

**UNIVERSITY OF NEWCASTLE-UPON-TYNE
DEPARTMENT OF CIVIL ENGINEERING**

**AN EXPERIMENTAL STUDY OF PILED EMBANKMENTS
INCORPORATING GEOSYNTHETIC BASAL
REINFORCEMENT**

**A THESIS SUBMITTED FOR THE DEGREE OF
DOCTOR OF PHILOSOPHY**

**BY
MAGDY A. DEMERDASH
NOVEMBER 1996**

Abstract

Basal reinforcement along with individually capped foundation piles is used in cases where both embankment stability and surface settlement control are required. The technique has been utilised to prevent differential settlement between new embankment construction over soft soil and an existing embankment where settlement has ceased. The piled embankment solution is also adopted to prevent differential settlement between an approach embankment constructed over soft soil and the piled foundations of a bridge abutment.

The study was conducted to investigate the behaviour of an idealised piled embankment incorporating basal geosynthetic reinforcement. Three-dimensional model tests at self-weight conditions were carried out to evaluate the effect of some of the factors affecting the arching mechanism and the development of surface settlement in piled embankments.

The physical model was designed to represent a square grid of individually capped piles centrally located within an embankment. Three different pile cap sizes and four different geosynthetic materials were employed in the experimental study. A movable base supported on hydraulically operated jacks was used to model the soft ground. The use of a movable base permitted the simulation of a worst case scenario in which the soft ground was not involved in the load sharing mechanism.

The experimental results indicated the existence of two modes of behaviour pertaining to a shallow and deep mechanism. The piled embankment geometry represented by a combination of height of fill, pile cap size and spacing was found to govern the mode of behaviour. The arching mechanism in the fill was found to be mobilised at a relatively small reinforcement deflection which supported the adoption of the two step approach utilised in designing the basal reinforcement. The circular and parabolic arc geometries were found to be adequate in describing the deflected shape of the reinforcement. The use a modified flexible cable formulation to describe the load-deflection response of the reinforcement was found to be in good agreement with the experimental results. In addition, the validity of a number of current methods and recommendations relating to the design of piled embankments was addressed.

A numerical study was undertaken using FLAC, a plane strain finite difference based programme. The calculated and measured results were compared to assess the suitability of modelling piled embankment behaviour using the finite difference programme. A parametric study was conducted to investigate the role of the basal reinforcement in the load transfer mechanism and in the prevention of surface settlement. The embankment geometry was identified as the significant factor influencing the reduction in differential settlement. A surface settlement mechanism was established based on results of the parametric study.

Acknowledgements

I wish to express my sincere gratitude for the help and companionship I received from members of the Geotechnical Group and Department of Civil Engineering as a whole. In particular, I am deeply grateful to my supervisor Professor C.J.F.P Jones for offering me the opportunity and resources to advance my knowledge and research skills and for his guidance and leadership.

I would also like to thank the British Council for granting me the sponsorship to undertake my research in the University of Newcastle-Upon-Tyne as a Chevening scholar.

I am grateful to Terram Ltd., specifically Chris Lawson and Geoff Kempton, for providing the financial support without which this research would not have been realised. The author would also like to extend his gratitude to Linear Composites Ltd., UK., for supplying the reinforcing materials.

My thanks are also forwarded to;

Dr. B. G. Clark was always kind to offer his assistance particularly during the analysis stage. Mr. A.I.B. Moffat with whom the Author has spent time discussing different aspects of the research. Dr. E. K. S. Passaris for his assistance in matters relating to the use of the numerical software.

I am especially grateful to Lindsey and John Moore for their advice, help, and enthusiasm during the study. I also thank Michael McKenna for his skill and expertise in manufacturing the test apparatus.

I would also like to thank the Group's secretaries for their co-operation and help. Mrs. C. Earle-Storey, Mrs. A.E. Bridges and Mrs. A. Meldrum always offered their assistance and help unstintingly.

On a more personal note, I would like to thank all my friends, especially, Yousef, Sami, Ali and Karim for their support and kindness during my period of study.

Last but not least, I am indebted to my wife, Rasha Naguib, for her encouragement, love and endurance, and my parents, Adel Demerdash and Nahed Hilmi, my in-laws, Ahamad Naguib and Maha Abou-el-Foutooh, and my brother Amr Demerdash, for their support, sacrifices, and belief in me. Thank you is not enough.

Table of Contents

Abstract

Acknowledgements

Chapter 1: Introduction Page

1.0 Introduction	1-1
1.1 Piled Embankments	1-2
1.2 Scope of Study	1-3
1.3 Layout of Thesis	1-4

Chapter 2: Literature Review Page

2.0 Introduction	2-1
2.1 Physical Models	2-1
2.2 The Phenomenon of Arching in Granular Soils	2-3
2.2.1 The Definition of Arching	2-4
2.2.2 The Mechanism of Arching	2-4
2.3 Theoretical Considerations	2-7
2.4 Arching in Piled Embankments	2-11
2.4.1 Analytical Solutions	2-11
2.4.2 Experimental Evidence	2-14
2.5 Tensioned Membranes	2-17
2.6 Modelling Using Continuum Methods	2-18
2.7 Design Philosophy	2-20
2.8 Case Histories	2-23
2.9 Summary	2-27

Chapter 3: Design of Apparatus Page

3.0 Introduction	3-1
3.1 Modelling at Reduced Scale	3-1
3.1.1 Identification of the Significant Physical Parameters	3-1
3.1.2 Dimensional Analysis	3-3
3.1.2.1 Determination of the ' π ' Parameters	3-3
3.1.3 Similitude and Scaling Laws	3-4
3.2 Selection of Model Components	3-5

3.2.1 Model Size	3-5
3.2.2 The Soil	3-6
3.2.3 The Reinforcement	3-7
3.3 The Apparatus	3-8
3.3.1 The Test Box	3-9
3.3.2 The Clamps	3-9
3.3.3 The Movable Base	3-10
3.3.4 The Pile Caps	3-11
3.3.5 The Sand Raining Box	3-12
3.4 Instrumentation	3-13
3.4.1 Load and Pressure Cells	3-14
3.4.2 Displacement Transducers	3-15
3.4.3 Surface Settlement	3-15
3.5 Data Acquisition	3-15
3.6 Summary	3-16

Chapter 4: Experimental Procedure and Test Results	Page
4.0 Introduction	4-1
4.1 Experimental Procedure	4-1
4.1.1 Installation of Geosynthetic Strips	4-1
4.1.2 Sandproofing	4-1
4.1.3 Lubrication of Sidewalls	4-2
4.1.4 Construction of Deposit	4-3
4.1.5 Lowering of the Platform	4-3
4.2 Material Properties	4-4
4.2.1 The Soil	4-4
4.2.2 The Geotextile Reinforcement	4-6
4.3 The Model Test Results	4-6
4.3.1 The Pile Cap Loads	4-7
4.3.2 Geotextile Mesh Deflections	4-10
4.3.3 Surface Settlement	4-11
4.4 Losses	4-12
4.5 Repeatability	4-13
4.6 Summary	4-13

Chapter 5: Interpretation and Analysis	Page
5.0 Introduction	5-1
5.1 Interpretation of Test Results	5-2
5.1.1 The Mechanism of Load Transfer	5-2
5.1.2 Shape of Deformed Mesh	5-7
5.1.3 Surface Differential Settlement	5-8
5.1.4 The Influence of the Settlement Ratio on Efficacy	5-9
5.2 Analysis of Basally Reinforced Piled Embankments	5-12
5.2.1 Prediction of Piled Embankment Efficacy	5-12
5.2.2 Dimensional Analysis of the Reinforcement Behaviour	5-18
5.3 Evaluation of Current Design Methods	5-21
5.4 Summary	5-22

Chapter 6: Finite Difference Analysis	Page
6.0 Introduction	6-1
6.1 The Finite Difference Method	6-1
6.2 The Computer Program	6-2
6.3 The Piled Embankment Problem	6-2
6.3.1 Modelling Considerations	6-2
6.3.2 The Finite Difference Grid	6-3
6.4 Preliminary Investigation	6-3
6.4.1 Evolution of the Gravitational Force	6-4
6.4.2 The Stiffness of the Yielding Support	6-6
6.4.3 The Piled Embankment Geometry	6-6
6.4.4 The Assumption of Plane Strain Conditions	6-6
6.5 Parametric Study	6-7
6.5.1 Un-Reinforced Piled Embankments	6-7
6.5.2 The Effect of Basal Reinforcement	6-9
6-6 Summary	6-11

Chapter 7: Conclusions and Design Recommendations	Page
7.0 Introduction	7-1
7.1 The Experimental Study	7-2
7.2 The Finite Difference Analysis	7-5

7.3 Design Recommendations	7-6
7.4 Recommendations for Future Research	7-7
References	
Figures	
Plates	

Notation

The following symbols have been used in the text. Deviations from the standard notations are defined locally.

Symbol	Definition
α	modification factor
A	pile cap tributary area
a/A	area ratio
a_c	internal radius of cavity
A_E, B_E, C_E, β	parameters pertaining to efficacy calculations
b	width of pile cap
B	width of trapdoor
b:s'	ratio of pile cap width to clear spacing
B _c	outside diameter of conduit
B _l	tensile breaking load
C	competency
C_c, m_r	arching coefficients
C_d	fill load coefficient for rigid conduit under a condition of positive projection
D	thickness of soft subsoil
$\Delta a, \Delta b, \Delta c$	average surface settlement
ds-max, ds-min	maximum and minimum surface settlement
E	efficacy of pile support
ε_G	the average tensile reinforcement in the reinforcement
M, E_m	modulus of elasticity of soft soil
ϕ	angle of internal friction
G	elastic shear modulus of soil
g	gravitational acceleration
γ	unit weight of fill
H	height of embankment
H/s'	depth of fill to clear spacing ratio

He	height of plane of equal settlement above crown of conduit
J	tensile stiffness of basal reinforcement
k	ratio between horizontal and vertical stresses
Ka	Rankine's active earth pressure coefficient
kn	normal spring stiffness
Kp	Rankine's passive earth pressure coefficient
l	finite length of trapdoor
L	unsupported span in cable formulation
m_v	coefficient of compressibility
ν	Poisson's ratio
P	failure load
Pa, Ta-avg.	average pile cap load due to overburden and arching in the fill
PL, Tn-avg.	net weight of fill per pile cap tributary area
q, w_s	surcharge applied to surface of soil
θ	half angle subtended by the radii of circular arc
qb, σ_s	vertical stress acting on the soft soil
R	dimensionless parameter pertaining to piled embankment surface deformation
RG	radius of circular arc
r_p	projection ratio
r_{sd}	settlement ratio pertaining to buried conduit
S	equivalent half line centre line spacing between piles
s'	clear spacing between adjacent pile caps
σ_o, σ_a	limiting radial stresses
SSR	stress reduction ratio
σ_v	vertical compressive strength
σ_{vo}	vertical overburden stress
Tl-avg	average load loss
Tv	vertical component of axial tensile load in reinforcement
TT	reinforcement tensile load

v	width of void
w	width of tributary grid zone
W _c	load on conduit per meter length
w _G	uniform load supported by reinforcement between adjacent pile caps
χ	$45^\circ + \phi/2$
ψ	angle of dilation
Y	yield strength of cable element
y _g	maximum vertical basal reinforcement deflection
y _g /s'	basal reinforcement settlement ratio
z	depth below surface of soil
z ₁	depth of plane of equal settlement below surface of soil

List of Tables

Table		Page
1-1	Main characteristics of the methods used for controlling settlement	1-5
2-1	Guidelines for the design of the necessary coverage by pile caps	2-29
4-1a	Nature of tests performed	4-14
4-1b	Nature of tests performed	4-15
5-1	Summary of maximum efficacy values for full height and incremental loading tests	5-26
5-2	Comparison between field measurements and experimental results	5-26
5-3	Summary of predicted efficacy values	5-27
5-4	Summary of dimensional analysis results	5-27
6-1	Material parameters and mesh size used in preliminary analysis	6-13
6-2	Material parameters and mesh size used in the simulation of the model tests	6-13
6-3	Material parameters and mesh size used in parametric analysis	6-14

Chapter 1

Introduction

1.0 Introduction

Over the last 15 years considerable use has been made of geotextiles to support the base of embankments constructed over piled foundations, especially in the Scandinavian countries and Southeast Asia, Broms and Wong (1985).

The principle behind a piled embankment construction is to use a grid of piles to support the fill with the assumption that all the embankment loading will be transferred through the piles down to a firm stratum. Consequently, the soft foundation soil itself no longer has direct relevance to the performance of the embankment.

The pile caps enable, through the development of arching in the fill material and the mobilisation of the tensile strength of the basal reinforcement, the transfer of the embankment load onto the piles and hence maximise pile efficiency.

Broms (1979) proposed that the fill above embankment piles should satisfy certain criteria so that it can transfer the weight of the fill through arching to the piles via the pile caps. In addition, the thickness of the fill should normally be at least 2.0 meters otherwise a geofabric reinforcement should be introduced in the fill.

The role of the geotextile is to support the weight of the fill in the embankment between the piles and to counteract the horizontal thrust at the sides of the embankment.

In supporting the embankment fill between the pile caps, the geotextile acts as a tension membrane transferring the vertical load of the embankment directly onto the piles which reduces the size of the pile caps. The geotextile also counteracts the horizontal thrust at the sides of the embankment and hence eliminating the need for raking piles.

The use of geosynthetic basal reinforcement in conjunction with piles to provide stability and reduce settlement represents a complex soil-structure interaction

problem. Experience shows that basal reinforcement can be safely designed but research is still needed in order to achieve an optimal design, Magnan (1994).

This study was, therefore, conducted to investigate, through model testing, the three dimensional behaviour of basally reinforced piled embankments under normal gravity conditions.

This Chapter provides a brief overview of the different methods available to provide settlement control for embankments on soft clays. In addition to highlighting the advantages gained by adopting the piled embankment construction technique. The scope of the study and the thesis layout are presented at the end of the Chapter.

1.1 Piled Embankments

Extensive deposits of very soft soils exist world-wide. Such soils are problematic due to their very low shear strength and high compressibility.

The difficulties encountered when constructing highway or rail embankments over such poor foundations are mainly due to bearing capacity failures and the associated lateral deformations, in addition to time-dependent consolidation and creep settlements.

It is often necessary to construct embankments over such poor subsoils for reasons of economy because alternative sites are simply not available or as extensions to existing road/rail networks. The difficulties of construction on soft ground can usually be avoided by designing a scheme to cope with the problem induced by the subsoils.

The techniques involved in overcoming such problems may be divided into several groups;

- i. preloading or staged construction in conjunction with vertical drainage to accelerate consolidation and, hence, increasing the load carrying capacity of the subsoil;
- ii. designing the embankment profile to be compatible with the bearing strength of the soft foundation, i.e., adopting gentle side slopes;
- iii. the use of light weight fill such as polystyrene;
- iv. specialised processes such as chemical treatment and electro-osmosis and;

- v. methods which reinforce or stiffen the subsoil using piles, sand/stone columns or geosynthetics.

Table 1-1 (after Magnan (1994)) gives some indications on the advantages and drawbacks of the available methods for controlling settlements.

The technique of driving piles into the soft ground to support embankments allows rapid construction with no fear of bearing capacity failure of the weak subsoil. In addition, vertical settlement is minimised, hence achieving considerable reduction in expense otherwise incurred to maintain the embankment crest at the specified level.

Additional problems arise when conventional embankments are constructed adjacent to piled structures such as at bridges, whereby the piled structure suffers a limited vertical settlement compared to the embankment leading to undesirable differential settlement and consequently loss of serviceability.

The embankment fill will also induce a lateral pressure to act on the structure's piled foundation which could lead to a structural failure of the piles. These problems are effectively controlled when resorting to a piled embankment in addition to minimising land use.

1.2 Scope of Study

The main purpose of this research programme is to study, through reduced-scale physical modelling, the principal features of an embankment supported on piles incorporating link geotextiles spanning between adjacent pile caps and assuming no support from the foundation soil.

In addition to modelling the essential features of the prototype, the goals of the experimental program were to:

- i. evaluate the effect of varying the ratio of the pile cap size to its centreline spacing and the height of the supported fill on the vertical stresses acting on top of the rigid pile caps and hence the degree of soil arching occurring;
- ii. measure the vertical deflections suffered by the geotextile reinforcement due to the fill load;

- iii. monitor the corresponding surface settlements;
- iv. validate a numerical model to investigate a wider range of parameters;
- v. develop a rational design methodology that will account for the 3-dimensional nature of piled embankments and which will include the fill characteristics, piled embankment geometry, and geotextile properties.

1.3 Layout of Thesis

The work described in this thesis is an attempt to address the design of piled embankments incorporating geosynthetic basal reinforcement. In Chapter 2, the mechanism of arching in granular soils is addressed to appreciate the governing factors. The current analytical solutions to the problem of arching in piled embankments are presented. The findings of recent experimental and numerical studies were summarised and presented to appreciate the different modelling strategies utilised by various researchers. The structural behaviour of the basal reinforcement and the different geometries used to represent the deflected shape were examined.

The different methodologies resorted to in the design of piled embankments were also reviewed. In conclusion a number of case histories from different locations world wide are presented.

The dimensional analysis involved in the study, design of the apparatus and the instrumentation scheme are described in Chapter 3. The experimental procedure and the overall testing approach as well as the test results are presented in Chapter 4. Chapter 5 includes the interpretation and analysis of the test results , together with comparisons between predictions made using current methods of analysis and the measured responses of the laboratory tests. The findings of a finite difference analysis undertaken to study a wider range of parameters are described in Chapter 6.

A summary of the main conclusions and design recommendations are presented in Chapter 7, along with recommendations for future research.

**Table 1-1. Main characteristics of the methods used for controlling settlement
(after Magnan (1994)).**

Method	Necessary data	Constraints	Reliability	Comments
Preloading	Compressibility permeability	Time necessary	Low if the desired settlements are low	Slow cheap
Preloading with vertical drains	Compressibility Horizontal and vertical permeability	Less time necessary	More flexible	Fast relatively expensive
Replacement of soft clay	Layer thickness	Disposal for extracted soil New fill	Good in case of total replacement	Expensive rapid
Stone columns, compaction sand piles	Soil resistance and moduli	Equipment Preliminary trials	Good after analysing a set of trial columns	Expensive rapid
Piled rafts and bridges	Soil resistance		Good	Very expensive
Electro- osmosis and injection	Physico-chem- ical properties compressibility permeability	Destruction of electrodes Electricity needed	Uncertain	Very expensive
Lightweight materials	Compressibility Permeability	Protection of the lightweight material	Low if the desired settlements are small	Expensive
Piled embankments	Soil resistance and moduli		Good	Expensive rapid
Jet-grouted columns	Soil resistance and moduli		Good	Expensive rapid

Chapter 2

Literature Review

2.0 Introduction

The main aim of the literature review is to draw upon the accumulated knowledge on the subject, identify the areas where research is required, and thus define the aims of this study. The review is discussed under the following headings

- Physical models
- The phenomenon of arching in granular soils
- Arching in piled embankments
- Tensioned membranes
- Design methods.
- Field experience.

2.1 Physical Models

It is of benefit to consider the aims and limitations attributed to physical modelling in the published literature.

Few researchers seem to have directly addressed the problem, and the following papers are noteworthy in having summarised the general purpose of physical modelling as well as expressing reservations concerning their applications.

Rocha (1957) and Kerisel (1967) considered that the ultimate goal of performing laboratory tests on scale models was to quantitatively predict the behaviour of full-scale structures and to have a knowledge of the confidence limits with which the results could be applied.

Both authors recognised the need to fulfil the laws of similarity, based upon the fundamental units of mass, length and time which should be satisfied when passing from one system of units to another.

Rocha acknowledged the fact that the availability of full-scale test results was often scarce but could see that the use of models, particularly ones satisfying the more general conditions of similarity, should provide a viable alternative for obtaining such data.

Kerisel emphasised the point that the smaller the scale of the tests, the larger the discrepancies were likely to be between the model predictions and the actual full-scale behaviour, suggesting that the relationship was hyperbolic in nature. He suggested therefore, that with reasonable size models, it should be possible to achieve good predictions of full-scale behaviour.

Bassett (1979) and Bassett and Horner (1979) posed several key questions regarding the use of physical models for geotechnical design purposes. These included:

- i. Can models be used to provide direct predictions of prototype behaviour ?
- ii. Is the use of models restricted by scaling relationships, as it is known that soil behaviour is dependant upon stress level, stress path and strain rate ?
- iii. Are particle size effects important?
- iv. One of the major components of stress fields in many geotechnical applications is due to the self-weight of the soil. Acknowledging the fact that this can be modelled by means of multi-gravity testing, the question was asked - when is such a technique justified, and under what circumstances could a normal laboratory test be equally useful ?
- v. How do boundary conditions and the type of apparatus influence model behaviour?

They also considered the advantages to be gained from testing small scale models over full-scale projects. These included :

- i. they are usually relatively cheap compared to full-scale situations;
- ii. the tests can be taken to failure without catastrophic or expensive results;
- iii. the soil properties can be chosen and to an extent controlled;

iv. the tests can be modified to try to highlight the effects of one variable at a time.

Bassett (1979) also suggested that whilst physical models can have several roles to play within the field of geotechnical engineering, they generally fall into two main categories:

- i. for the direct prediction of full-scale behaviour;
- ii. for the validation of numerical methods.

Bassett correctly stated that the most direct use of models would be to provide predictions of full-scale performance. The use of a single model does however raise a fundamental problem of how to achieve material properties that most likely represent the insitu soil conditions. It was suggested that samples chosen to represent the best and worst possible site conditions, subjected to loading representative of the full-scale event, and well in excess of this, should cover the range of possible responses, and allow engineering design to proceed.

The most rewarding field for future model work would lie in the validation of complex numerical relationships. Full-scale tests yield insufficient data to allow definite correlations to be made between numerical predictions and observed behaviour. It was concluded therefore that model testing offered an ideal alternative for providing controlled and repeatable data in these situations.

Craig (1979) felt that the use of physical models primarily for the validation of numerical predictions was unnecessarily restrictive. He presented views clearly on how physical models should fit into the design process, including their role with numerical models and constitutive relationships, but with the more direct prediction of full-scale responses from physical models also emphasised.

To achieve extrapolation, both from one model scale to another and model scale to full-scale, modelling laws need to be applied correctly. These consist of the laws of similarity which should be satisfied when passing from one scale to another.

2.2 The Phenomenon of Arching in Granular Soils

The load sharing mechanism in piled embankments is dependant on the formation of an arched condition in the fill that transfers the larger portion of the embankment

weight onto adjacent pile caps. The role of arching in this process cannot be over-emphasised.

Consequently, within this section, the conditions leading to and affecting arching in granular soils are described. A select number of theoretical approaches to analysing the arching phenomenon in soil mechanics with special relevance to piled embankments are also reviewed.

2.2.1 The Definition of Arching

If only a localised area of the support for a mass of soil yields, the soil adjoining the yielding zone tends to displace with the yielding support while the rest of the soil remains stationary. In the transition zone between the moving and stationary soil masses, shear stresses are developed by the relative displacement of the two masses. Since the shearing resistance tends to keep the yielding mass in its original position, it reduces the pressure on the yielding part of the support and a corresponding increase in the pressure on the stationary part.

The transfer of pressure from a yielding mass of soil onto adjacent stationary parts is referred to as the arching effect, and the soil is said to arch over the yielding part of the support, Terzaghi (1943).

Tschebotarioff (1973), however, pointed out that the term arching is often used loosely to explain the reduction in the vertical stress. Equating the bin action in silos to arching is not entirely correct despite the similarity in the end effect. Bin action develops primarily due to fill friction along the silo walls resulting in a reduction of vertical stresses in the soil mass with depth.

On the other hand, a pre-requisite for true arching is a process of progressive wedging and jamming of individual sand grains. Thus arching must involve a transfer of vertical stress by shear. Conversely a pressure reduction due to shearing stresses does not necessarily produce a true arch.

2.2.2 The Mechanism of Arching

Arching occurs whenever there is a localised displacement along any restraining structure, horizontal or vertical, which confines a soil mass. Since arching is maintained solely by shearing stresses in the soil; it is no less permanent than any other state of stress in the soil (Terzaghi, 1943)

Some of the earliest experimental investigations into the stress distribution above a yielding trap door were conducted by Terzaghi (1936). The tests were conducted under plane strain conditions using a deflecting trapdoor incorporated in the base of a rectangular container full of sand.

The results of one of Terzaghi's experiments are shown in **Figure 2-1**. A trapdoor 73 mm wide and 463 mm long was mounted in the base of a bin containing 310 mm of sand. As the trapdoor was deflected downwards, its movement and the total load upon it were measured. It was observed that the total load on the door decreased to less than 10% of its initial value by the time the trapdoor had been deflected 0.005 to 0.10 times the door width, depending upon the density of the sand. After reaching a minimum value, the load increased slightly to less than 13% of its original value.

Terzaghi (1936) explained the mechanism of arching in two stages. During the first, when the downward movement of the trap door is less than 10% its width, shear stresses develop along the inclined planes a'-a" and b'-b" (**Figure 2-2**). These shearing stresses transfer part of the weight of the sand located between the inclined shear planes onto the adjacent soil mass.

The second stage is induced upon further trapdoor deflection, the shear planes shift to re-orient almost perpendicular to the yielding surface accompanied by an increase in the trapdoor load.

Further experiments by Terzaghi, in which the force required to pull out flat metal tapes embedded at different depths, suggested that the ratio between horizontal to vertical stresses increased from unity immediately over the trapdoor to a value of 1.5 at an elevation of B above the centreline of the trapdoor. The movement of the trapdoor, however, did not have a significant effect on the state of stress in the fill at elevations greater than $2.5(B)$.

McNulty (1965) carried out an experimental investigation similar to that undertaken by Terzaghi (1936). The tests, however, were carried out under conditions of axisymmetry, i.e., in plan the trap door was circular. The test results demonstrated the ability of a soil arch to transfer loads of much greater magnitude than its own dead

weight. In addition for axi-symmetrical conditions, a soil cover in excess of 1 to 1.5 diameters had an insignificant effect on the arching mechanism as opposed to a ratio ranging between 2 to 3 for plane strain conditions.

The influence of the trap door surface profile was the subject of a series of laboratory tests carried out by Getzler et al. (1968). The three different profiles employed in the testing programme were: (a) triangular, (b) semi-circular and (c) flat. The ratio of height to width was referred to as the aspect ratio of the trap door.

For the triangular and semi-circular profiles, two different aspect ratios were considered, the aspect ratio of the flat door being zero. Getzler et al. concluded that an increase in the aspect ratio of the trap door enhanced the formation of arching and that no great distinction was observed between the triangular and the semi-circular profiles. However, the arching mechanism was observed to diminish considerably with increasing depth of soil cover.

The classical trap door experiment was not always undertaken using natural soils. Ladanyi et al. (1969), conducted a model study on soil structure-interaction using an apparatus similar to that used in the classical trap door experiments. The model tests were carried out under plane strain conditions and the granular mass was represented by a stack of aluminium rods supported by a U-shaped rigid steel frame.

The test results for the case where the trap door was moved downwards were similar to those obtained by Terzaghi (1936). For dense packing, the pressure on the trap door decreased to a minimum which was attained at about 8 to 10% of the door width. At further lowering, there was a gradual increase of pressure up to a constant ultimate value at downward door movement of about 50% of its width. The ultimate arching ratio, which represents the reduction in the trapdoor load, was observed to be independent of the depth of soil for depth to width of door ratios ranging from 2 to 3.

Vardoulakis et al. (1981) conducted a set of trapdoor experiments in both the passive and active modes. The granular sand mass above the trapdoor was placed in regularly spaced horizontal layers of coloured sand. The objective of the tests was to investigate the mechanism of shear band formation for both upward and downward

trap door movement, i.e., in both the passive and active modes respectively. For the active mode, which is of more relevance to the current study, Vardoulakis et al. observed that for relatively small downward displacements, a small dilatant zone developed above the trap door. A clear delineation was evident separating the dilatant zone from the remaining mass. These boundaries start vertically at the edges of the trap door and converge towards the axis of symmetry. With further downward movement of the trap door, the dilatant zone continued to expand upwards until it finally reached the free surface .

The development of powerful computers capable of carrying out laborious and complicated mathematical operations within a reasonable time scale led to an increase in the popularity of numerical modelling. Koutsabeloulis and Griffith (1989) modelled the trap door problem using the finite element method. Both passive and active modes of displacement were analysed. **Figure 2-3** shows a typical finite element discretisation of the trap door problem. The soil was assumed to be cohesionless and to behave as an elastic perfectly plastic material. The Mohr-Coulumb failure surface was used together with a non-associated flow rule.

The arching mechanism was initiated by giving the trap door a prescribed set of displacements. Failure was considered to occur when the averaged stresses above the trap door level out and having reached this stage remain so despite further displacement increments.

Figure 2-4 shows the failure load (P) normalised by the hydrostatic load (γH) plotted against (H/B) where (H) refers to the height of fill cover and (B) is the door width. Koutsabeloulis et al. (1989) identified two modes of failure depending on the geometry ratio (H/B) , a shallow and deep mechanism. The transition from the shallow to a deep failure mechanism was observed to occur at a depth ratio (H/B) of about 2.5.

2.3 Theoretical Considerations

Terzaghi (1943) presented an analytical solution based on Janssen's silo equation to predict the variation in the vertical stress above the trapdoor as shown in **Figure 2-5a**. The analysis was based on the vertical equilibrium of forces for the yielding element shown in **Figure 2-5b**.

The following equation was obtained by vertical force equilibrium on a unit length of the yielding element ;

$$B\gamma dz = B(\sigma_v + d\sigma_v) - B\sigma_v + 2cdz + 2k\sigma_v dz \tan(\phi) \dots (2-1).$$

The differential equation shown above was solved to give the vertical stress at a depth (z) below the surface of the soil;

$$\sigma_v = \frac{B(\gamma - 2(c/B))}{2k \tan(\phi)} * [1 - e^{-k \tan(\phi)(2z/B)}] \dots (2-2).$$

For granular soils the cohesion (c) is zero and the above equation reduces to;

$$\sigma_v = \frac{B\gamma}{2k \tan(\phi)} * [1 - e^{-k \tan(\phi)(2z/B)}] \dots (2-3).$$

where k = ratio between the horizontal and vertical pressures; γ = unit weight of the soil; B = width of trapdoor; ϕ = angle of internal friction; z = depth below the surface of the soil. Terzaghi (1943) modified the above expression to account for the plane of equal settlement, which represents the location above the yielding trap door where the state of stress reverts to hydrostatic conditions;

$$\sigma_v = \frac{B\gamma}{2k \tan(\phi)} * [1 - e^{-k \tan(\phi)(2z/B)}] + (\gamma(z - z_1) + q)e^{-k \tan(\phi)(2z_1/B)} \dots (2-4)$$

where q = surcharge applied to the surface of the soil;

z_1 = depth of plane of equal settlement below surface of soil.

Mckelvey III (1994) recommended that (k) should be taken equal to that proposed by Handy (1985). In his analysis of the state of stress in the arched soil above the yielding surface, Handy showed that the path of the minor principal stress takes the shape of a catenary. The equation shown below was proposed by Handy (1985) to obtain a stress ratio (k) compatible with the catenary representation;

$$k = 1.06 * (\cos^2(\chi) + K_a \sin^2(\chi)) \dots (2-5)$$

where K_a = Rankine's active earth pressure coefficient,

and $\chi = 45^\circ + \Phi/2$.

The analysis presented above pertains to plane strain conditions, i.e., the trapdoor has infinite length. Van Horn (1963) showed that for a yielding element having a finite length (l) and width (B), a more general form of Terzaghi's equation can be obtained by replacing the term (B) with (L_E);

$$\sigma_v = \frac{L_E \gamma}{2k \tan(\phi)} * [1 - e^{-k \tan(\phi)(2z/L_E)}] + (\gamma(z - z_1) + q) e^{-k \tan(\phi)(2z_1/L_E)} \quad (2-6)$$

where $(L_E) = (B \times l) / (B + l)$.

To conclude this section two examples of the manifestation of soil arching in engineering applications are described. The two cases presented below have direct relevance to the arching mechanism in piled embankments as will be shown in later sections of this Chapter.

[A] Buried Conduits

Marston and Anderson (1913) proposed the following load formula for positive projecting conduits with an external diameter (B_c);

$$W_c = C_d \gamma B_c^2 \dots\dots\dots (2-7)$$

where γ = unit weight of the soil;

and
$$C_d = \frac{e^{\pm k \tan(\phi)(2H/B_c)} - 1}{\pm 2k \tan \phi}$$
 when $H \leq H_e$;

or
$$C_d = \frac{e^{\pm k \tan(\phi)(2H_e/B_c)} - 1}{\pm 2k \tan \phi} + \left(\frac{H}{B_c} - \frac{H_e}{B_c} \right) e^{\pm k \tan(\phi)(2H_e/B_c)}$$

when $H > H_e$.

H_e = height of the plane of equal settlement above the crown of the conduit.

The term C_d in the above equations represents a load coefficient, the +ve sign refers to a rigid conduit under a condition of positive projection. Marston derived a complex expression to determine the height of the plane of equal settlement (H_e) in terms of the height of soil cover (H), the outside diameter of the conduit (B_c) and the

projection and settlement ratios, (r_p) and (r_{sd}), respectively. The projection and settlement ratios are defined in **Figure 2-6** for a rigid conduit under positive projection conditions.

Spangler (1960) derived a relationship between the ratio ($\sigma_v/\gamma B_c$), where σ_v = vertical stress at the crown of the conduit, and the ratio (H/B_c) for a range of ($r_{sd} \cdot r_p$). The relationship is shown in **Figure 2-7** (Bulson (1985)).

[B] Shallow Circular Tunnels

More recently Atkinson and Potts (1977) studied soil arching in connection with the stability of shallow circular tunnels in soils. Their experimental investigation consisted of small-scale model tests in the laboratory and in a large diameter centrifuge. The objective of the study was to determine the influence of various parameters on the tunnel pressure at collapse. A theoretical study carried out in parallel with the experimental work was based on the upper and lower bound theorems for perfectly plastic materials.

Bolton (1979) analysed the stability of the crown of an underground cylindrical cavity subject to an external surcharge σ_o and internal cavity pressure σ_a , **Figure 2-8**. Self-weight of the soil was included in the differential equation of radial equilibrium to give;

$$\frac{d\sigma_r}{dr} + \frac{(\sigma_r - \sigma_\theta)}{r} = -\gamma \dots\dots\dots (2-8).$$

Bolton solved the differential equation at limiting conditions to obtain;

$$\frac{\left(\frac{\sigma_o}{\gamma R}\right)^{\left(k_p - 2\right) - 1}}{\left(\frac{\sigma_a}{\gamma a}\right)^{\left(k_p - 2\right) - 1}} = \left(\frac{R}{a}\right)^{k_p - 2} \dots\dots\dots (2-9)$$

- where
- R = radial distance from centre of cavity to surface of soil cover;
 - a = internal radius of cavity;
 - k_p = limiting stress ratio corresponding to the Rankine passive failure coefficient;
 - σ_o, σ_a = limiting radial stresses.

Attempts have been made to solve the problem through the use of the theory of elasticity (Finn (1963)). Such solutions, however, are restricted to the narrow range within which soil is assumed to behave as an elastic material. For the deformations usually encountered in typical field situations, soil does not exhibit linear elastic properties. Consequently, the use of elasticity solutions will yield an unrealistic estimate of the pressure distribution resulting from the arching mechanism and will not be pursued further.

2.4 Arching in Piled Embankments

The following section presents a review of current analytical solutions to the problem of arching in piled embankments. The findings of previous experimental studies are also summarised to demonstrate the available physical evidence of the soil-structure interaction inherent in piled embankment behaviour.

2.4.1 Analytical Solutions

Although a number of theoretical models were developed in the past to quantify the arching process in a variety of field situations, these formulations were essentially two-dimensional. The aforementioned formulations, however, were modified to address the three-dimensional nature of piled embankments. In this section the assumptions and simplifications leading to modified theoretical equations are reviewed in order to appreciate their limitations.

John (1987) modified Marston and Anderson's (1913) load equation for positively projecting conduits to calculate the pile cap load due to the load transfer mechanism. Thus replacing the term (B_c) with (b), the pile cap width, and re-arranging terms Marston's and Anderson's (1913) equation for positively projecting conduits becomes;

$$\frac{p_c}{\sigma_{vo}} = \left(\frac{C_c b}{H} \right)^2 \dots\dots\dots (2-10)$$

where p_c = vertical stress on the pile cap;
 σ_{vo} = overburden stress;
 C_c = arching coefficient;
 H = height of fill above pile cap
 b = width of pile cap.

The coefficient of arching (C_c) in the above equation is identical to the (C_d) parameter in Marston's analysis. John (1987), however, recommended the use of 0.2 and 5 for the projection and settlement ratios, respectively, to obtain the following expression for (C_c):

$$C_c = \frac{1.69H}{b} - 0.12 \dots\dots\dots (2-10).$$

Bergdahl et al. (1979) proposed the following semi-empirical relationship to obtain the average bearing pressure (q_b) supported by the soft soil in a piled embankment system;

$$q_b = \left(\frac{\gamma H}{k \tan(\phi)} \right) \cdot \left(\frac{s^2 - b^2}{4b} \right) \dots\dots\dots (2-11);$$

where s = pile cap centre line spacing

b = pile cap width

ϕ = angle of internal friction for the fill

H = height of embankment

k = empirical constant ranging between 0.7 for $H/s < 1$ and 1.1 for $H/s > 1$;

While this equation may enable an estimate of the vertical stress between the pile caps, for a specific centreline spacing, to be made, it does not account for the development of a plane of equal settlement.

Hewlett and Randolph (1988) idealised the arching of granular fills in a piled embankment as a system of vaulted domes of hemispherical shape supported on diagonally opposite pile caps (**Figure 2-9**). The principal element of the assumed stress field is the semi-circular zones of arched sand. These arches of sand transfer the weight of the embankment onto the pile caps. Although the arches of sand lie within a continuum, their action is similar to that of masonry arches. The theoretical expressions developed were based on an analytical approach similar to that adopted by Bolton (1979). Hewlett and Randolph defined the term "efficacy" (E) as the proportion of the embankment weight carried by the piles. The piled embankment system was analysed by considering the radial force equilibrium for two possible failure modes (**Figures 2-10 and 2-11**).

For low fill heights, failure was considered to occur at the crown of the arch and the corresponding efficacy was obtained as follows;

$$E = 1 - (1 - \delta^2)(A_E - A_E B_E + C_E) \dots \dots \dots (2-12)$$

where $A_E = (1 - \delta)^2 (k_p - 1)$; $B_E = \frac{s}{\sqrt{2H}} \left[\frac{2k_p - 2}{2k_p - 3} \right]$; $C_E = \frac{s - b}{\sqrt{2H}} \left[\frac{2k_p - 2}{2k_p - 3} \right]$; $\delta = b/s$;

and $k_p = (1 + \sin \phi) / (1 - \sin \phi)$.

The second possible failure mode was assumed to occur in the fill above the pile cap and the efficacy for such a case was given by ;

$$E = \frac{\beta}{\beta + 1} \dots \dots \dots (2-13)$$

where $\beta = \frac{2k_p}{k_p + 1} \left(\frac{1}{1 + \delta} \right) \left[(1 - \delta)^{-k_p} - (1 + \delta k_p) \right]$.

Hewlett and Randolph suggested that the lower value of these two estimates was to be used for design. The variation of the efficacy (E) with pile geometry and embankment fill properties is shown in **Figure 2-12**.

Combarieu (1989) presented the following semi-empirical equation to determine the vertical stress (σ_s) bearing on the soft foundation soil;

$$\sigma_s = \frac{H \gamma}{m_r} (1 - e^{-H m_r}) \dots \dots \dots (2-14)$$

Combarieu expressed (m_r) in terms of the piled embankment geometry and the fill properties as follows:

where $m_r = \frac{(b/2) \cdot k \cdot \tan(\phi)}{(S)^2 - (b/2)^2}$;

b =the lateral width of the pile cap;

H = height of embankment;

and $2S$ =the equivalent centre line spacing between pile caps;

The pile spacing (2S) corresponds to a 2-D representation of the actual 3-D geometry. Combarieu (1989) proposed that the centre line spacing (2S) is related to the pile grid spacing (s) by the following expression;

$$\frac{S}{b} = \frac{s}{b} \sqrt{\frac{4}{\pi}} \dots\dots\dots (2-15);$$

where s = pile grid spacing.

2.4.2 Experimental Evidence

In recent years a number of laboratory controlled experimental investigations have been carried out with the aim of providing a better understanding of the mechanism of piled embankment behaviour and identifying the controlling parameters. The different test procedures adopted and the results obtained in carrying out these experimental investigations are summarised in this section.

[A] Test Procedures

Bergdahl et al. (1979), working at the Swedish Geotechnical Institute for the State road board carried out a series of model tests to examine the influence of the pile cap size and spacing for different embankment heights. The model consisted of a test box with square plan dimensions filled with sand. The box was supported on four screw jacks which allowed a controlled downward movement simulating subgrade settlement. A regular pattern of openings was provided in the base to accommodate the pilecaps supported on piles fixed firmly to the laboratory floor, as shown in **Figure 2-13a**.

A generally similar method was used by Ting et al. (1983) and Ali (1990), where the settlement of the subgrade was simulated by a mechanically controlled movable base (**Figure 2-13b**).

Hewlett and Randolph (1988), however, used a bed of foam rubber chips to model the soft subsoil (**Figure 2-13c**).

The use of geotextile reinforcement in piled embankments was investigated by Tang (1992) in a series of plane strain laboratory scale tests. In these model tests, cap-beams were employed as opposed to the individual square caps with the subsoil simulated by rubber foam.

The sand was placed on a layer of geotextile supported on the model cap beams and rubber foam. A series of control tests were carried out in which the geotextile reinforcement was absent to assess the effect of the geotextile on the load transfer mechanism.

All the above mentioned tests were carried out at normal self-weight ('1g') conditions in which no attempt was made to achieve identical stress magnitudes between the model and the full-scale events.

Bujang (1990), carried out centrifuge model tests at a 1:100 scale to investigate the behaviour of a prototype piled embankment. On the basis of the test results, Bujang recommended for further research the investigation of incorporating geosynthetic basal reinforcement on the behaviour of piled embankments. **Figure 2-14** shows a typical cross section of the model embankment showing the pertinent dimensions and details of its instrumentation.

[B] Test Results

In their experiments carried out at the Swedish Geotechnical Institute, Bergdahl et al. (1979), found that the sand fill on top of the pile cap showed two distinct profiles. Fills with low heights (H) relative to a given ratio of pile cap size (b) to centreline spacing (s), ($H/(s-b) < 1$), exhibited an uneven surface with the minimum settlement occurring above the pile cap increasing to a maximum midway between diagonally opposite pile caps. Increasing the height of fill for the same (b/s) ratio produced an even surface settlement for ($H/(s-b) > 1$).

A small downward movement of the base of the test box induced the measured vertical stress carried by the square plates to reach a maximum. Further lowering of the base caused the vertical stresses on the plates to reduce to a value slightly larger than that corresponding to hydrostatic conditions. Average pressure measurements of vertical stress supported by the yielding base ranged between 10 to 90% of (γH) where the lower vertical stress value corresponds to fills with heights satisfying the condition that ($H/(s-b) > 1$).

By placing the sand in layers of alternate colours, Hewlett et al. (1988) observed the deformation of the sand in the vicinity of the foam and the pile caps.

The shear distortion was concentrated in fans emanating from the corners of the pile caps. The coloured band of sand directly above the foam between the pile caps, however, remained level indicating a relatively uniform vertical stress distribution. Hewlett et al., attributed the observed deformation patterns to the formation of an arched region of sand spanning the adjacent and diagonally opposite pile caps.

Ali (1990) concluded that arching in the fill played an important role in the load sharing between the compressible foundation soil and pile caps. The model test results indicated that a higher capping ratio ($b:s'$) was conducive to the formation of a stable arching mechanism. A stable arching mechanism was observed to transfer a greater portion of the fill weight to the piles and to maintain a constant level of load transfer despite an increasing downward movement of the movable base. The lowering of the movable base, for a capping ratio ($b:s'$) not conducive to the formation of stable arches, results in a punching shear failure mechanism to develop in the fill characterised by a significant drop in the pile loads and large surface settlements.

In the model tests carried by Bujang (1990), the insitu foundation soil was simulated using a troll clay with properties matching those of the field material. Bujong carried out the model piled embankment study in a centrifuge to overcome scale effects. The purpose of the experimental study was to simulate field structures in Malaysia and investigate the influence of various parameters affecting the performance of a piled embankment. The pile support efficacy (E) obtained from the experimental study was compared with that obtained from the field.

Good agreement was obtained for the efficacy (E) which was found to approach 60% in both model and prototype for the piled embankment coincided. The settlement of the subsoil caused an initial increase in the efficacy (E). Furthermore, the efficacy decreased from 60 to 40% in response to a corresponding reduction in the area ratio from 0.26 to 0.17 for the same height of embankment and pile cap size.

Tang (1992), investigated the role of geotextile basal reinforcement in the load transfer process occurring within the granular fill of a piled embankment. The bulk of the tests were carried out under plane strain conditions.

The individual pile caps were modelled as beams placed perpendicular to the longitudinal axis of the embankment.

Simulations involving individually capped piles were attempted but, due to the poor quality of the test results, were discontinued. The spacing of the cap beams was varied to give four different capping ratios ranging from 1:4 to 1:9.

The model test results indicated that the efficacy of the system increased with a reduction in the capping ratio, i.e., the pile spacing was increasing relative to the cap width. However, for a given capping ratio, the efficacy reached a limiting maximum value when the fill thickness exceeded 3 to 4 times the clear spacing between the cap beams.

The use of geotextile basal reinforcement was observed to increase the efficacy (E) of the system by 15 to 30% .

2.5 Tensioned Membranes

The structural behaviour of the geotextile spanning between adjacent pile caps, can be idealised as that of tension membrane, Jones et al. (1990). A tension membrane is a structure that supports loads by tensile stresses with no compression or flexure allowed. The behaviour of tension membranes is load-adaptive in that the structure changes geometry to accommodate changes in load rather than by an increase in stress level.

The deformed shape of a tension membrane depends on the assumptions made regarding the applied loads and whether the self-weight of the structure is accounted for or not. Fluet et al. (1986) idealised the problem of a geotextile reinforcement supporting embankments spanning a void as shown in **Figure 2-15**. The circular arc concept gives;

$$v = 2R_G \sin \theta \dots\dots\dots (2-16);$$

and $y_g = R_G (1 - \cos \theta) \dots\dots\dots (2-17);$

where v = void width;

y_g = maximum vertical deflection of the reinforcement

and R_G = the radius of circular arc subtending an angle (2θ) at its centre.

The strain (ϵ_G) suffered by the geotextile under the imposed loads and for the assumed circular geometry is given by;

$$\epsilon_G = \left(\frac{R_G \pi \theta}{90} - v \right) / v \dots \dots \dots (2-18)$$

A more simple equation for the analysis of the geotextile's behaviour was presented by Jones et al. (1990) based on a parabolic geometry for the deformed shape. This assumption was based on the fact that when the self-weight of the geotextile is very small compared to the imposed loads then the catenary shape may be approximated by that of a parabola (Leonard, (1988)).

The tensile load (T_T) generated in the geotextile reinforcement due to the application of a vertical distributed load (w_G) for a parabolic geometry is given by;

$$T_T = \frac{w_G (s-b)}{2} \cdot \sqrt{\left(1 + \frac{1}{6} \epsilon_G \right)} \dots \dots \dots (2-19);$$

where s =pile centreline spacing;
 b =pile cap width.

Regardless of the method adopted a preliminary estimate of the reinforcement's centreline deflection (y_g) is required to enable determination of (T_T). John (1987) recommended that a preliminary estimate of (y_g) should be in the region of 20% of the anticipated soil settlement without the presence of the piles. The calculated value of (T_T) is then used to deduce the corresponding strain from the geotextile's load-extension data. The calculated strain (ϵ_G) is then compared to that obtained from the geosynthetic load-extension data. The analytical procedure is repeated if found significantly different until compatibility is achieved.

2.6 Modelling Using Continuum Methods

Jardaneh (1988) studied the behaviour of the BASP (Bridge Approach Support Piling) system using the finite element program FELSTA (Finite Element Stability Analysis). The stress-strain relationship of the foundation and embankment were

assumed to follow the hyperbolic relationships proposed by Kondner and Zelasko (1963) and described by Duncan and Chang (1970).

In the analysis, the three-dimensional nature of the BASP system was idealised as a two-dimensional plane strain problem. The piles and geosynthetic reinforcement were assumed to be elastic and the analysis was undertaken assuming stage construction. The study was carried out to highlight the interaction complexity that exists in a piled embankment incorporating basal reinforcement.

The finite element program FELSTA was used to carry out a parametric study to determine the tensile force in the geotextile reinforcement supporting a number of embankments of different heights built upon a range of foundation soils with varying pile spacing.

The parametric analyses indicated that loads carried by the piles could reach up to 80% of the total embankment weight depending on the piled embankment geometry. The reinforcement tensile loads predicted using the finite element method were found to be lower in comparison to those obtained analytically for similar piled embankment geometries and fill characteristics. The conclusion drawn by Jardeneh (1988) was that the simplified design procedures were conservative in as much as they were overestimating the tensile requirements of the geotextile reinforcement.

Adachi et al. (1989) used a finite element method to analyse the behaviour of piles in landslide stabilisation. The soil movement is restrained by the piles acting as dowels and the lateral loads are transferred to the piles by arching thus restraining the slip from progressing. As the mechanism of arching is in some aspects similar to that in piled embankments, the analysis of Adachi et al. is summarised below.

In the finite element analysis, the soil was assumed to be cohesionless and to behave as an elastic-perfectly-plastic material obeying a Drucker-Prager failure criterion. Because of symmetry, only half the spacing between rectangular piles was modelled (**Figure 2-16**). The soil movement due to a landslide was simulated by applying a prescribed vertical displacement to the nodes at the base of the mesh. **Figure 2-17** shows the results of a typical analysis for a 30 mm pile width (d) and a pile spacing (s) ranging between two to eight pile widths.

On comparing the results obtained using the finite element analysis to those from model test results, Adachi et al. concluded that (1) there was good agreement provided that (s) does not exceed $4(d)$, and (2) that for (s) greater than $4(d)$ the numerical analysis overestimated the pile loads. The model test results and the predictions from the numerical analyses both indicated that interaction between adjacent piles did not occur for a spacing (s) greater than $8(d)$.

Tang (1992) conducted a numerical study of piled embankments supported by cap beams using the finite element program SSTIPN (Soil Structure Interaction Program). The program allows the soil to be modelled by hyperbolic stress-strain relationships, as described by Duncan et al. (1970). The analysis was carried out under plane strain conditions and construction stages were modelled. A comparison between the predicted and the measured results indicated that the numerical method overestimated the efficacy. The discrepancy was observed to increase the larger the pile spacing for a constant cap beam width.

Pyrah et al. (1996) proposed a method of analysis for piled embankments based on the Finite Difference technique. The downward displacement of the subsoil was modelled as a "trapdoor" problem. The ratio of the embankment height to the clear span was shown to have a significant effect on the behaviour and the transfer of load onto the pile caps. The soil was modelled as an elastic-plastic material, and a cut-off method was used to limit the dilation (ψ). The method limits the dilation in Drucker's theory by implementing a cut-off at the intersection of the Drucker line and the horizontal line representing shearing at constant volume. The authors concluded that modelling dilation behaviour using a cut-off provides a more realistic prediction of the load transfer due to the arching occurring in the embankment fill.

2.7 Design Philosophy

A review of published literature pertaining to the design of piled embankments shows that the current procedures are either empirical, based on small scale model studies, or analytical. The latter category involves both idealisations and simplifying assumptions regarding the arching of the embankment fill and the behaviour of the geosynthetic reinforcement.

Broms (1979) described the procedure adopted in the Scandinavian countries to design pile embankments. It is assumed that the total embankment loading will be carried by the piles and transferred to a firm stratum. Consequently, the soft foundation soil plays no role in supporting the embankment loads and is only considered with regards to pile installation and type. The vertical embankment loads are transferred by arching onto closely spaced pile caps. The close spacing is required to prevent fill settlement between adjacent pile caps. The design curve shown in **Figure 2-18** developed by the Swedish Road Board (1974) is used to obtain the size and spacing of pile caps for a given embankment height. The design curve is based on the results of reduced scale model tests carried out using dry sand to simulate the embankment fill.

Low et al. (1994) presented an elaborate analysis for piled embankments with cap beams and incorporating geotextile reinforcement which relates the arching in the fill, the corresponding strain mobilised in the geotextile and the soft subgrade reaction. The basic assumptions in their analysis were as follows:

- i. plane strain arching occurs above the cap beams
- ii. the deformed shape of the geotextile is idealised to be a circular arc
- iii. the net pressure acting on the geotextile is uniform
- iv. the soft subgrade behaves in a linearly elastic fashion

Low et al. (1994) presented the results of their analysis in the form of dimensionless plots. The chart shown in **Figure 2-19** permits the determination of the tensile strain (ϵ_G) in the geosynthetic reinforcement. The strain is a function of the two dimensionless parameters given by;

$$\left(\frac{DK_G}{s' 2 M} \right) \text{ and } \left(\frac{\sigma_s D}{s' M} \right) \dots\dots\dots (2-20) \text{ \& } (2-21)$$

- where
- D = original thickness of soft subsoil;
 - K_G = tensile stiffness of geosynthetic reinforcement;
 - M = modulus of a linearly elastic soft ground;
 - s' = clear span between adjacent cap beams;
 - σ_s = vertical stress acting downwards on the soft subsoil.

The vertical stress acting on the soft subsoil can be estimated from the piled embankment efficacy (E) given by;

$$E = 1 - \alpha \left(\omega + \frac{m}{H/s} \right) \dots \dots \dots (2-22)$$

where (m) and (ω) are parameters determined from the charts shown in **Figure 2-23**. The coefficient (α) was introduced by Low et al. to account for possible non-uniformity in the vertical stress acting on the soft subsoil.

The British Standard code of practice for the design of strengthened/reinforced soils (BS 8006:1995) follows a similar approach to that proposed by Jones et al. (1990) whereby the tension membrane theory and soil arching are combined together.

The ratio of the vertical stress exerted on the pile caps to the average vertical stress exerted at the base of the embankment is estimated in a similar manner to that proposed by John (1987):

$$\left(\frac{p_c}{\sigma_{v0}} \right) = \left[\frac{C_c b}{H} \right]^2 \dots \dots \dots (2-23)$$

where C_c =arching coefficient; p_c =vertical stress on pile caps; b =pile cap size; s =spacing between adjacent piles; $\sigma_{v0}=(f_{fs}\gamma H+f_q w_s)$; γ =unit weight of embankment fill; H =embankment height; w_s =uniformly applied surcharge loading; f_{fs} =partial load factor for soil unit weight; and f_q =partial load for externally applied loads

The arching coefficient (C_c) depends on the pile type where a distinction in this method is made between end-bearing and friction piles to account for the relative movement of the pile cap and is calculated from the following expressions:

$$C_c = 1.95H/b - 0.18(\text{for end-bearing piles}) \dots \dots \dots (2-24)$$

$$C_c = 1.5H/b - 0.07(\text{for friction piles}) \dots \dots \dots (2-25)$$

The ratio of embankment height (H) to the clear spacing ($s'-b$) between pile caps governs the portion of embankment load supported by the geotextile reinforcement.

The magnitude of the distributed load (W_G) which the geotextile membrane has to support between the pile caps can be determined as follows;

for $H > 1.4(s'-b)$;

$$W_G = \frac{1.4sf_{fs}\gamma(s-b)}{s^2 - b^2} \left[s^2 - b^2 \left(p_c / \sigma_{v0} \right) \right] \dots\dots\dots (2-26)$$

and for $0.7(s'-b) \leq H \leq 1.4(s'-b)$;

$$W_G = \frac{s \left(\gamma H + f_q w_s \right)}{s^2 - b^2} \left[s^2 - b^2 \left(p_c / \sigma_{v0} \right) \right] \dots\dots\dots (2-27)$$

However, for $s^2/b^2 \leq p_c/\sigma_{v0}$ the distributed load (W_G) can be taken as zero and the pile caps carry the entire embankment load. Furthermore, to ensure that differential settlement of the embankment surface cannot occur, which is a problem associated with low embankments, it is recommended that the relationship between embankment height and pile cap spacing be maintained at:

$$H \leq 0.7(s-b).$$

The equation governing the tensile force and the extension in the unsupported geotextile segment when subjected to a vertical distributed load (W_G), (Leonard (1988)) is given by:

$$T_T = \frac{W_G(s-b)}{2b} \sqrt{1 + \frac{1}{6\varepsilon_G}} \dots\dots\dots (2-28)$$

where T_T = the tensile load in the reinforcement;

ε_G = reinforcement strain.

The above equation is solved for (T_T) by taking into account the maximum allowable strain in the reinforcement and by assuming an understanding of the load/strain characteristics of the reinforcement at different load levels.

2.8 Case Histories

The preceding sections have been concerned mainly with theoretical aspects or laboratory investigations into the behaviour of piled embankments under laboratory controlled conditions.

In the case of a field structure, the behaviour is also controlled to a considerable extent by the strength and stiffness as well as the time-dependant properties of the subsoil. These other considerations are not amenable to simplified mathematical analyses or to reduced scale modelling techniques. It is therefore useful to present a select number of piled embankment case histories from different parts of the world.

The method of supporting soil structures on piles is an established construction technique. Broms (1979) and Broms and Hansbo (1981), reported that timber and concrete piles have been used to support small road embankments on soft clays in Finland and Sweden for more than 40 years.

The Geotechnical Laboratory of the Technical Research Centre of Finland commissioned a research programme to investigate the behaviour of piled embankments, Rathmayer (1975). The investigation consisted of compiling records from 46 existing piled embankment sites representing a total of 7 kilometres in length. In addition the behaviour of three instrumented trial embankments were monitored. For the existing structures, no signs of distress were observed in piled embankments with heights greater than 2.5 meters and a capping ratio of 30 to 40 %. However, in a number of cases, embankments with heights less than 2.5 meters, supported on piles with a similar capping ratio, showed signs of damage. The road surface was uneven and cracks were observed in both longitudinal and transverse directions.

The structural failure of low height embankments was attributed to the low capping ratios and to the lack of batter piles to support the side slopes.

The conclusions drawn from the investigation led to the recommendations shown in **Table 2-1** regarding the required capping areas for different embankment heights and fill materials.

Holtz and Massarch (1976) described the use of a polyester fabric as a basal reinforcement in a piled approach embankment leading to the Gota bridge in south-western Sweden. The piling scheme consisted of end-bearing timber piles placed at 1.5 meters centres. Pile caps were used to transfer the embankment weight to the piles the caps increasing surface area of the piles to 44%. Three layers of the fabric were used with a 150 mm thick layer of compacted sand as shown in **Figure 2-21**. Three

years after construction settlements were reported to be very small. There was no change in the pore water pressure measurements during the construction of the embankment suggesting that almost the entire weight of the fill was transferred to the pile caps.

Holmberg (1978) described the construction and performance of a pile supported bridge approaches on the Bang Pa-In Sawan highway in Thailand. About 20 km of this road embankment traverses an area characterised by subsurface deposits of soft clay ranging between 2.5 and 5.0m in thickness. At bridge locations, the approach embankments with heights ranging between 3-6m were supported on timber or concrete piles in order to prevent large differential settlements. A typical layout of the pile arrangement is shown in **Figure 2-22**. Each pile was provided with a concrete cap 0.8m square. The length and spacing of the piles were varied such that the piles closest to the bridge were end-bearing with a centreline spacing of 1.5m, with the pile caps covering 28% of the ground area.

Reid and Buchanan (1984) also mention the advantages gained by the use of piles beneath bridge approach embankments on the link motor way between the M876 and M9 near Glasgow in Scotland. The piles near the bridge abutments were long and designed to carry the full weight of the embankment while further away the piles were shorter and settled more to effect a gradual transition from the bridge to the embankment founded on soft alluvial deposits (**Figure 2-23**). All the piles were installed vertically at a grid spacing of 3.0m and 4.5m below the main embankment and the transition sections, respectively. Each pile was provided with a circular pile cap varying from 1.1 to 1.5 meters in diameter to maintain a capping ratio of 10.6%. A membrane consisting of two mutually perpendicular layers of Terram reinforced with Paraweb strapping was placed above the pile caps. The membrane was provided to prevent excessive settlements from occurring in the zone between adjacent caps by transferring the embankment weight to the pile caps.

Reid and Buchanan (1984) reported that pile load cell readings at the top of the piles indicated that 82% of the weight of a ten meter high embankment was carried by the piles. They also noted that there had been no differential settlement in the road surface adjacent to the bridge where the system had been used.

Another major highway project incorporating piled embankment structures was reported by Chin (1985). The site was at Jalan Deiga in the north of Malaysia where the foundation soils consisted of a soft clay deposit 9.0 to 11.0m thick underlain by clayey sand and a bedrock of shale.

A similar piling scheme was adopted as that reported by Reid and Buchanan (1984). Two embankments were instrumented to allow monitoring of the pile support efficacy as the fills were raised. The reported values of efficacy (E) ranged from 60% to 70%; the larger value pertaining to the higher embankment. The results also showed the tendency for (E) to increase with time after the end of construction, Reid and Buchanan (1984) made similar observations.

Azzam et al. (1990) described settlement problems occurring at bridge approach embankments and at transition zones between rigid and flexible embankments along the Alor Setar-Gurun and Jitra-Alor Setar highways in the north of Malaysia. Since opening the highways to traffic, repair works had been carried out regularly to maintain an acceptable riding surface on the carriageway.

The following observations were reported following inspections of the problematic sites:

- i. Large settlements of the embankment surface and sinkholes were evident around the individual pile caps. The excessive settlements were attributed to the penetration of the embankment fill in between the pile caps.
- ii. Lateral deflection of the pile heads located outside the carriageway zone were probably due to the lateral thrust developed by the embankment fill at the side slopes.
- iii. Large differential settlement of the embankment fill was evident at the transition zone between piled and un-piled sections of the highway.

The second Severn River crossing in the United Kingdom required embankment construction over highly compressible soils to form a toll plaza. Bell et al. (1994) described the use of a geogrid reinforced granular mattress that was used to transfer

through arching the embankment loads to a grid of Vibro concrete columns. The Vibro concrete columns were formed with enlarged mushroom heads during contraction. A cross-section through the embankment showing details of the geogrid reinforced mattress is depicted in **Figure 2-24**.

Card et al.(1995) reported the use of the geogrid reinforced granular mattress to support the road embankment on either side of the conventionally piled Docklands Light Railway channel in the London dockland area. The piles were installed on a 3.0 meter square grid and were provided with 1m square caps. The granular mattress was 1.5m thick and reinforced with geogrids at 0.5m vertical spacing.

2.9 Summary

A brief review of the various theoretical solutions and numerical models available to quantify the vertical stress re-distribution occurring due to arching in granular soils has been presented. The results of experimental trapdoor tests were investigated to appreciate the physical conditions affecting the arching mechanism. The angle of internal friction of the fill and the ratio of the height of fill to the width of the trapdoor have been identified as the significant controlling parameters.

Laboratory model tests have been carried out to simulate piled embankment behaviour in the centrifuge and under normal gravity conditions. The majority of the model tests were designed to simulate piled embankments not incorporating basal reinforcement. Tang (1992) carried out an experimental study of piled embankments incorporating geosynthetic reinforcement, the tests, however, involving individual pile caps were abandoned due to difficulties in simulating the boundary conditions. The study was continued for a plane strain geometry in which the pile caps were replaced with beams. The experimental procedure precluded the development of any surface settlement since the placement of the fill in stages resulted in any surface deformations being built out.

Piled embankment design methods are either empirical, based on the results of experimental tests, or analytical. However, analytical methods involve the following simplifying assumptions;

- i. the foundation soil between the pile caps does not support any vertical embankment loading;
- ii. a two step approach in which the arching action is decoupled from the structural behaviour of the basal reinforcement.

The first step concerns the quantifying of the load transfer process due to the arching in the fill. The most commonly proposed soil arching models are based on projecting subsurface conduits John (1987) and Jones et al. (1990) or suspended hemispherical vaults, Hewlett and Randolph (1988).

BS 8006:1995 utilises the arching model proposed by John (1987) which results in ratios of vertical stress applied to pile caps to the average overburden stress at the base of the embankment. The structural behaviour of basal reinforcement is idealised as a tensioned membrane. The deflected reinforcement is assumed to take the shape of either a parabolic or circular arc. Adopting a geometrical shape is necessary to estimate the tensile loads and strains sustained by the reinforcement.

The methods available to assess the serviceability limit states of basal reinforced embankments on soft foundations are much less prevalent than those used to assess the ultimate limit states. The reason for this is that sophisticated analytical procedures are required, typically, continuum methods. Consequently, serviceability limits have been based on empirical values which have been observed to work in practice. The BS 8006:1995 proposed a maximum of 5% for short term reinforcement strain and a minimum value of 0.7 for the ratio of embankment height to the clear span between adjacent pile caps to ensure that differential surface deformations cannot occur.

Several empirical recommendations and analytical models have been proposed to evaluate the behaviour of basally reinforced piled embankments. However, no systematic three-dimensional experimental study of piled embankments incorporating geosynthetic basal reinforcement that addresses the various controlling parameters has been made to date.

**Table 2-1. Guidelines for the design of necessary coverage by pile caps,
(Rathmayer (1974)).**

Height of embankment (H), m	Coverage by pile caps , %	
	Crushed-rock fill	Gravel fill
1.5 to 2.0	50 to 70	> 70
2.0 to 2.5	40 to 50	55 to 70
2.5 to 3.0	30 to 40	45 to 55
3.0 to 3.5	30 to 40	40 to 45
3.5 to 4.0	> 30	> 40

Chapter Three

Design of Apparatus

3.0 Introduction

In order to tackle the main issue of investigating the behaviour of piled embankments incorporating geotextile reinforcement, a deliberately simple approach was adopted.

The complexity of traffic loading, non-homogeneity in ground conditions combined with an inherently three-dimensional geometry makes the full scale real-life situation an extremely difficult problem to analyse.

It was decided to design and construct a three-dimensional reduced scale model of a grid of centrally located piles. A worst case scenario was adopted which entailed the absence of any support from the subgrade, i.e. the embankment load is shared between the tension membrane and the pile caps. The worst scenario methodology was considered suitable to enable an understanding of the basic mechanisms involved.

3.1 Modelling at Reduced Scale

When conducting model tests at reduced scale it is necessary to reduce all the geometrical dimensions of each component by a chosen scale factor. The adoption of a reduced geometrical scale at self weight conditions necessitates the scaling down of material properties in the system, such as strengths and stiffnesses, if similarity is to be maintained between model and prototype.

Establishing the scaling laws and hence the extent to which each property should be reduced is obtained by carrying out a dimensional analysis. Dimensional analysis, described in detail by Langhaar (1951), provides the basis for establishing similitude requirements, and it is applied herein to the load-deflection behaviour of basal geosynthetic reinforcement in piled embankments.

3.1.1 Identification of the Significant Physical Parameters

As previously mentioned the two important mechanisms involved in the piled embankment behaviour are reinforcement structural response and the arching occurring in the embankment fill.

The identification of the significant physical parameters are presented separately for each mechanism in the following paragraphs.

In the classical trapdoor problem the arching action in a granular soil can be mobilised in either of two ways; (a) the passive mode or (b) the active mode. In the passive mode the trapdoor movement is upwards and into the soil mass, a downward movement on the other hand is associated with the active mode. The arching action occurring in piled embankments can be identified with the active mode described previously.

The importance of the mode of action inducing the arching in the fill was investigated by Tanaka et al. (1993). In their study, Tanaka et al., carried out trapdoor experiments involving both the active and passive modes. The experiments involved the use of trapdoors of different widths for which load displacement measurements were obtained.

In addition, the development of shear bands was monitored through the use of thin horizontal layers of coloured sand interbedded within the sand mass. The influence of size effects and progressive failure in the trap door experiments was evaluated on the basis of results obtained from both an experimental and numerical investigation. The experimental and numerical results led Tanaka et al. to conclude that the presence of progressive failure in the sand mass due to arching in the active mode was not sufficient to introduce any appreciable scale effects. Consequently the arching action involved in the piled embankment problem can be reproduced adequately at reduced geometrical scale. The significant physical parameters were identified as being the ratio of the height of fill to the width of the trapdoor and the angle of internal friction of the sand.

In a piled embankment system the structural behaviour of the basal reinforcement is that of a tension membrane, Jones et al. (1990). Consequently, the maximum mid span vertical deflection of the membrane (y_g) is a function of the applied stress (w_G), the piled embankment geometry, and the reinforcement "stiffness" (J).

The stiffness of the geotextile is a term which is often used loosely, so it is important to define its meaning here fully. The quantity (J) is the tensile stiffness per unit width,

whose units are [kN/m] and is defined as the secant modulus at a specified strain as obtained from a plot of load per unit width against strain. The vertical load (w_G) acting on the reinforcement is a function of the degree of arching occurring in the soil mass. The mechanism of arching in turn depends primarily on the shear strength of the soil mass, the piled embankment geometry and the ratio of the reinforcement deformation (y_g) to width of the clear span (s') between adjacent pile caps. **Figure 3-1** depicts an idealised representation of the significant physical parameters involved in the reduced scale model used in the experimental study.

3.1.2 Dimensional Analysis

The purpose of the dimensional analysis is to determine the dimensionless parameters usually called " π " groups. This is accomplished by constructing a dimensional matrix. The matrix comprises of columns which represent the physical parameters and rows which correspond to the basic units necessary for establishing the dimensions of the physical parameters. Thus the elements of the matrix correspond to the dimensional exponents of each physical parameter. The basic units necessary to establish the dimensions of the physical parameters are; (i) length; and (ii) force.

3.1.2.1 Determination of the " π " Parameters

Having established the controlling physical parameters, the vertical deflection (y_g) of the geotextile reinforcement in the piled embankment system can be determined as a function of:

$$y_g = f (s' , H , J , \gamma , \phi , G) \dots\dots\dots (3-1)$$

where H = height of embankment [m]
 s' = clear span between adjacent pile caps [m]
 G =elastic shear modulus of fill material [kN/m²]
 γ =unit weight of fill material [kN/m³]
 ϕ = angle of internal friction for fill material
 J =stiffness of reinforcement per unit width [kN/m']

By inspection the following set of (π) groups can be identified:

$$(a) \pi_1 = \phi; (b) \pi_2 = \frac{y_g}{s'}; (c) \pi_3 = \frac{\gamma H}{G}; (d) \pi_4 = \frac{\gamma H s'}{J}.$$

3.1.3 Similitude and Scaling Laws

In order to obtain complete similarity the physical model test must be designed in such a way that the independent dimensionless products attain the same numerical values in both model and prototype, i.e., the model and the prototype are then said to be completely similar.

Consequently, for a geometrical scale factor of (λ_L), the following scaling laws were established:

$$\lambda_G = \lambda_\gamma * \lambda_L \dots\dots\dots (3-2)$$

$$\lambda_J = \lambda_\gamma * (\lambda_L)^2 \dots\dots\dots (3-3)$$

where	$\lambda_G =$ shear modulus scale factor	$=$	$\frac{G_{\text{prototype}}}{G_{\text{model}}}$
	$\lambda_\gamma =$ unit weight scale factor	$=$	$\frac{\gamma_{\text{prototype}}}{\gamma_{\text{model}}}$
	$\lambda_J =$ stiffness scale factor	$=$	$\frac{J_{\text{prototype}}}{J_{\text{model}}}$

Since the physical modelling was carried out at self-weight conditions, i.e., the unit weight scale factor (λ_γ)=1, the stiffness (J) of the geotextile must be reduced by the square of (λ_L). Similarly, the elastic shear modulus (G) of the fill should be reduced by (λ_L) if the scaling laws are to be satisfied.

In a model study of geogrids in unpaved roads, Love (1985), reported that the shear modulus (G) of sand was assumed to be adequately scaled down for the following reasons:

- i. The shear modulus of sand is proportional to (p')ⁿ where (n) has a value of 0.5 and (p') is the mean normal stress. Hence, the model p' is reduced by (λ_L), causing the shear modulus of the soil to reduce by $0.45(\lambda_L)$.
- ii. The additional reduction factor is achieved by a small increase in the voids ratio.

3.2 Selection of Model Components

3.2.1 Model Size

For a successful laboratory investigation, physical models of geotechnical structures must be constructed of a size that involves volumes of fill which can be placed and removed in a reasonable time span.

The model must also be of a size which permits adequate instrumentation without significant interference of instrumentation with expected behaviour of the model. Models which are too small are subject to amplified experimental errors, scale effects and are difficult to reliably relate to full-scale structures.

On the other hand, models which are too large may involve volumes of materials exceeding the handling capacity of available laboratory equipment and can be difficult to construct. The physical dimensions of the model piled embankment were chosen to maximise use of the fill placement method available.

A geometrical scale factor of (5) was used to model a central portion of a piled embankment system. A square grid was adopted for the piles with a centre-line spacing of 0.6 meters. This value corresponds to 3.0 meters in the prototype which is a typical grid spacing adopted in practice. To fulfil conditions of symmetry in the reinforcement and to avoid locating the pile caps close to the side walls, a test box 1.2mx1.2m in plan was considered appropriate.

The minimum height of the test box was dictated by the pile cap size. Three different cap sizes were investigated, the smallest produced a maximum clear spacing of 0.4m between adjacent pile caps. This maximum lateral dimension influences the depth at which the plane of equal settlement is expected to occur.

The plane of equal settlement is the surface at which no relative movement exists i.e. arching ceases to affect the state of stress in the soil. This plane of equal settlement has been observed in the laboratory to be approximately 2-2.5 times the width of the trap-door, Terzaghi(1943). The clear spacing between two adjacent pile caps was considered equivalent to the trapdoor width in Terzaghi's experiment. This assumption resulted in a minimum height ranging between 0.8 to 1.0 meters.

In addition to considerations of practicability, the maximum height investigated was limited by the friction developed between the side walls and the soil. Tang (1992), carried out tests to determine the effect of wall friction as a part of a laboratory investigation into the behaviour of piled embankments under plane strain conditions. The test box had two sides constructed of perspex while the other two were lined with Teflon sheets and the fill consisted of a sand possessing an angle of internal friction of approximately 37° and an insitu unit weight of 14.2 kN/m^3 . A reported wall friction of 6.25 N/m^2 per 10 mm of fill height was obtained from the difference between the actual weight and the load cell readings.

Using these results as a guideline, it was decided that a maximum fill height of 1.0 meters would limit the side wall friction to an acceptable level.

The presence of the silo effect or "Janssen" arching was another factor affecting the choice of height and width of the test box. Jarret et al. (1995) carried out tests to investigate the pressures exerted by Leighton Buzzard sand stored in a rectangular flexible-wall silo possessing a height to width ratio of $1.5:1$.

The vertical pressure measurements at the centre of the silo were found to approximate to the geostatic condition. In comparison with the dimensions of the proposed test box, i.e., the fill height to test box width ratio of $1:1.2$, the silo effect should be small enough to be considered negligible.

3.3.2 The Soil

The soil used in the study was standard Leighton Buzzard sand falling between sieve numbers 14 and 25. The main reasons for using the Leighton Buzzard sand grade 14/25 as a fill material in the experimental study were;

- i. The behaviour of uniform sands is easier to interpret and conceive than non-uniformly graded soils or soils with large values of uniformity coefficients since the different shapes and particle sizes present a more complex inter-particle mechanism.
- ii. Although fills with a wider range of particle sizes and more angular grains are used in the prototype, the stress-strain properties of the Leighton Buzzard sand

at low stresses existing in the laboratory tests are comparable to the properties of the more angular sands and gravel at full scale stresses, Milligan (1982).

- iii. The grading was easier to use in test preparation than materials with very fine particle sizes, especially when testing in a dry condition. Mechanical compaction is not required as the material can be poured through a sand rainer to give the required density by varying the drop height.
- iv. Leighton Buzzard sand is a well documented material (Jewell (1980), Stroud (1971), Palmeira et al. (1989)). This reduced the number of unknown quantities and the test results were easier to interpret.

3.2.3 The Reinforcement

The geotextile reinforcement used in the study was a scaled down version of "Paralink". This material is composed of high tenacity polyester fibres encased in a durable polyethylene sheath. The polyester fibres provide the strength whereas the polyethylene cover gives high resistance to chemical attack and good reinforcement/soil frictional characteristics. The resulting strips are joined together to form a geotextile sheet with uni-directional tensile properties. For piled embankments it is necessary to use a double layer of "Paralink" laid at right angles to each other to satisfy the bi-directional load shedding action. The use of "Paralink" for piled embankments is shown in **Figure 3-2**.

To satisfy the scaling laws, the tensile stiffness of the reinforcement has to be reduced by the geometrical factor squared, i.e. by 25. This meant that the stiffness (J) for a reduced scale model fabricated from the same material as the prototype, should fall within the range of 80 to 500 kN/m.

Linear Composites Ltd., the manufacturers of "Paralink" provided two miniaturised versions of the Paralink in strip form. The two model strips were designated P165 and P500 and possessed nominal breaking loads of 1.65 and 5.0 kN respectively and a corresponding failure strain of approximately 10%. The strips were 50mm in width and required a clamping arrangement with a minimum lateral dimension of 100 mm.

Consequently, the maximum number of adjacent strips per linear meter was 10, i.e. the stiffness moduli were approximately 165 and 500 kN/m' for the P165 and P500 respectively. Another two materials made from polyester were used to investigate the influence of the tensile stiffness on the piled embankment behaviour. The two materials are commercially known as Textomur and Stratagrid and are made of polyester high tenacity filament yarns. Textomur is a nonwoven needlepunched geotextile while Stratagrid is a woven geogrid. The breaking loads and corresponding failure strains for the Textomur and the Stratagrid, as supplied by the manufacturers, are 44 kN/m' at 44% strain and 80 kN/m' at 14% strain respectively. The reported material load-strain properties should give stiffness moduli of 45 kN/m' and 285 kNm' for the Textomur and Stratagrid respectively for strips spaced 100 mm centre to centre.

3.3 The Apparatus

The apparatus was designed to meet the following general requirements:

- i. The test box was sufficiently rigid and stiff such that the sand could be contained without causing excessive lateral bulging of the walls. The test box was constructed of detachable segments to allow the modelling of embankments of different heights.
- ii. The need to assemble and dismantle the test box meant that the segments should not be excessively heavy to allow ease of manhandling.
- iii. A mobile A-frame fitted with a beam trolley and chain block with enough head room to clear the combined height of the sand raining tank and the fully assembled test box.
- iv. The test box was provided with a movable base to simulate the yielding subgrade.
- v. The clamped ends of the geotextile strips were restrained from movement in the horizontal direction only to satisfy boundary conditions.

3.3.1 The Test Box

The test box was assembled from three separate segments which could be bolted together to enable the simulation of embankments with different heights. The use of several segments was necessary to maintain a relatively constant drop height when placing the sand fill. The walls of each segment consisted of 20 mm thick plywood panels to give internal dimensions of 1200x1200x400mm. The walls of each segment were held in place and stiffened at the top and bottom with ring beams consisting of 6 mm thick 76x38 steel channels. The ring beams in turn were supported at the corners with 6 mm thick 76x76 mm steel angles. The total height of the segments was 1200 mm high when fully assembled. The inner face of each panel was lined with PTFE sheets to minimise wall friction and hence reduce the silo effect which would have adverse effects on the test results.

The bottom ring beam of the first segment was supported at the corners (on plan) by means of columns 495 mm in height and consisting of steel angles, 100x100 mm and 6 mm in thickness. The columns were braced laterally at the floor level by means of steel channels which in turn were anchored to the laboratory floor by means of Rawl bolts. Schematic diagrams of the of the test box and supporting columns are shown in **Figures 3-3a and 3-3b**.

3.3.2 The Clamps

To construct the geotextile mesh, each individual strip of reinforcement had to be clamped at both ends. The clamping system was a miniaturised version of the bollards used to carry out tensile strength tests on Paralink and other similar products. To satisfy the boundary conditions, the clamps were provided with guide rollers fitted with ball raced bearings that ran on tracks mounted perpendicular to the laboratory floor. The tracks were formed from angles welded back to back and buttressed against the ring beam of the first segment and the steel channel sections used to brace the test box. To impart a slight pretension to the strips, the clamps were provided with an adjusting nut. The weight of the clamps was accounted for by the provision of a counterweight effected through a pulley mechanism. **Figures 3-4a and 3-4b** show the clamps and the general arrangement of the pulley system.

3.3.3 The Movable Base

Foam rubber has been used to represent a soft subgrade in reduced scale models (Milligan (1982), Tang (1992) and Hewlett et al. (1988)). An alternative method of simulating the subgrade adopted, is the use of a movable base controlled by mechanical or hydraulic systems (Bergdahl et al. (1979), Ting et al.(1983).

The use of a movable base to model the subgrade was adopted in the current study. This choice was based on the following:

- The primary function of a piled embankment scheme as a ground improvement technique is to limit the post-construction settlement that would otherwise result in loss of serviceability of the fill structure. Hence, the observation of surface settlement was considered an integral part of the investigation.

The use of rubber foam or some other similar material to represent the subgrade would preclude any surface measurements since they would be "built out" as the construction of the deposit progresses.

- The modelling philosophy of a "worst-case" scenario dictates that the subgrade contributes no support in the load sharing mechanism. This condition can only be achieved if a movable base is adopted.

The movable base comprised of a platform consisting of a plywood deck supported on a square frame formed of hollow steel sections welded together to form a grillage. Each of the four plywood sheets making up the platform deck had a square shape cut out to accommodate the pile caps as shown in **Figure 3-5**. The platform was in turn supported on four single acting spring return hydraulically operated cylinders. The four cylinders were connected to a 6 way manifold block to allow simultaneous contraction and extension of the rams using one hand operated pump.

The governing criterion in the choice of cylinder was a minimum stroke length and a maximum extended height of 150 mm and 375 mm. The cylinders used were type HS-106, manufactured by Hi-Force Hydraulics Limited, which satisfied the stroke length and extended height requirements.

3.3.4 The Pile Caps

The pile caps were supported on hollow steel sections 6 mm in thickness and 100 mm in width and breadth which represented the piles. The length of each section was based on the height of the movable base with the hydraulic cylinders fully extended. The hollow sections were welded to anchor plates which in turn were secured to the laboratory floor via four Rawl bolts.

To assess the load transfer mechanism, however, it was considered necessary to obtain measurements of the following:

- i. The net load per pile cap tributary area.
- ii. The average vertical stress acting on the pile cap after lowering of the movable base.

Each pair of diagonally opposite pile caps was designed to accommodate the appropriate instrumentation required to permit measurement of the required parameters.

Two different instrumentation schemes were employed to obtain the required measurements. The need to obtain such measurements resulted in the design and construction of two different pile caps to accommodate the appropriate instruments.

Scheme No.1

In the first design, the pile caps consisted of a square 8 mm thick steel plate. Each steel plate was provided with a plywood cushion 16 mm in thickness secured by means of two countersunk screws. The plywood cushions possessed bevelled edges to avoid damage to the geotextile reinforcement resulting from stress concentrations developed at the plate edges.

For the first pair of diagonally opposite pile caps, the plywood cushions were provided with circular centrally located recesses 58mm in diameter to accommodate the "Kulite" pressure cells locked flush to the pile cap surface to allow accurate vertical pressure measurements to be made in the fill, Jarret et al., (1992). The second pair of pile caps were instrumented to record the net load acting on the piles. The pile

caps were secured to the N.C.B cells via threaded bolts which screwed into base plates welded inside the pile section.

Scheme No.2

The pile cap design was subsequently changed to accommodate a different array of instruments for reasons that will be presented in a later section of the thesis.

The Kulite and N.C.B units were replaced with RDP tension/compression load cells. The plywood cushion was maintained and each pile cap was formed of an upper and lower steel plate separated by an annular steel bearing plate.

One pair of pile caps was designated for the measurement of the vertical loads influenced by the arching mechanism. This was made possible by transferring the vertical stresses acting on the upper plate of each pile cap to the RDP load cell via a threaded circular bar with a collar to distribute bearing stresses. The geotextile strips were supported on the lower plate which was in turn bolted to two steel angles welded to the steel pile sections.

The second pair of pile caps was used to record the total load per pile tributary area. To fulfil this purpose, the upper and lower plates were connected to the load cell via a threaded bolt. An annular bearing plate of suitable thickness was inserted between the bottom plate and the load cell. The bearing plate maintained a sufficient clearance between the bottom plate and the upper end of the pile section.

Another annular plate was used to maintain a clearance of 5 mm between the upper and lower plates to accommodate the geotextile strips. The load cells, for both pile cap arrangements were fastened to a steel base plate welded to the inside of the hollow steel sections by eight socket head screws.

Figure 3-6a and **3-6b** shows the details of the different pile cap designs employed in this experimental investigation.

3.3.5 The Sand Raining Box

Different techniques are available to prepare sand deposits in the laboratory (such as pluviation, vibration and tamping). Mori et al., (1977) and Oda et al., (1978) both

commented on the suitability of the air pluviation technique in obtaining sand deposits of uniform and repeatable densities.

Bieganousky et al. (1976) investigated different techniques of air pluviation and concluded that perforated plate sand rainers produced best results with regards to reproducibility and homogeneity of the deposit.

Rad et al.(1987) carried out a series of tests to investigate the factors affecting sand specimen preparation using the perforated plate method. The size and pattern of the holes in the perforated plate in addition to the height of fall were identified as the two variables most affecting the relative density of the deposit.

Consequently, the air pluviation technique using a perforated steel plate was adopted in this study to construct the required sand deposits. The drop height and the specifications of the perforated plate adopted in this study were similar to those used by Hassan (1991) to construct medium dense deposits from Leighton Buzzard sand grade (14/25).

The internal dimensions of the raining tank were 1200mmx1200mm on plan and 250 mm in depth. The frame of the box and the supporting legs were fabricated from 40x40 steel angles 3mm in thickness. The length of the supporting legs was 700 mm to allow for the required drop height. The base of the box consisted of a perforated plate with holes 3.15 mm in diameter and 6.35 mm centre to centre arranged in a triangular pattern. Two sheets of plywood were used as trap doors, to prevent the flow of sand from the raining tank during the filling process. Once the raining tank was in position, the trap doors were allowed to swing open by releasing two trip levers permitting the sand to flow freely and evenly into the test box.

3.4 Instrumentation

The choice of instrumentation was based on the need to furnish the necessary data required to establish a) a philosophical understanding of the soil-structure interaction mechanism and b) to obtain through, dimensional analysis, a quantitative relationship between the independent and dependant parameters.

Accordingly, the following parameters were measured and recorded:

- i. the vertical stress acting on the pile caps
- ii. the load bearing on the pile caps due to the arching mechanism

- iii. the net load supported by the geotextile mesh and pile caps.
- iv. surface settlement
- v. geotextile deflection
- vi. pile caps deflection under the weight of the fill

The positioning of the different instruments used to measure the above mentioned parameters is shown in **Figure 3-7**.

3.5.1 Load and Pressure Cells

A. "Kulite" Cells

The vertical stress changes in the vicinity of the pile caps were monitored by using "Kulite" pressure cells. These cells have a working range of 0 to 200 kN/m² and use a semiconductor diaphragm that incorporates a monolithic diffused Wheatstone Bridge as the basic sensing element. The semi-conductor diaphragm is located behind a stainless steel isolated diaphragm, and a silicon fluid is used to transfer the load from the isolation diaphragm to the pressure diaphragm. Each cell was calibrated under hydrostatic stress and in soil conditions that closely resemble those it was used in, as recommended by Weiler et al. (1978).

B. "NCB" Load Cells

NCB/MRE load cells were employed in "scheme no.1" to measure the net loads per pile cap tributary area. The load cells are of the electrical resistance strain gauge type, capable of measuring compressive loads up to 15 tons to an accuracy of 0.25% of the applied load. The readings of the load cell were transmitted through a 4-conductor, shielded cable to a Vishay P350A Read-out Box. The cells were calibrated using an Avery compression testing machine.

C. "RDP" Load Cells

The loads acting on the pile caps whether hydrostatic or due to arching were measured using RDP model 41 tension/compression load cells. The load cells used a bonded foil, strain gage for the sensing element to which two stabilising diaphragms were welded to reduce off-centre and side-loading effects. Each load cell was provided with a threaded hole running completely through the centre of the cell. The cells were calibrated using an Avery compression testing machine.

3.4.2 Displacement Transducers

A. Direct Current Differential Transducer (DCDT)

A DCDT transducer was used to measure the displacement of the upper plate, used in the modified pile cap design, under the applied weight of the fill. It was considered essential to ascertain that the edge of the upper plate did not excessively deflect to come into contact with the geotextile strips.

The procedure was considered only necessary for the plate with the largest width i.e. 300 mm. The DCDT was secured to the steel pile via a clamp with a magnetic base and positioned to allow the DCDT to come in contact with the lower surface of the upper steel plate and hence record the plate deflection.

B. Draw-Wire Transducers (DWT)

Each of the five draw wire transducers used in the experimental programme were mounted vertically on an "L" shaped plate. The base of each unit was fixed to the laboratory floor via "Velcro" strips at designated locations directly below the measurement points. The DWT unit was attached to the geotextile mesh by bolting the threaded rod at the free end of the cable to a flexible anchor plate cut from a 1 mm PTFE sheet. The DWT units were connected to a transformer that supplied a 12 volt regulated direct current. Prior to use, the units were adjusted in both the fully retracted and extended positions to give 0 and 10 volts respectively through a trimmer screw. The DWT units were calibrated using a manually operated extensometer fitted with a Vernier gage.

3.4.3 Surface Settlement

A simple method was adopted for the measurement of surface settlement, which consisted of using a measuring rule fitted with an end plate, the end plate allowed the rule to rest on the surface of the sand with minimal disturbance. A graduated steel cross-bar was used as a reference level against which the settlement was measured.

3.5 Data Acquisition

The recording and storage of the instrument readings was carried out using an ELONEX 486 personal computer that supported the data acquisition software, Spectra-DAS version 4, together with a Spectra MSI data logger.

Full description and technical specifications can be found in the manufacturer's user manual and technical brochure. In brief, the Spectra-MSI system is a microprocessor controlled, precision measurement and control module which communicates with the host computer via a serial data link. Input devices such as the load cells and draw-wire extensometers are connected to the system through individual channels provided by a remote connection module connected to the system.

Using the Spectra-Das system allowed on-screen scanning of the different data channels being logged versus time, in addition to recording the data on hard disk. The files were exported in a format amenable to spreadsheet software and saved on 'Floppy' disks.

3.6 Summary

The significant physical parameters controlling the behaviour of piled embankments were identified. A dimensional analysis of the different parameters was carried out to establish the scaling laws. Similitude requirements necessitated the scaling down of the reinforcement tensile stiffness by the square of the geometrical scale.

The overall dimensions of the test box were determined and a range for the pile cap sizes selected taking into account considerations of practicability and boundary effects due to side wall friction. The reinforcement was connected to roller camps designed to simulate the idealised boundary condition of translation in a vertical plane only.

The simulation of the foundation soil was carried out using a movable base system to achieve the worst scenario condition where the subgrade no longer participates in the load sharing mechanism.

The method of sand placement was the air pluviation technique using a raining box with a plan area similar to that of the test box. The raining box drop height and perforated plate specifications were similar to those used by Hassan (1991).

Two instrumentation schemes were adopted regarding the measurement of the pile cap loads. The pile caps were designed to allow the measurement of two loads; (a) the load transferred due to the arching in the fill and (b) the total load per pile cap tributary area.

The deflection of the basal reinforcement was monitored using draw-wire transducers fixed to the laboratory floor and installed in an extended state. The retraction of the wire corresponded to the deflection of the reinforcement at that point.

CHAPTER 4

EXPERIMENTAL PROCEDURE AND TEST RESULTS

4.0 Introduction

In the first part of the chapter the steps followed in constructing the sand deposit and in installing the geotextile reinforcement are described in detail. The properties of the materials used in the physical model tests as well as the results of both simulations are presented in graphical form in the latter part of the thesis. The experimental results are described under three topics; load transfer, geotextile deflection, and surface settlement.

4.1 Experimental Procedure

The test procedure is best described as consisting of two major activities, 1) the installation of the geotextile and preparation of the test box with regards to lubrication of side walls and sand proofing; 2) the construction of the sand deposit.

4.1.1 Installation of Geosynthetic Strips

The geotextile mesh consisted of twenty four individual strips, each spanning the width of the test box. The ends of each strip were connected to a clamping device as shown in **Figure 4-1**. A slight pretension was applied to the reinforcement by using a calibrated torque wrench. By changing the tension of the torque spring the desired pretension could be imparted to the geotextile strip.

The ratchet mechanism incorporated within the wrench ensured that the pretension applied each time was the same. The set-up adopted to calibrate the torque wrench is shown in **Figure 4-2**.

4.1.2 Sandproofing

The use of discrete elements to construct the geotextile mesh and the use of clamps that can translate vertically resulted in the formidable problem of sand loss through a multitude of openings and gaps. The use of a membrane overlying the geotextile mesh

was deemed essential if sand was to be prevented from pouring through the openings in the mesh.

The membrane, however, should not influence the structural behaviour of the reinforcing mesh. With that requirement in mind, a material commercially known as "Cling-film" was found to be ideally suited for this purpose due to its very low tensile stiffness. The membrane was not spread in one single coherent section, but in individual sheets approximately 0.3m by 0.3 m in plan dimensions. The sheets were overlapped to provide continuity and to prevent the ends from parting allowing the sand to pour out.

Corner and edge sections were made from strips of polythene which were designed to fit snugly at the intersection of the geotextile mesh and the side-walls of the test box and to overlap with Cling-film membrane. These sections followed the downward movement of the sand and the supporting geotextile strips thus preventing the loss of sand from the resulting openings at the bottom of the test box segment.

4.1.3 Lubrication of Sidewalls

The use of friction reducing inserts was considered necessary to reduce the frictional forces generated on the side walls of the test box and to reduce the possibility of the silo effect influencing the test results. Demiris (1987) used a variety of friction reducers to investigate the effect of boundary friction in polyaxial tests.

Similarly, Tatsuoka et al. (1985) carried out a series of direct shear tests between sand and various kinds of smooth and lubricated surfaces for a wide range of normal stresses to evaluate the shear resistance.

The results of both the above mentioned experimental studies indicated that the use of Teflon (PTFE) sheets along with a silicon based grease as a lubricant were quite effective in reducing the frictional forces. Consequently, a similar approach was adopted with the side walls of the test box lined with PTFE sheets which were then coated with a silicone oil. To prevent contamination of the adjacent sand, the PTFE lining was covered with strips of Cling-film. This arduous process was repeated for every test. Furthermore, a set of friction-breakers were fashioned from strips of PTFE

and inserted at the junction between the lower edge of the test box and the geotextile mesh.

4.1.4 Construction of Deposit

The total volume of sand involved in the experimental study was approximately one cubic meter. The sand was stored in three skips mounted on rollers to allow ease of movement during the deposit construction and emptying phases.

The process of constructing the deposit consisted of positioning the skip adjacent to the pluviation tank then manually filling it with the sand to a pre-set level. The pluviation tank was lifted via a pulley block mounted on a beam trolley and connected to the mobile gantry frame. A set of eight clamps were used as locators to enable the positioning of the tank onto the test box quickly and accurately since any misalignment resulted in jamming of the trap doors and a termination of the test.

A manual pulley block system was used despite the availability of an electric hoist to allow positioning of the pluviation tank with minimum disturbance. The trapdoor mechanism was subsequently released and the sand was allowed to pour forming a sand deposit that was uniform and repeatable. The number of times this process was repeated per test depended on the height the piled embankment being investigated. The volume of sand in the pluviation tank was such that the height of the deposit slightly exceeded a lift thickness of 200 mm. The surface was levelled by means of a wooden board for each increment of fill. The aforementioned process was repeated until the desired height of fill was achieved. Upon completion of the test the sand was removed and stored in the skips. Each test box segment was unbolted and lifted using the pulley block system and mobile gantry to be lowered on to the laboratory floor.

Section elevation and plan views of the testing area and apparatus depicting the overall dimensions are shown in **Figure 4-3**.

4.1.5 Lowering of the Platform

It was considered an essential part of the investigation to adopt the two loading procedures representing the two possible loading regimes the geotextile reinforcement might encounter during its design life.

The simulation of the yielding subgrade was achieved by lowering of the mobile platform. This process was accomplished by contracting the pistons of the hydraulic cylinders simultaneously via a manifold connected to a hand pump. The platform would start to settle slowly and the weight of the sand deposit gradually transferred to the geotextile mesh and the pile caps.

The post construction behaviour of the piled embankment was simulated by lowering of the mobile platform after achieving the required height of fill. On the other hand, the construction behaviour was modelled by lowering the loading platform after deposition of the first fill layer. The geotextile mesh under the weight of the fill deformed incrementally with each successive lift, the sequence of events is outlined in **Figure 4-4**.

4.2 Material Properties

The materials used in the model tests consisted essentially of the Leighton Buzzard sand and the geotextile strip reinforcement. The tests carried to characterise the properties of these materials are described in the following sections.

4.2.1 The Soil

The soil used was found to be a uniformly graded medium to fine sand with particle sizes ranging between 0.6 to 1.2 mm. The effective grain size (D_{10}) was 0.67mm with a uniformity coefficient (C_u) of 1.38. The specific gravity of the Leighton Buzzard sand is 2.65 (Hassan (1992)).

Relative Density

The dry unit weight for Leighton Buzzard sand ranges between 17.8 kN/m³ (maximum) and 14.8kN/m³ (minimum) according to results obtained by Stroud (1971). The minimum and maximum void ratios corresponding to the unit weights mentioned previously are 0.49 and 0.79.

In the present study, unit weight measurements were made at various depths to ensure repeatability of the sand deposit properties. Density cups were placed at chosen depths and locations in the deposit, and sand was rained over them. After the cups were filled, they were retrieved from the deposit, levelled with a straight edge,

and weighed. Knowing the volume of the cup and the weight of the retrieved sand, the unit weight of the sand can be calculated. The average unit weight obtained was 17.1 kN/m³ with a void ratio of 0.55. The insitu void ratio achieved relates to a relative density of 80% which can be classified as dense (Lambe and Whitman 1969)

Mechanical Properties

The angle of shearing resistance of granular material depends upon many factors including the mineral composition, angularity, shape, texture, and size of grains, as well as the overall grading characteristics, state of compaction and moisture of the material. The shear strength parameters of sand can be found in several ways using such equipment as the direct shear box, simple shear, and ring shear apparatus, as well as from triaxial testing devices.

The advantages and disadvantages of each method over the others and has been the subject of detailed studies by previous researchers including, Butterfield and Andrawes (1972) and Yoshimi and Kishida (1981). Probably the most commonly used method is the direct shear test. It has the main advantage in that the test is simple in terms of sample preparation and execution.

On the other hand, its main drawbacks are :

- i. unequal strain distributions occur across the shear plane, with larger strains observed at the edges of the samples. This induces a progressive failure mechanism;
- ii. the interface area decreases with increasing shear displacements;
- iii. the relatively small size of the test sample limits the accuracy to which target densities can be achieved;
- iv. boundary friction between the test sample and the walls of the upper half of the shear box result in lower normal loads transmitted to the shear plane than are actually applied.

The simple shear test eliminates the problems associated with a reduction in the shearing area as the tests progress, but still suffers from stress concentrations at the edges of the samples.

The ring torsion apparatus has the main advantage that stresses and strains are fairly uniform hence progressive failure mechanisms cannot develop.

The triaxial test, although generally regarded as a better test than the direct shear method, suffers from inherent difficulties associated with preparing dry samples and achieving target densities. These findings coupled with availability, led to the use of the direct shear box method in the present research.

Several tests were performed under increasing normal loads to allow shear stress versus normal stress relationships to be plotted and hence the determination of the angles of shearing resistance.

Particular emphasis was placed on evaluating the angle of shearing resistance of the sand at the test density. This was made possible by placing the lower half of the shear box inside the test box and raining in the sand. The test results indicated peak and residual angles of internal friction of 45° and 36° for the peak and residual states, respectively.

4.2.2 The Geotextile Reinforcement

A series of tensile strength tests were carried out to obtain the load-strain characteristics of the four materials used in the experimental study. The set-up used in the testing of the specimens consisted of a mechanically controlled Shimadzu Autograph AG-E tensile testing machine. The geotextile strips were held in locked roller jaws connected to the speed controlled cross-bars. The load-strain results of the tests for the four different materials are shown in **Figure 4-5** and **4-6**.

4.3 The Model Test Results

The behaviour of piled embankments incorporating geotextile strip reinforcement was investigated by carrying out a series of reduced-scale physical model tests. The testing programme addressed the piled embankment geometry by varying the pile cap size and the height of the fill column. The influence of the geotextile reinforcement was investigated by using geotextile materials of varying extensibility. The response of the piled embankment system to two different methods of loading was also incorporated within the testing program.

The behaviour of the system was assessed by measurements taken of the following physical parameters:

- i. pile cap loads;
- ii. geotextile mesh deflection;
- iii. surface settlement.

The centre line spacing between the pile caps was maintained unchanged at 600 mm for all tests. The plan dimensions of the three pile caps investigated were 200x200, 250x250 and 300x300 millimetres to give pile cap width (b) to clear spacing (s') ratios of 1:2, 1:1¼ and 1:1, respectively.

The fill thickness was increased in five equal increments to give a maximum height of 1.0 meters that is the ratio of height (H) to clear spacing (s') ranged between a maximum and minimum of 3.33 and 0.5, respectively.

Four different geotextile materials were considered in the experimental investigation to assess the influence of the tensile stiffness on the behaviour of the piled embankment. Only one unit weight for the soil deposit was investigated due to constraints on the available time. Furthermore, the labour intensive nature of the test procedure precluded an exhaustive testing programme .

A total of 33 tests were carried out (**Table 4-1**), three of which were to establish the reproducibility of the test results. The individual test results, presented in Chapter 4 represent the ultimate steady state values for the pile cap loads and geotextile mesh deflections.

4.3.1 Pile Cap Loads

The objective of measuring the pile cap loads was to assess the influence of pile cap size and geotextile stiffness on the vertical stress re-distribution occurring due to the downward movement of the fill supported by the geotextile mesh. As mentioned in an earlier section, each pair of diagonally opposite pile caps were designed differently to enable the assessment of the load transfer mechanism. The load transfer process was evaluated on the basis of the parameters (T_n -avg) and (T_a -avg) which represent the arithmetic average of the individual loads obtained from the instrumented pile caps and are defined as follows:

- i. T_{a-avg} : represents average pile cap load due to both the hydrostatic stress and that transferred by the arching process mobilised by the arching action in the fill.
- ii. T_{n-avg} : average net weight of fill per pile cap tributary area.

[A] Effect of Geotextile Tensile Stiffness

For the full height tests, the influence of the reinforcement tensile stiffness on the load transfer mechanism was investigated for a pile cap width of 200 mm. The materials involved in the investigation were Stratagrid 200 and Paraweb grades 165 and 500.

Figure 4-7 depicts the variation of (T_{a-avg}) and (T_{n-avg}) with the height of fill for the three different geotextile materials.

The instrumentation scheme, however, was changed as the testing programme progressed. For the tests involving Paraweb 165 and Stratagrid, the vertical stresses acting on the pile cap and the net load per tributary area were obtained through the use of Kulite pressure cells and N.C.B "donut" cells, respectively.

In the tests mentioned above, the parameter (T_{a-avg}) was not obtained directly from the Kulite cell readings. The experimental procedure followed in calibrating the Kulite cells produced readings in units of stress.

The product of the pile cap plan area and the calibrated Kulite cell readings was then considered to be the average load (T_{a-avg}). The readings of the N.C.B cells were expressed in units of force.

The standard deviation of the results represented by the error bars indicated an unacceptable level of variability in the measurements acquired using the Kulite cells. The variability obtained was typical of measurements associated with assessing the state of stress in a granular mass and has been reported by several investigators, including, Jarret et al. (1992), and Agaiby (1991). The variability in the load measurements acquired using the combination of Kulite and N.C.B. cells is exemplified in the tests involving the Stratagrid reinforcement (**Figure 4-7**).

In addition to the difficulties associated with stress measurements in granular masses, the following points were identified as contributing to the variability in the load measurements:

- i. One Kulite cell was installed per pile cap, which represents a relatively small portion of the pile cap surface area. Consequently, the stress measured by the Kulite cell reflects only the conditions at that discrete point. Several cells would then be required per pile cap if an average value is to be obtained.
- ii. The readings of the Kulite cells were affected by the impact of positioning the upper test box sections into place to achieve the required height of fill, despite using a manual hoist to effect the process gently.

The corresponding net load measurements (T_n -avg.), obtained through the use of the NCB cells, represented by the dashed line displayed a more uniform trend and smaller error bars. However, the NCB cells possess a maximum capacity of 150 kN in compression at an accuracy of 0.25% which represents an error of ± 0.375 kN. This level of sensitivity was considered to be incompatible with the relatively low loads involved in the piled embankment model tests. Consequently, the use of the Kulite and NCB cells was discontinued and the pile caps were modified to accommodate the RDP load cells. RDP-1 and -2 were installed in the pile caps designed to measure that portion of the net load affected by the load transfer process.

The measurement of the net load was effected through RDP-3 and -4 installed in the two remaining diagonally opposite pile caps. The improvement in the average readings obtained using the RDP cells is evident in the variation of (T_a -avg.) and (T_n -avg.) with the height of fill for Paraweb 500 as shown in **Figure 4-7**.

The influence of the geotextile stiffness on the load transfer process was also investigated for the incremental loading procedure. In these tests the geotextile materials used were again the Paraweb grades 165 and 500. The third material was a needlepunched polyester commercially known as Textomur. The Textomur sheets were cut into strips of the same width as the Paraweb and the reinforcing mesh constructed following the same procedure. The high extensibility of Textomur material was considered important in assessing the influence of the reinforcement tensile stiffness on the load transfer mechanism. The results of tests (31) to (33) showing the variation of (T_a -avg.) and (T_n -avg.) with height of fill are depicted in **Figure 4-8**. The trends shown indicated the insensitivity of (T_a -avg.) to the tensile

stiffness of the basal reinforcement mesh constructed using the aforementioned geotextile materials

[B] Effect of Pile Cap Width

In addition to increasing the height of the fill, the piled embankment geometry was changed by varying the pile cap size (b) to achieve different fill height (H) to clear span (s') ratios, ($b:s'$). Paraweb 500 was used to construct the basal reinforcing mesh in the tests carried out to investigate the effect of the pile cap width (b). The variation of ($T_{a-avg.}$) and ($T_{n-avg.}$) with height of fill was investigated for pile caps 200, 250 and 300 mms in widths. The test results for both the full height and incremental loading simulations are shown in **Figures 4-9** and **4-10**, respectively.

In general, both ($T_{a-avg.}$) and ($T_{n-avg.}$) show an almost linear variation with the height of fill. The pile cap load measurements influenced by the arching in the fill, ($T_{a-avg.}$), were found to be consistently larger for the full height simulations than those obtained from the incremental loading tests (**Figure 4-11a**). The difference in the ($T_{a-avg.}$) load measurements was observed to be more prominent the greater the height of the fill. The net load per pile cap tributary area ($T_{n-avg.}$) was found to be independent of both the pile cap size and loading procedure (**Figure 4-11b**). The relatively constant values obtained for ($T_{n-avg.}$) with changing the pile cap size for both simulations attests to the repeatability of the procedures carried out to minimise the losses due to the frictional forces developed between the sidewalls of the test box and the granular fill.

4.3.2 Geotextile Mesh Deflection

The deflection of the geotextile mesh was monitored at five different points using the draw wire transducers. The measurement points were located along three different lines of symmetry to investigate the deflected shape of the mesh. The location of the measurement points are shown in **Figure 3-7**.

The variation of the mesh deflection for the five measurement points obtained using the draw-wire transducers (DWT-1 to -5) with height of fill for the two loading conditions are shown in **Figures 4-12** to **4-15**. The geotextile deflection, for the full height simulations, was observed to increase up to a fill height of 0.4 meters. For

heights of fill exceeding 0.4 meters the deflections were observed to decrease gradually regardless of both pile cap size or the tensile stiffness of the reinforcing material. The deflection measurements obtained for any full complement of five consecutive full height tests represent an envelope of values. In contrast, the deflection of the mesh for the incremental loading represents a continuous process with the values increasing with the fill height. Furthermore, the deflection suffered by the geotextile mesh due to the full height loading were found to be less in magnitude than those obtained from the incremental loading simulations for a similar reinforcement stiffness and piled embankment geometry. The difference in the magnitude of the measured deflections obtained became more evident the greater the height of fill.

4.3.3 Surface Settlement

The full height tests allowed the influence of the basal reinforcement tensile stiffness and the piled embankment geometry on the magnitude of the fill surface settlements to be investigated.

The surface settlement resulting from the downward movement of the basal mesh reinforcement was measured at nine different points. The change in the surface profile was represented by three settlement measurements (Δ_a), (Δ_b) and (Δ_c). The surface settlement at the centre of the mesh was designated by (Δ_a) while the terms (Δ_b) and (Δ_c) denote the average values above the pile caps and mid-span between adjacent piles, respectively. The influence of the different pile cap sizes and the geotextile material used in constructing the basal reinforcement on the surface deformations were investigated. The variation of the surface settlement of the fill represented by (Δ_a), (Δ_b) and (Δ_c) with the height of fill (H) is shown in **Figures 4-16** and **4-17**, respectively. A distinctive pattern was observed regardless of pile cap size or geotextile material involved:

- i. the surface settlement directly above the pile caps increased with the height of fill to reach a limiting value;
- ii. the pile cap size controlled the height and at which the limiting value was attained and to a certain extent the magnitude of the threshold value.

On the other hand, the mid span surface settlement along both the diagonal and transverse lines of symmetry decreased in value and to attain a similar limiting value. The height at which the limiting values coincide is referred to as the plane of equal settlement.

4.4 Losses

The losses in the system were quantified by obtaining the difference between the theoretical total load per pile cap tributary area and the T_n -avg. to give;

$$T_l - \text{avg} = (\gamma s^2 H) - (T_n - \text{avg}) \dots\dots\dots (4-1)$$

where T_l -avg = average load lost in system, (kN);

γ = insitu unit weight, (kN/m³);

s = pile spacing;

H = height of fill above pile caps, (m);

T_n -avg = average net load, (kN).

The losses were attributed to the combined effects of the friction between the PTFE lining of the test box side walls and the sand, in addition to the losses in the pulley system of the roller clamps.

Stress concentrations at the edges of bottom edges of the test box also contributed to the losses.

Equation (4-1) was used to estimate the losses due to the combined factors mentioned above. The average percentage losses were found to range between 5% to 15% of the total load for the minimum and maximum heights of fill, respectively.

It was not possible to separate the losses into individual components to estimate the magnitude of the side wall friction. However, Tang (1992) using a PTFE lining to reduce wall friction reported percentage losses of a similar magnitude to those encountered in the current study.

The sidewall friction encountered was considered to have no significant effect on the experimental test results.

4.5 Repeatability

Repeatability is a major concern in this type of testing. If a series of tests is conducted in which the effect of a changing parameter is being studied, it becomes imperative to establish the amount of agreement that is obtainable between the results of two tests for which the parameter was not varied. It is easy to attribute apparent trends in data to the variables being changed, and to draw involved conclusions from the results, when very often the observed variations in test results are smaller in magnitude than the accuracy of the experimental repeatability. Tests (26-28) were carried out to ascertain the reproducibility of the testing procedure. The results obtained from the aforementioned tests indicated that the reproducibility of the observed trends was satisfactory.

4.6 Summary

Model tests simulating the three dimensional behaviour of piled embankments incorporating geosynthetic reinforcement have been carried out using a granular soil. The parameters varied were the geosynthetic material, the piled embankment geometry and the test procedure. The testing facilities, experimental programme and procedures have been outlined.

The test results and methods used to characterise the materials involved in the experimental study were reported. The model test results were presented in graphical form to show the trends obtained from varying the different parameters described above.

The full height tests were found to result in a greater load to be transferred on to the pile caps in comparison with the incremental loading procedure. The reinforcement deflection for the full height tests was observed to decrease with height of fill for the full height tests. The full height tests provided an envelope of values corresponding to the post- construction behaviour of different piled embankment geometries.

The full height test procedure was employed to permit measurements of the surface deformations which were "built-out" in the case of the incremental loading simulations. The surface deformation results indicated that beyond a certain height of fill the settlements occurring were uniform, i.e., the settlement was total and not differential.

Table 4-1a. Nature of tests performed.

Test No.	b (m)	H (m)	Loading Method	Geotextile Material
1	0.20	0.2	Full height	P500
2	0.20	0.4	Full height	P500
3	0.20	0.6	Full height	P500
4	0.20	0.8	Full height	P500
5	0.20	1.0	Full height	P500
6	0.25	0.2	Full height	P500
7	0.25	0.4	Full height	P500
8	0.25	0.6	Full height	P500
9	0.25	0.8	Full height	P500
10	0.25	1.0	Full height	P500
11	0.30	0.2	Full height	P500
12	0.30	0.4	Full height	P500
13	0.30	0.6	Full height	P500
14	0.30	0.8	Full height	P500
15	0.30	1.0	Full height	P500
16	0.20	0.2	Full height	Stratagrid
17	0.20	0.4	Full height	Stratagrid
18	0.20	0.6	Full height	Stratagrid
19	0.20	0.8	Full height	Stratagrid
20	0.20	1.0	Full height	Stratagrid
21	0.20	0.2	Full height	P165
22	0.20	0.4	Full height	P165
23	0.20	0.6	Full height	P165
24	0.20	0.8	Full height	P165
25	0.20	1.0	Full height	P165
26	0.20	0.2	Full height	P500
27	0.20	0.4	Full height	P500
28	0.20	0.6	Full height	P500

Table 4-1b. Nature of tests performed.

Test No.	b (m)	H (m)	Loading Method	Geotextile Material
29	0.20	0.2	Incremental	P500
		0.4		
		0.6		
		0.8		
		1.0		
30	0.25	0.2	Incremental	P500
		0.4		
		0.6		
		0.8		
		1.0		
31	0.30	0.2	Incremental	P500
		0.4		
		0.6		
		0.8		
		1.0		
32	0.30	0.2	Incremental	P165
		0.4		
		0.6		
		0.8		
		1.0		
33	0.30	0.2	Incremental	Textomur
		0.4		
		0.6		
		0.8		
		1.0		

CHAPTER 5

INTERPRETATION AND ANALYSIS

5.0 Introduction

The objective of the experimental study was to investigate the influence of geotextile reinforcement on the behaviour of piled embankments. A square grid of central piles has been modelled at a reduced geometrical scale of 1:5.

The usefulness of model test programmes lies in the following areas:

- i. The laboratory scale model may be used to try out the effect of a number of variables in several different situations and conduct a parametric study in order to find out which variables are important, and discover what relationships exist between them. The results of the parametric study can be of use in a wide range of situations since a set of 'general' rules will have been established.
- ii. The use of laboratory models permits the important variables to be isolated and studied in a cost-effective manner. The cost of model tests is only a fraction of the cost for similar tests under field conditions on full-size prototypes. The potential disadvantage, however, is how closely the model represents the behaviour of full-scale piled embankments.
- iii. The model test results may be used to validate current design methods which might be based on simplifying assumptions and idealisations that may result in over conservative solutions.

The results of the model tests were used to study the validity of a number of frequently used analytical solutions to the problem of load transfer in piled embankments. In addition the observed trends from the experimental study were compared with the recommendations of BS 8006:(1995) and the Swedish Road Board (1974) for piled embankment design. A worst case scenario was adopted where the natural subgrade was assumed to possess no strength, i.e., the weight of the embankment fill is shared between pile cap and geotextile reinforcement.

The weight of the fill was applied to the pile cap and geotextile mesh in two different ways, as follows:

- i. In the first method, the required height of fill was first achieved before permitting the movable base to settle and is referred to as the full height simulation.
- ii. In the second method, the height of fill was increased in lifts 200 mm in thickness with no support from the movable base, i.e., the geotextile mesh was allowed to deflect incrementally with increasing fill height.

The parameters varied were the geotextile stiffness and the piled embankment geometry. The influence of the geometry on the piled embankment behaviour was investigated by varying the ratio defined by the height of the fill to the clear spacing between the adjacent pile caps. In addition, the full height simulations described above were considered representative of the post-construction stage behaviour of the piled embankment system. The construction stage process, on the other hand, was simulated by the second procedure whereby the geotextile mesh deflects with the increasing height of fill.

5.1 Interpretation of Test Results

In order to discern the relationships governing the piled embankment mechanism, the results of the model test study have been presented in non-dimensional form in order to dissociate them from the geometrical scale factor. The test results are examined separately under the following topics:

- i. the mechanism of load transfer;
- ii. shape of the deformed mesh;
- iii. surface differential settlement
- iv. influence of the settlement ratio on the efficacy

5.1.1 The Mechanism of Load transfer

It is of benefit at this stage, to examine the components of the load transfer mechanism with reference to **Figure 5-1** which depicts an idealised two-dimensional representation of the piled embankment problem. The load (P_L) transferred onto the

pile cap consists of two components. The primary component (P_a) is due to the arching in the fill. The secondary (T_v) is the vertical component of the tensile force (T_T) generated in the geotextile reinforcement and equals the difference between the applied load (P_s) and the subgrade reaction force (Q_{rf}). In the current study the modelling philosophy precluded the presence of the natural foundation, i.e., (Q_{rf}) is zero. Consequently, the efficacy (E) is a direct measure of the arching occurring in the fill.

It is then possible to define three terms to express the degree of load transfer, namely: the efficacy (E), competency (C) and the stress reduction ratio (SRR) (Low et al.(1994)).

The abovementioned load transfer terms are defined below prior to the interpretation of the model test results (assuming $Q_{rf} = 0$):

$$E(\%) = \left(\frac{P_a}{A \gamma H} \right) \times 100 \dots\dots\dots (5-1)$$

$$C = \frac{P_a}{a \gamma H} \dots\dots\dots (5-2)$$

$$SRR = \frac{P_s}{\gamma H(A - a)} \dots\dots\dots (5-3)$$

where A =pile cap tributary area, m^2 ;

a =pile cap plan area, m^2 ;

γ =unit weight of fill, kN/m^3 ;

H =thickness of fill above the pile cap, m .

The efficacy, competency and the stress reduction ratio are inter-related and the following equations can be identified:

$$E(\%) = C \left(\frac{a}{A} \right) \times 100 \dots\dots\dots (5-4)$$

$$SRR = \frac{1 - (E/100)}{1 - (a/A)} \dots\dots\dots (5-5)$$

where (a/A) is the area ratio.

The above expressions have all been derived assuming that no wall friction exists. The pile caps were instrumented to enable the measurement of (T_{a-avg}), and the average net load (T_{n-avg}). These parameters correspond to the terms (P_a) and ($A_y H$), respectively, in the idealised piled embankment system described previously.

Hence, using the parameters (T_{n-avg}), which implicitly accounts for wall friction and other losses in the system, and (T_{a-avg}) equations (5-1) to (5-3) can be expressed as follows:

$$E(\%) = \frac{T_{a-avg}}{T_{n-avg}} \times 100 \dots\dots\dots (5-6)$$

$$C = \frac{T_{a-avg}}{T_{n-avg}} \cdot \frac{b^2}{s^2} \dots\dots\dots (5-7)$$

$$SRR = \frac{1 - (T_{a-avg}) / (T_{n-avg})}{1 - (b^2 / s^2)} \dots\dots\dots (5-8)$$

For reasons outlined in Chapter 4 the test results obtained using the RDP load cells only were considered in analysing the load transfer process.

Although the above expressions all pertain to the load transfer mechanism each one is more suited to describing a different aspect of the piled embankment system. The importance of each parameter is as follows:

- i. The efficacy (E) is a measure of the overall performance and provides a good measure when comparing between different piled embankment geometries. The competency on the other hand gives a direct measure of the stresses bearing on the pile cap and is of more relevance to the structural design process.
- ii. The stress reduction ratio, however, relates to the loads the basal reinforcement is expected to sustain for the given piled embankment geometry.

The dimensionless parameter (H/s') is ideally suited to represent the variation of the load transfer parameters in that it accounts for the two important dimensions defining the piled embankment geometry. The variation of the load transfer parameters with the depth ratio (H/s') for the two loading procedures and the different geotextile materials used in the model tests are shown in **Figures 5-2 to 5-4**.

Figure 5-4 shows the competency curves for the three different pile cap sizes which correspond to three different capping ratios ($b:s'$) as a function of the depth ratio (H/s'). For any given (H/s') value, the competency was largest for the smallest capping ratio ($b:s'$). The fact that the tributary area (A) was maintained constant accounts for the increased vertical stresses acting on the pile caps of smaller size and consequently a corresponding increase in the associated competency values. Hence, if the capping ratio ($b:s'$) was taken to an extreme value of 1, the competency assumes the a minimum value of 1 regardless of (H/s').

On the other hand, the competency cannot exceed the reciprocal of the capping ratio ($b:s'$) since it implies that the pile cap is supporting the entire weight of fill within the tributary area which is physically impossible.

The two loading procedures adopted were designed to simulate the construction and post-construction phases that a prototype might exhibit in response to the applied loading regime. The efficacy (E) shown in **Figure 5-2** indicated that the pile cap loads ($T_{a-avg.}$) were lower for the incremental loading procedure. Consequently, the stress reduction ratio (SRR) for the full height simulations was consistently lower than for the incremental loading method. The difference between the load transfer parameters obtained for both simulations was observed to increase with the depth ratio (H/s').

Fluet et al.(1986) reported a similar response in their full scale experimental investigation into the use of geosynthetic reinforcement to bridge voids beneath embankments. The two cases simulated were analogous to the full height and incremental construction tests of the current study. Fluet et al. observed that the gradual settlement of the reinforcement as the fill height increases promoted less arching in the soil.

The tendency for the pile cap loads to increase was reported by Reid et al. (1983). An efficacy of 66% measured at the end of construction increased to 85% in the long term. It was concluded that the settlement of the subsoil due to consolidation or other time dependant deformations subsequent to achieving the full embankment height induced a further increase in the system efficacy (E).

For the incremental procedure, however, the efficacy at a given height was the cumulative contribution due to the placement of each successive lift of fill material. The load transfer in the case of the full height tests, however, was induced by differential settlement occurring within one single coherent mass of fill. A condition that permits the settling soil to transfer a greater portion of its weight to the stationary fill supported on the pile cap. The trends obtained for the load transfer parameters versus the depth ratio, however, were observed to be reproduced for both loading procedures, i.e., the load transfer mechanism is independent of the test procedure.

The shape of the efficacy and stress reduction curves suggest the existence of two modes of behaviour for the investigated range of (H/s') and $(b:s')$ ratios. By inspection, the point of departure from a shallow to a deep mode of behaviour occurs at a relatively constant depth ratio (H/s') of approximately (2) which corresponds to an efficacy value ranging between (80) to (83) %.

The portion of the efficacy curve beyond the point of departure represents a primarily deep failure mechanism. The maximum efficacy values and the corresponding depth ratios at which they were attained are summarised in **Table 5-1**. The shape of the curves, **Figure 5-2**, indicated that the maximum values are very close to a threshold level. The capping ratio $(b:s')$ appears to influence both the magnitude and corresponding depth ratio (h/s') at which the ultimate state is achieved. The larger the capping ratio the greater the ultimate efficacy and the corresponding depth.

Although dimensional analysis was considered in designing the experimental apparatus, "modelling of the model" to investigate scale effects was unrealistic. The size and geometry of the apparatus would necessitate major modifications that rendered the task impracticable both with regards to time and cost.

The field measurements reported from three case histories, however, showed reasonable agreement with experimental results for tests with a similar geometry as shown in **Table 5-2**. The results of the two dimensional capping beam system proposed by Tang (1992) are shown in **Figure 5-5a**. In addition, the area ratios (a/A) versus the efficacy corresponding to a depth ratio of (3) for both the current study and the capping beam system are shown in **Figure 5-5b**.

The plotted curves suggest the following points:

- i. The efficacy of the individually capped piles was consistently higher. The difference in efficacy was most evident for area ratios less than 15%.
- ii. The change over from a shallow to a deep mechanism for the cap-beam system occurs at a depth ratio of approximately 2 for the capping ratios considered

The second observation is similar to that obtained in the present study. This observation indicates that the depth ratio at which the load transfer mechanism changes is independent of the capping ratio ($b:s'$).

5.1.2 Shape of Deformed Mesh

The fact that the reinforcing mesh possesses negligible bending stiffness implies that it resists loads applied transverse to its longitudinal axis by a change in geometry. Consequently, the mesh reinforcement behaves as a tensioned membrane that can only sustain tensile loads. The importance of attributing a specific geometry to the deflected shape is necessary in order to estimate the magnitude of the tensile loads and the corresponding strains developed in the mesh. The ultimate aim is to provide a basis for selecting a geotextile reinforcement capable of sustaining the imposed loads.

In that regard, three shapes have been proposed, namely:

- i. a catenary
- ii. a parabolic arc
- iii. a circular arc

The catenary will not be investigated since for settlement ratios (y_g/s') much less than a value of (1) and where the self weight is negligible the catenary degenerates to the parabolic arc, Leonard (1988). The geometry and governing equations for the parabolic and circular arc segments are shown in **Figure 5-6**.

The deflected shape of the mesh reinforcement was investigated along two lines of symmetry to encapsulate the three dimensional nature of the system. The measured mid-span deflections for each line of symmetry were used to calculate the

corresponding quarter-span deflections (d) for both the parabolic and circular arc geometries.

Figures 5-7 and 5-8 show the experimental versus the calculated quarter-span deflections normalised by the clear span (L) along both lines of symmetry and for the full height and incremental loading simulations. A 45° line corresponding to a perfect fit relationship was superimposed as a comparative measure aid.

The circular and parabolic arc analyses were observed to show a reasonable degree of agreement with the experimental values. In fact both methods for the investigated range of geotextile materials and embankment geometry were found to give almost identical results. The discrepancy between the measured and calculated values was found to range between 5-15%.

It was therefore concluded that the deflected shape of the mesh reinforcement can be adequately described by both the parabolic and circular arc geometries.

5.1.3 Surface Differential Settlement

The piled embankment solution is adopted primarily to overcome the development of excessive surface settlement. The second objective is to expedite the construction of the embankment which would otherwise require a much longer time if conventional ground improvement methods were adopted.

Investigating the factors influencing the development of surface settlement was one of the main targets of the experimental study. The post-construction behaviour of a piled embankment was represented by the full height simulations and the surface settlement measurements provided the basis for a comparative analysis.

The effect of varying the capping ratio ($b:s'$) is shown in **Figure 5-9**. The maximum surface differential settlement is plotted against the height of embankment for the geotextile material, Paraweb 500. The results show clearly that for the same height of fill a marked decrease in the differential surface settlement occurs with an increase in the capping ratio ($b:s'$), a trend evident for both lines of symmetry. The maximum differential settlement, however, was observed to diminish sharply for heights of fill greater than 0.4 meters. The results indicated clearly that the depth ratio (H/s') is the

dominant parameter controlling the magnitude of the maximum surface differential settlement .

On the other hand, for a capping ratio ($b:s'$) of 1:2, the influence of the geotextile stiffness on maximum differential settlement is shown in **Figure 5-10**. The three different materials used were Paraweb-500, Stratagrid and Paraweb-165 representing a nominal tensile stiffness range values of 500, 285 and 165 kN/m' respectively.

The surface differential settlement was found to be relatively insensitive to the change in the tensile stiffness of the basal reinforcement for the investigated range of geotextile materials.

The maximum surface differential settlement was normalised by the corresponding clear span for both lines of symmetry and plotted against the depth ratio (H/s'). The resulting dimensionless parameter is a measure of the angular distortion occurring on the embankment surface between adjacent pile caps.

The angular distortion parameter was plotted against the depth ratio for the investigated piled embankment geometry and reinforcement materials. The results for both lines of symmetry (the transverse and diagonal) are shown in **Figure 5-11**.

The plane of equal settlement represents the height above the pile caps beyond which surface differential settlements were no longer manifest. With reference to **Figure 5-11** the plane of equal settlement occurs at depth ratios (H/s') ranging between (1.7 to 2) and (1.3 to 1.4) for the transverse and diagonal lines of symmetry. The plane of equal settlement and the departure from a shallow to a deep failure mechanism were observed to occur at the same depth ratios (H/s').

5.1.4 The Influence of the Settlement Ratio on Efficacy

The process by which the efficacy of the piled embankment system is influenced by the settlement of the natural subgrade is associated with the concept of strain compatibility. The concept of strain compatibility is the essence of the load sharing mechanism occurring between the different components of the piled embankment system. In the current study the modelling philosophy precluded the presence of a subsoil between adjacent pile caps, i.e., the efficacy is representative of the load transfer due to arching in the fill. Consequently, it was only possible to study the

influence of the downward deflection of the geosynthetic reinforcement on the arching mechanism in the fill. The effect of foundation stiffness on the efficacy of the system and the tensile loads developed in the reinforcement was investigated using a continuum method to take into account the response of the foundation soil. In this case strain compatibility becomes a function of the problem (Chapter 6).

Figure 5-12 shows the efficacy (E) plotted versus the settlement ratio (y_g/s') for the results of the full height simulations involving the Paraweb 500 geotextile reinforcement. The settlement ratio is defined as the maximum geotextile mesh deflection (y_g) normalised by the clear span (s') between the adjacent pile caps.

The three plots shown in **Figure 5-12** pertain to three different capping ratios ($b:s'$). There was an initial rapid increase in the efficacy to a peak value further downward settlement resulted in a decrease to a relatively constant value. The peak values were attained for a reinforcement deflection of about 0.8% to 2% of the clear span between adjacent pile cap. At further lowering, there was a gradual decrease in the efficacy (E) up to a settlement ratio of (0.03) to (0.05) beyond which an ultimate value was achieved.

The plot depicting the results for a capping ratio of 1:1, however, did not conform to the trend described previously except for the test with a depth ratio of 0.67. The reason for the deviation was that the hydraulically supported movable base representing the soft foundation was yielding gradually during the sand placement. The yielding of the movable base prior to achieving the full test height resulted in the efficacy increasing gradually with no discernible peak value. In general, the plotted results were observed to be analogous to the curves obtained by Terzaghi (1936) and Ladanyi et al. (1969) for the trapdoor load versus settlement ratio (**Figure 2-1**).

Ali (1990) carried out a series of model tests to investigate piled embankment behaviour. The soft soil was simulated by a mechanically operated movable base. Unlike the current study, the use of geotextile basal reinforcement was not incorporated in the reduced scale laboratory model. The efficacy versus the settlement ratio plots for tests carried out for capping ratios of 1:1.8 and 1:1 are shown in **Figure 5-13**.

The efficacy versus settlement ratio plots obtained from Ali's unreinforced model study suggest the following:

- a capping ratio of 1:1, i.e., an area ratio (a/A) of 25%, produced a stable arching mechanism despite the large settlement ratios attained. The ultimate efficacy values for a capping ratio of 1:1 were in good agreement with the results of the reinforced fill system of the current study.
- For a capping ratio of 1:1.8 (area ratio of approximately 12%), a sharp decrease in the efficacy was observed to occur in response to an increase in the settlement ratio. The effect was exacerbated for fill heights with a depth ratio ($H:s'$) less than (2) .

The second observation highlights the importance of geotextile reinforcement and points to the conditions under which basal geotextile reinforcement would be of most value. In the current study an area ratio of as low as 11.1% was sufficient to induce a stable arching mechanism. This was made possible because the geotextile reinforcement arrested further settlement from occurring. In Ali' s tests the arching mechanism collapsed due to a disintegration of the soil structure under the continuous settlement of the movable board for a similar piled embankment geometry. Furthermore, with reference to **Figure 5-13**, the efficacy of the unreinforced system was observed to reduce considerably at a settlement ratio of about (0.15) for the capping ratio ($b:s'$) of 1:1.8.

The following scenario further emphasises the importance of the geotextile basal reinforcement:

- consider a typical design configuration where; (b) and (s) are 1.0 and 3.0 meters respectively to give a corresponding area ratio of 11%. A settlement in the soft subgrade of 0.3 meters (assuming a settlement ratio of 0.15) would then result in a potentially unstable arching mechanism. Further settlement will probably result in loss of serviceability of the piled embankment.

A settlement of 0.3 meters for the fill supported on the subsoil in between adjacent pile caps and more is not unlikely in areas where very soft highly compressible soils exist.

Barry et al.(1995), described the construction of a reinforced piled embankment road over a deep layer of peat in East Sumatra, Indonesia. Settlements in excess of 0.7 meters were reported for an unpiled section of the road where the height of fill was only 0.5 meters. Without the basal reinforcement to control the settlement of the fill between the adjacent pile caps, an area ratio of 11% would not be a feasible solution.

In conclusion, the ultimate pile cap load due to the arching mechanism was observed to occur at small reinforcement settlement ratios (0.03 to 0.05). However, relatively large settlement ratios can de-stabilise the mechanism. Consequently, the use of geotextile basal reinforcement is essential to arrest foundation settlement occurring due to consolidation or other time dependant mechanisms. The most benefit is attained for area ratios less than 20% and for relatively shallow depth ratios (H/s').

5.2 Analysis of Reinforced Piled Embankments

The objective of this section is to examine the current methods of analysing the behaviour of a reinforced piled embankment with regards to a) the arching mechanism, i.e., the efficacy and b) the load deflection response of the geotextile reinforcement.

5.2.1 Prediction of Piled Embankment Efficacy

The main methods used to quantify the arching mechanism in piled embankments have been reviewed in Chapter 2. These methods are based on either limit equilibrium solutions or on semi-empirical equations. Three methods were selected as being representative of those reviewed in Chapter 2, and they are perhaps the most commonly quoted methods of analysis.

The first two methods are limit equilibrium solutions based on either vertical shear plane or cylindrical arch models. The former has been proposed by John (1987) and is a modified version of Marston's (1913) equation for buried circular conduits under incomplete positive projection conditions.

John (1987) based his proposed solution on the analogy between a buried conduit with an external diameter (B_c) and a pile cap with an equivalent lateral width (b). The ratio of the vertical compressive stress acting on the pile cap to the overburden pressure corresponding to hydrostatic conditions was obtained in accordance with the following expression:

$$\frac{p_c}{\gamma H} = \left(\frac{C_c b}{H} \right)^2 \dots\dots\dots (5-9)$$

where p_c =vertical stress on pile cap, kN/m²;
 C_c =arching coefficient;
 γ =unit weight of fill, kN/m³;
 H =thickness of fill above the pile cap, m;
 b =width of pile cap.

The pressure ratio as defined above is equivalent to the competency (C), hence the efficacy (E) of a piled embankment can be expressed in terms of John's pressure ratio as follows:

$$E(\%) = \left(\frac{C_c b}{H} \right)^2 \times \frac{b^2}{s^2} \times 100 \dots\dots\dots (5-10)$$

Hewlett et al.(1988) analysed the arching of granular fill over a square grid of pile caps by considering the radial equilibrium of domed arches (**Figure 2-10**). As in the earlier work of Atkinson and Potts (1977), self-weight was included in the differential equation of radial equilibrium of an element of arched sand at the crown of the dome.

The solution of the differential equation leads to the stress at the inner surface of the dome (σ_i). The vertical pressure (σ_s) acting on the soft ground comprised the sum of (σ_i) and the weight of soil extending to the inner surface of the dome.

The portion of the fill weight borne by the pile caps, and hence the efficacy (E), was obtained from the overall vertical force equilibrium. The efficacy thus calculated was based on the limit condition at the crown of the domed arch.

Hewlett et al. also entertained the possibility of a bearing type failure in the sand at the pile cap. By considering the radial equilibrium of the arched sand immediately above the pile cap, the overall force that may be taken by the cap was obtained.

Analysis of the two regions leads to two separate estimates of the piled embankment efficacy, the lower of which governs the design. The details of the governing equations for efficacy at the crown and pile cap are to be found in Chapter 2 and will not be reproduced again.

Combarieu (1989) presented the following semi-empirical equation to determine the vertical stress (σ_s) bearing on the soft foundation soil;

$$\sigma_s = \frac{H \gamma}{m_r} (1 - e^{-H m_r}) \dots\dots\dots (2-14).$$

Combarieu expressed (m_r) in terms of the piled embankment geometry and the fill properties as follows:

$$\text{where } m_r = \frac{(b/2) \cdot k \cdot \tan(\phi)}{(S)^2 - (b/2)^2};$$

b = the lateral width of the pile cap;

H = height of embankment;

and $2S$ = the equivalent centre line spacing between pile caps.

Consequently the pile spacing ($2S$) appearing in the arching coefficient (m_r) pertains to that of an equivalent plane strain condition. The term $k \tan(\phi)$ which brackets the state of stress and the shear strength of the fill was determined empirically and found to range between 0.8 and 1 for granular fills.

The efficacy expressed in terms of the bearing pressure (σ_s) was obtained as follows:

$$E(\%) = \left(1 - \frac{\sigma_s (s^2 - b^2)}{\gamma H s^2} \right) \times 100 \dots\dots\dots (5-13)$$

where s = centre-line spacing of a square grid of piles;

b = width of pile cap.

A comparison between the efficacy values of the model tests and predictions made using the above mentioned methods has been carried out. The purpose of the exercise was to assess the accuracy of the assumptions made in deriving the proposed solutions. Each method was used to calculate the efficacy for the three different piled embankment geometries pertinent to the experimental study. The results of both the full height and incremental loading simulations were used as the basis for comparison since they bracket the anticipated load regime the structure will encounter during its design life. The calculated efficacies were based on properties of the test deposit, i.e., a unit weight (γ) of 17.1 kN/m³ and a shear strength corresponding to a residual angle of internal friction of 36°.

Table 5-3 summarises the efficacies using the above mentioned methods together with the corresponding measured values. The results of the comparative analysis are shown plotted in **Figures 5-14 to 5-16** .

In general, the three methods used to calculate the efficacy were found to give pessimistic results when compared with the experimentally obtained values. Although the general trend was to underestimate the efficacy, the method proposed by John (1987) gave slightly unconservative efficacy values for low depth ratios (H/s'). Another point of interest, was the insensitivity of the calculated efficacy, using John's method, to the depth ratio (H/s') which was indicated by the relatively flat shaped curves. The capping ratio ($b:s'$) on the other hand appears to have a significant effect on the ultimate efficacy value.

The efficacy values obtained using Combarieu's semi-empirical method did not vary greatly for the proposed range of the experimentally determined factor $k \tan(\phi)$. The element of over conservatism however seems to be less when compared to John's shear plane method. The trend obtained from the calculated efficacy curves were observed to follow a pattern similar to that obtained for the measured values.

The domed arch analytical model proposed by Hewlett et al.(1988) yielded the closest overall predictions for the range of experimental parameters investigated. In particular, good agreement was obtained between the predicted efficacy governed by crown stability and the incremental loading results. The cap stability predictions, on the other hand, were found to agree with the maximum measured efficacy obtained from the full height tests.

A parametric study was also undertaken to examine further the validity of the three different methods. A wider range of piled embankment geometries were investigated involving capping and depth of cover ratios ranging between (0.5 to 5.5) and (1:1 to 1:3), respectively.

However, a constant pile cap width was maintained at 1.0 meters. The selected range for piled embankment geometry mentioned previously was chosen to represent typical design configurations. The results of the parametric study are shown in **Figure 5-17**. The method proposed by John (1987) was found to produce unrealistic predictions with regards to efficacy.

The two main reasons thought to contribute to the shortcomings of this method are as follows:

- i. The fact that the proposed solution is not sensitive to the depth of cover ratio is due to adopting the same arching coefficient as that proposed by Marston (1913) in his analysis of the loads on buried conduit. The arching coefficient (C_d) pertaining to the buried conduit analogy is a function of the soil shear strength and the height at which the plane of equal settlement is attained. In Marston's solution, the height of the plane of equal settlement was governed primarily by the external diameter of the buried conduits. The experimental evidence however, indicates that the analogy between the buried conduit problem and piled embankments is not appropriate. The experimental results of the current study indicate quite clearly that the depth ratio (H/s') is the governing parameter affecting the height at which equal settlement occurs.
- ii. The second reason is due to the squaring of the pressure ratio to obtain an equivalence between the plane strain conditions of the buried conduit solution and the three dimensional geometry of the piled embankment problem. This process can produce unexpected results for the efficacy especially for capping ratios ($b:s'$) less than 1:1.

The semi-empirical solution proposed by Combarieu (1987) presents a more reasonable approach to the problem of predicting the efficacy. The main area of concern is that the solution appears to be based on an exponential type equation. The calculated efficacy will continue to increase with the depth ratio (H/s') extending asymptotically towards 100% efficacy. The experimental results indicate that at a specific depth ratio depending on the piled embankment geometry the efficacy attains a limiting value .

Combarieu's solution does not account for an ultimate efficacy governed by the capping ratio ($b:s'$). With increasing depth ratios the predicted efficacy can then exceed the ultimate value governed by the capping ratio hence eliminating the element of conservatism with regards to the load supported by the basal reinforcement.

The domed arch analysis proposed by Hewlett al.(1988), however, is based on the following three assumptions:

- i. The vertical stress (σ_s) supported by the soft soil is uniformly distributed.
- ii. The vertical stress (σ_s) is equal to the internal pressure (σ_i) corresponding to the stability of the crown of the dome plus the weight of the underlying column of soil.
- iii. The major principal stress is the tangential component and describes a semi-circular path.

In their analysis, Hewlett et al. have shown that the crown stability governs the efficacy for shallow embankments. Consequently the internal stress supporting the element of arched sand at the crown of the dome represents a maximum value. An element of over-conservatism is introduced into the calculated efficacy due to the assumption that the internal stress at that location is uniformly distributed on the subsoil or basal reinforcement. In addition, the proposed solution is not valid for $(H/s) < 0.5$ due to the assumed circular geometry. To allow for a possible non-uniform vertical distribution on the soft ground, a modifying factor (α) was proposed such that ($\alpha\sigma_s$) is an equivalent uniform pressure (similar to that proposed by Low et al.(1994) in their plane strain analysis). The efficacy corresponding to the crown stability can then be expressed as follows:

$$E(\%) = \left(1 - \alpha \left[\omega + \frac{m}{\sqrt{2}(h/s)} \right] \right) \dots\dots\dots (5-14)$$

where $\omega = (1 - \delta^2)(1 - \delta)^{2(k_p - 1)}$;
 $m = (1 - \delta^2) \left(\frac{2k_p - 2}{2k_p - 3} \right) \cdot \left((1 - \delta) + (1 - \delta)^2(k_p - 1) \right)$;
 $s =$ centre-line spacing of a square grid of piles;
 $\delta = b/s$ and $K_p = \frac{1 + \sin \phi}{1 - \sin \phi}$.

Figure (5-18) shows the calculated efficacies based on the above equations for a range of (α) values. An (α) value of 0.57 was found to produce good agreement between the predicted efficacy (E) based on crown stability and the measured values corresponding to the full height tests. However, when compared to the results of the incremental loading tests, a value of 0.8 for (α) was observed to produce a closer fit

to the measured efficacy. In addition, the use of the modifying factor (α) extended the range of the closed form solution to encompass depth ratios (H/s') as low as (0.5).

5.2.2 Dimensional Analysis of the Reinforcement Behaviour

In investigating a function describing the behaviour of the geotextile mesh the structural response of the reinforcement will be divorced from the load transfer mechanism. This assumption was shown to be justifiable since the efficacy values at ultimate conditions were attained at relatively small settlement ratios and were not sensitive to further reinforcement deflection.

In Chapter 2 it was proposed that the dimensionless parameters governing the behaviour of the geotextile mesh is a function of the following dimensionless parameters :

$$\pi_1 = \phi \quad ; \quad \pi_2 = \frac{y_g}{s'} \quad ; \quad \pi_3 = \frac{\gamma H}{G} \quad ; \quad \pi_4 = \frac{\gamma H s'}{J}$$

Consequently, of the dimensionless parameters mentioned above, only two are considered relevant to analysing the structural response of the reinforcing mesh. Hence by isolating (π_3) and (π_4) then substituting the applied load (w_G) for the (γH) term in the selected (π) parameters, the following function can be obtained:

$$\left(\frac{y_g}{s'} \right)_{\text{exp}} = f \left(\frac{w_G s'}{J} \right) \dots \dots \dots (5-15)$$

- where y_g = mid span deflection
 s' = clear span between adjacent pile caps
 w_G = applied load on reinforcement
 J = stiffness of geotextile

Furthermore, it was shown in a preceding section that the geometry of a parabolic arc adequately describes the deformed shape of the geotextile mesh. The parabolic shape was evident for both the transverse and diagonal lines of symmetry. John (1987) proposed that behaviour of the basal reinforcement is very similar to that of suspension cables which deform to take the shape of a parabolic arc when supporting a uniformly distributed load .

The load-deflection of flexible cable structures for an assumed parabolic geometry is described by the following equation, Roark (1989):

$$\left(\frac{y_g}{L}\right)_{\text{calc}} = \left(0.0467 \cdot \frac{w_G L}{J}\right)^{1/3} \dots\dots\dots (5-16)$$

where y_g = mid span deflection

L = unsupported span

w_G = uniformly distributed load

J = tensile stiffness

The mid span deflection (y_g) normalised by the unstretched span (L) in the parabolic cable formulation is expressed in terms of the tensile stiffness and a uniformly distributed load (w_G) acting vertical to the span.

The suitability of using equation (5-16) was investigated by plotting the experimental versus the calculated values for the parameter (y_g/L). The results used in the comparative analysis pertained to the incremental loading simulations. They were considered appropriate for the following reasons:

- i. the loading procedure of the basal reinforcement was a gradual and continuous process that resembles the field behaviour;
- ii. the geotextile materials investigated in carrying out the incremental loading simulations encompassed a broader range of tensile stiffnesses.

The reinforcement stiffness (J) used in equation (5-16) was equal to the secant modulus calculated using the load extension curves shown in **Figures 4-5 and 4-6**.

The reinforcement strain corresponding to the calculated secant moduli was estimated using the following equation for parabolic cables, Marshall et al. (1986):

$$S_o = L + \frac{8}{3} \left(\frac{y_g^2}{L}\right) \dots\dots\dots (5-17)$$

where S_o = the stretched length of cable, m

L = unsupported span, m

y_g = maximum midspan deflection, m

Equation (5-17) can be expressed as follows:

$$\varepsilon_G(\%) = \left(\frac{8}{3} \left(\frac{yg}{L} \right)^2 \right) \cdot 100 \dots\dots\dots (5-18)$$

to give an estimate of the strain (ε_G) suffered by the reinforcing strips spanning between adjacent pile caps. The input data used in obtaining the calculated and measured values for the parameter (yg/L) are shown on **Table 5-4**.

The trend shown in **Figure 5-19a** suggests that equation (5-16) representing the parabolic cable load-deflection behaviour is suitable despite its tendency to underestimate the midspan deflections.

The disparity between the experimental and calculated values can be attributed to the following factors:

- i. the theoretical solution for the parabolic arc is derived for a uniformly distributed load which is unlikely to be representative of the real stress distribution.
- ii. the three dimensional nature of the piled embankment system contributes to the disparity between the calculated and measured values.

It is possible to reduce the three dimensional geometry with its geotextile reinforcement spanning across regularly spaced pile caps into an equivalent plane strain representation (**Figure 5-19b**).

Donovan et al. (1984) suggested that a linear scaling of material properties is a simple and convenient method of distributing the discrete effect of elements over the distance between elements in a regularly spaced pattern. Consequently the parameter (yg/L) was re-calculated using the equation (5-16). The secant moduli used in the calculations were modified by using a scaling factor (f) defined as the ratio of the cap width (b) to the pile spacing (s), i.e., $f = b/s$.

The measured versus the calculated values for the (yg/L) parameter are shown plotted in **Figure 5-20a**. The points corresponding to the modified solution converged around the 45° line which attests to the suitability of the rationale developed above.

Figure 5-20b depicts the measured values of the diagonal versus the transverse parameter (yg/L) for the incremental test results. The trend shown, clearly indicates that the maximum midspan deflection along the diagonal line of symmetry can be expressed by;

$$(yg)_{diag.} = \left(\frac{L_{diag.}}{L_{trans.}} \right) * (yg)_{trans.} \dots\dots\dots (5-19)$$

where (yg) and (L) represent the midspan deflection and the unsupported span for the transverse and diagonal lines of symmetry, respectively.

5.3 Evaluation of Current Design Methods

The objective of the following section is to examine the philosophy behind the two most comprehensive and most commonly used methods employed in the design of piled embankments, namely:

- i. The Swedish Road Board (1974);
- ii. BS (8006):1995.

[A] Swedish Road Board Method

The Swedish Road Board (1974) proposed a design curve (**Figure 2-18**) established on the basis of laboratory model tests. The load of the embankment fill is assumed to be supported totally by the piles via the arching mechanism in the fill. Inspection of the design curve indicates that the ratio $(s/b)^2$, where (s) and (b) are the pile spacing and the cap width respectively, attains a threshold value of (5.7). The implication of such a maximum allowable value is that the capping ratio cannot decrease beyond (1:1.4), i.e. a minimum area ratio of 17.5%. The experimental results of the current study have shown that a capping ratio of (1:2) (corresponding to an area ratio of 11.1%) can be used with no detrimental surface deformations taking place (providing the depth ratio $H/s' \geq 2$). Achieving a reduction in the capping ratio to achieve cost-effectiveness cannot be over-emphasised when adopting an expensive solution such as the piled embankment technique. The ability to employ a smaller capping ratio was made possible by incorporating basal reinforcement into the piled embankment system. The limitations mentioned above suggest that the design curve proposed by the Swedish Road Board can result in uneconomic piled embankment configurations.

[B] BS 8006:1995

Analysis of the piled embankment problem as proposed by the new British Standard Code of Practice for Reinforced Fills, BS 8006:1995, is based on the decoupling of the two basic components responsible for the load transfer mechanism occurring in piled embankments, namely, the soil arching and the geotextile reinforcement. In addition, the foundation soil between the pile caps is considered non-existent and hence does not contribute to the load sharing process.

The soil arching model proposed by John (1987) is utilised in BS 8006:1995 to determine the pressure ratio which relates the pile cap pressure to the hydrostatic overburden. The magnitude of the distributed load (W_G) which the geotextile membrane has to support between the pile caps can be determined as follows;

for $H > 1.4(s'-b)$;

$$W_G = \frac{1.4sf_{fs}\gamma(s-b)}{s^2 - b^2} \left[s^2 - b^2 \left(p_c / \sigma_{vo} \right) \right] \dots\dots\dots (5-20)$$

and for $0.7(s'-b) \leq H \leq 1.4(s'-b)$;

$$W_G = \frac{s(\gamma H + f_q w_s)}{s^2 - b^2} \left[s^2 - b^2 \left(p_c / \sigma_{vo} \right) \right] \dots\dots\dots (5-21)$$

BS 8006:1995 requires that the full embankment height (H) should be used providing that the condition $(H) \leq 1.4(s-b)$ is fulfilled. However, should (H) exceed $1.4(s-b)$ then the embankment height (H) is taken equal to $1.4(s-b)$ where $(s-b)$ represents the clear span between adjacent pile caps. The justification lies in that the greater the embankment height the smaller is the portion of the total weight supported by the reinforcement due to the arching in the fill.

Consequently, the arching mechanism in equation (5-20) is accounted for by using the pressure ratio concept proposed by John (1987) and by limiting the height of fill (H). Furthermore, a dimensional analysis of the equations proposed by BS 8006:1995 indicates that the units of the distributed load (W_G) are (kN/m'). The units of load per meter run are a function of the distributed load and the pile spacing (s).

The piled embankment geometry and material properties corresponding to the experimental study were used to calculate (W_G) following the BS 8006:1995 method. The load (W_G) was also calculated using the results of both the incremental and full

height tests. For the sake of consistency the values calculated using the test results were multiplied by the pile spacing (s) to enable a direct comparison with (W_G) obtained from the BS 8006:1995 method. The results of the comparative analysis are shown in **Figure 5-21**. The drawbacks of adopting the soil arching model proposed by John (1987) has been discussed previously and are manifested in the disparity between the measured and calculated values obtained for the distributed load (W_G).

In catering to the serviceability requirements, BS 8006:1995 identifies two surface deformation modes and are shown in **Figure 5-22**. However, only the limit state pertaining to the development of differential surface deformations is of relevance to the current study. To ensure that localised differential deformations cannot occur at the surface of embankments, BS 8006:1995 recommends that the relationship between the embankment height and the pile cap spacing be maintained as;

$$H \geq 0.7(s - b) \dots\dots\dots (5-20)$$

where b = pile cap width;
 s = spacing between adjacent piles;
 H = height of embankment.

The above limit on the embankment height implies that a depth ratio (H/s') should not decrease below a value of (0.7) to preclude the development of surface differential settlement.

The test results suggest that a minimum depth ratio (H/s') of (1.7) should be maintained if the development of differential settlement is to be prevented. Adoption of the minimum depth ratio specified by the BS 8006:1995 of (0.7) could result in the development of differential surface deformations

5.4 Summary

A reduced scale experimental investigation into the behaviour of piled embankments incorporating geotextile reinforcement was carried out. The controlling parameters investigated were the geometry and the tensile stiffness of the geosynthetic reinforcement. A worst case scenario was considered in which the foundation soil did not participate in the load sharing mechanism.

The pile caps were so instrumented to permit measurement of the average net load per pile tributary area and the component of the load transfer mechanism influenced the arching in the fill.

The ratio of the two load measurements expressed as a percentage was referred to as the efficacy (E) of the system.

The variation of the efficacy with the depth ratio indicated the existence of two mechanisms. The transition from one mechanism to another was observed to occur at depth ratio of approximately (2). In addition the maximum values for the efficacy appeared to increase with a corresponding increase in the pile cap size. It was concluded that the deep mechanism resulted in achieving the ultimate efficacy value and was influenced by the capping ratio, i.e., by the pile cap size.

Although it was not possible to test the modelling assumptions by 'modelling the model', the measured efficacy compared well with reported field measurements.

The differential surface settlement was found to be influenced mainly by the piled embankment depth ratio. The plane of equal settlement was observed to occur at a depth ratio range of (1.7-2) which coincides with the transition from a shallow to a deep piled embankment behaviour.

The deflected shape of the reinforcement was found to be adequately represented by both the circular and parabolic arc geometry.

Efficacy predictions were made using three frequently used analytical methods. On average, predictions made using the domed arch method proposed by Hewlett et al. (1988) showed a good overall agreement with the measured efficacy values. A modification factor (α) was proposed which improved the matching obtained between the predicted and measured values. Two values for (α) were proposed, (0.57) and (0.8), the latter value was found to produce a better fit with the incremental loading efficacy.

A rationale was proposed whereby the three-dimensional geometry of the basal reinforcement can be represented by a plane strain suspended cable formulation. The tensile stiffness used in the plane strain formulation should be reduced by the ratio of the cap width to the pile spacing (b/s) to achieve a load-deflection response equivalent to that of the three-dimensional system.

The Swedish Road Board (1974) recommends that the pile caps should cover a minimum of 17.5% of the embankment base. The current study has indicated that the provision of basal reinforcement permits the use of area ratios as low as 11%.

The British Standards for reinforced fills, BS 8006:1995, utilises the soil arching model proposed by John (1987) to obtain the distributed load acting on the basal reinforcement. A comparison between the measured and experimental values indicated that a disparity exists between the measured and calculated values.

Furthermore, the minimum depth ratio of 0.7 recommended by the BS 8005:1995 to avoid the development of differential surface deformations appears to be too liberal when compared with the surface settlement measurements obtained from the full height tests.

Table 5-1. Summary of maximum efficacy values for the full height and incremental loading tests

Capping Ratio (b/s')	Maximum Efficacy (%)	Depth Ratio (H/s')
1:1	93 (83)	3.33
1:1.4	89 (78)	2.86
1:2	85 (74)	2.5

() incremental loading values

Table 5-2. Comparison between field measurements and experimental results.

Piled Embankment Location	Area Ratio(%)	E (%)
M9 and M876 Motorways, Scotland. Individual concrete caps, geotextile strips used as reinforcement (Reid et al. (1983)).	10.6 (11.1)	82 (85)
Molasses storage tank, Scotland. Individual concrete caps, 1m ² , spaced at 2m apart on triangular grid. Dense granular fill 2m thick placed over pile caps (Thorburn et al. (1983)).	27.8 (25)	>90 (93)
Seremban-Air Hitam toll expressway, Malaysia. Individual concrete caps, 0.72m ² , spaced at 1.9 meters on square grid (Ooi et al. (1987))	19.9 (25)	86-90 (93)

() experimental results

Table 5-3. Summary of predicted efficacy values

b:s'	H/s'	E _{meas.} , (%)		E _{calc.} , (%)				
		I.L.	F.H.	A	B		C	
					cap	crown	K _r =1	K _r =0.8
1:2	0.5	21.0	23.7	27.4	75		26.1	23.4
	1.0	45.1	51.4	29.4	75	26.3	37.98	33.5
	1.5	59.7	73.2	30.3	75	48.0	47.1	41.8
	2.0	71.5	82.9	30.6	75	58.8	54.5	48.7
	2.5	73.6	85.2	30.8	75	65.3	60.4	54.47
1:1.4	0.57	27.3	35.1	41.1	86		35.1	32
	1.14	53.2	62.3	45.3	86	39.1	47.9	43.3
	1.71	65.9	78.3	46.7	86	58.1	57.5	52.1
	2.29	74	87	47.4	86	67.7	64.5	59
	2.86	78.1	90.2	47.8	86	73.4	69.9	64.5
1:1	0.67	40.6	43.1	57.0	92	5.9	44.9	41.6
	1.33	63.3	70.1	64.0	92	52.2	58.1	53.4
	2.00	71.8	83.3	66.4	92	67.7	64.1	62.1
	2.67	79.6	89.9	67.6	92	75.4	73.3	68.5
	3.33	82.8	93.1	68.4	92	80.1	77.9	73.4

(A) John (1987) - (B) Hewlett et al. (1988) - (C) Combarieu (1989) - (I.L.) incremental loading - (F.H.) full height

Table 5-4. Summary of the dimensional analysis results.

Material	b (m)	s (m)	wg (kN/m')	yg (m)	εg (%)	J _{avg.} (kN/m')	J _{mod} (kN/m')	$\left(\frac{yg}{L}\right)_{exp}$	$\left(\frac{yg}{L}\right)_{calc}$
P500	0.20	0.60	2.94	0.026	1.11	533	178	0.064	0.068
			3.97	0.029	1.43			0.073	0.075
			4.09	0.03	1.49			0.075	0.076
			4.25	0.031	1.59			0.077	0.077
			4.31	0.031	1.64			0.078	0.077
P500	0.25	0.60	2.91	0.018	0.72	612	257	0.052	0.057
			3.56	0.02	0.87			0.057	0.061
			3.73	0.021	0.91			0.059	0.062
			3.75	0.021	0.95			0.06	0.062
			3.82	0.022	1.03			0.062	0.062
P500	0.30	0.60	2.46	0.014	0.59	643	321	0.047	0.048
			3.24	0.015	0.69			0.051	0.052
			3.39	0.016	0.72			0.052	0.053
			3.41	0.016	0.76			0.053	0.053
			3.43	0.017	0.78			0.054	0.053

Table 5-4 (cont'd).

Material	b (m)	s (m)	wg (kN/m')	yg (m)	εg (%)	Javg. (kN/m')	Jmod (kN/m')	$\left(\frac{yg}{L}\right)_{exp}$	$\left(\frac{yg}{L}\right)_{calc}$
P165	0.30	0.60	2.56	0.018	0.99	220	110	0.061	0.069
			3.24	0.02	1.21			0.067	0.075
			3.26	0.021	1.25			0.068	0.075
			3.46	0.021	1.29			0.07	0.076
			3.48	0.021	1.33			0.071	0.076
Textomur	0.30	0.60	2.46	0.039	4.55	32	16	0.131	0.129
			3.32	0.043	5.48			0.143	0.143
			3.32	0.044	5.81			0.148	0.143
			3.42	0.045	5.98			0.15	0.144
			3.44	0.045	6.08			0.151	0.145

Chapter Six

Finite Difference Analysis

6.0 Introduction

The laboratory physical model was constructed to simulate an idealised case where the natural subgrade was not a participant in the load sharing process. Consequently, the control case consisting of an un-reinforced piled embankment was not possible to achieve. In addition, the practicality of scaling down the prototype geotextile reinforcement dictated a rather narrow tensile stiffness range. The numerical model, however, does not suffer from such limitations. A wider spectrum of stiffness values can be involved in a parametric study designed to assess the contribution of the reinforcement to the overall piled embankment behaviour. The objective of the numerical study was to examine some aspects of the piled embankment behaviour not covered by the experimental investigation.

6.1 The Finite Difference Method

The finite difference method is an established numerical technique used for the solution of differential equations. In the finite difference method, every derivative in the set of governing equations is replaced directly by an algebraic expression written in terms of the field variables at discrete points in space, Desai et al. (1977). Finite difference programs have been used with success in diverse areas of geomechanics, Cundall (1976) and Pyrah (1987).

Many finite difference programs use an explicit time-marching method to solve the algebraic equations whereas implicit matrix oriented schemes are more commonly used with finite elements. One of the attractions of the finite difference methods is that non-linearities can be treated without recourse to equivalent stiffnesses or initial stresses and initial strains.

Such techniques are required for matrix oriented programs to preserve the linearity dictated by the matrix formulation, Cundall (1976).

6.2 The Computer Program

The two-dimensional continuum code FLAC (Fast Lagrangian Analysis of Continua, ITASCA Consulting Group (1991)) was used to perform a parametric study. FLAC models continuum behaviour using an explicit Lagrangian finite difference technique. The numerical formulation of FLAC is described in detail by Cundall and Board (1988).

6.3 The Piled Embankment Problem

Only conditions close to the centre of a wide embankment resting on a layer of soft soil of finite depth underlain by a stiff stratum are considered in the numerical study. The analyses involves one unit cell as shown in **Figure 6-1**. Such a cell was assumed to be under one dimensional loading conditions, where no lateral movement occurs along the vertical boundaries. No consideration were given to the effect of the end conditions, leading to lateral spreading, which may significantly modify the behaviour close to the side slopes.

6.3.1 Modelling Considerations

The fill was idealised as an isotropic linear elastic-perfectly plastic material operating in the drained state, with its properties defined by a Young' modulus (E), Poisson's ratio (ν), angle of shearing resistance (ϕ), cohesion intercept (c) and angle of dilation (ψ). A Mohr-Coulomb failure surface was used in conjunction with a non-associated flow rule. The geosynthetic reinforcement was modelled using one dimensional cable elements that can sustain uniaxial tension only and have no lateral stiffness. The constitutive model governing the behaviour of these elements is elastic/perfectly plastic and is described by a yield strength (Y), a cross sectional area (A) and a tensile stiffness (J). The soft subsoil in the current study was represented by springs possessing a normal stiffness (k_n). The stiffness (k_n) was obtained by the following equation;

$$k_n = \frac{wE}{D} \dots\dots\dots (6-1)$$

where E = the elastic modulus, (N/m²);

D = the thickness of the soft subsoil, (m);

and w = width of the tributary grid zone, (m).

The solution procedure consisted of performing the required alterations, in the form of deleting or adding grid zones to simulate the required geometry then stepping the model to equilibrium under the action of the gravitational force (g). Equilibrium was conceived to be approached when the out-of-balance forces were less than a user defined value; in the study taken equal to $0.01N$.

In general the overall mesh dimensions and element size were chosen to ensure that for the geometry studied a balance between the time taken for the analysis and the accuracy of the results was achieved.

6.3.2 The Finite Difference Grid

A unit cell was considered to be of width, L , and height, H , resting on pile caps and subsoil as shown in **Figure 6-2**. The width of each pile cap was denoted by (b) . The width of the subsoil referred to as (s') , represents the clear span between adjacent pile cap edges.

The subsoil (a-a), was modelled as a Winkler type foundation consisting of springs possessing a normal stiffness (kn).

The vertical boundaries of the embankment, (b-b) and (c-c), were considered to be rigid and smooth. Typical grid discretisation and boundary conditions employed in the analyses are shown in **Figure 6-3**.

6.4 Preliminary Investigation

The load transfer process, the associated surface deformations and the reinforcement behaviour must be predicted with a reasonable degree of confidence to achieve a meaningful parametric study. Consequently, it was considered necessary to investigate the sensitivity of FLAC to the development of the gravitational stresses, the piled embankment geometry and the foundation stiffness prior to conducting the parametric study. In addition, the suitability of using a plane strain code to investigate the three dimensional geometry piled embankments was also examined.

The experimental investigation carried out by Tang (1992) was considered ideally suited for verification purposes. The plane strain conditions under which the experimental model was carried out would allow a direct comparison between the predicted and measured results.

As the three parameters (efficacy, competency and stress reduction ratio) are mathematically related, comparison between the results obtained from the finite difference analysis and the physical model tests were based only on the efficacy.

The two dimensional experimental study involved four capping ratios. Only the model tests involving the (1:4) and (1:9) ratios, however, were simulated numerically. The specified capping ratios were chosen since they represented the upper and lower limits of the investigated range. The analysis was limited to a depth ratio of (H/s') of 3. The piled embankment geometry, mesh size and the material properties used in the validation exercise are shown in **Table 6-1**.

6.4.1 Evolution of the Gravitational Force

The traditional approach to inducing the arching process is to apply a prescribed displacement to the nodes representing the surface of the yielding subsoil (Pyrah et al. (1996) and Koutsabeloulis et al. (1986)). It is then possible to specify the rate of displacement application to effect gradual process similar to that occurring in the prototype situation.

The presence of geotextile reinforcement at the interface between the yielding soil and the fill in the case of reinforced pile embankments precluded this approach.

In a discussion regarding the method of setting up the geostatic stresses, Chandler (1994) proposed that the gravitational force (g) should be 'switched on' in a gradual manner. The modelling philosophy adopted involved the application of the full gravitational force (g) in several equal increments. Although not duplicating the natural process, the procedure provided a convenient method to avoid shocking the system.

The influence of the number of increments used to attain the full gravitational force (g) was investigated for a capping ratio of (1:4) and depth ratios of (0.5) and (3). **Figure 6-4a** depicts the effect of applying the gravitational force gradually on the efficacy (E). It was observed that a limiting value for (E) was attained for a gravitational force applied in five equal increments. The effect of the number of increments used to achieve (g) on the vertical stress distribution bearing on the pile cap is shown in **Figure 6-4b**.

The stress was found to increase in the vicinity of the pile cap's edge for the case where the gravity was applied in five increments. On the other hand, applying gravity in one single increment produced larger stresses close to the centre of the pile cap. The predicted profile of the vertical stress distribution obtained by gradually applying the gravitational force was compared with field measurements reported by Rathmayer (1975) (**Figure 6-4b**). The similarity between the measured vertical stress profile and that obtained numerically attests to the suitability of applying the gravity incrementally.

6.4.2 The Stiffness of the Yielding Support

The soft subsoil in the experimental study conducted by Tang (1992) was simulated by the use of soft rubber foam. Tang proposed a constrained modulus of 200 kN/m² based on results of compression tests carried out on the rubber foam. The modulus value proposed by Tang was obtained by inspection of the initial linear elastic portion of the stress strain curves. The element of bias in selecting the elastic modulus justified investigating the influence the elastic modulus on the load transfer behaviour. The analysis was carried out for the same piled embankment geometry adopted in the previous section and using the proposed modelling methodology. Five different values for the elastic modulus of the soft foam were used in a parametric investigation, in addition the case of no support, i.e., an elastic modulus of zero was also analysed.

The variation of the efficacy (E) versus the elastic modulus of the rubber foam is shown plotted in **Figure 6-4c**. A comparison between the measured and predicted efficacy for the capping and depth ratios of (1:4) and (3), respectively, indicated the following:

- a. the predicted value of the efficacy was found to be sensitive to the elastic modulus of the rubber foam;
- b. an elastic modulus of 110 (kN/m²) resulted in better agreement between the predicted and measured efficacy values.

The load sharing process in a piled embankment is depicted in **Figure 6-4c**. The vertical component of the reinforcement tensile load (T_v) was also observed to

decrease with an increase in the foundation stiffness. A threshold value was attained for a modulus of elasticity of approximately 200 kN/m². Consequently, the efficacy of the system was found to decrease as more of the embankment weight is supported by the foundation. The maximum efficacy (E) was achieved for the theoretical case where the foundation does not contribute to the load sharing process.

It was not possible to extrapolate the previously described trends to full scale behaviour because scaling laws have not been rigorously considered, Low et al. (1994).

6.4.3 The Piled Embankment Geometry

The variation between the measured and calculated efficacy for the two capping ratios (b:s') investigated is shown in **Figure 6-5**. A good agreement was obtained between the predicted and measured values. The numerical technique was found capable of reproducing the load transfer mechanism of piled embankments incorporating geosynthetic basal reinforcement under plain strain conditions.

6.4.4 The Assumption of Plane Strain Conditions

Jardenah (1988) questioned the suitability of using a plane strain numerical model to represent piled embankment behaviour. To address this issue, the three dimensional geometry of the reduced scale laboratory model used in the current study was simulated using the plane strain finite difference code.

The finite difference grids and material properties used in comparison between the physical and numerical models are shown **Table 6-2**. The experimental measurements used to compare between the physical and numerical models were obtained from the full height simulations. Furthermore, only the tests involving the geotextile material Paraweb 500 were considered in the comparative study. The appropriate secant modulus value was obtained from the load-extension results of tensile strength tests performed on the Paraweb 500 strips.

The equivalence factor proposed in Chapter 5 was used to obtain a modified modulus value. The modified value was adopted in the subsequent numerical analyses to account for the three-dimensional geometry of the piled embankment system.

The following parameters provided the basis for comparison between the numerical and physical model results:

- i) the efficacy;
- ii) the stress reduction ratio;
- iii) the reinforcement deflection
- iv) the maximum and minimum surface settlement.

The above mentioned parameters were plotted against the depth ratio (H/s') for capping ratios (1:1) and (1:2). **Figures 6-6a** and **6-6b** show the predicted and the corresponding measured values. In general a reasonable agreement was achieved between the measured and predicted parameters.

The discrepancy between the predicted and measured values, however, was most evident for the surface deformations occurring above the pile cap centreline (ds_{min}). The numerical code was observed to under-estimate (ds_{min}), more so for the (1:1) capping ratio. The tendency to under-estimate (ds_{min}) led inevitably to a conservative prediction for the differential settlement. The disparity, however, was observed to reduce beyond a depth ratio of 2.5.

6.5 Parametric Study

A parametric study of the influence of reinforcement stiffness on the load transfer mechanism and the surface settlement in piled embankments was carried out using FLAC. The purpose of the study was not the production of a comprehensive set of design charts, the limitations imposed by the available time made such a task untenable. Instead, a series of limited scenarios were analysed to highlight the role of the geosynthetic reinforcement within the piled embankment system. The size of the finite difference grids and material properties are shown in **Table 6-3**. The parameters used for the embankment fill are typical of a compacted granular soil (Lawson et al. (1996)).

6.5.1 Un-reinforced Piled Embankments

It was considered useful at this stage to appreciate the limitations of adopting the piled embankment solution without incorporating geotextile reinforcement. The

stiffness of the foundation was arbitrarily chosen to correspond to a layer of soft highly compressible material six meters in depth overlying a rigid base.

Tomlinson (1986), recommended a coefficient of compressibility (m_v) of $1.5 \text{ m}^2/\text{MN}$ for organic clays and peat. The theory of elasticity was used to relate (m_v) and the Young's modulus (E_m) as follows:

$$E_m = \frac{(1 + \nu) \cdot (1 - 2\nu)}{(1 + \nu)} \cdot \frac{1}{m_v} \dots\dots\dots (6-2)$$

where (ν) = Poisson's ratio.

The piled embankment geometries investigated were limited to three capping ratios: i) 1:1; ii) 1:2 and iii) 1:3. A minimum value of 3 for the depth ratio was maintained to achieve the transition between the deep and shallow failure mechanisms.

The load transfer in the case of an un-reinforced piled embankment is achieved mainly through the arching process occurring in the granular fill. **Figure 6-7** shows the variation of the efficacy (E) with the depth ratio (H/s') for the three different capping ratios. The trends were found to be comparable to those obtained from the physical model tests. The ultimate efficacies increased with a decrease in the capping ratio. The transition from a shallow to a deep mechanism was achieved at a depth ratio of approximately 2. The influence of the piled embankment geometry on the differential settlement was investigated by plotting the angular distortion against the depth ratio (**Figure 6-8**).

The maximum angular distortion was found to occur at a depth ratio of (1) and ranged between (10.5-13.5)% for the investigated capping ratios. On exceeding a depth ratio of (1) the angular distortion was observed to decrease to a minimum value ranging between 0 and 1.1 (%) at a depth ratio of (3). At a depth ratio of (2), however, the angular distortion was observed to decrease considerably for a capping ratio of (1:3). The transition from a capping ratio of (1:1) to (1:3) resulted in a 70% reduction in the angular distortion, i.e., increasing the clear span between pile caps reduced the surface differential settlement. The tendency for 'uniform settlement' to develop in response to increasing the pile cap spacing, however, induced relatively large total surface settlements.

Figure 6-8 depicts the maximum and minimum surface settlements plotted against the depth ratio. The uniform surface settlement for a capping ratio of (1:3) was found to be approximately five times that obtained for the (1:1) capping ratio for a depth ratio (H/s') of (3). In contrast to the considerable reduction in the angular distortion achieved at a similar depth ratio (H/s').

The trend described above implies that increasing the pile cap spacing reduces the magnitude of the differential settlement. Bergdahl et al. (1979) reported the same pattern in their physical model tests. They concluded that the use of smaller pile caps and a larger centreline spacing induced uniform surface settlements to occur.

6.5.2 The Effect of Basal Reinforcement

The effect of introducing geosynthetic basal reinforcement on the load transfer process and the surface deformations of piled embankments was investigated for a wide range of tensile stiffnesses. The reinforcement load-extension behaviour was governed by;

$$J = 10B_L \dots \dots \dots (6-3)$$

where J = the tensile stiffness, (kN/m');

and B_L = breaking load, (kN/m').

The above relationship was maintained throughout to ensure consistency with current polymeric reinforcement (Lawson et al., 1996).

The influence of the introduction of the basal reinforcement on the performance of the piled embankments is shown in **Figure 6-9**. The increase in the efficacy is attributed to the vertical component of the axial tensile load developed in the reinforcement. The results indicate that the improvement in the system efficacy due to incorporating the geotextile reinforcement was greatest for fill heights with depth ratios (H/s') less than (2). A considerable reduction in the surface deformation was also observed to occur due to the incorporation of the geotextile reinforcement.

The effect of increasing the reinforcement stiffness (J) on reducing the surface deformations is depicted in **Figure 6-10**. The results show that the depth ratio (H/s') has a major effect on reducing the angular distortion and the maximum total

settlement. Furthermore, a relatively large increase in reinforcement stiffness is required to reduce the surface deformations significantly.

The influence of the depth ratio in reducing the angular distortion, however, was more pronounced for capping ratios less than (1:1). The marked reduction in the angular distortion in response to an increase in the depth ratio signified the onset of the uniform surface settlement mechanism. It was concluded that the surface settlement mechanism was similar to that identified in the un-reinforced piled embankment.

A maximum allowable surface deformation was established by the BS 8006:1995 to maintain serviceability of highway embankments. The BS 8006:1995 recommends that the maximum differential surface deformation should be limited to 1% and 2% for principal and non-principal roads, respectively. The angular distortion used in the current study is analogous to the parameter (ds/Ds) defined by BS 8006:1995. The results shown in **Figure 6-11** indicate that the adoption of a depth ratio (H/s') of (3) ensured that the differential surface deformations are within the 1% limit specified by BS 8006 (1995) for the investigated range reinforcement stiffness. A significant reduction, however, is achieved in the differential settlements using basal reinforcement for piled embankments with depth ratios less than a value of (1.5).

Satisfying the serviceability criteria pertaining to differential surface deformation does not preclude the occurrence of excessive total settlements. In addition, the adoption of restrictions on the depth ratio does not ensure that the maximum total settlements are within specified limits. It may be possible to control the total surface settlement by specifying an upper limit on the maximum mid span deflection suffered by the basal reinforcement. Consequently, the dimensionless parameter (R) is suggested;

$$R = \left(\frac{ds - \max}{y_g} \right) \cdot \left(\frac{b}{s} \right) \dots\dots\dots (6-3)$$

where H = height of fill, (m);
 b = width of pile cap, (m);
 s = pile cap centreline spacing, (m);
 y_g = maximum geotextile deflection, (m).

The parameter (R) combines the reinforcement deflection, the ratio of the cap width to the pile centreline spacing and the maximum surface settlement.

The above parameter was plotted against the depth ratio for three different geotextile stiffnesses (**Figure 6-12**). The results clearly indicated that the reinforcement stiffness does not influence the proposed dimensionless parameter. The piled embankment geometry represented by the height of fill pile cap size and spacing ratios were found to have the most significant effect. The parameter (R) was observed to achieve a common value of approximately 0.2 at a depth ratio of (3) for the investigated range of capping ratios. **Figure 6-13** depicts the dimensionless parameter (R), calculated using the experimental results, plotted against the depth ratio. The trend indicates that the parameter (R) attained a threshold value ranging between 0.2 to 0.24 for depth ratios exceeding 1.5.

6.6 Summary

The suitability of the finite difference code (FLAC) for the numerical simulation of piled embankment behaviour has been investigated. The sensitivity of the code to the method of applying the gravitational force was demonstrated. The lower the depth ratio (H/s') the more sensitive the results were to the number of increments required to achieve the full gravitational force.

The vertical stress distribution across the pile cap was shown to compare well with field measurements for the incremental method of applying gravity. The foundation stiffness was shown to have a significant effect on the load transfer mechanism.

The use of the plane strain code to simulate the three-dimensional behaviour indicated that for the reinforcement deflection and the system efficacy reasonable agreement was achieved between the calculated and measured values. However, the numerical method was found to over-estimate the surface differential settlement.

A parametric study using the finite difference code was carried out for three capping ratios ($b:s'$); (i) 1:1, (ii) 1:2 and (iii) 1:3. The three pile cap spacings used were 1.0m, 2.0m and 3.0m. The cap width, however, was maintained at 1.0 meters. The depth ratio varied from 0.5 to 3.0 to encompass both the shallow and deep mechanisms.

The parametric study carried out demonstrated that an increase ranging from 18% to 40% in the efficacy can be achieved as result of incorporating basal geotextile reinforcement in piled embankment systems. A reduction in the angular distortion was also brought on by the reinforcement. However, the depth ratio was identified as the parameter having the most significant effect in eliminating the surface differential settlement.

For the reinforced piled embankment scenario, the same geometries and fill properties were adopted. However, four different tensile stiffness values for the reinforcement were considered ranging from 500 kN/m' to 10000 kN/m' were employed in a parametric study to investigate the effect of the reinforcement on serviceability.

The results show clearly that the depth ratio has a major effect on reducing surface differential deformation with the reinforcement having a relatively minor secondary effect. A relatively large increase in the reinforcement stiffness is required to reduce the surface differential deformation significantly.

Satisfying serviceability requirements pertaining to angular distortion does not necessarily preclude the development of undesirable total settlements. A reduction in the angular distortion can be accompanied by unacceptable uniform surface settlement.

Consequently, for specified piled embankment geometry and an allowable maximum total surface settlement (d_{s-max}), the maximum geotextile deflection (y_G) can be determined through the dimensionless parameter (R).

The parameter (R) provides a convenient method of restricting the maximum reinforcement deflection to comply with a specified maximum allowable surface settlement.

Table 6-1. Material parameters and mesh size used in the preliminary analysis

Geometry and Mesh Size			
Capping Ratio, (b:s')	Depth Ratio, (h/s')	Cap Width (b), m	No. of Grid zones
1:4	0.5 - 3	0.025	1240
1:9	0.5 - 3	0.0125	2140
Material Properties			
Material	Parameter	Value	
Fill	Friction, ϕ	38	
	Cohesion, c	0	
	Dilation, ψ	0	
	Bulk modulus, (N/m ²)	5.13e6	
	Shear modulus, (N/m ²)	1.46e6	
	Unit weight, (kN/m ³)	14.2	
Foundation	kn, (N/m')	varies	
Geotextile	Stiffness, J (N/m')	varies	

Table 6-2 Material parameters and mesh size used in the simulation of the 3-D model tests

Geometry and Mesh Size			
Capping Ratio, (b:s')	Depth Ratio, (h/s')	Cap Width (b), m	No. of Grid zones
1:1	0.67 - 3.33	0.3	820
1:2	0.5 - 2.5	0.2	615
Material Properties			
Material	Parameter	Value	
Fill	Friction, ϕ	36	
	Cohesion, (N/m ²)	0	
	Dilation, ψ	0	
	Bulk modulus, (N/m ²)	5.13e6	
	Shear modulus, (N/m ²)	1.46e6	
	Unit weight, γ	17.1	
Foundation	kn, (N/m')	N/A	
Geotextile	Stiffness, J, (N/m')	varies	

Table 6-3. Material parameters and mesh size used in the parametric analysis

Geometry and Mesh Size			
Capping Ratio, (b:s')	Depth Ratio, (h/s')	Cap Width (b), m	No. of Grid zones
1:1	0.5 - 3	1.0	840
1:2	0.5 - 3	1.0	630
1:3	0.5 - 3	1.0	630
Material Properties			
Material	Parameter	Value	
Fill	Friction, ϕ	38	
	Cohesion, c	0	
	Dilation, ψ	0	
	Bulk modulus, (N/m ²)	70e6	
	Shear modulus, (N/m ²)	25e6	
	unit weight, (kN/m ³)	20.0	
Foundation	k_n , N/m'	varies	
Geotextile	Stiffness, J, (N/m')		

Chapter 7

Conclusions and Design Recommendations

7.0 Introduction

Embankments are supported on piles and basal reinforcement to reduce costs, to overcome the problem of differential surface deformations and to expedite the construction process.

The current design techniques are based on analytical solutions that involve simplifying assumptions that have yet to be verified. The current research was carried out to evaluate, through a parametric study, the influence of various factors on the behaviour of piled embankments incorporating basal reinforcement and to assess the validity of a number of analytical formulations.

The test apparatus represented a square grid of centrally located piles sufficiently distant from the side-slopes to represent the centre of a piled embankment. The piles were provided with individual caps to represent the three dimensional nature of the system. The use of roller clamps capable of restraining the reinforcement from horizontal movement yet allowing vertical translation permitted modelling of the boundary conditions.

Thirty-three model-scale tests were carried out during the study, the parameters investigated include:

i. Embankment Geometry:

The embankment geometry was represented by two parameters, the depth ($H:s'$) and capping ($b:s'$) ratios. Five different embankment heights (H) were investigated to encompass a range of depth ($H:s'$) ratios ranging from (0.5) to (3.33). The pile caps were square in plan and varied in width from 0.2m to 0.3m to give a capping ($b:s'$) ratio ranging from (1:1) to (1:2). The depth ratio was limited to 3.33 to avoid the development of excessive wall friction that could affect the experimental results. The capping ratios used in the study resulted in an area ratio of (11%) to (25%). These area ratios represent typical piled embankment schemes used in the construction industry.

ii. Reinforcement Tensile Stiffness

The basal reinforcement consisted of a mesh made up of geosynthetic strips. The materials used were Paraweb 500, Paraweb 165, Stratagrid and Textomur.

The materials were chosen to give a tensile stiffness range of 50 to 500 kN/m'. According to the scaling laws, established on the basis of a dimensional analysis, the aforementioned values correspond to full scale polymeric materials possessing stiffness moduli ranging from 1250 kN/m' to 12500 kN/m'.

iii. Loading Conditions:

The experimental procedure was varied in an attempt to bracket the possible loading regimes the basal reinforcement might encounter during its design life. The two procedures adopted were the full height and incremental loading methods. The full height tests were carried out by achieving a height of fill representing a specified depth (H/s) ratio first before the movable base was released. The basal reinforcement was not provided with any support from the movable base during the construction of the sand deposit. The full height method provided the means to investigate the development of post construction surface settlement while the incremental procedure represented the loading regime the geotextile reinforcement might encounter during the construction process.

7.1 The Experimental Study

The model pile caps were instrumented to obtain the following load measurements:

- i. Ta-avg.: the pile cap load influenced by the arching process;
- ii. Tn-avg.: the average net load per pile cap tributary area.

The load transfer process was investigated by the variation of the efficacy, defined as the ratio of Ta-avg to Tn-avg expressed as a percentage, versus the depth ratio. The effect of using different capping ratios, tensile stiffnesses and loading conditions indicated the following:

- i. the shape of curves depicting the variation of the load transfer parameters with the depth ratio for different pile cap sizes indicated the presence of two modes

of behaviour. The initial portion of the curve up to a depth ratio of approximately (2) pertained to a shallow failure mechanism influenced primarily by the depth ratio. Beyond a depth (H/s') ratio of (2), the slope of the curves was observed to flatten indicating that a deep failure mechanism had been attained. The deep mechanism was found to be affected predominantly by the pile cap size and spacing.

- ii. T_a -avg. was observed to be insensitive to the tensile stiffness of the basal geosynthetic reinforcement. The variation of the efficacy with the settlement ratio also indicated that the load contributed to the pile by the arching mechanism attains a threshold value at a relatively small settlement ratio.

Predictions of the piled embankment efficacy were made using different analytical solutions for the model geometries and the insitu sand properties. Three different analytical solutions to the problem of arching in piled embankments were used. The solutions were based on the concept of projecting subsurface conduits, or assuming a model formed as suspended hemispherical vaults model.

On average the predictions made using the suspended hemispherical vaults method (Hewlett and Randolph (1988)) were closest to the measured efficacy values.

The method also accounts for the shallow and deep modes of behaviour identified in the load transfer curves obtained from the experimental test measurements. The efficacy of the system was found to be governed by crown stability for the shallow mechanism. The pile cap size and spacing governed the magnitude of the ultimate system efficacy for the deep mechanism.

The results of the full height simulations provided the surface deformation measurements which indicated the following:

- i. The differential settlement was found to be insensitive to the investigated range of tensile stiffnesses. The dominant parameter affecting the development of differential settlement was found to be the depth ratio (H/s').
- ii. The plane of equal settlement was observed to occur at a depth ratio ranging from (1.7) to (2) beyond that a uniform total settlement developed.

A rationale was proposed whereby the three-dimensional geometry of the basal reinforcement can be represented by a plane strain suspended cable formulation.

The tensile stiffness used in the plane strain formulation should be reduced by the ratio of the cap width to the pile spacing (b/s) to achieve a load-deflection response equivalent to that of the three-dimensional system.

The Swedish Road Board recommends a maximum limit on the permissible capping ratio which implies a minimum pile cap coverage of 17.5 % of the base of the embankment. The experimental results, however, have demonstrated that a coverage of as low as 11.1% is feasible.

BS 8006:1995 method employs a two step approach in designing the basal reinforcement used in piled embankments.

The distributed load acting on the reinforcement is obtained by using the soil arching model proposed by John (1987). The tensile loads generated in the reinforcement are then calculated using a parabolic arc formulation.

The method treats each mechanism separately assuming that the tensile strain developed in the reinforcement is compatible with the load obtained from the arching in the soil. In the current study the measured efficacy of the system was found to be insensitive to the reinforcement settlement ratio. The efficacy is a direct measure of the arching in the fill due to the instrumentation arrangement in the pile caps, it was concluded that the de-coupling approach used by BS 8006:1995 is appropriate.

The distributed load calculated using BS 8006:1995 was found to exhibit the drawbacks of the soil arching model proposed by John (1987) when compared with the measured values. It is possible to conclude that the formulations used by BS 8006:1995 to calculate the distributed load (W_G) are inappropriate due to the unjustified assumptions employed in the soil arching model proposed by John (1987).

Furthermore, the minimum depth ratio of (0.7) recommended by the BS 8006:1995 to preclude the development of differential surface deformations was found to be less than the depth ratios (H/s') corresponding to the plane of equal settlement obtained from the experimental study.

7.2 The Finite Difference Analysis

The numerical study was carried out to examine a wider range of parameters and conditions than those investigated in the experimental study. The analysis was performed in three stages, as follows:

Stage 1: The results of a plane strain experimental study were used to assess the suitability of the numerical code to simulate the behaviour of piled embankments incorporating geosynthetic reinforcement. The setting up of the gravitational stresses was carried out incrementally to simulate the gradual process occurring in the field. The numerically predicted parameters were found to be in good agreement with their measured counterparts which attests to the suitability of the modelling strategy.

Stage 2: The program was used to simulate the model tests of the current study. The numerical results were then compared with the measured values to assess the suitability of using a plane strain formulation to model the behaviour of an essentially three-dimensional system.

The numerical results were found to achieve reasonable matching with the measured values with regards to the reinforcement deflection and the system efficacy. However, the program was found to over-estimate the magnitude of the surface differential settlement.

Stage 3: A parametric analysis was carried out to investigate the behaviour of an unreinforced piled embankment and the role of the basal reinforcement in limiting the surface deformations. The following points summarise the main conclusions:

- i. Increasing the pile cap spacing for a constant pile cap size induces the development of uniform settlements, the magnitude of the associated total settlement, however, can be unacceptable from the serviceability point of view.
- i. The results indicated that the depth ratio has a major effect on reducing the surface differential settlement with the reinforcement having a relatively secondary effect. Increasing the depth ratio induces the development of the deep mechanism which is associated with uniform rather than differential surface settlement. A relatively large increase in reinforcement settlement is required to reduce the surface differential deformation significantly.

- iii. It was also noted that a unique combination of both reinforcement stiffness and a specified depth ratio is required to satisfy a prescribed serviceability requirement. Thus continuum methods are the only techniques that can carry out a serviceability limit analysis of basally reinforced piled embankments.
- iv. Satisfying serviceability requirements pertaining to differential settlement does not necessarily preclude the development of undesirable total settlements. A reduction in the differential settlement can be accompanied by unacceptable uniform surface settlement.
- v. Consequently, for a specified piled embankment geometry and an allowable total surface settlement (d_{s-max}), the maximum geotextile deflection (y_g) can be determined through the dimensionless parameter (R).

7.3 Design Recommendations

A general set of recommendations to be followed in the design of piled embankments incorporating geosynthetic reinforcement is described in the following:

- a. For a given embankment height (H), the pile cap spacing shall be chosen to achieve a minimum depth ratio of (1.7) to prevent the development of surface settlement.
- b. For a maximum allowable total settlement and a specified pile cap size the maximum mid-span deflection of the reinforcement can be determined using the parameter (R) which attains an average value of 0.2 for depth ratios greater than (1.5).
- c. The efficacy can then be calculated using the equations proposed by Hewlett and Randolph (1988) modified by the (α) value. The average uniformly distributed load acting on the reinforcement can then be obtained by equilibrium of vertical forces.
- d. The required tensile stiffness can then be obtained for the reinforcement deflection and applied uniformly distributed load obtained from steps (b) and (c) using the modified cable formulation .

7.4 Recommendations for Future Research

The following points represent areas where further research is still required

- i. The current experimental study has been carried out under static self-weight conditions, the effect of dynamic loads and vibration effects have not been investigated.
- ii. A study carried out under multi-gravity conditions in a centrifuge to investigate the influence of scale effects.
- iii. The effect of utilising a well graded material to represent the embankment fill.
- iv. The measurement of the insitu stiffness of sand deposits is associated with difficulties, therefore it is recommended to use the results of the experimental study to calibrate a three-dimensional numerical analysis to investigate the influence of the soil stiffness on the system behaviour. The calibrated model can also be used to produce a set of comprehensive design charts that embrace a wide range of field conditions.

REFERENCES

References

- Adachi, T., Kimura, M., and Tada, S. (1989). 'Analysis on the Preventative Mechanism of Landslide Stabilising Piles', Proceedings, 3rd International Symposium on Numerical Models in Geomechanics, Elsevier Applied Science, London, pp. 691 - 698.
- Agaiby, S.W. (1991). ' An Experimental Study of The Behaviour of Drilled Shaft Foundations Subjected to Static and Repeated Lateral and Moment Loading Under Drained Conditions', D.Ph. thesis, Cornell University, Ithaca, NY.
- Ali, F.H., (1990). 'A Model Study on Embankment Piles', Proceedings, Piletalk International, Jakarta, Indonesia, pp. 35 - 40.
- Atkinson, J. H. and Potts, D.M. (1977). 'Stability of A Shallow Circular Tunnel in Cohesionless Soil'. *Geotechnique*, Vol. 27, No.2, pp. 203 - 215.
- Azzam T., Raman K., Ali, F. H. (1990). 'Geotechnical Assessment of Distressed Piled Embankments on Soft Ground', Proceedings, Seminar on Geotechnical Aspects of the North-South Expressway, Kuala Lumpur, Malaysia, pp. 269 - 274.
- Barry, A. J., Trigunarsyah, B., Symes, T. and Younger J. (1995). 'Geogrid Reinforced Piled Road Over Peat', *Engineering Geology of Construction*, The Geological Society, London, pp. 205 - 210.
- Basset, R.H. (1979). 'The Use of Physical Models in Design', Proceedings, 7th European Conference, Soil Mechanics and Foundation Engineering, Brighton, Vol.4, pp. 253 - 270.
- Basset, R.H. and Horner, J.N. (1979). 'Prototype deformations from Centrifugal Model Tests', Design Parameters in Geotechnical Engineering, Proceedings, 7th European Conference, Soil Mechanics and Foundation Engineering, Brighton, Vol.2, pp.1 - 10.
- Bell, A.L., Jenner, C., Maddison, J.D. and Vignoles, J. (1994). 'Embankment Support Using Geogrids with Vibro Concrete Columns', Proceedings, 5th International

Conference on Geotextiles, Geomembranes and Related Products, Vol. 1, Singapore, pp.335 - 338.

Bergdahl, U., Lingfors, R., and Nordstrand, P. (1979). 'The Mechanics of Piled Embankments', Swedish Geotechnical Institute, Report No. SG3-79, pp. 310 - 320.

Bieganousky, W. A. and Marcuson, III, W.F. (1976). 'Uniform Placement of Sand', Journal of the Geotechnical Engineering Division, American Society of Civil Engineering, Vol. 102, No.GT3, pp. 229 - 232.

Bolton, M.D. (1979). A Guide to Soil Mechanics, Macmillan Education Ltd., London.

Bolton, M.D. (1986). 'The Strength and Dilatancy of Sands', Geotechnique, Vol.36, No.1, pp. 65 - 78.

Broms, B. B. (1979). 'Problems and Solutions to Construction in Soft Clay', Proceedings, Sixth Asian Regional Geotechnical Conference on Soil Mechanics and Foundation Engineering, Bangkok, Vol.2, pp. 3-38.

Broms, B. B. and Hansbo, S. (1981). Soft Clay Engineering, Elsevier Publishing Company, pp. 417 - 480.

Broms, B. and Wong, K. (1985). 'Embankment Piles', Proceedings, 3rd International Geotechnical Seminar on Soil Improvement Methods, Singapore, pp. 167 - 178.

BS 8006 : 1995. 'Code of Practice for Strengthened/Reinforced Soils and Other Fills', British Standards Institution.

Bujang, B. K. H., Craig, W.H., and Merrifield, C.M., (1991). 'Simulation of a Trial Embankment Structure in Malaysia', Centrifuge 91, (editors) Ko and Mclean, Balkema, Rotterdam, pp. 51 - 58.

Bujong, B. K. H. (1990). 'Simulation of Field Trial Structures in Malaysia', D.Phil. thesis, University of Manchester, U.K.

Bulson, P.S. (1985). 'Buried Structures: Static and Dynamic Strength', Chapman and Hall, London.

Butterfield, R. and Andrawes, K. Z. (1972). 'On Angles of Friction Between Sand and Plane Surfaces', *Journal of Terramechanics*, Vol.8, pp. 15 - 23.

Butterfield and Andrawes, K.Z., (1976). 'An Air Activated Sand Spreader for Forming Uniform Sand Beds', *Geotechnique*, Vol.20, pp. 77 - 90.

Card, G.B. and Carter, G. R. (1995). 'Case History of A Piled Embankment in London's Docklands', *Engineering Geology of Construction*, The Geological Society, London, pp. 79 - 84.

Chandler, H. W.(1994). Personal communication.

Chin, F. K. (1985). 'The Design and Construction of Highway Embankments on Soft Clay', *Proceedings, 8th South East Asian Geotechnical Conference, Kuala Lumpur*, Vol.2, pp. 42 - 60.

Combarieu, O. (1989). 'Embankments on Soft Soils Improved by Vertical Rigid Inclusions', *Proceedings, 12th ICSMFE, Rio de Janiero*, pp. 1723 - 1724.

Craig, W.H. (1979). Discussion, Design Parameters in Geotechnical Engineering, *Proceedings, 7th European Conference, Soil Mechanics and Foundation Engineering, Brighton*, Vol.4, p.341.

Cundall, P.A. and Board, M.(1988). 'A Microcomputer Program For Modelling Large-Strain Plasticity Problems', *Proceedings, 6th International Conference on Numerical Methods in Geomechanics, Innsbruck, Austria*.

Cundall, P.A. (1976). 'Explicit Finite-Difference Methods in Geomechanics', *Proceedings, The EF Conference on Numerical Methods in Geomechanics, Blacksburg, Virginia, 1976*, Vol.1, pp. 132-150.

Demiris, C. A. (1987). 'Investigation of Boundary Friction Effects in Polyaxial Tests', *Geotechnical Testing Journal*, Vol.10, No.2, pp. 86 - 90.

Desai, C.S. and Christian, J.T., (1977). 'Numerical Methods In Geomechanics', McGraw-Hill, New York.

Donovan, K., and Cepak, M. (1984). 'Finite Element Approach to Cable Bolting in Steeply Dipping VCR Stopes', *Geomechanics Applications in Underground Hardrock*

- Mining, editor (Pariseau, W. G.), New York Society of Mining Engineering, pp. 65 - 90.
- Duncan, J.M. and Chang, C. Y. (1970). 'Non-Linear Analysis of Stress and Strain in Soils', Journal of Soil Mechanics and Foundation Engineering, ASCE, SM5, pp. 1629 - 1653.
- Finn, W. D. (1963). 'Boundary Value Problems of Soil Mechanics'. Journal of Soil Mechanics and Foundations Division, ASCE, Vol. 89, No.SM5, pp. 39 - 51.
- FLAC (Fast Lagrangian Analysis of Continua, Version 3.0), (1991). Itasca Consulting Group, Inc., Minneapolis, Minnesota 555414, USA.
- Fluet, J. E., Christopher, B. R., and Slaters, A. R., Jr., (1986). 'Geosynthetic Stress-Strain Response Under Embankment Loading Conditions', Proceedings, Third International Conference on Geotextiles, Vienna, Vol. 1, pp. 175 - 180.
- Getzler, Z. and Komornik, A. (1968). 'Model Study on Arching Above Buried Structures', Journal of Soil Mechanics and Foundations Division, ASCE, Vol. 94, SM5, pp. 1123 - 1141.
- Handy, R. L. (1985). 'The Arch in Soil Arching'. Journal of Geotechnical Engineering, ASCE, Vol. 111, No.3, pp. 302 - 318.
- Hassan, C.B. (1992). 'The Use of Flexible Transverse Anchors in Reinforced Soil', D.Phil thesis, University of Newcastle-Upon-Tyne.
- Hewlett, W. J. and Randolph, M. F. (1988). 'Analysis of Piled Embankments', Ground Engineering, Vol.21, No.3, pp. 12 - 18.
- Holmberg, S. (1978). 'Bridge Approaches on Soft Clay Supported by Embankment Piles', Journal of Geotechnical Engineering, Vol. 10, No.1, pp. 77 - 89.
- Holtz, R. D., and Massarch, K. R. (1976). 'Improvement of the Stability of an Embankment by Piling and Reinforced Earth', Proceedings, 6th European Conference on Soil Mechanics and Foundation Engineering, Vol. 1.2, Vienna, pp.473 - 478.
- Jardaneh, I. G., (1988). 'Finite Element Analysis For Preliminary Study of BASP System', M. Sc. thesis, University of Newcastle-Upon-Tyne.

-
- Jarret, N. D., Brown, C. J. and Moore, D. B. (1995). 'Pressure Measurements in a Rectangular Silo', *Geotechnique*, Vol.45, No.1, pp. 94 - 104.
- Jarret, N. D., Brown, C. J. and Moore, D. B. (1992). 'Obtaining Accurate Pressure Measurements in a Stored Granular Medium', *Canadian Geotechnical Journal*, Vol.29, pp. 217 - 224.
- Jewel, R. A. (1980). 'Some Effects of Reinforcement on the Mechanical Behaviour of Soils', D.Ph. thesis, University of Cambridge, U.K.
- John, N. W. M. (1987). *Geotextiles*, Blackie, Chapman and Hall, New York.
- Jones, C. J. F. P., Lawson, C. R. and Ayres, D. J., (1990). Proceedings, Fourth International Conference on Geotextiles, Geomembranes and Related Products, The Hague, Vol. 1, pp. 155 - 160.
- Jones, C.J.F.P., Lawson, C.R., Kempton, G.T. and Passaris, E.K.S. (1994). 'Advanced Analysis of Reinforced Fills over Areas Prone to Subsidence', Proceedings, 4th International Conference on Geosynthetics, Singapore, Vol.1, pp. 311 - 316.
- Kerisel, J.L. (1967). Scaling laws in soil Mechanics. Proc. 3rd Pan-American Conf. SMFE, Venezuela, Vol. 3 pp. 69-92.
- Kondner, R. L. and Zelasko, J.S. (1963). 'A Hyperbolic Stress-Strain Foundation for Sands', Proceedings, Second Pan-American Conference Soil Mechanics and Foundation Engineering, Brazil, Vol. 1, pp. 289 - 324.
- Koutsabeloulis N. C. and Griffiths D. V. (1989). 'Numerical Modelling of the Trap Door Problem'. *Geotechnique*, Vol. 39, No.1, pp. 77 - 89.
- Ladanyi, B. and Hoyaux, B. (1969). 'A Study of the Trapdoor Problem In a Granular Mass', *Canadian Geotechnical Journal*, Vol. 6, No.1, pp. 1 - 14.
- Lambe T.W. and Whitman, R. V. (1969). 'Soil Mechanics', John Wiley and Sons Inc., New York, NY.
- Langhaar, H.C. (1951). 'Dimensional Analysis and the Theory of Models'. John Wiley and Sons Inc., New York, NY.

Lawson, C. R., Jones, C.J.F.P. and Kempton, G. T. (1996). 'Some Factors Affecting the Structural Performance of Reinforced Fills Spanning Voids', Proceedings, I.S. Kyushu, Japan.

Leonard, J.W. (1988). Tension Structures, McGraw-Hill, New York.

Love, J. P. (1984). 'Model Testing of Geogrids in Unpaved Roads', D. Phil. Thesis, University of Oxford, Oxford, U.K.

Low, B. K., Tang, S. K. and Choa, V. (1994). 'Arching in Piled Embankments', Journal of Geotechnical Engineering, ASCE, Vol. 120, No.11, 1917 - 1938

Magnan, J. (1994). 'Methods to Reduce the Settlement of Embankments on Soft Clay: A Review', Speciality Conference on the Foundations and Emabankments Deformations, American Society of Civil Engineers, (Geotechnical Sprcial Publication No. 40), pp. 77 - 90.

Marshall, W. T. and Nelson, H. M. (1986). 'Structures', Longman Scientific and Technical, Essex, U.K.

Marston, A. and Anderson, A.O. (1913). 'The Theory of Loads on Pipes in Ditches and Tests of Cement and Clay Drain Tile and Sewer Pipe', Bulletin No. 31, Iowa Engineering Experiment Station, Ames, Iowa.

Mckelvey J. A. (1994). 'The Anatomy of Soil Arching', Journal of Geotextiles and Geomembranes, Vol. 13, pp. 317 - 329.

McNulty, J.W. (1965). 'An Experimental Study of Arching in Sand', D. Ph. thesis, 1961, University of Urabana, Illinois, U.S.A.

Milligan, G. W. E. (1982). 'Some Scale Model Tests to Investigate the Use of Reinforcement to Improve the Performance of Fill on Soft Soil', Journal of Engineering Geology, Vol.15, pp.209 - 215.

Mori, K., Seed, H. B., and Chan, C. K. (1977). 'Influence of Sample Disturbance on Sand Response to Cyclic Loading', Report UCB/EER-77/03, University of California, Berkley, California.

- Oda, M., Koishikawa, I. and Higuchi, T., (1978). 'Experimental Study of Anisotropic Shear Strength of Sand by Plane Strain Test', *Soils and Foundations*, Vol. 18, No.1, pp. 25 - 38.
- Ooi, T. A., Chan, S. F., and Wong, S. N. (1987). ' Design, Construction and Performance of Pile Supported Embankments', *Proceedings, 9th Southeast Asian Geotechnical Conference, Bangkok, Thailand*, pp. 2-1 - 2-12.
- Palmeira, E.M. and Milligan, G.W.E (1989). 'Scale and Other Effects Affecting the Results of Pull-out Tests of Grids Buried in Sand', *Geotechnique*, Vol.39, No.3, pp.511 - 524.
- Pyrah, I. C. and Othman, M.Z. (1996). 'Analysis of Piled Embankments', *Proceedings, 12th Southeast Asian Geotechnical Conference, Kuala Lumpur*, Vol. 1, pp. 271 - 278.
- Pyrah, I.C. (1987). 'Elasto-Plastic Analysis in Geotechnical Engineering Using Finite Differences', *Proceedings, International Conference on Computational Plasticity*, Vol.2, Spain, pp. 1607 - 1620.
- Rad N. S. and Tumay, M.T., (1987). 'Factors Affecting Sand Specimen Preparation by Raining', *Geotechnical Testing Journal*, Vol.10, No.1, pp. 31 - 37.
- Rathmayer, H. (1975). 'Piled Emabnkment Supported By Single Pile Caps', *Proceedings, Istanbul Conference on Soil Mechanics and Foundation Engineering*, pp.283 - 290.
- Reid, W. M., and Buchanan, N. W. (1983). 'Bridge Approach Support Piling', *Proceedings, The International Conference on Advances in Piling and Ground Treatment for Foundations*, Institution of Civil Engineering, London, pp. 267 - 274.
- Roark, R. J. (1989). 'Roark's Formulas for Stress and Strain', (editor W.C. Young) McGraw-Hill Book Co., New York.
- Rocha, M. (1957). The possibilty of solving soil mechanics problems by the use of models. *Proc. 4th Int. Conf. SMFE, London*, Vol. 2 pp.183-188.
- Spangler, M.G., (1960). 'Soil Engineering', International Textbook Company, Scranson, Pennsylvania.

Stroud, M. A. (1971). 'The Behaviour of Sand at Low Stress Levels in the Simple Shear Apparatus', D.Phil thesis, University of Cambridge.

Swedish Road Board (1974). Embankment Piles, Report No.TV121.

Tanaka, T. and Sakai, T. (1993). 'Progressive Failure and Scale Effect of Trapdoor Problems with Granular Materials', Soils and Foundations, Japanese Society of Soil Mechanics and Foundation Engineering, Vol. 33, No.1, pp. 11 - 22.

Tang, S., K. (1992). 'Arching in Piled Embankments', M.E thesis, Nanyang Technological University, Singapore.

Tatsuoka, F. and Haibara, O. (1985). 'Shear Resistance Between Sand and Smooth or Lubricated Surfaces', Soils and Foundations, Japanese Society of Soil Mechanics and Foundation Engineering, Vol.25, No.1, 89 - 98.

Terzaghi, K. (1943). Theoretical Soil Mechanics, John Wiley and Sons, New York.

Terzaghi, K. (1936). 'Stress Distribution in Dry and in Saturated Sand Above a Yielding Trapdoor', Proceedings, 1st International Conference on Soil Mechanics and Foundation Engineering, Cambridge, Mass., Vol. 1 pp. 307 - 311.

Thorburn, S., Laird, C. L., and Randolph, M. F. (1983). 'Storage Tanks Founded on Soft Soils Reinforced with Driven Piles', Proceedings of the International Conference on Advances in Piling and Ground Treatment for Foundations, ICE, London, pp. 157 - 164.

Ting, W. H. and Toh, C. T. (1983). 'Pile Supported Fill', Proceedings, Symposium on Recent Developments in Laboratory and Field Tests and Analysis of Geotechnical Problems, Bangkok, pp. 95 - 100.

Tomlinson, M.J. (1986). 'Foundation Design and Construction', Longman Scientific and Technical, Essex, U.K. p. 536.

Tschebotarioff, G.P. (1973). Foundations, Retaining and Earth Structures, McGraw-Hill, New York.

Van Horn, A. D. (1963). 'A Study of Loads on Underground Structures', part III, Iowa Engineering Experiment Station.

Vardoulakis, I. Graf B. and Gudehus G. (1981). 'Trapdoor Problem with Dry Sand: A Statical Approach Based upon Model Test Kinematics'. International Journal for Numerical and Analytical Methods in Geomechanics, Vol. 5, pp. 57 - 78.

Weiler, W.A., Jr. and Kulhawy, F.H. (1978). 'Behaviour of Stress Cells in Soil', Geotechnical Engineering Report 78-2, Cornell University, Ithaca, 312 p.

Yoshimi, Y. and Kishida, T. (1981). 'Friction between Sand and Metal Surfaces', Proceedings, 10th International Conference of Soil Mechanics and Foundation Engineering, Stockholm, Vol.2, pp. 831 - 834.

FIGURES

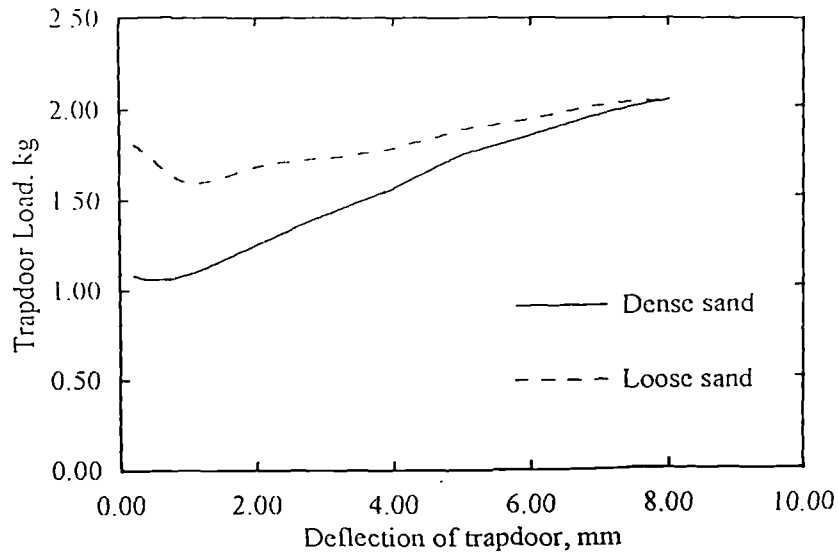
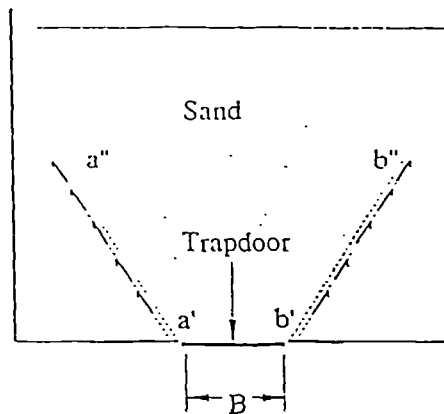
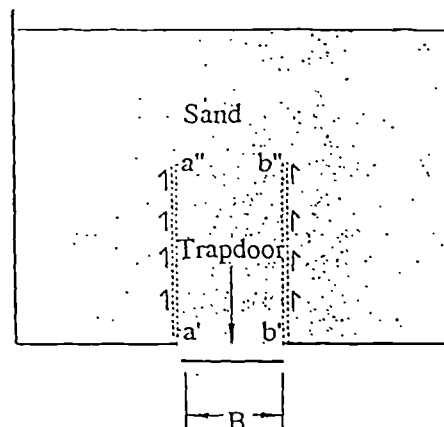


Figure 2-1. The variation of the trapdoor load with downward deflection
Terzaghi(1936))



Stage 1: Small downward displacement of trapdoor



Stage 2: Large downward displacement of trapdoor

Figure 2-2. Terzaghi's idealisation of the arching mechanism occurring in sand due to deflection of trapdoor (Terzaghi (1936)).

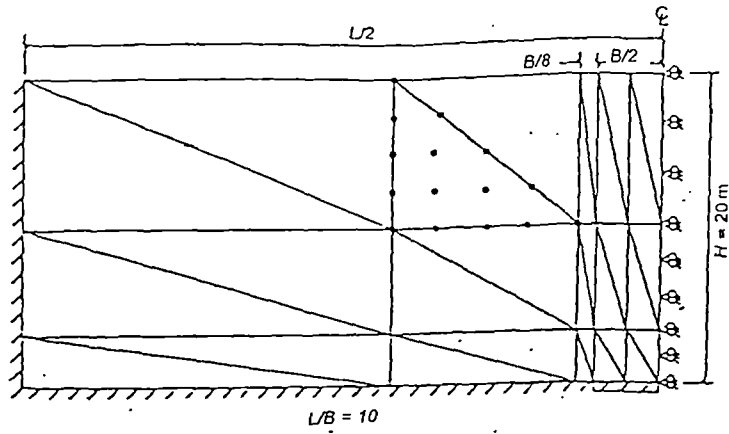


Figure 2-3. Finite element grid discretisation used to model the tradoor problem by Koutsabeloulis et al. (1989).

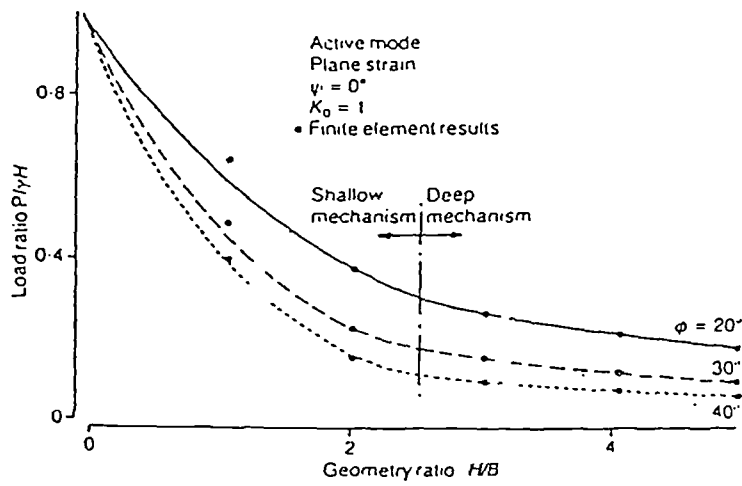


Figure 2-4. Load ratio plotted against (H/B) (Koutsabeloulis et al. (1989)).

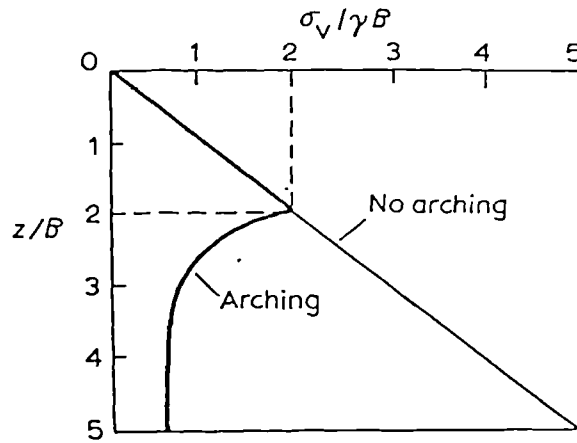


Figure 2-5a. The theoretical variation of vertical stress above trapdoor (Terzaghi (1943)).

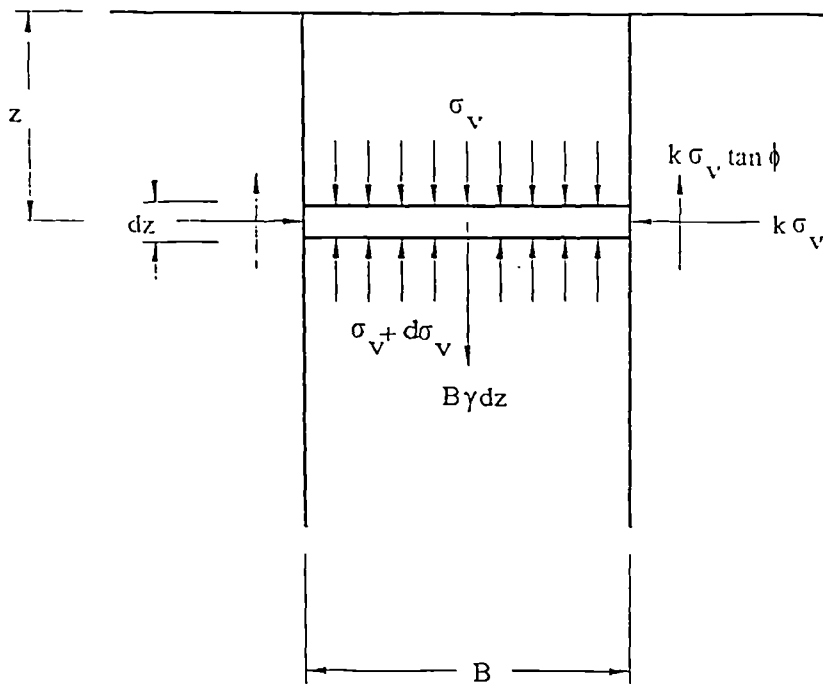


Figure 2-5b. Diagram showing the differential element utilised by Terzaghi (1943) to compute pressure acting on trapdoor.

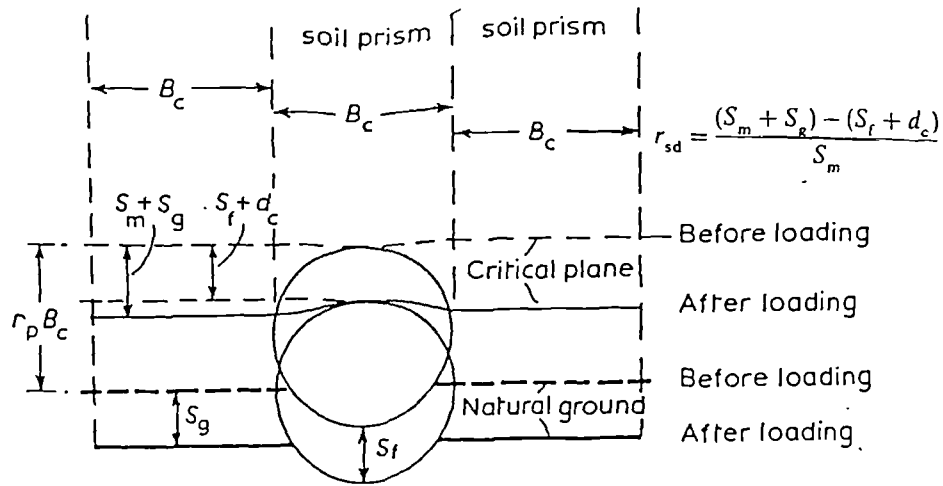


Figure 2-6. Definition of (r_{sd} and r_p) for buried conduits under positive projection conditions (Bulson (1985)).

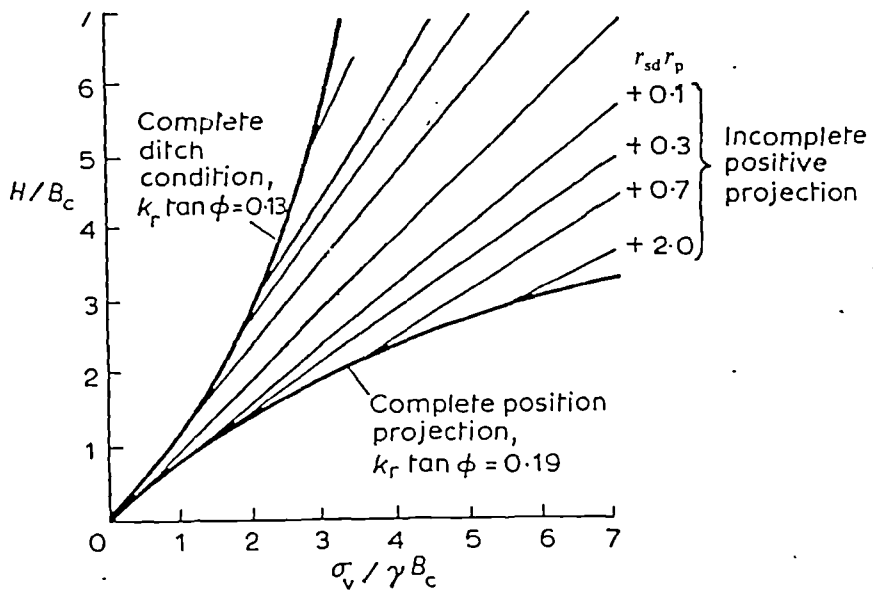


Figure 2-7. Relationship between (H/B_c) and ($\sigma_v/\gamma B_c$) for a range of (r_{sd}).(r_p) values (Spangler (1960)).

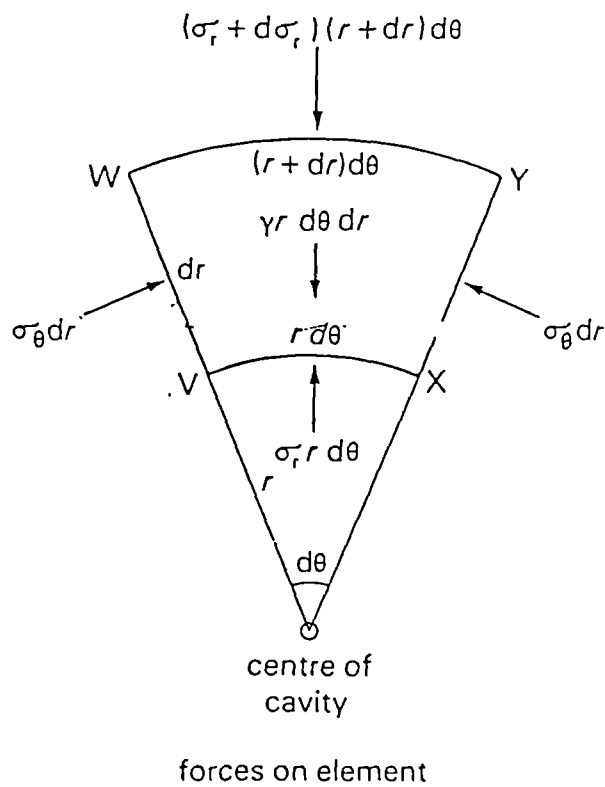
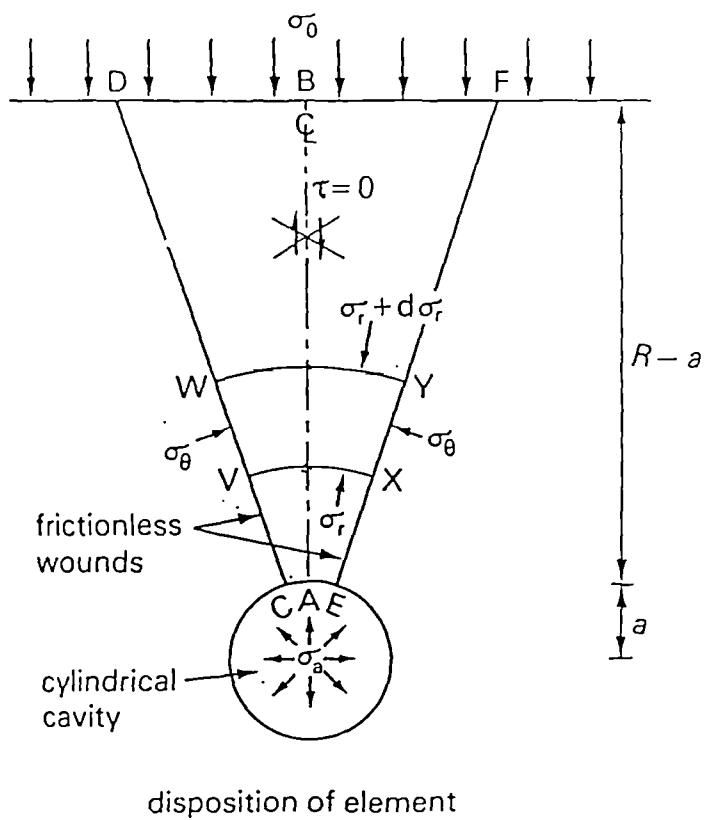


Figure 2-8. Idealisation of the state of stress above a buried circular cavity (Bolton (1979)).

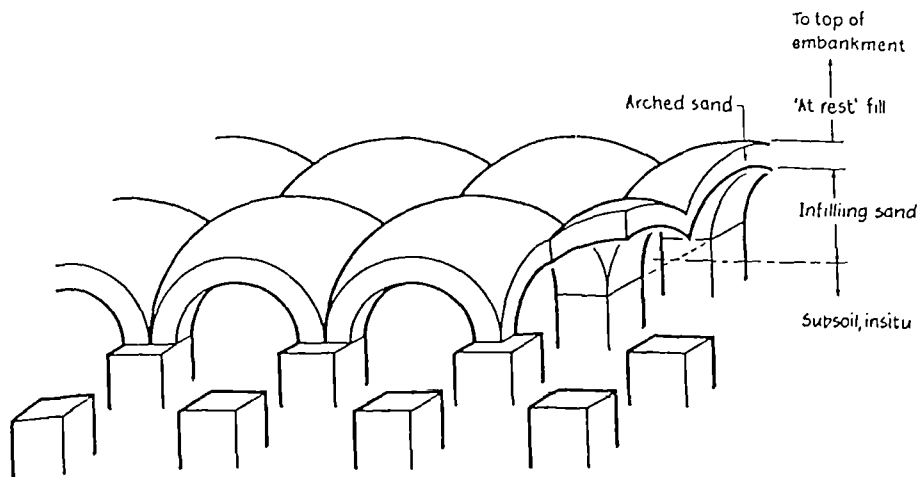


Figure 2-9. The vaulted domes idealisation proposed by Hewlett and Randolph (1988).

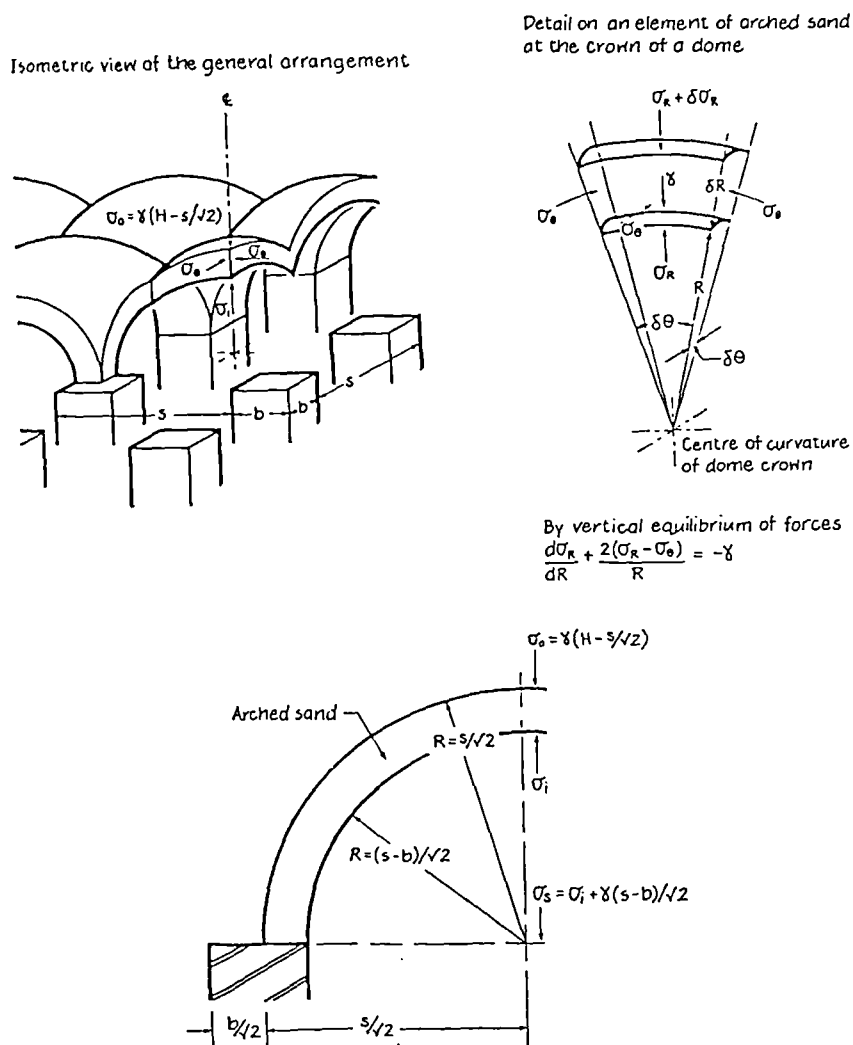


Figure 2-10. Crown stability, domed arches in piled embankments (Hewlett and Randolph (1988)).

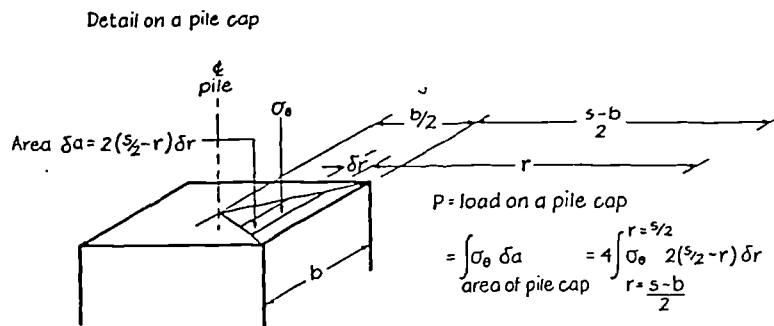
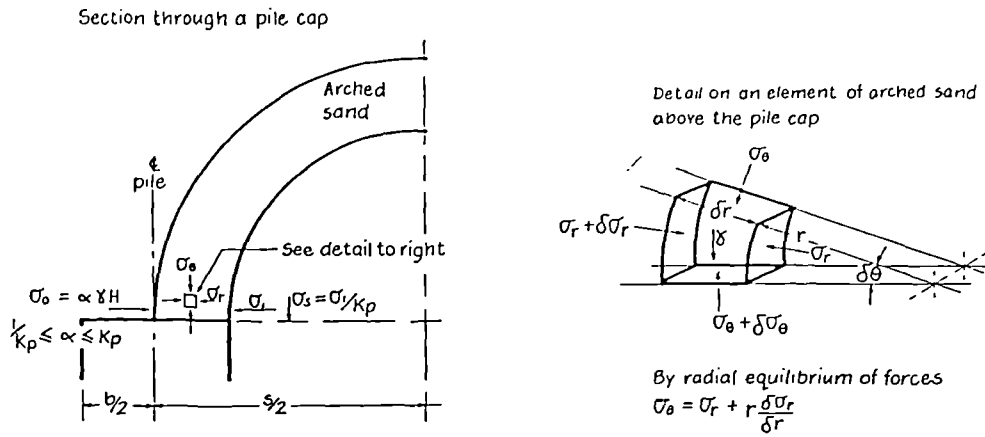


Figure 2-11. Cap stability analysis, domed arch idealisation (Hewlett and Randolph (1988)).

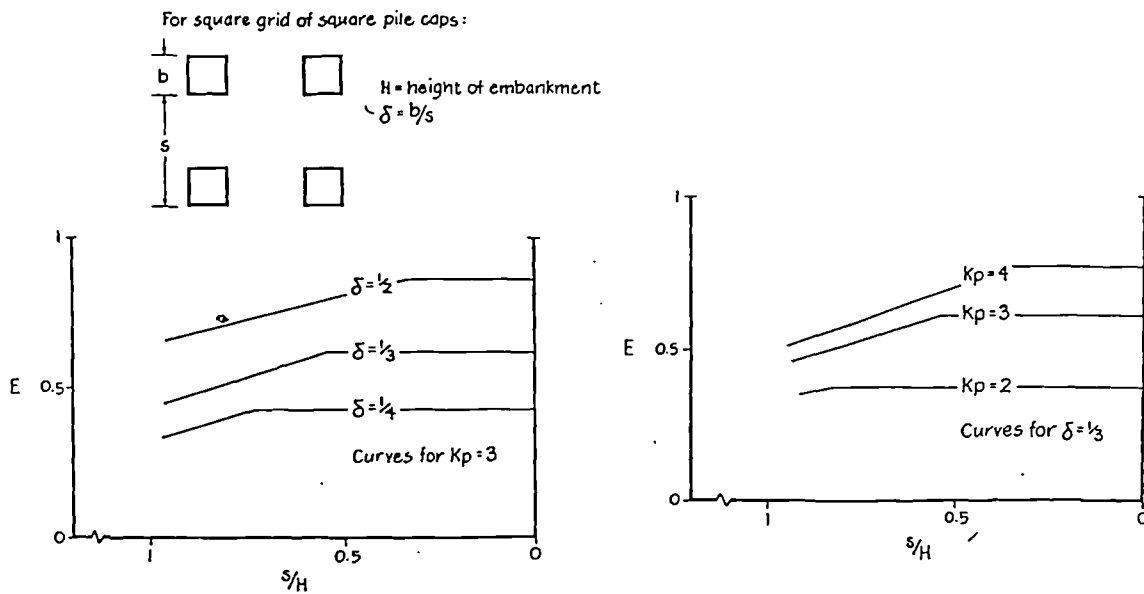


Figure 2-12. The variation of efficacy with the embankment geometry and the fill properties (Hewlett and Randolph (1988)).

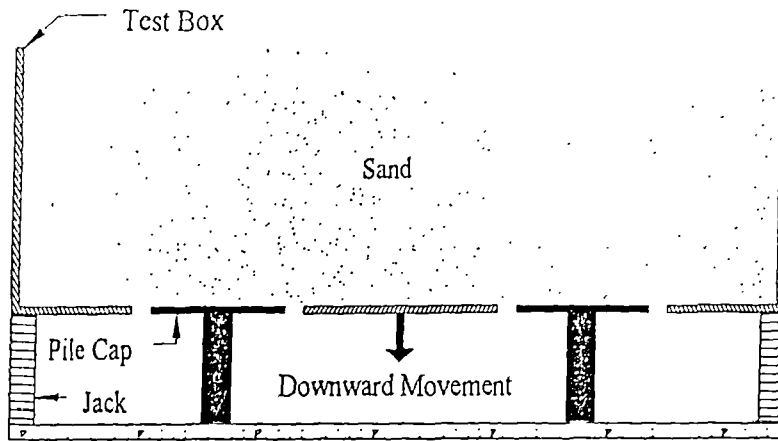


Figure 2-13a. The test apparatus used by Bergdahl et al. (1979).

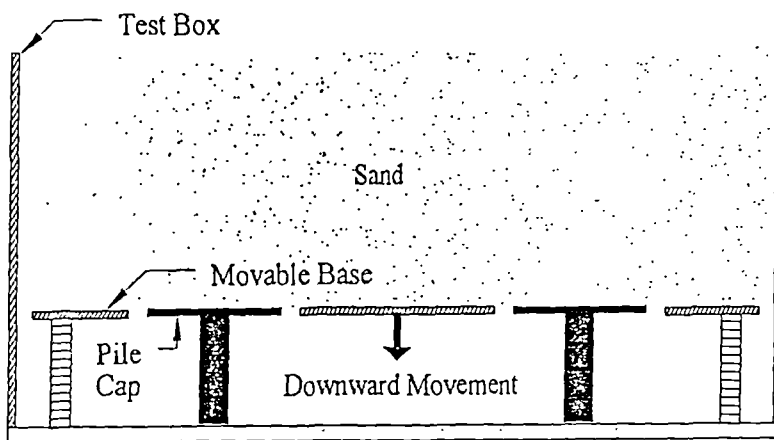


Figure 2-13b. The movable base method employed by Ting et al. (1983) and Ali (1990).

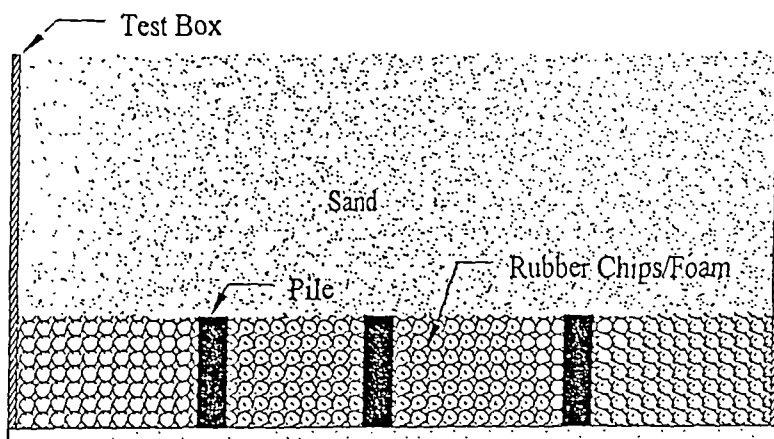


Figure 2-13c. Test procedure used by Hewlett and Randolph (1988).

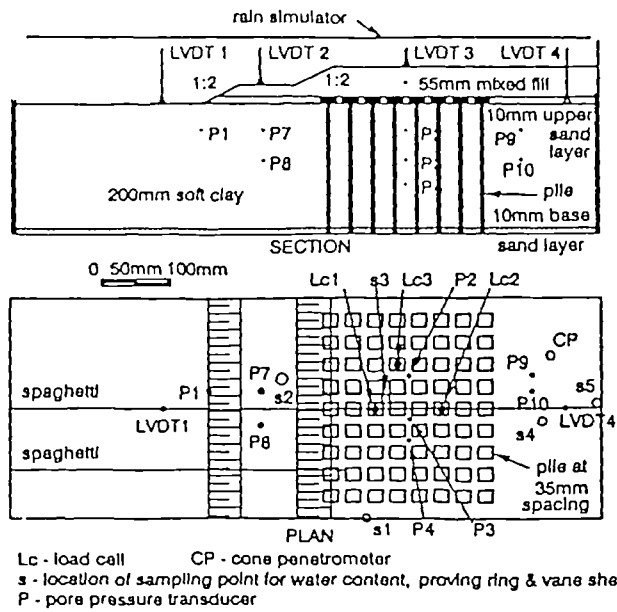


Figure 2-14. Typical cross section through model embankment used by Bujang (1990).

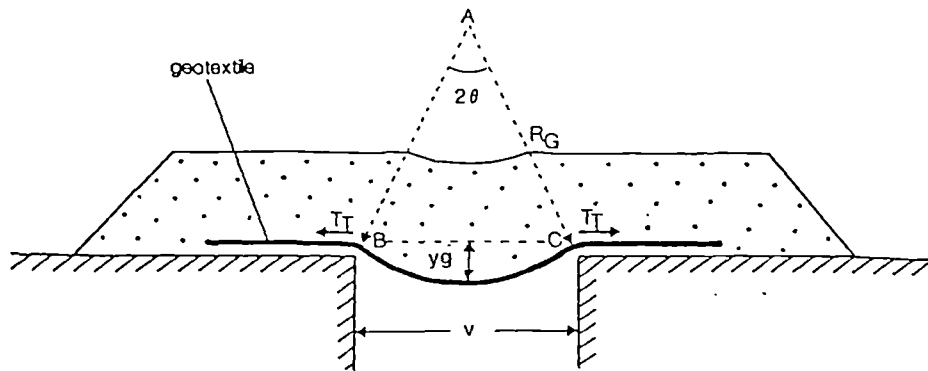


Figure 2-15. Circular arc analysis of geosynthetic basal reinforcement (Fluet et al. (1986)).

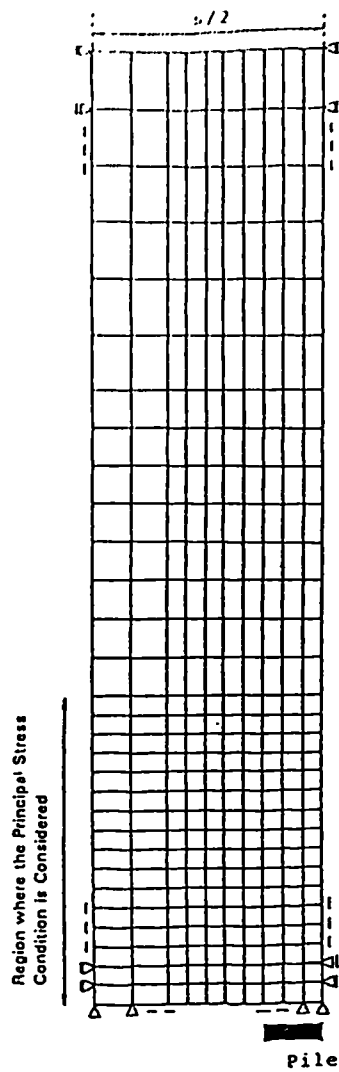


Figure 2-16. Finite element mesh used by Adachi et al. (1989) to study the use of piles in stabilising landslides.

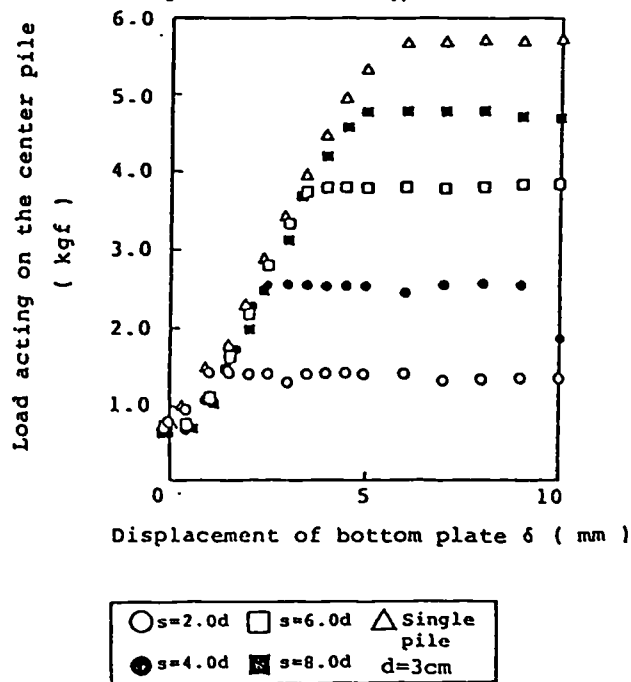
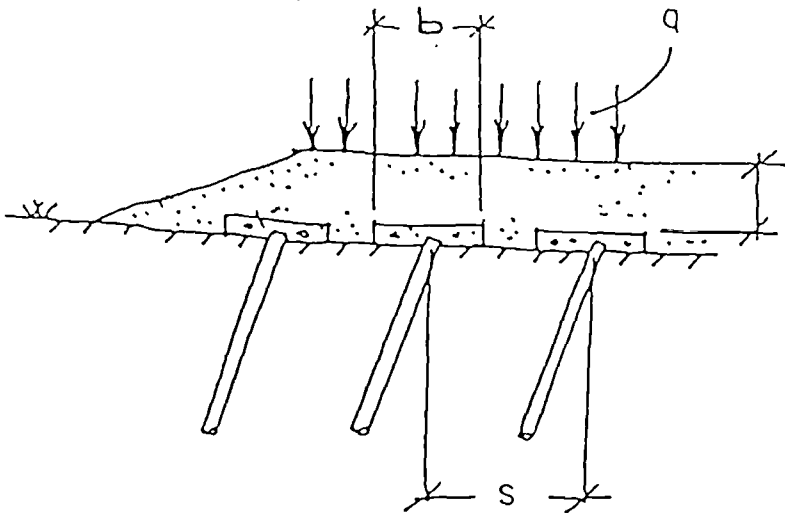


Figure 2-17. The variation of the load acting on a central pile and displacement (Adachi et al. (1989)).



$$\left[\frac{q}{\gamma H} + 1 \right] \frac{s^2}{b^2}$$

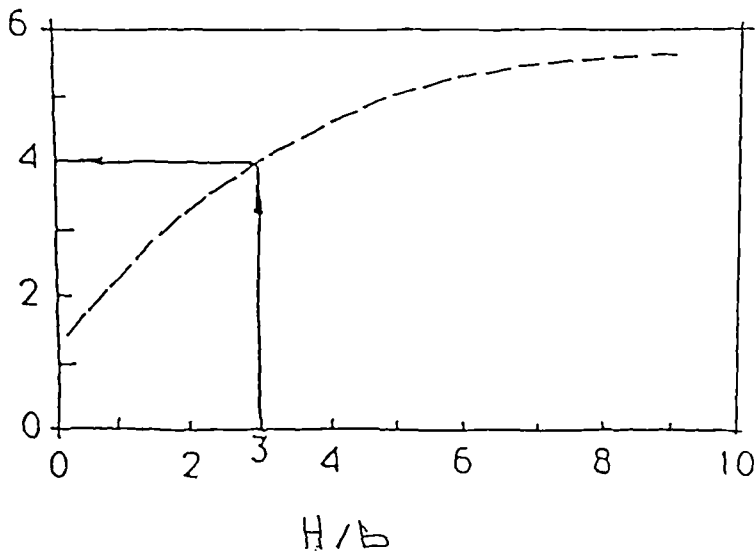


Figure 2-18. Design curve proposed by the Swedish Road Board (1974).

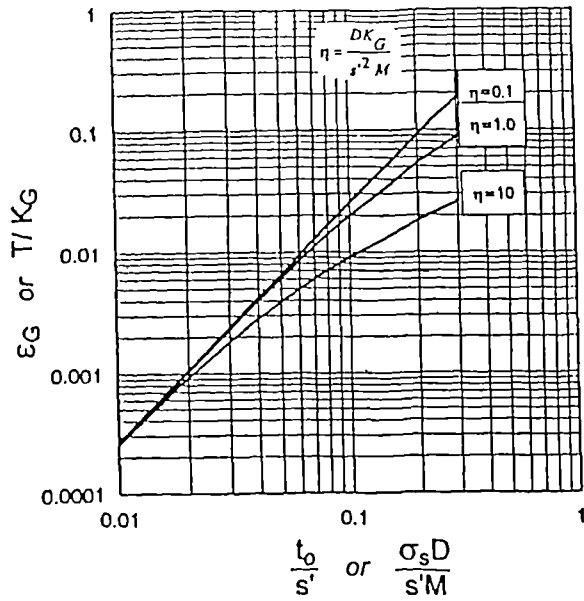


Figure 2-19. Design chart to determine the reinforcement strain (ϵ_G) proposed by Low et al. (1994).

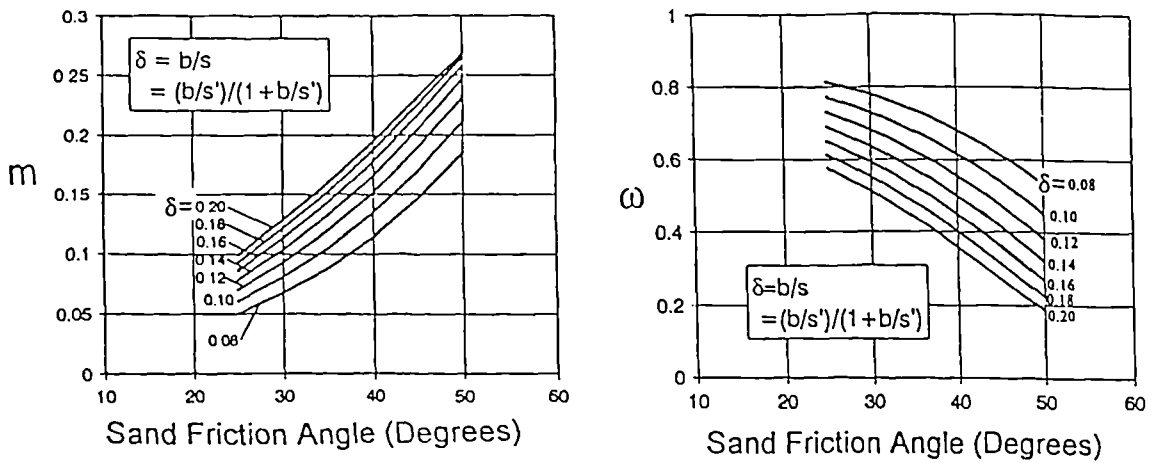


Figure 2-20. Charts proposed by Low et al. (1994) to determine the efficacy (E).

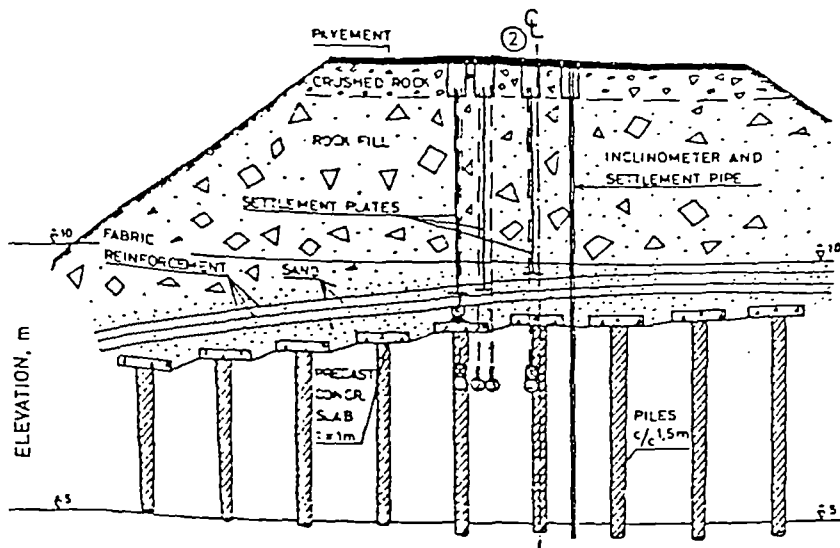


Figure 2-21. Cross section of completed embankment with piles and fabric reinforcement at the Gota River Valley (Holtz and Massarch (1976))

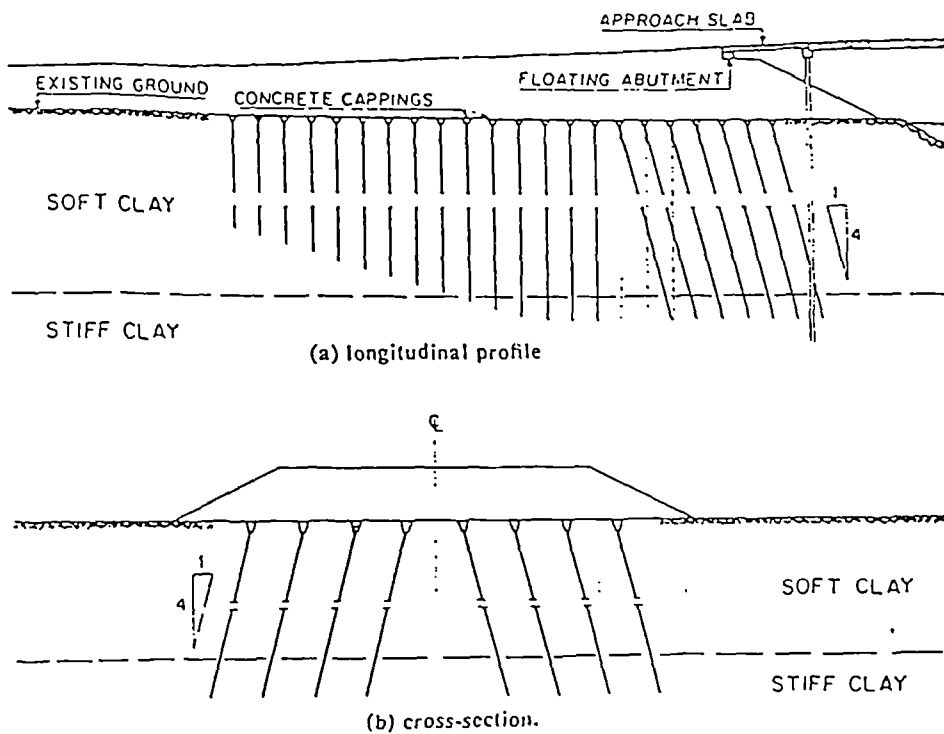


Figure 2-22. Typical layout of embankment piles for bridge approaches on the Bank Pa-in to Sawan Highway (Holmberg (1978)).

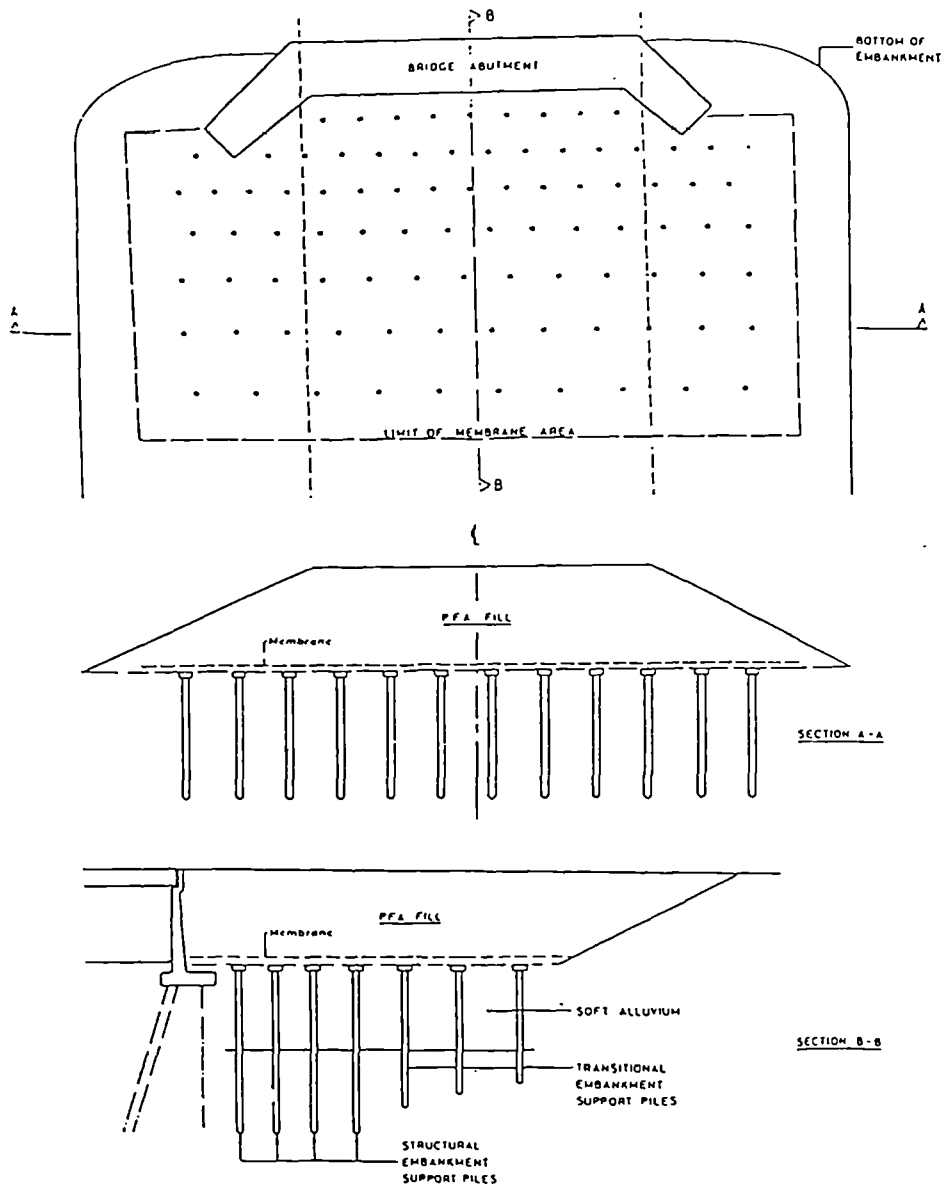


Figure 2-23. Typical Basp installation at the M9 and M876 Motorways (Reid and Buchanan (1983).

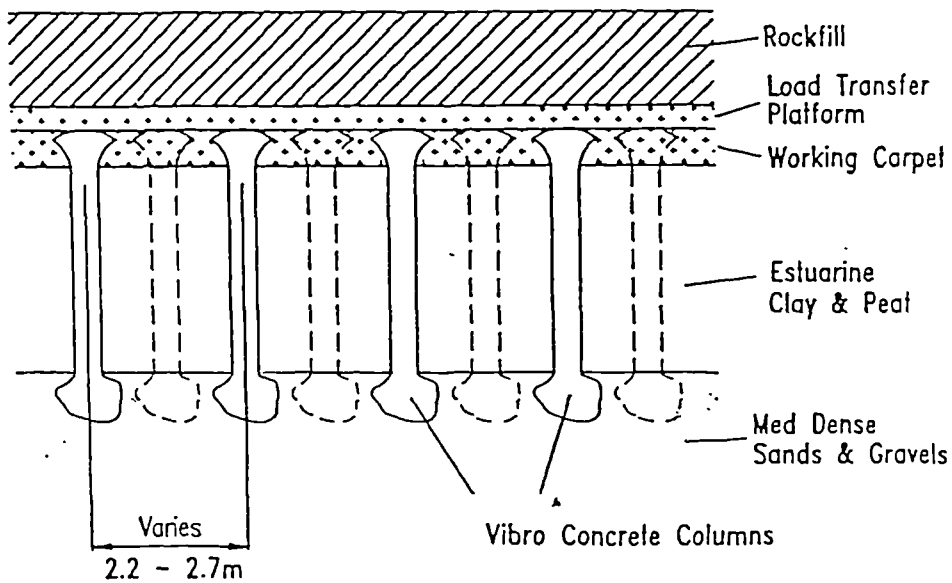
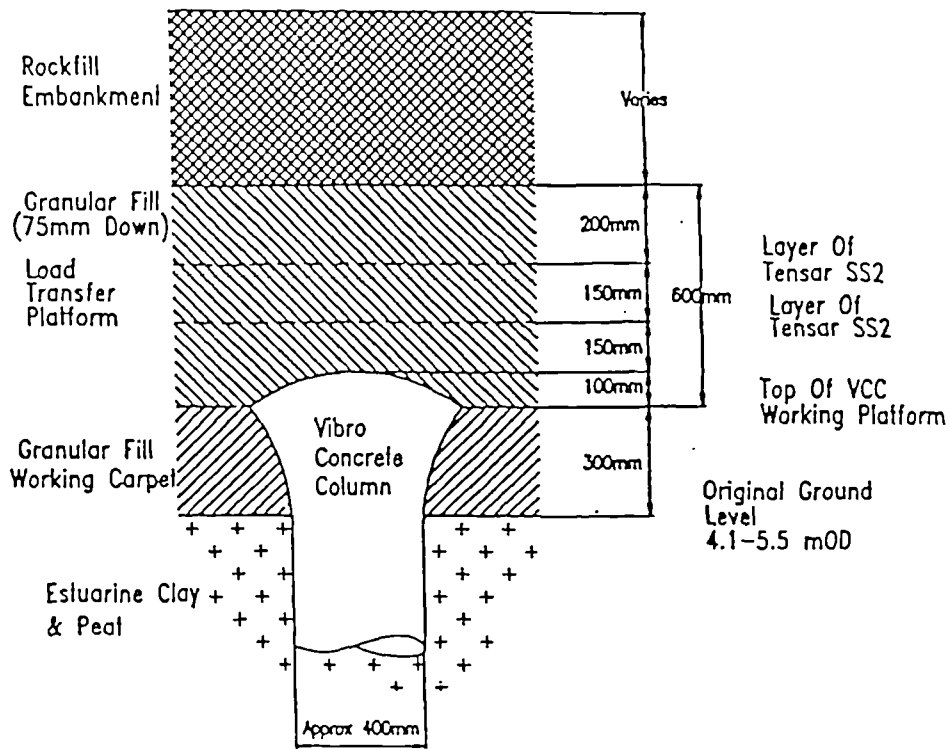


Figure 2-24. Geogrid reinforced granular mattress used in conjunction with Vibro concrete columns (Bell et al. (1994)).

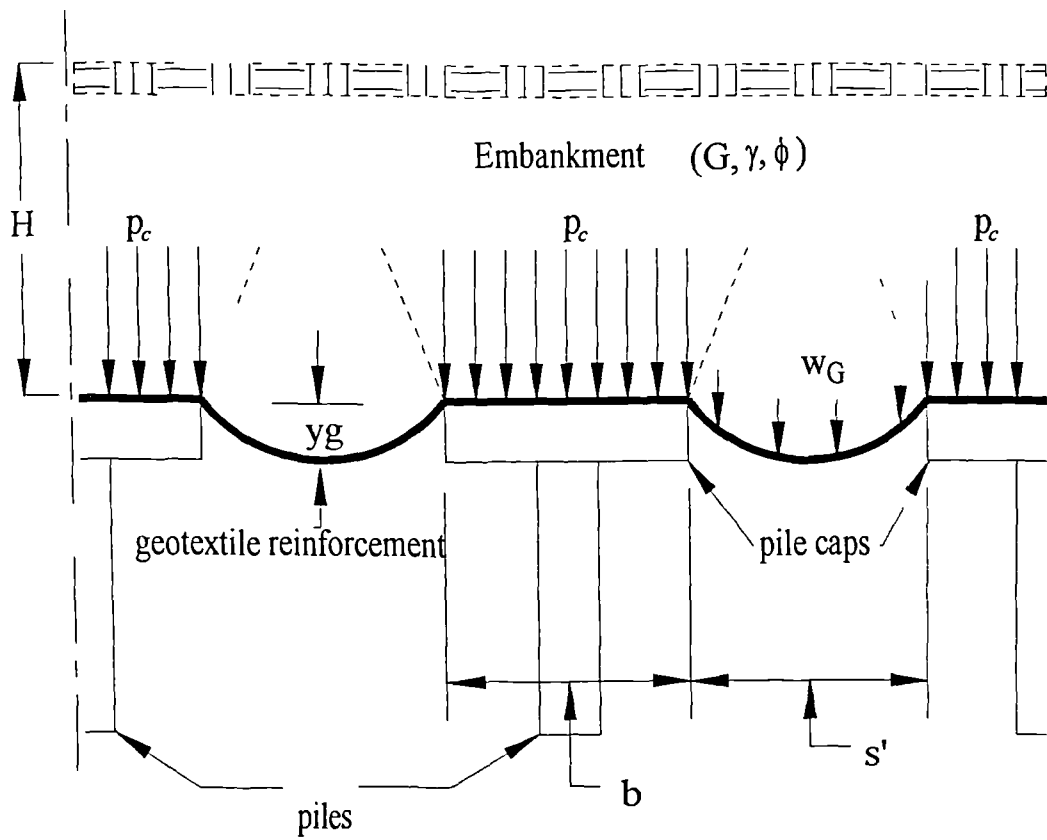


Figure 3-1. Significant physical parameters in piled embankment model.

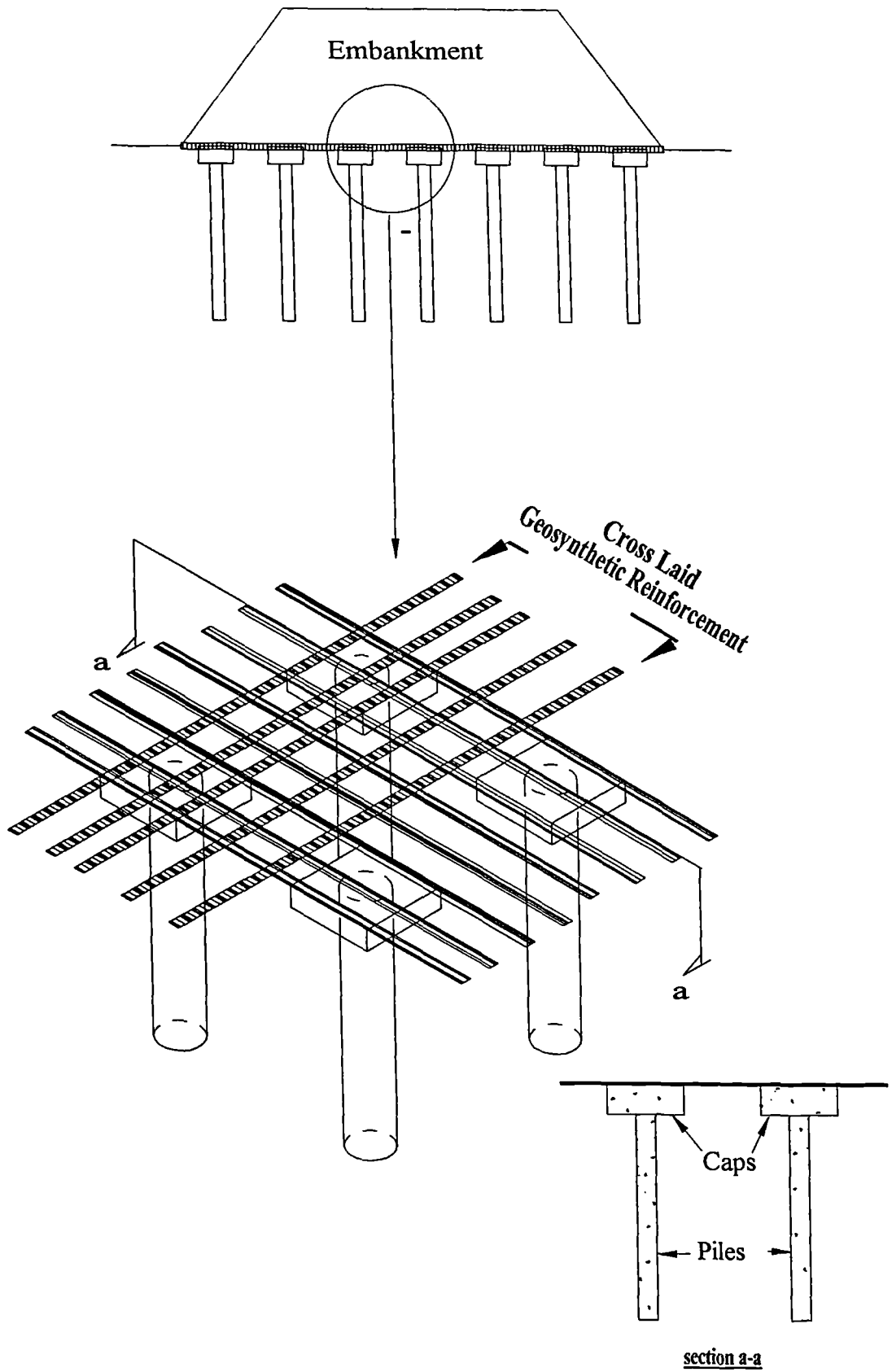


Figure 3-2. The use of geosynthetic strip reinforcement in piled embankments

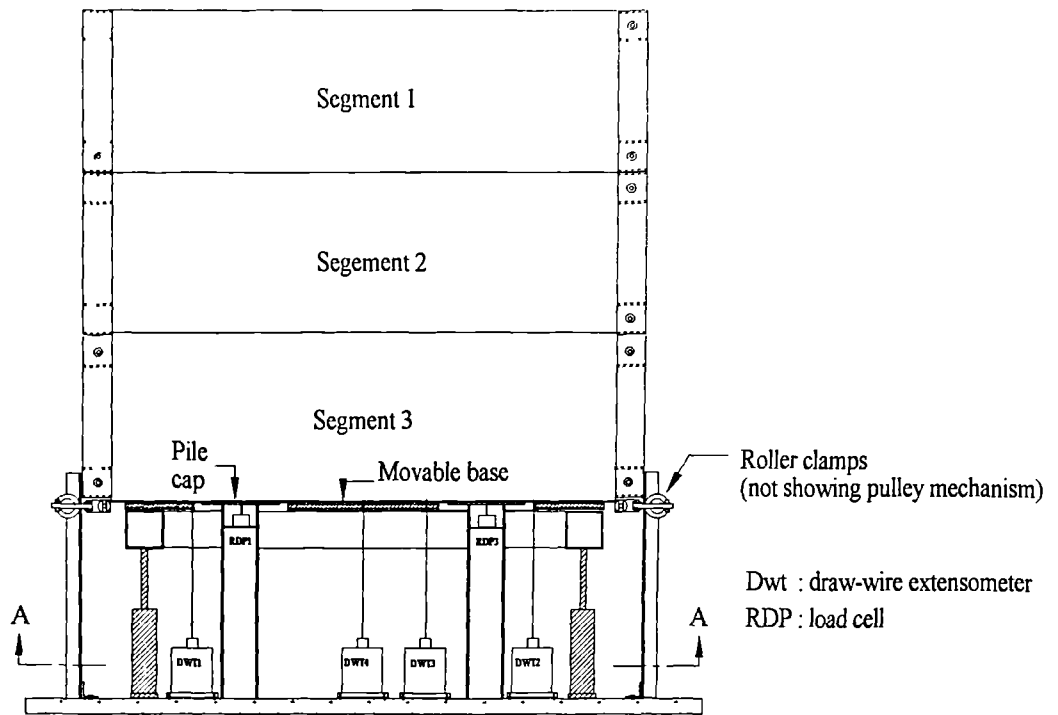


Figure 3-3a. Cross section through test box and movable base showing location of instruments.

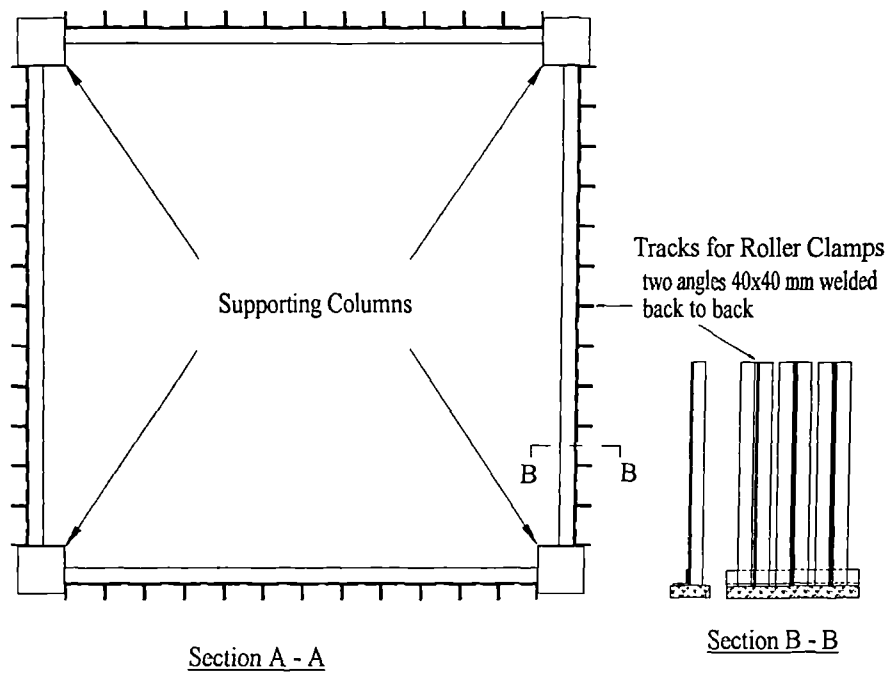


Figure 3-3b. Section through test box base (not showing movable base)

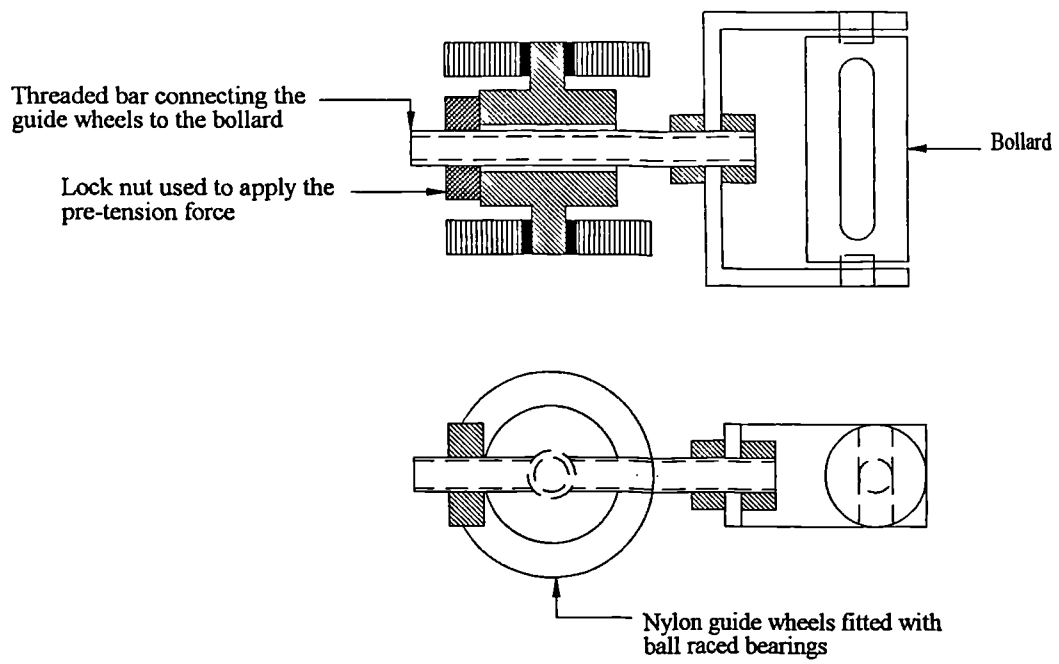


Figure 3-4a. Schematic cross section and plan view showing the roller clamp.

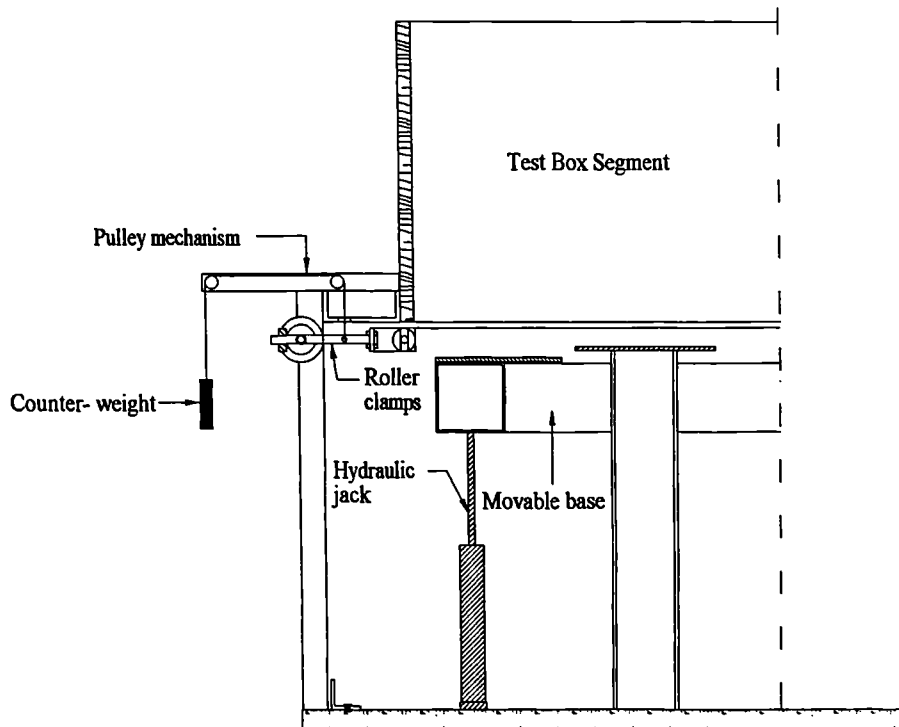
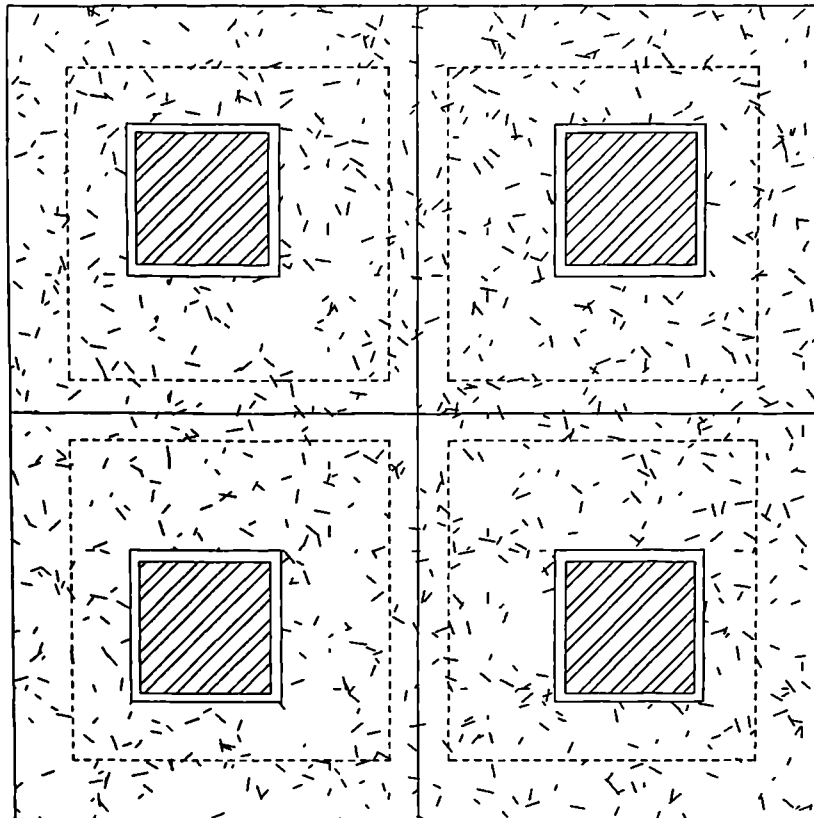
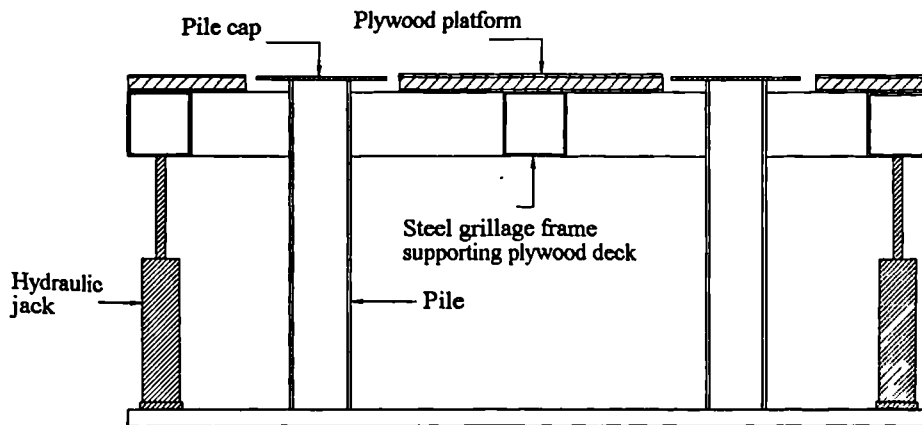


Figure 3-4b. Schematic section elevation showing the pulley mechanism.

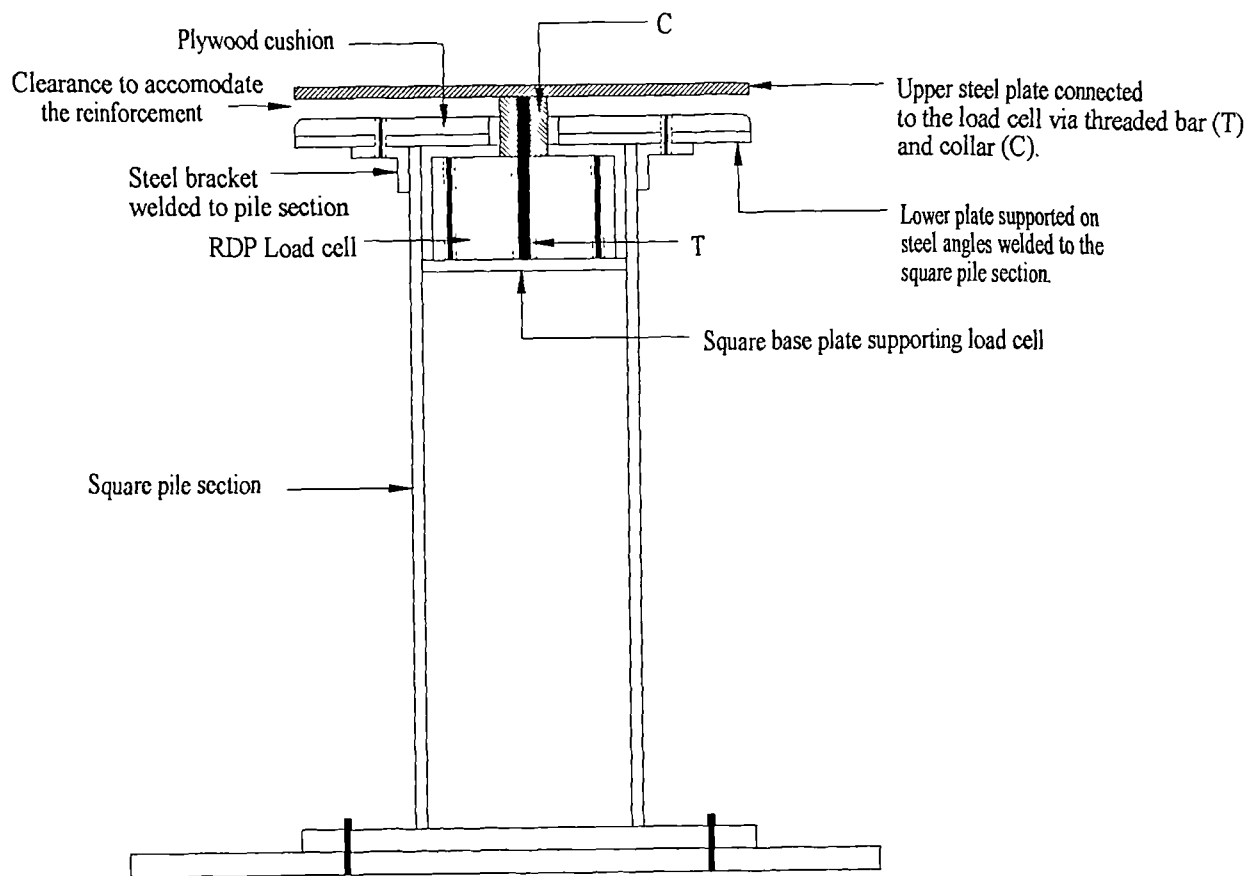


Plan View of Movable base



Section Elevation

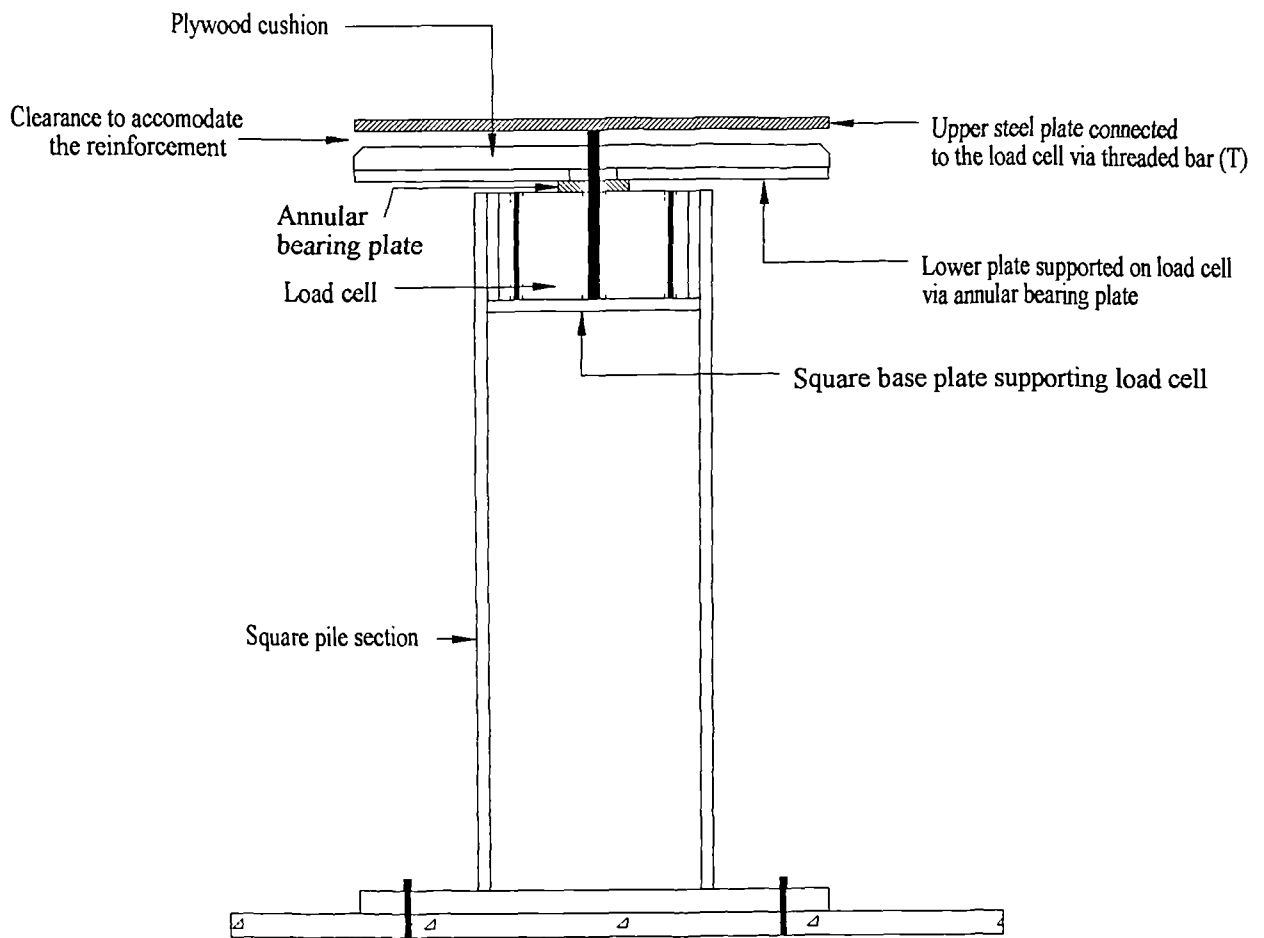
Figure 3-5. Plan and section elevation of the movable base.



Pile Cap [A]

Measures load on pile cap due to arching in fill

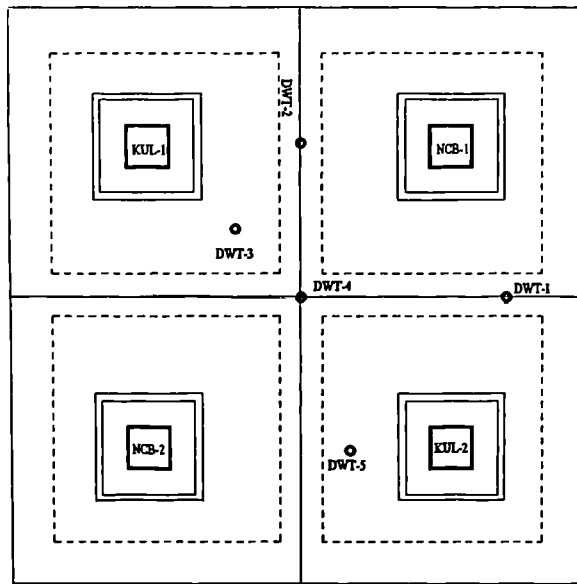
Figure 3-6a. Section through pile caps used to assess load transfer.



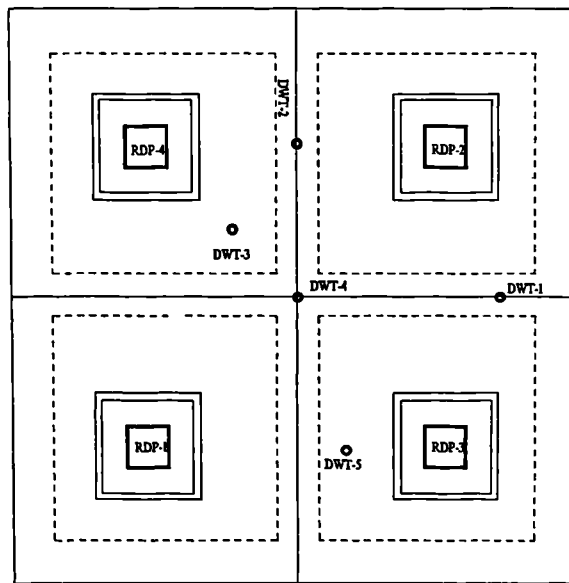
Pile Cap[B]

Measures net load per pile cap tributary area

Figure 3-6b. Section through pile caps used to assess load transfer



SCHEME NO.1



SCHEME NO.2

Legend :

DWT : Draw-wire extensometer

RDP : Load cell

KUL : pressure cell

NCB : load cell

Figure 3-7. Plan view of the movable base showing location of different instruments.

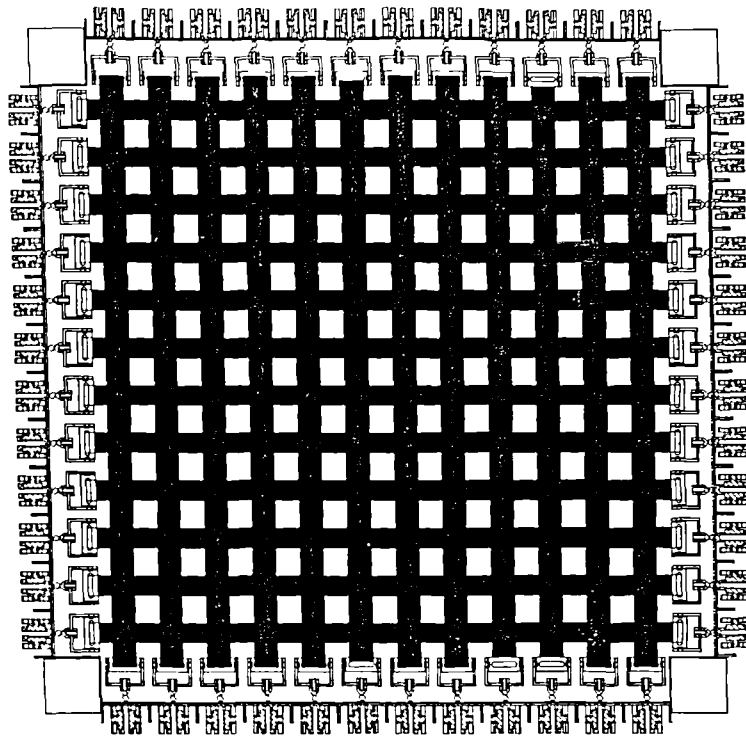


Figure 4-1. Plan view of the test box base showing the installed geotextile mesh.

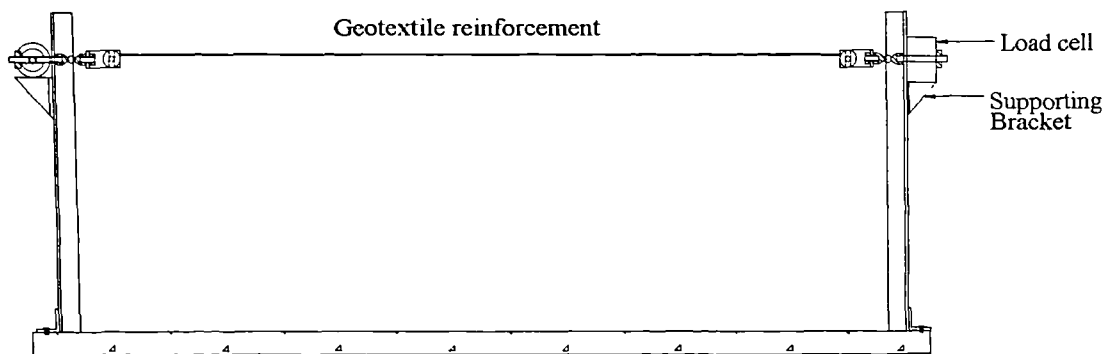
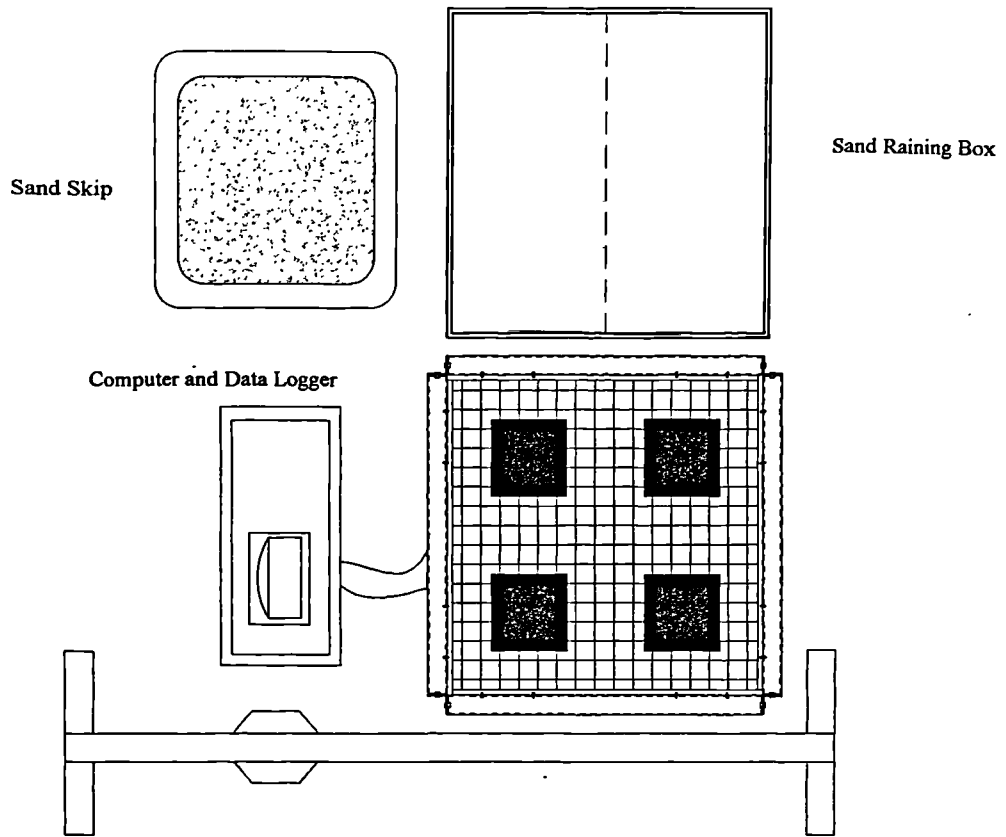
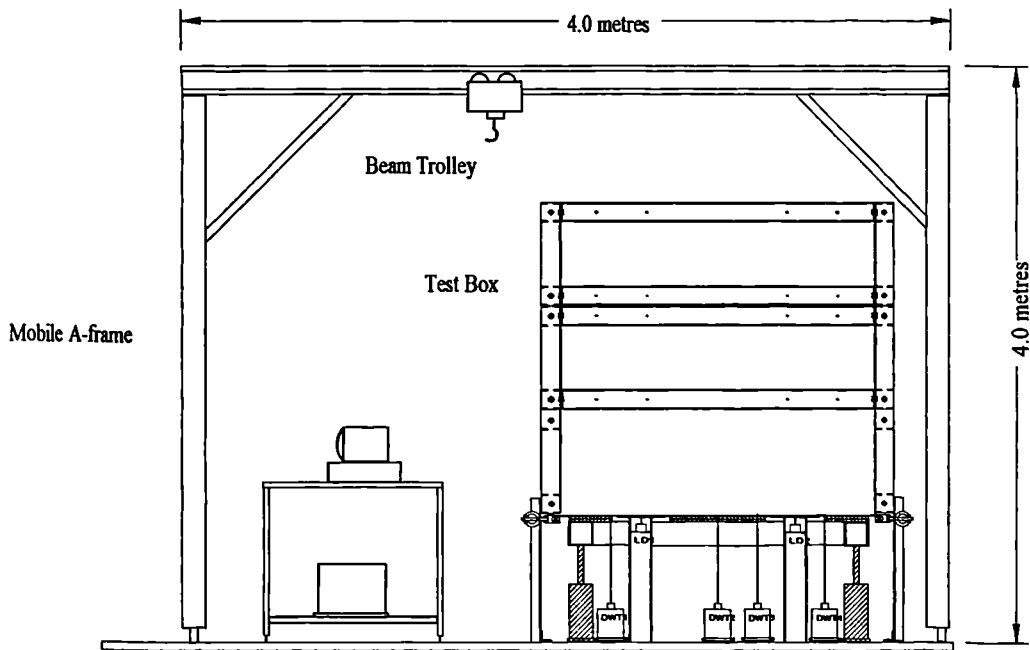


Figure 4-2. Section elevation showing the set-up used to calibrate the torque wrench.

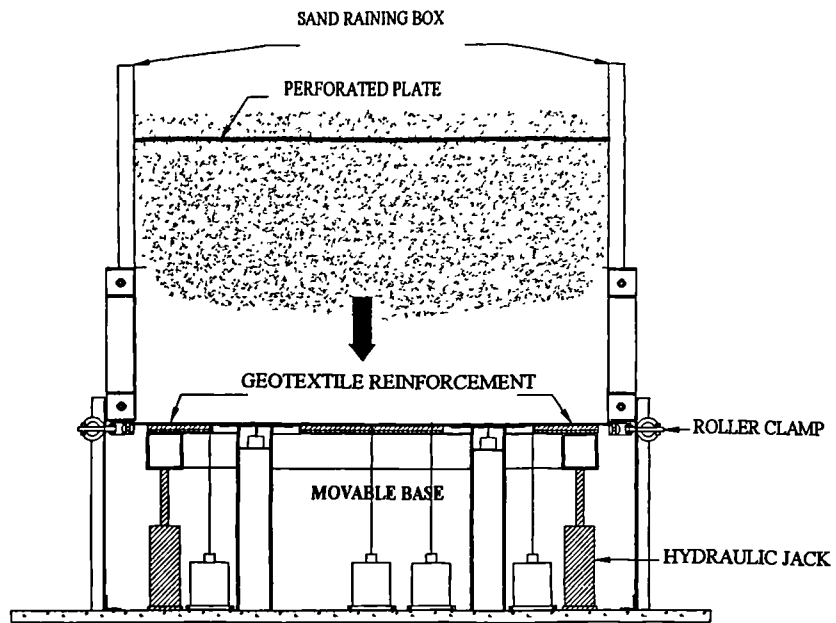


PLAN VIEW

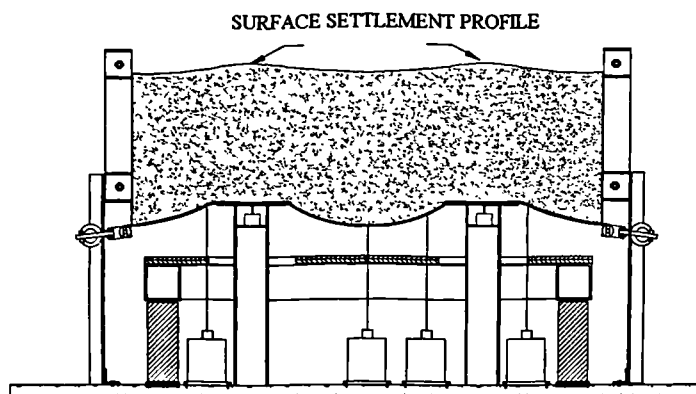


SECTION ELEVATION

Figure 4-3. Layout of apparatus, mobile A-frame and sand raining box.



STAGE 1 : PLACEMENT OF SAND DEPOSIT



STAGE 2 : MOVABLE BASE LOWERED

Figure 4-4. Schematic of the test procedure.

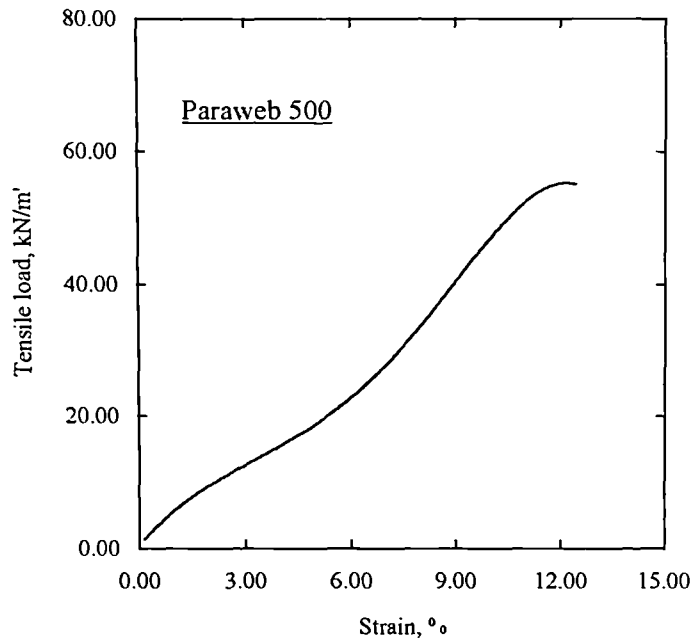
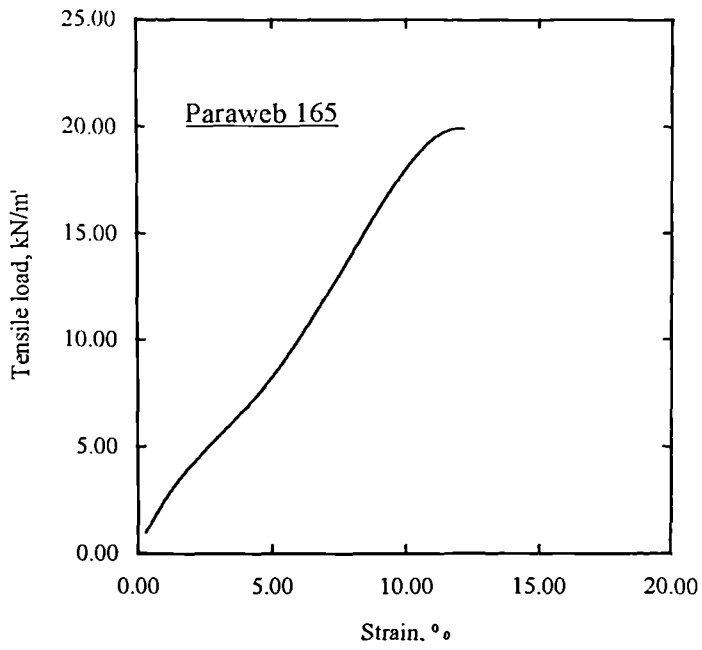


Figure 4-5. Load-strain curve for Paraweb 165 and 500.

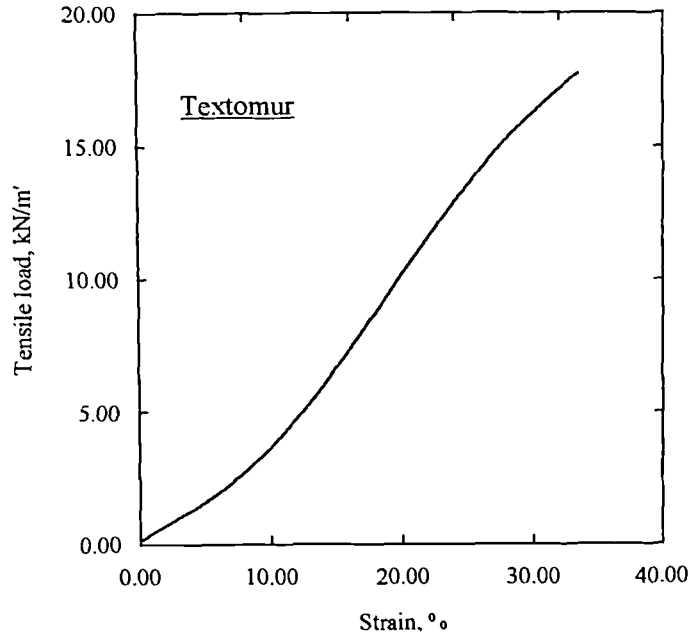
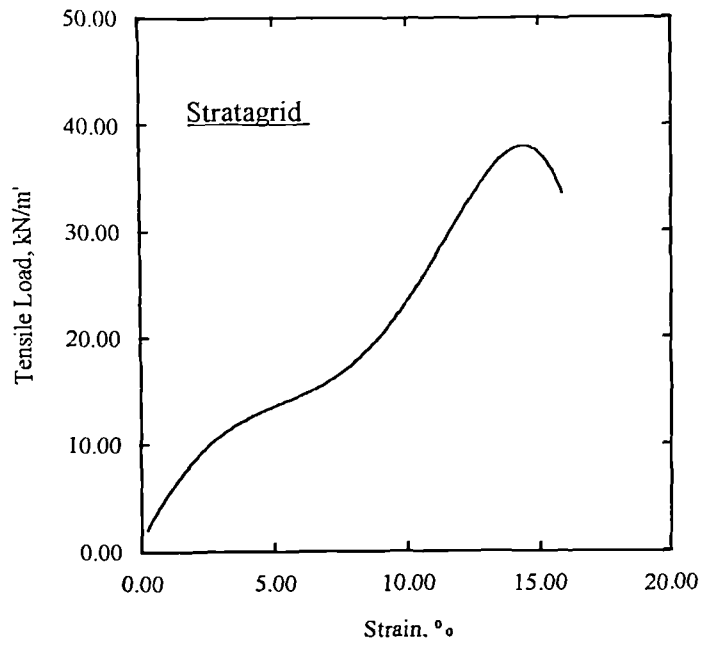


Figure 4-6. Load-strain curve for Stratgrid 200 and Textomur.

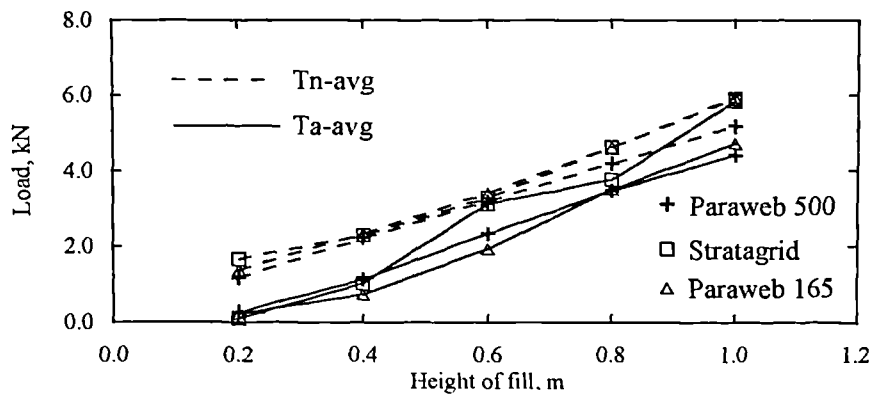
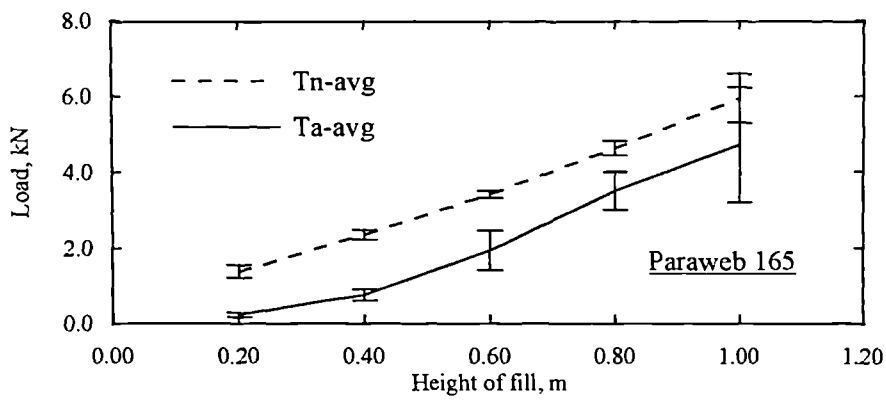
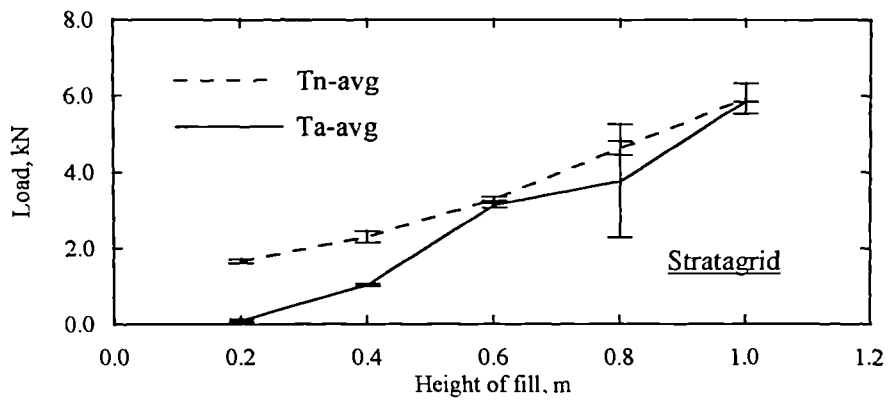
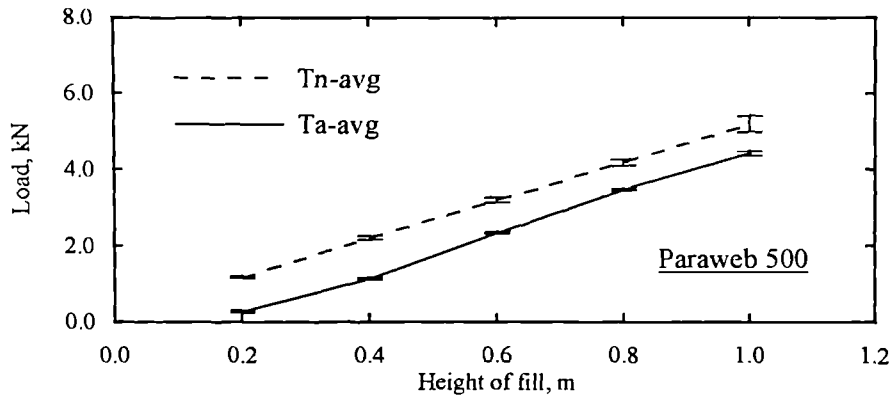


Figure 4-7. The variation of load with fill height for the full height simulations (effect of geotextile stiffness).

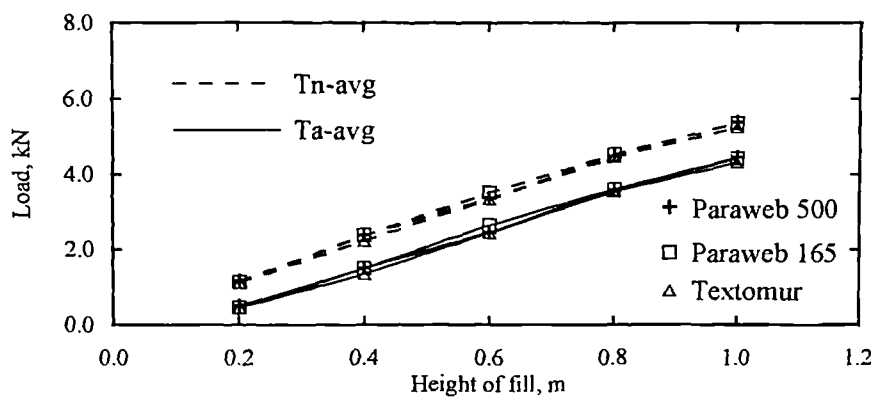
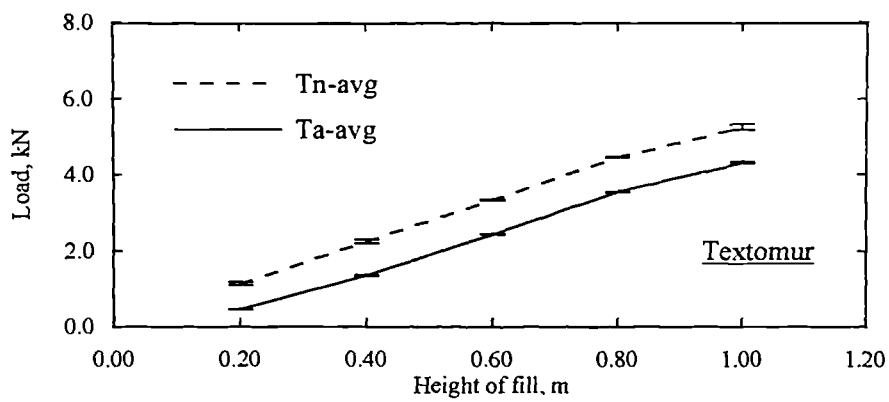
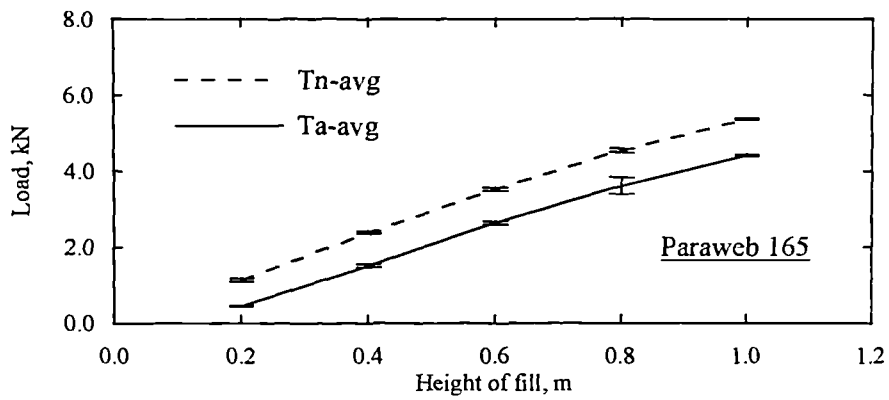
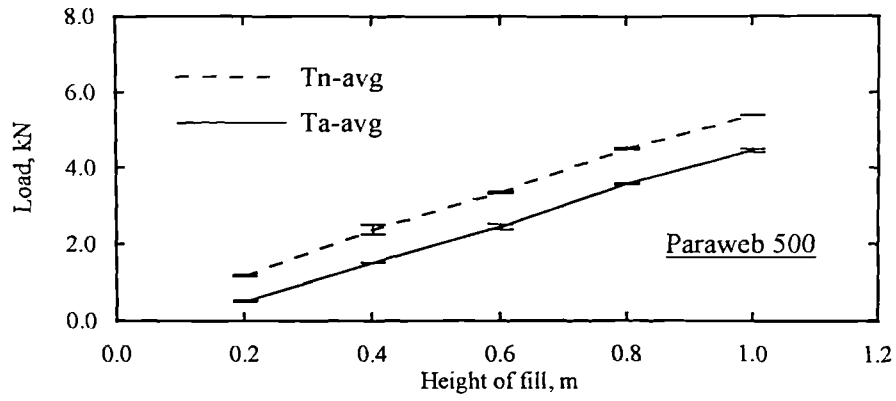


Figure 4-8. The variation of load with fill height for construction stages simulation (effect of geotextile stiffness).

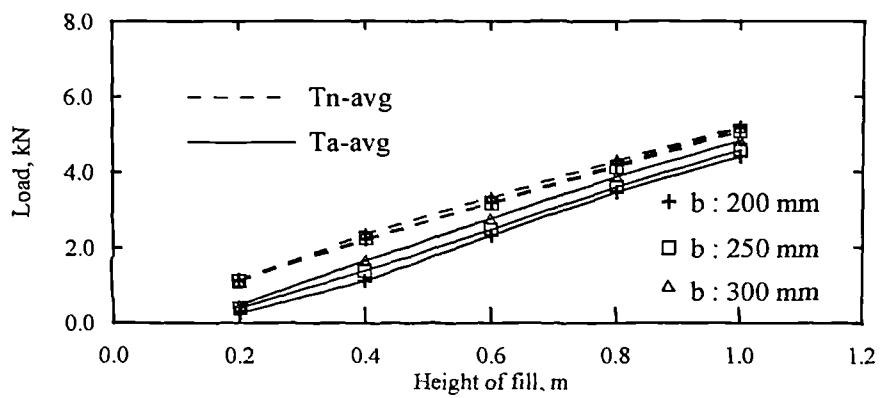
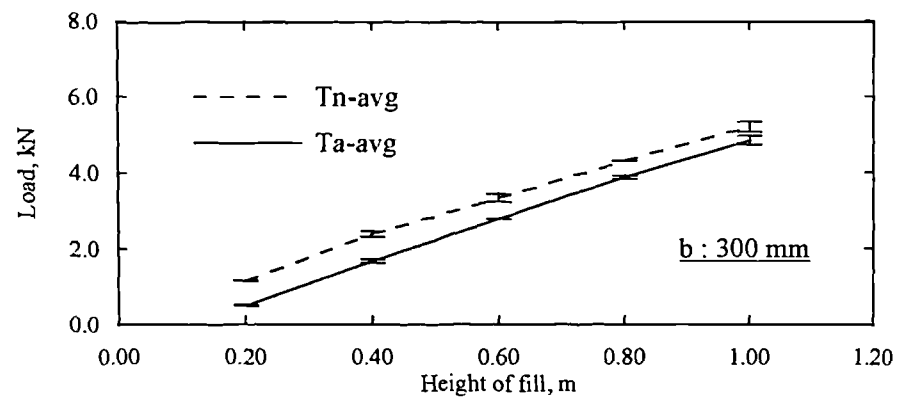
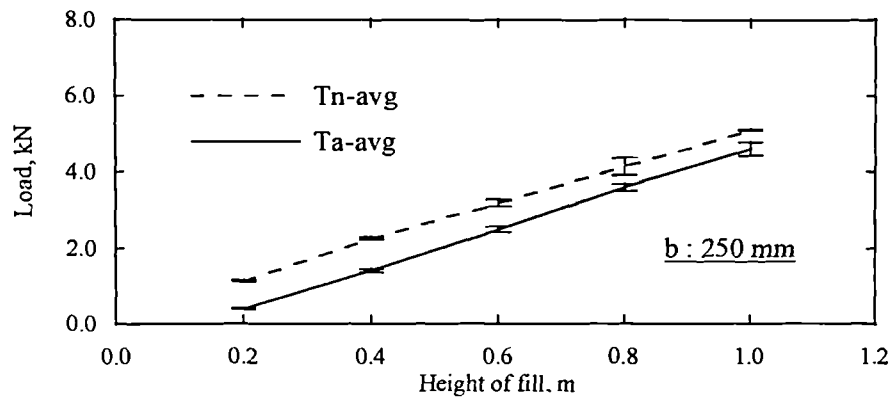
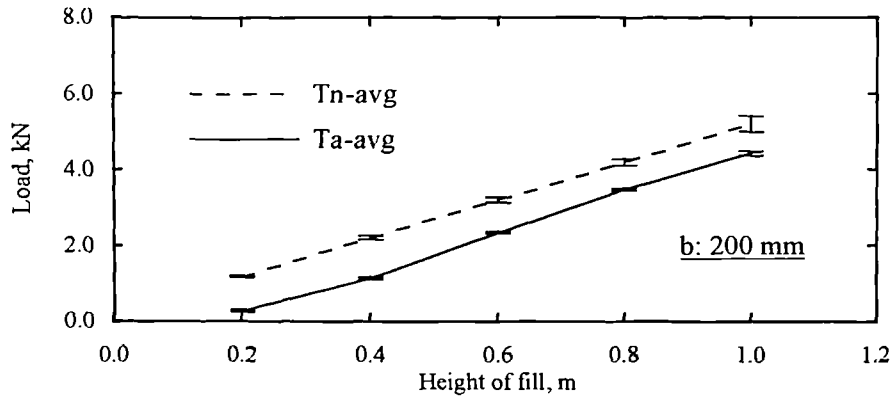


Figure 4-9. The variation of load with the height of fill for the full height simulations (effect of pile cap width).

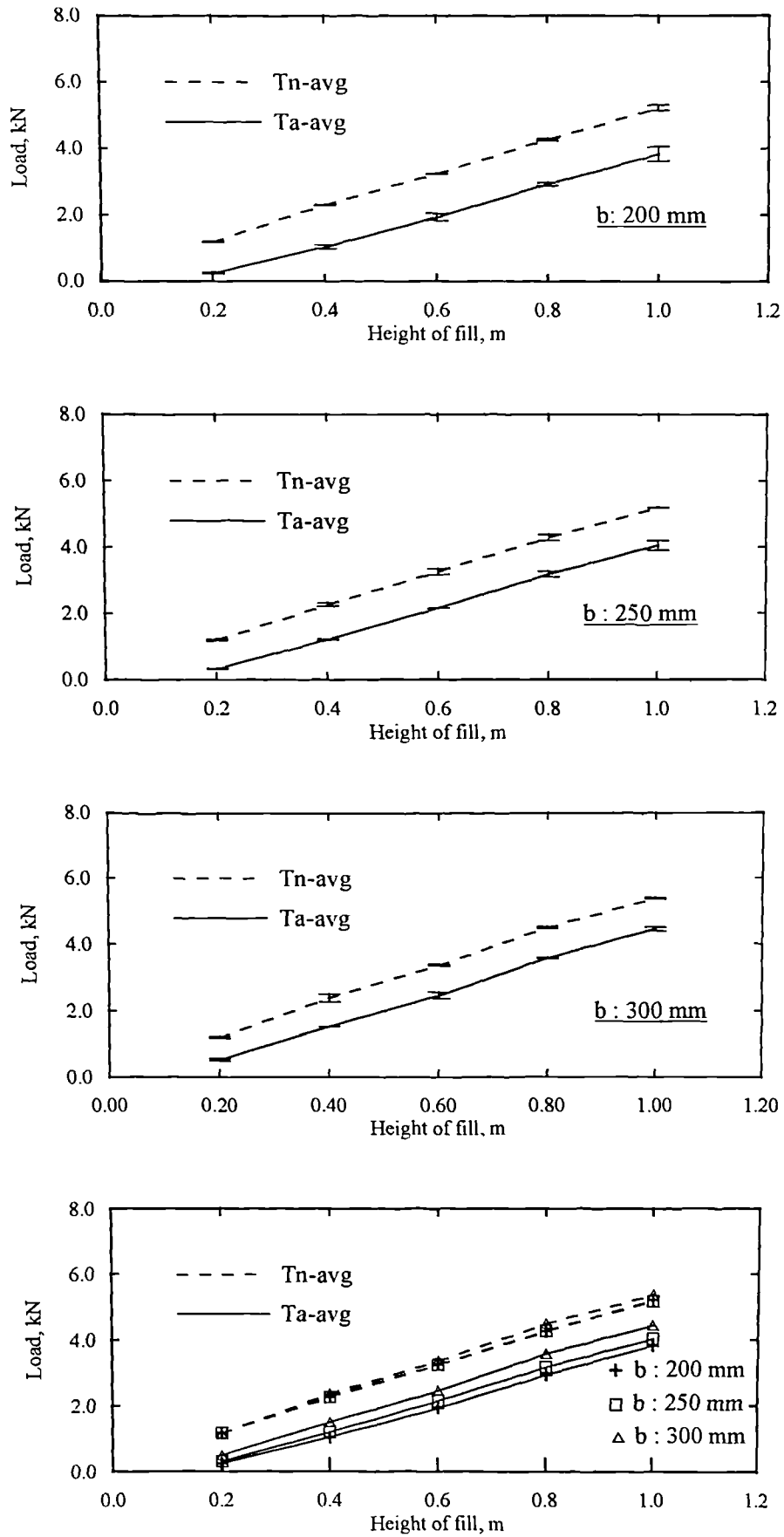
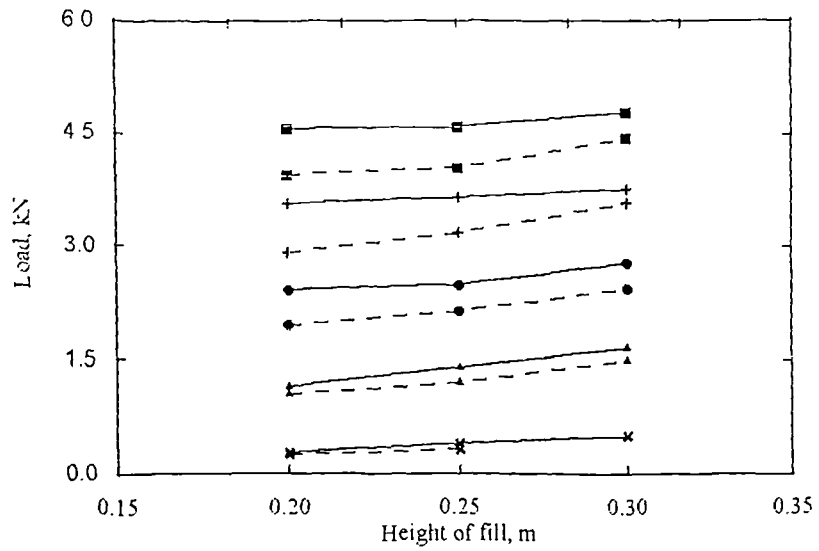
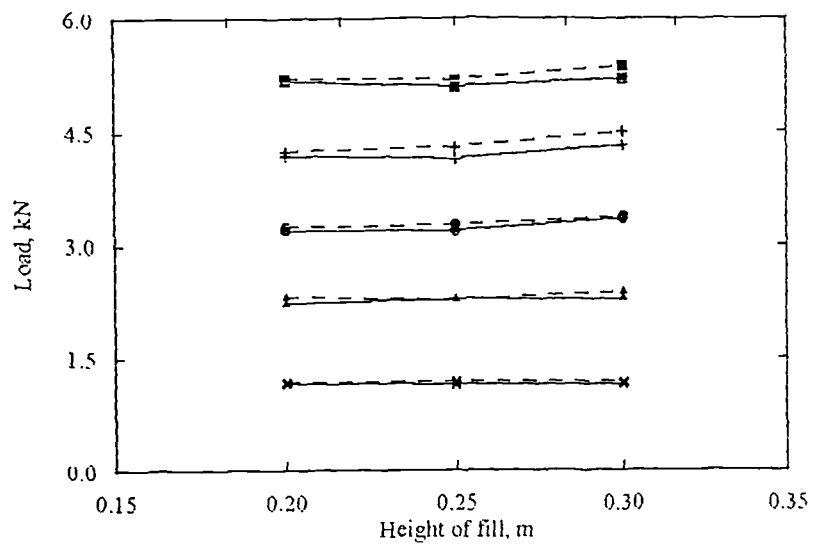


Figure 4-10. The variation of load with the height of fill for the incremental loading simulations (effect of pile cap width).



(a) Variation of Ta-avg with pile cap width.



(b) Variation of Tn-avg. with pile cap width.

Legend:

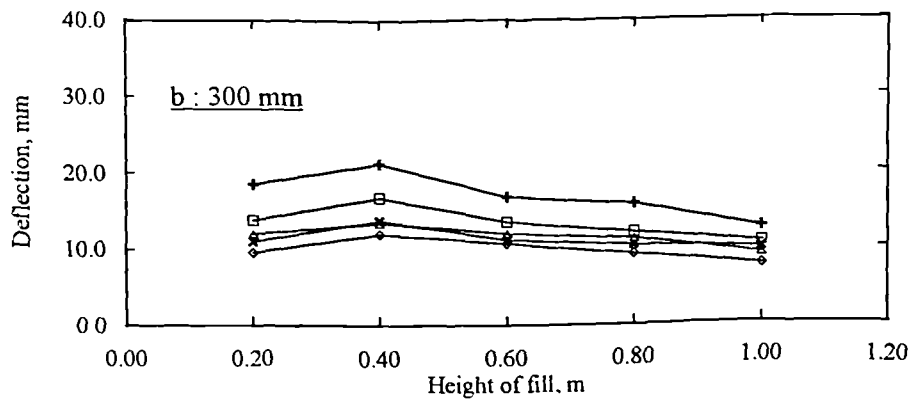
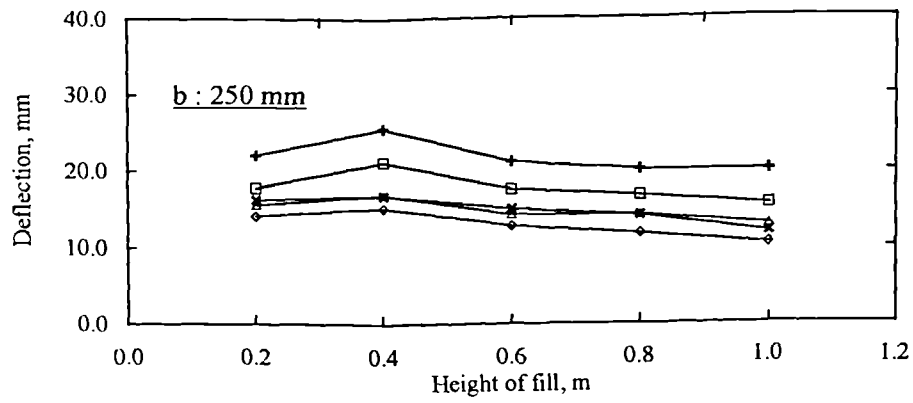
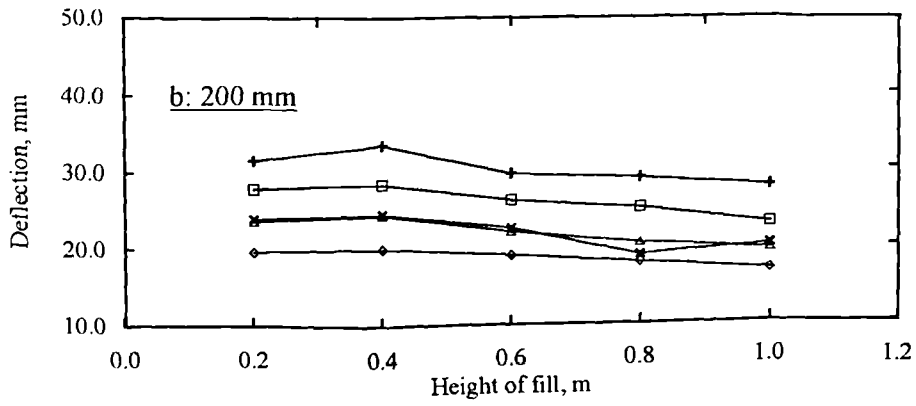
Height of fill :

- 1.0 m
- + 0.8 m
- 0.6 m
- ▲ 0.4 m
- × 0.2 m

Loading Procedure :

- Full height
- - Incremental

Figure 4-11. The variation of load with the pile cap width for the incremental and full height loading procedures.



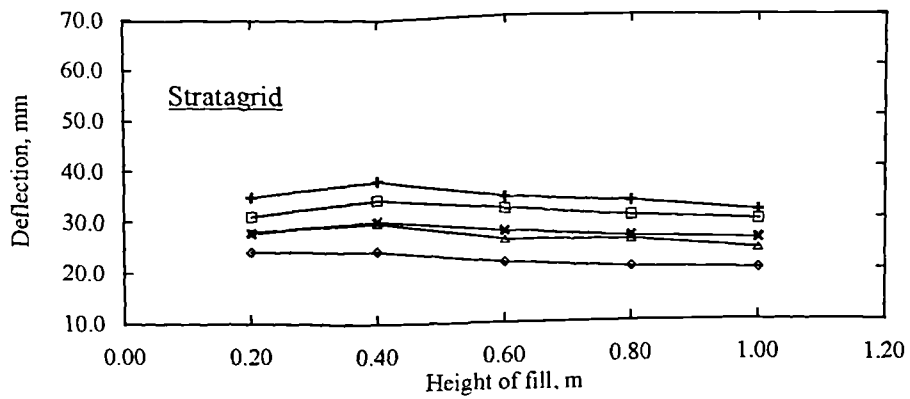
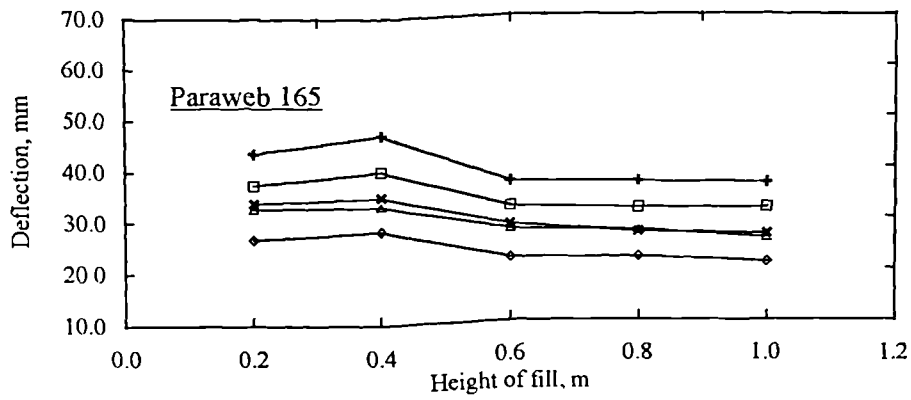
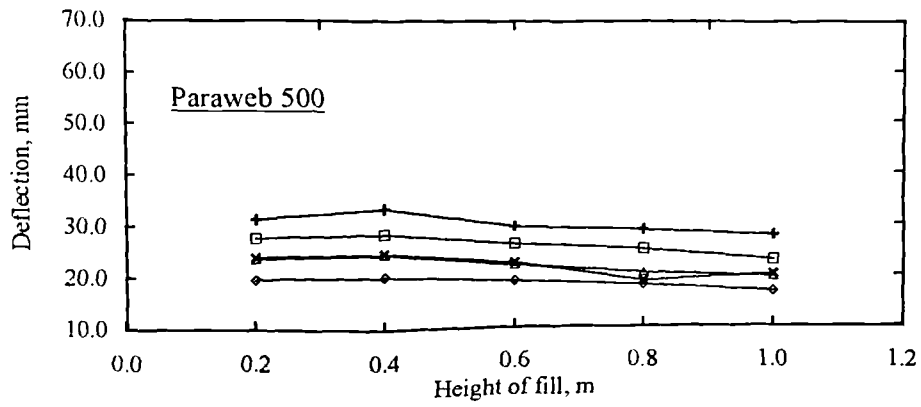
Legend :

- | | |
|---------|----------------------------|
| × Dwt-1 | + Dwt-4 |
| ● Dwt-2 | ◇ Dwt-5 |
| □ Dwt-3 | Dwt : Draw-wire transducer |

Note:

The geotextile material used Paraweb 500

Figure 4-12. The variation of mesh deflection with height of fill for the full height simulations (effect of cap width).



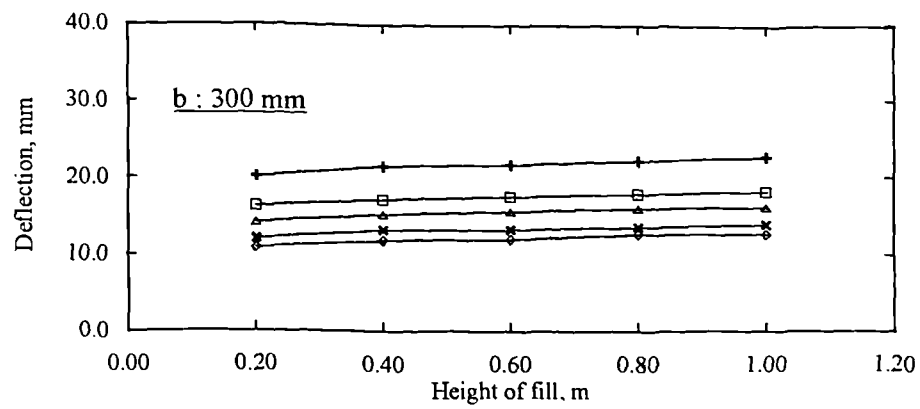
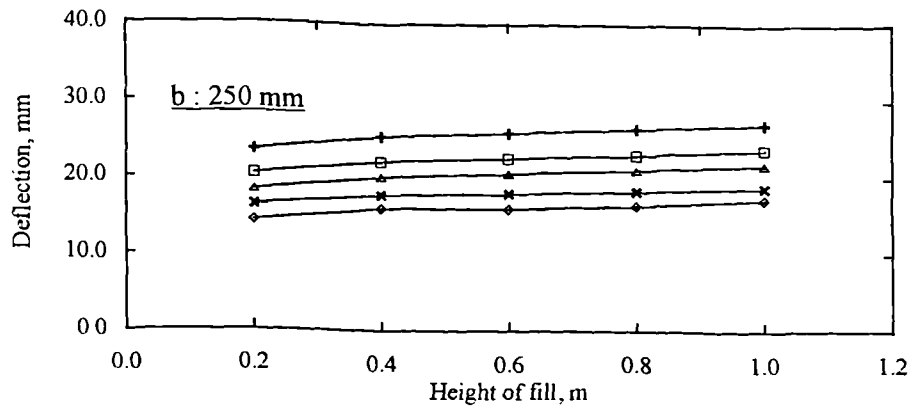
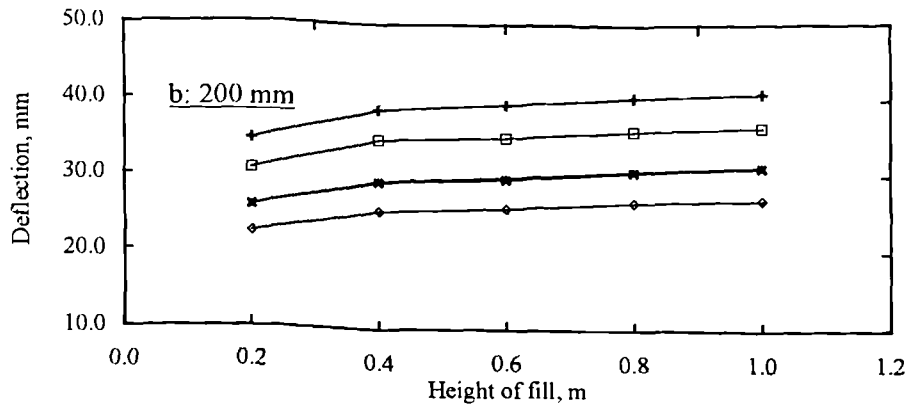
Legend :

- × Dwt-1 + Dwt-4
- Dwt-2 ◇ Dwt-5
- Dwt-3 Dwt : Draw-wire transducer

Note:

The pile cap width (b) = 200 mm

Figure 4-13. The variation of mesh deflection with height of fill for the full height simulations (effect of geotextile material).



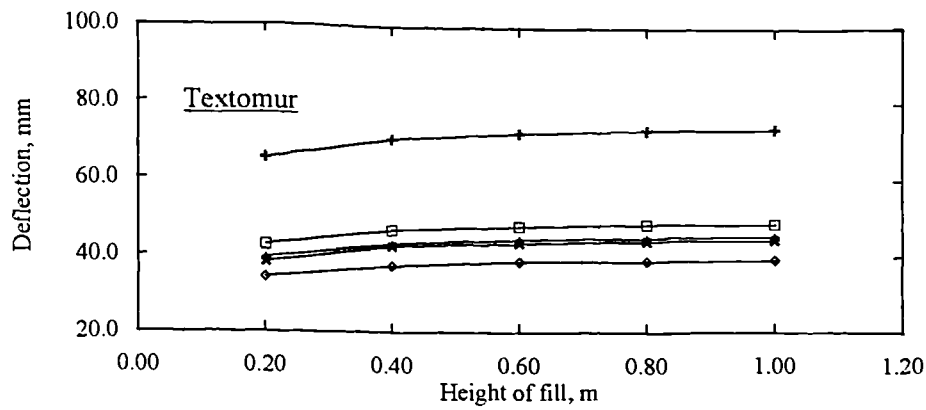
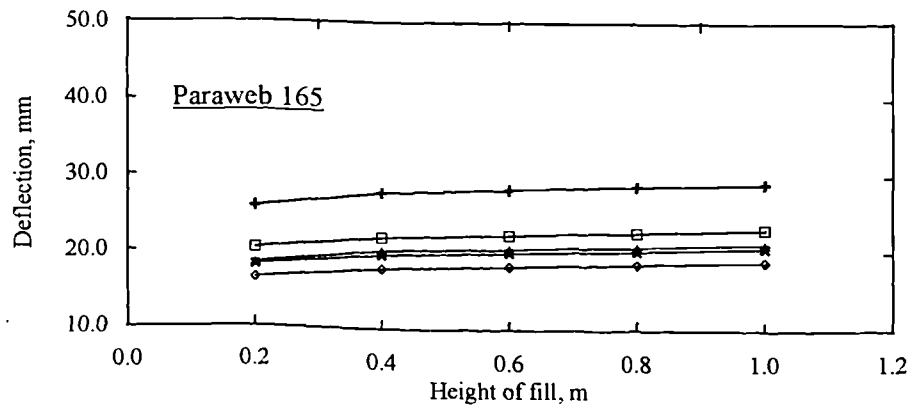
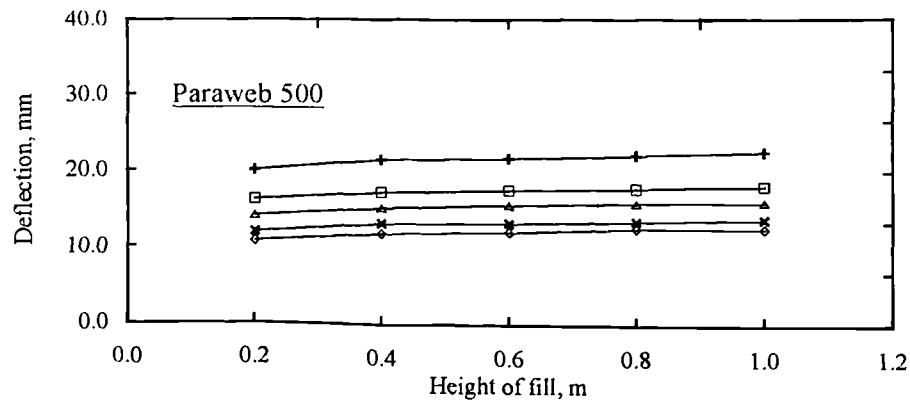
Legend :

- × Dwt-1 + Dwt-4
- Dwt-2 ◇ Dwt-5
- Dwt-3 Dwt : Draw-wire transducer

Note:

The geotextile material used Paraweb 500

Figure 4-14. The variation of mesh deflection with height of fill for the incremental loading simulations (effect of cap width).



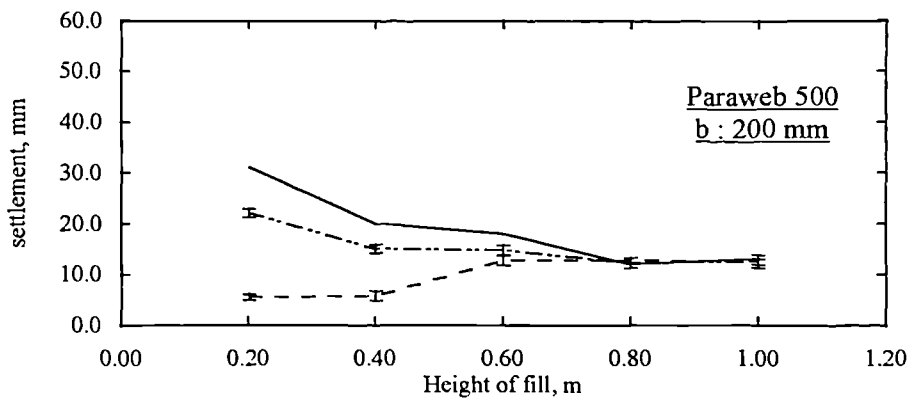
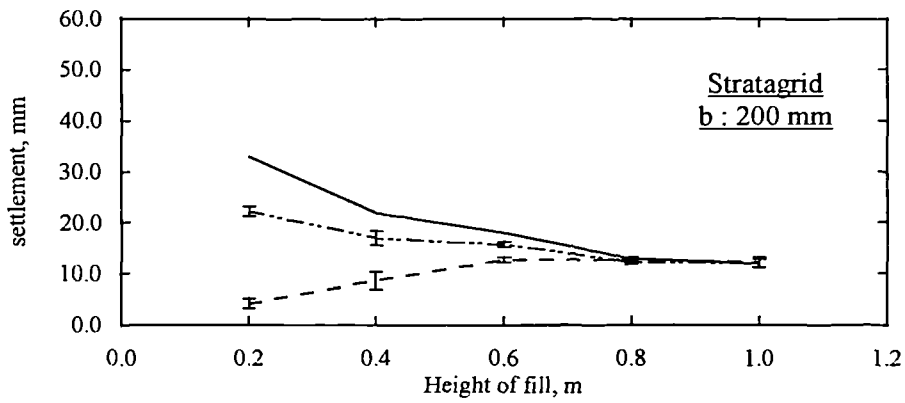
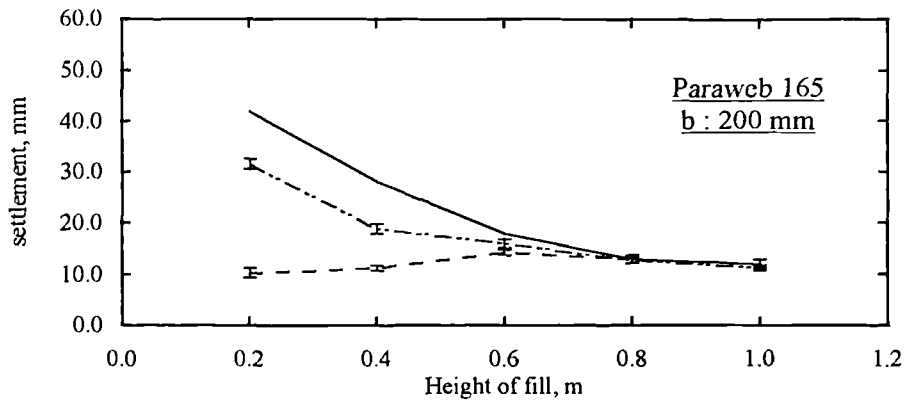
Legend :

- × Dwt-1 + Dwt-4
- Dwt-2 ◇ Dwt-5
- Dwt-3 Dwt : Draw-wire transducer

Note:

The pile cap width (b) = 200 mm

Figure 4-15. The variation of mesh deflection with height of fill for the incremental loading simulations (effect of geotextile material).



Legend:

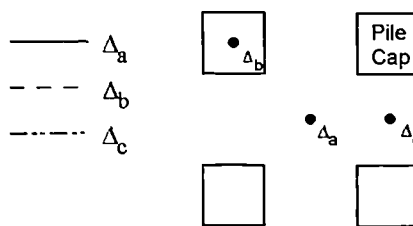
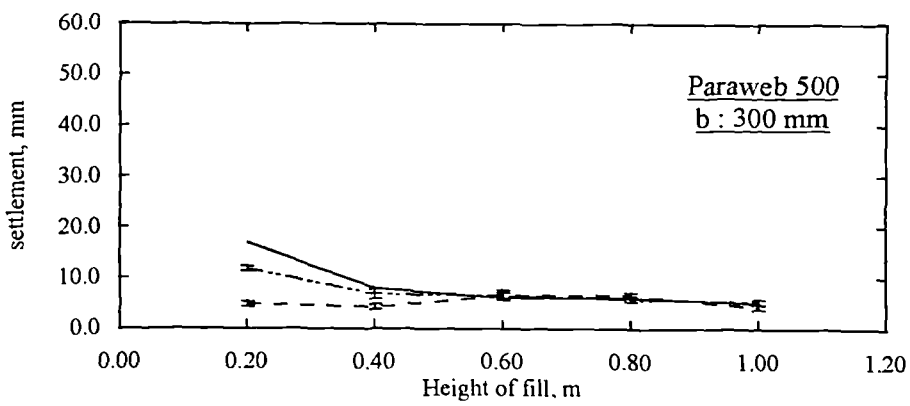
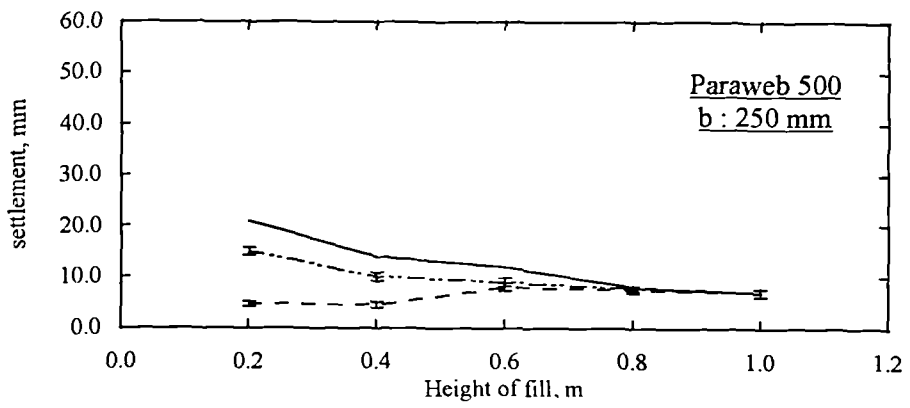
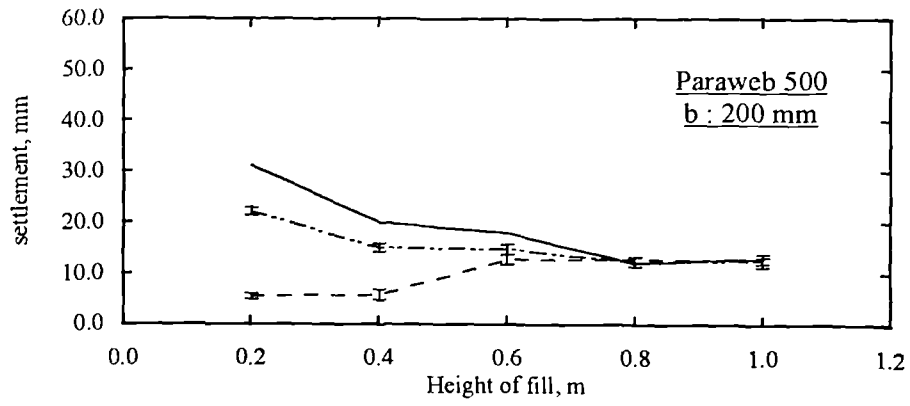


Figure 4-16. The variation of surface settlement with height of fill for geotextile materials Paraweb 165, 500 and Stratagrid.



Legend:

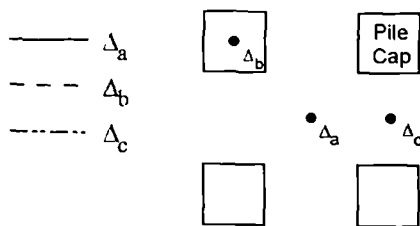
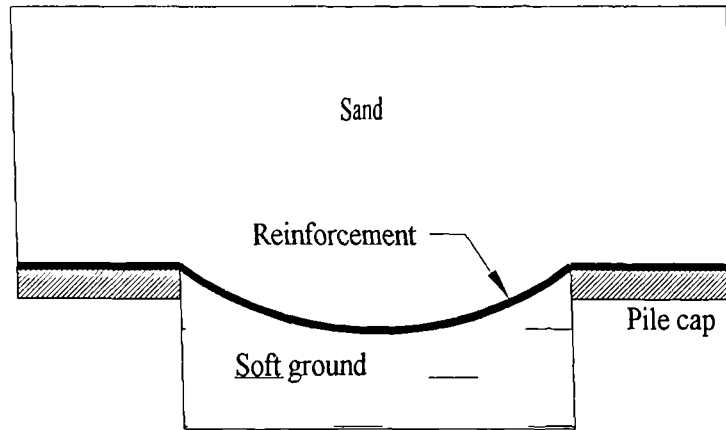
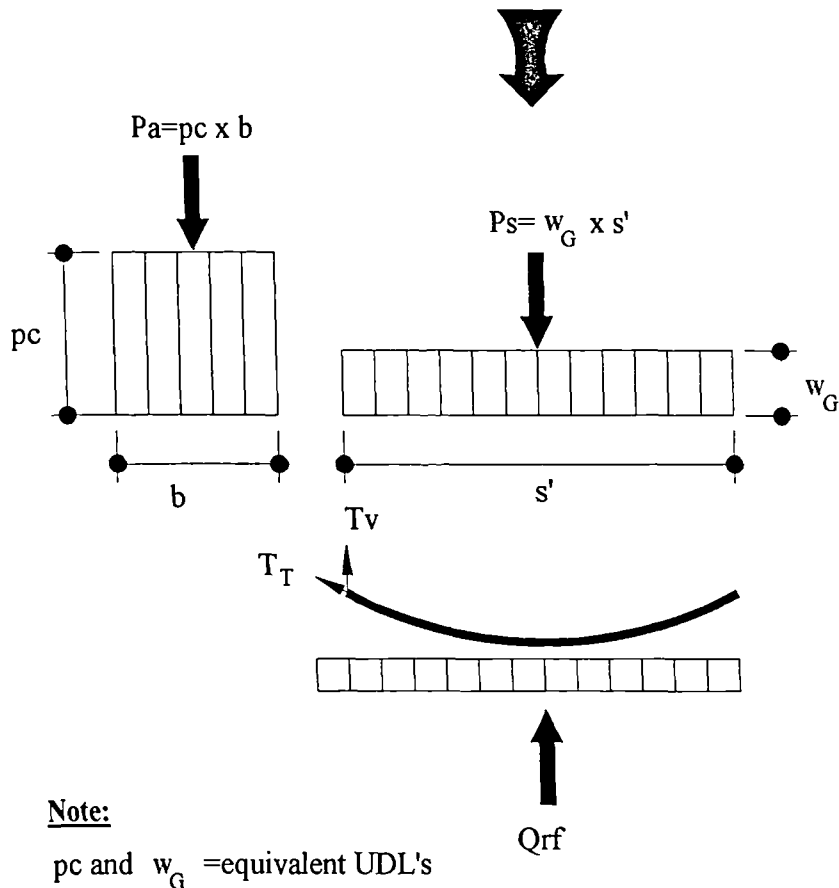


Figure 4-17. The variation of surface settlement with height of fill for different pile cap widths.



Typical Piled Embankment System



Idealised Vertical Stress Distribution

Figure 5-1. Idealised vertical stress distribution on the geosynthetic reinforcement

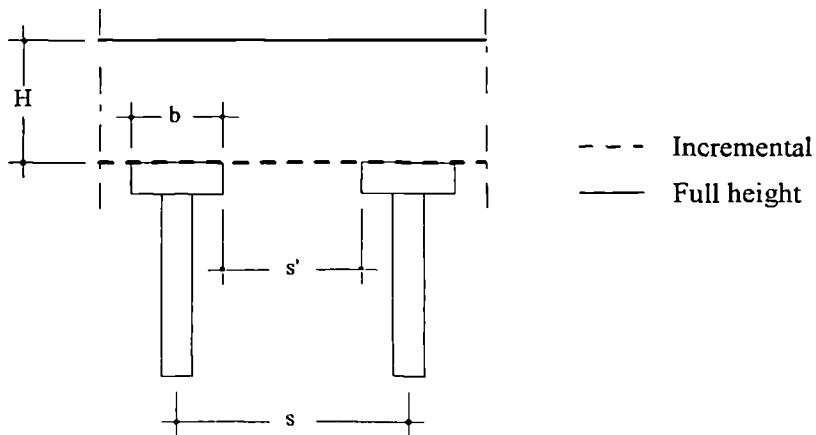
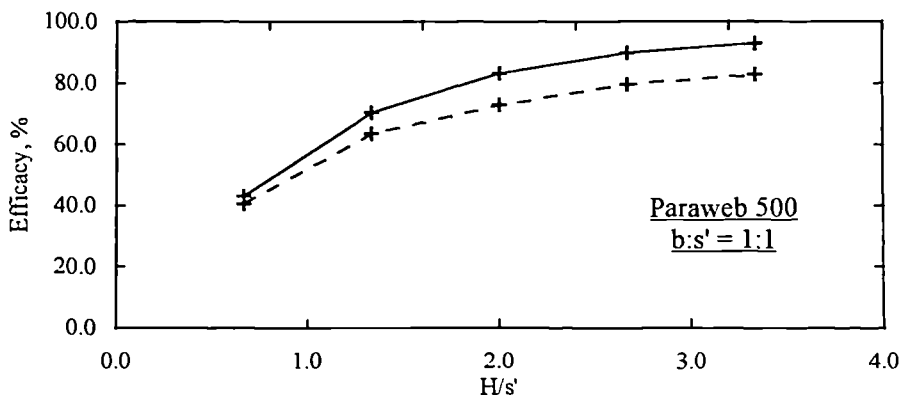
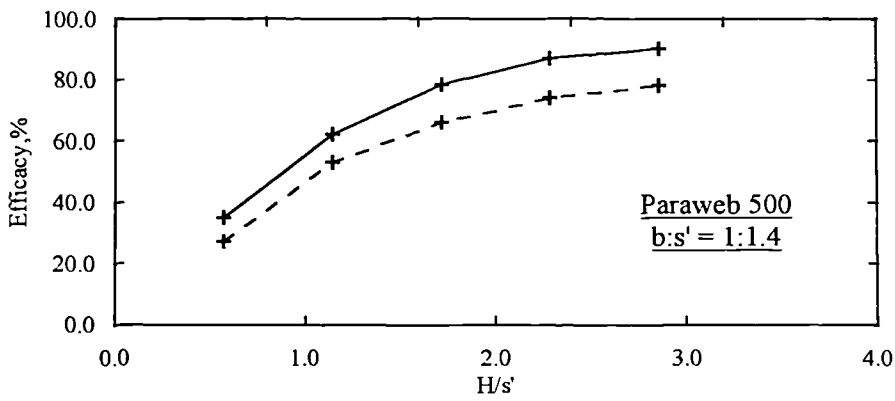
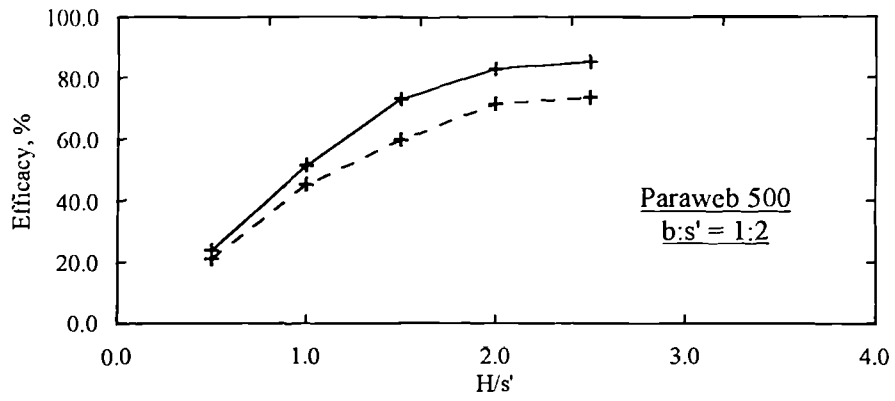


Figure 5-2. The variation of efficacy with the (H/s') for different b/s' ratios.

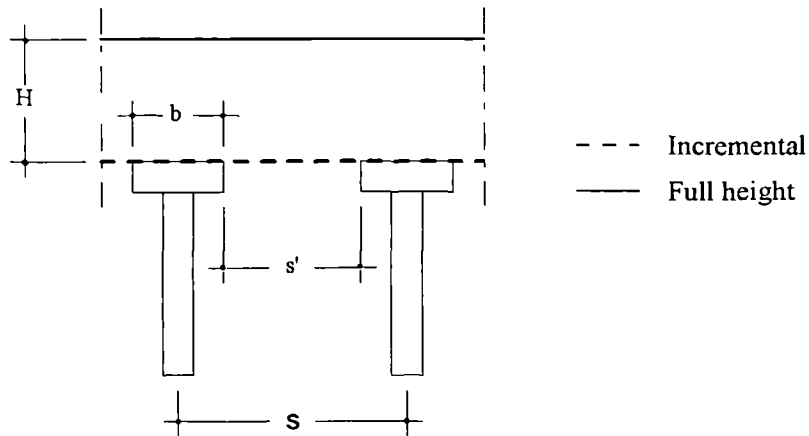
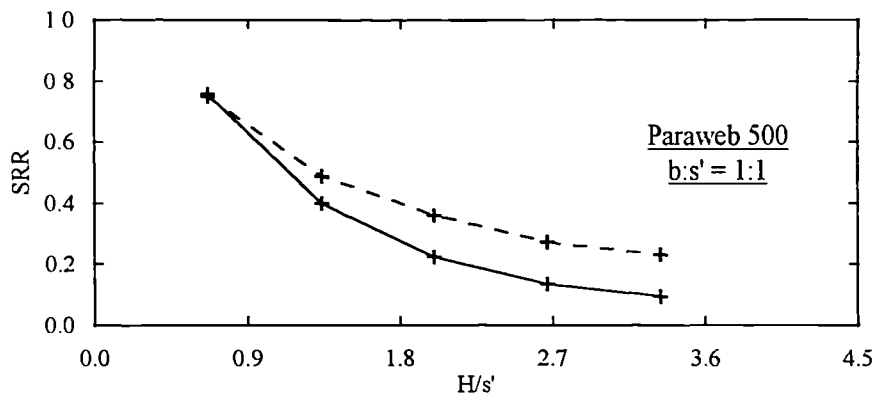
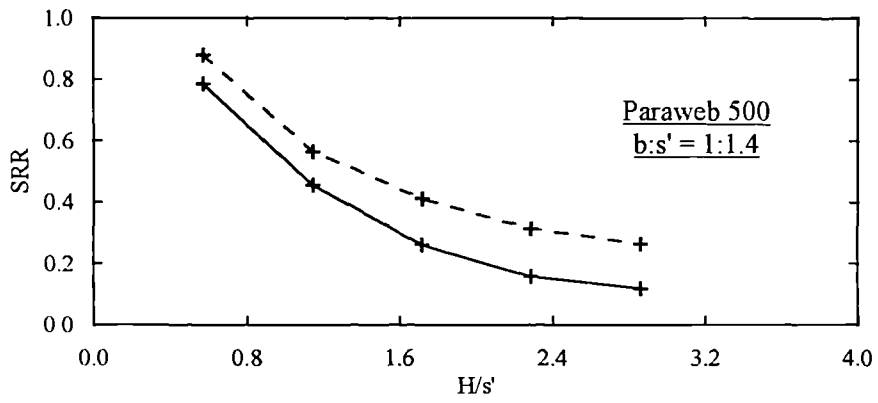
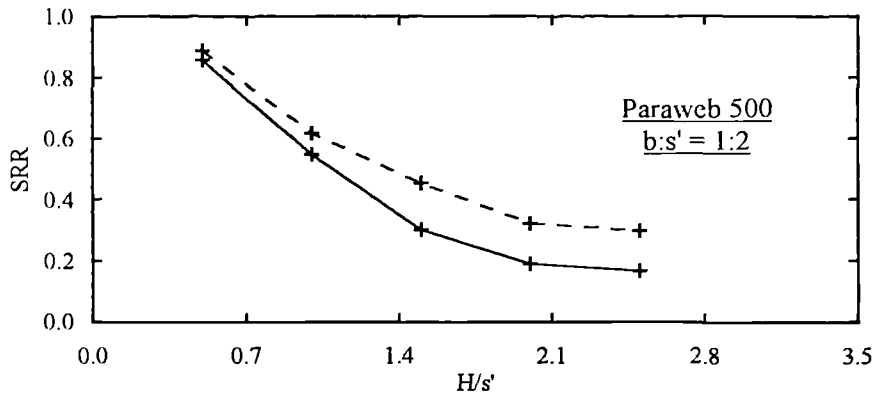


Figure 5-3. The variation of the stress reduction ratio (SRR) with the (H/s') for different b/s' ratios.

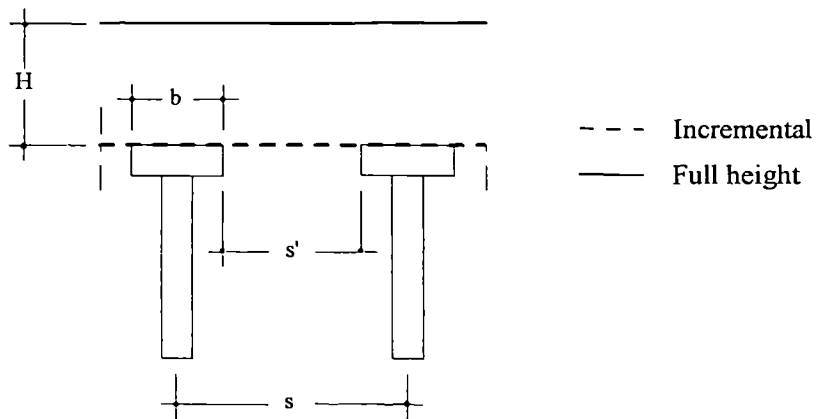
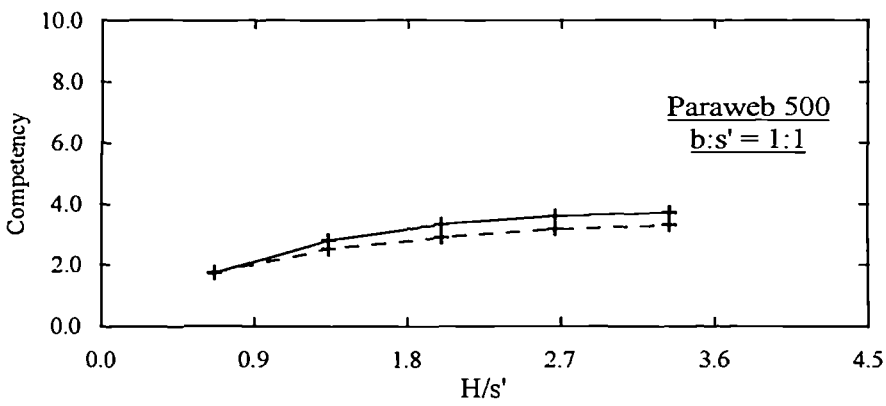
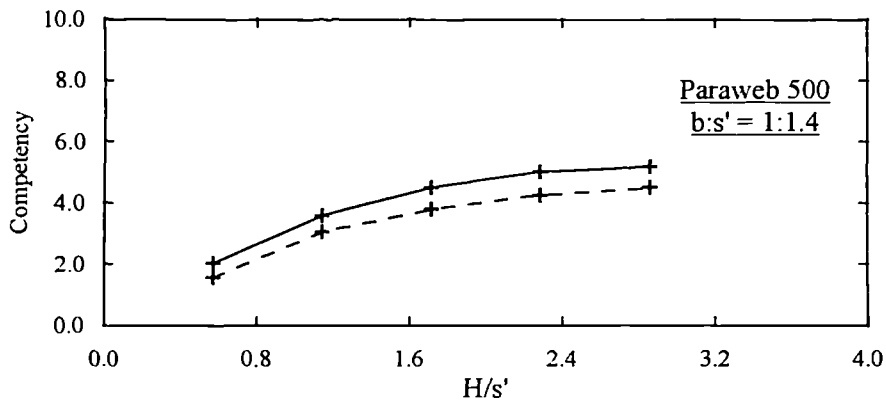
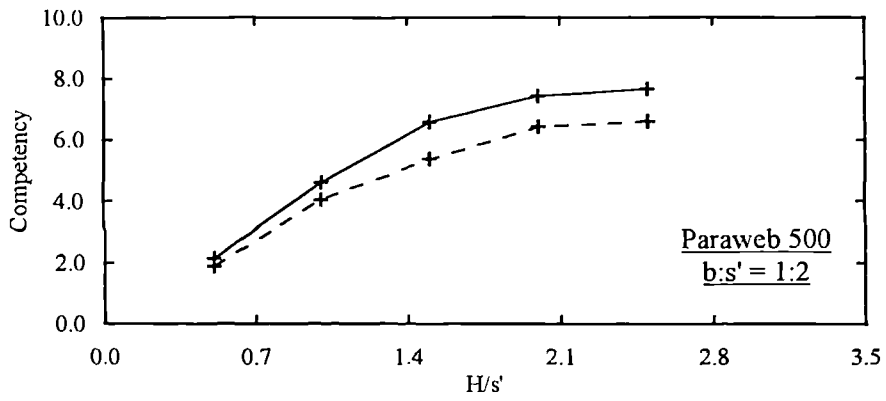


Figure 5-4. The variation of competency with the (H/s') for different b/s' ratios.

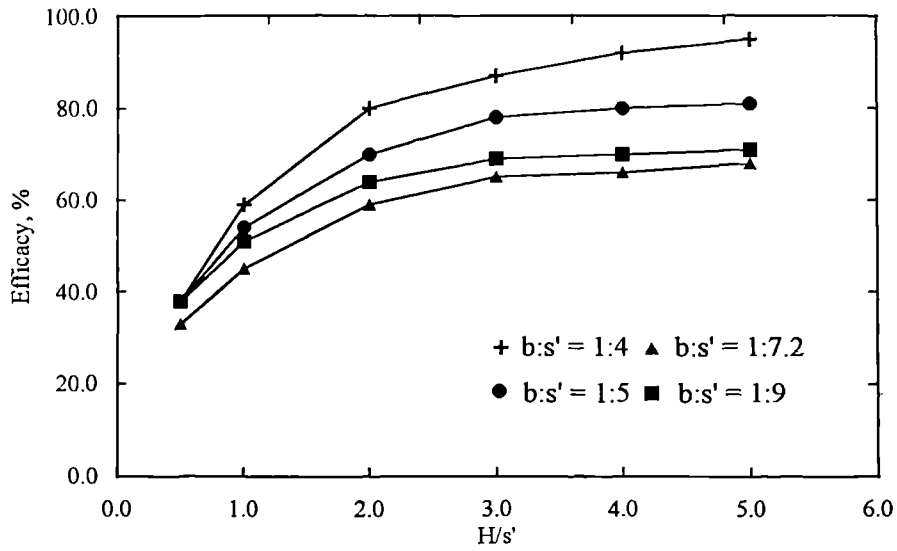


Figure 5-5a. The variation of the efficacy versus the depth ratio for the cap beam system proposed by Tang (1992).

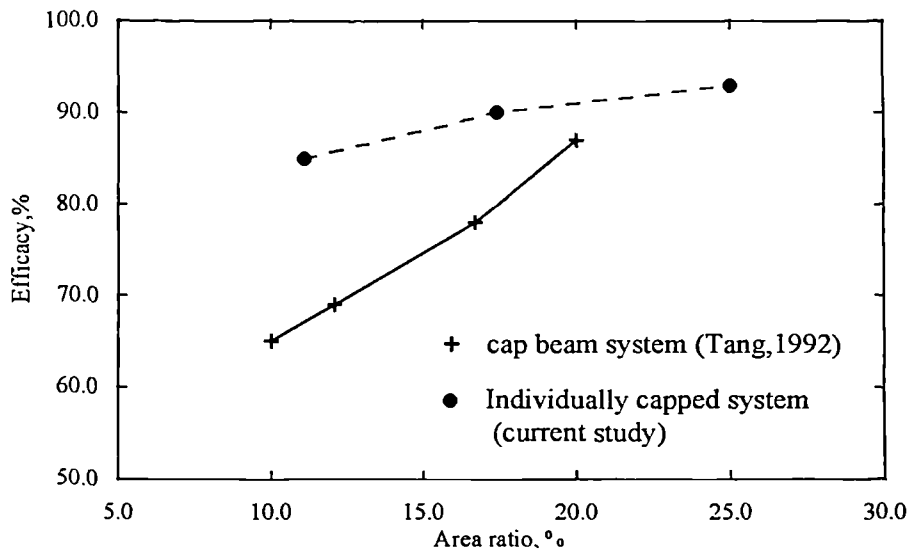
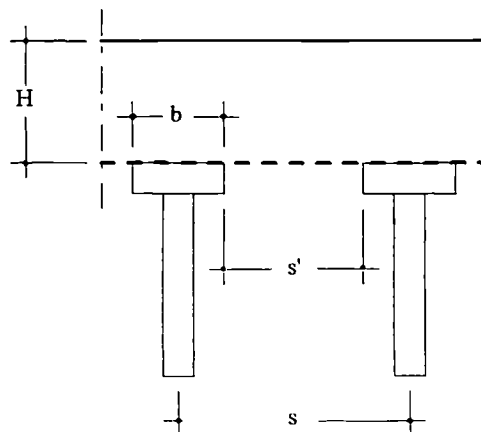


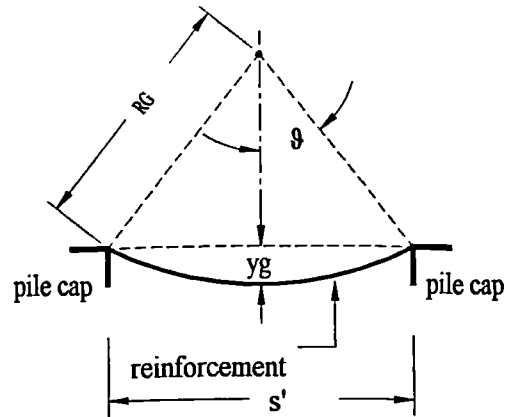
Figure 5-5b. A comparison between the efficacy of the individually capped system and the cap beam method at depth ratio of $H/s' = 3$.



Circular Arc Geometry

$$s' = 2 * R * \sin(\vartheta)$$

$$y_g = R (1 - \cos\left(\frac{\vartheta}{2}\right))$$



Parabolic Arc

$$y = \frac{4 * y_g * x * (s' - x)}{(s')^2}$$

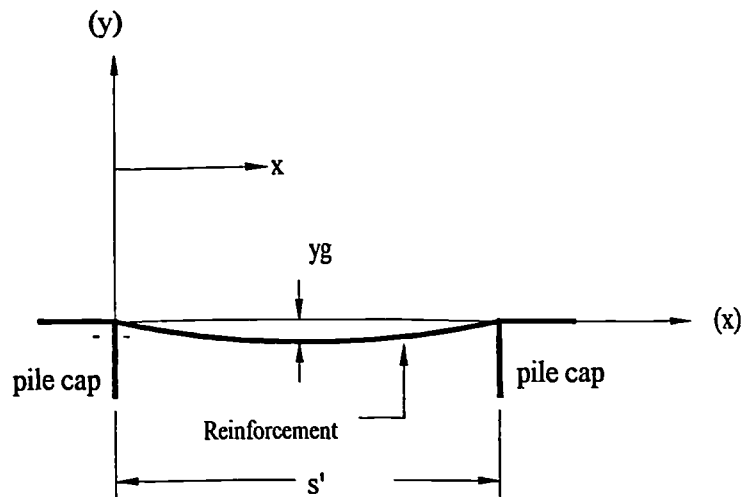
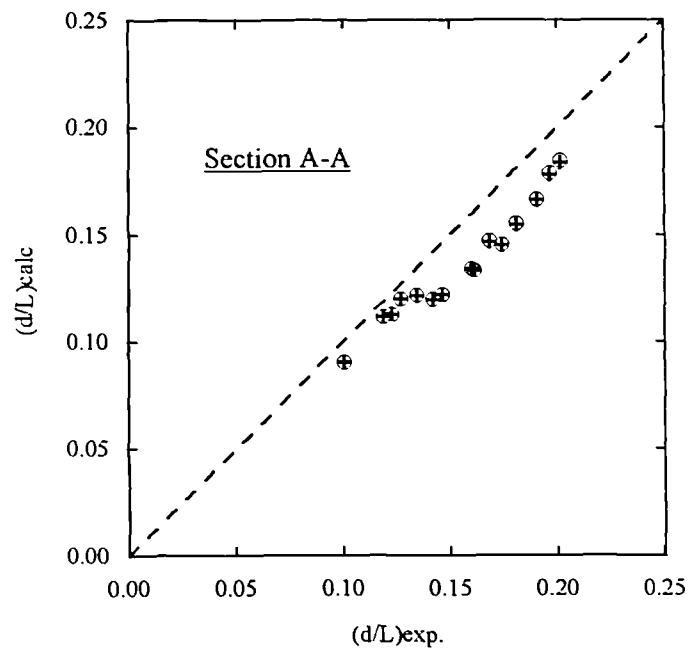
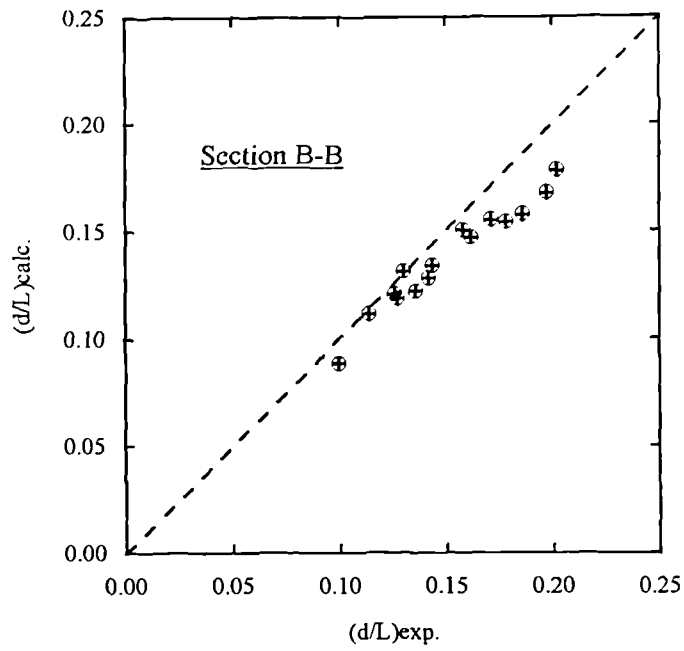


Figure 5-6. Idealised representation of the circular and parabolic arc geometries used in the comparative study.



Legend:

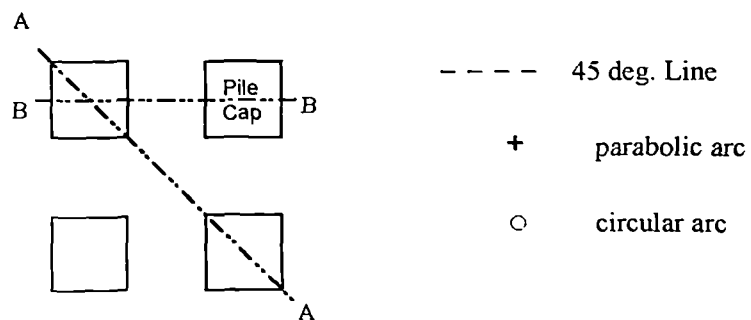
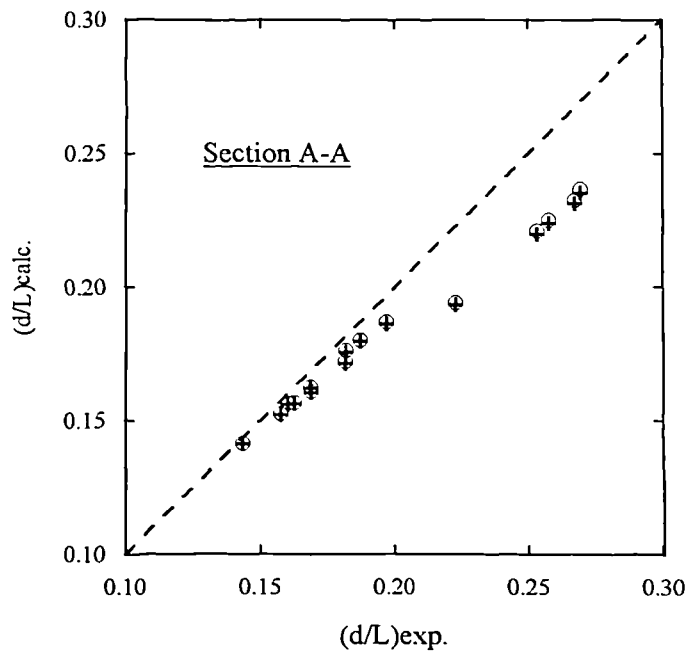
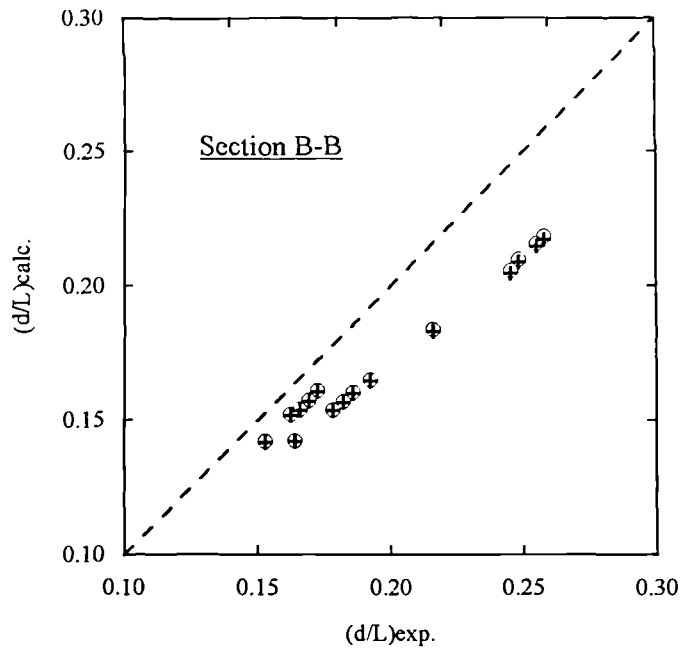


Figure 5-7. Experimental versus calculated (d/L) values for full height simulations.



Legend:

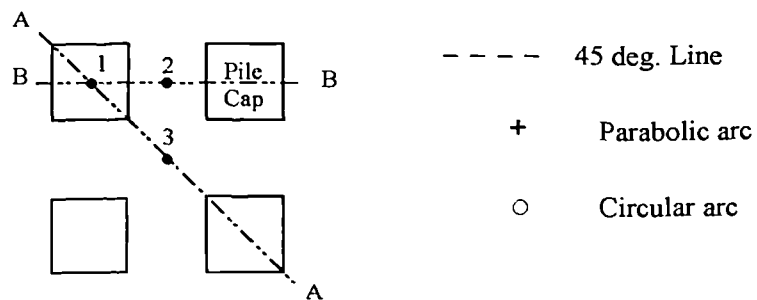


Figure 5-8. Experimental versus calculated (d/L) values for incremental loading simulations.

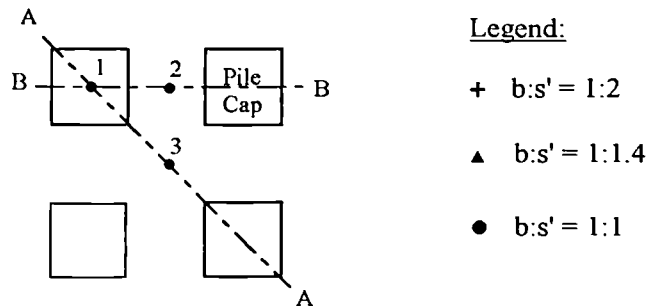
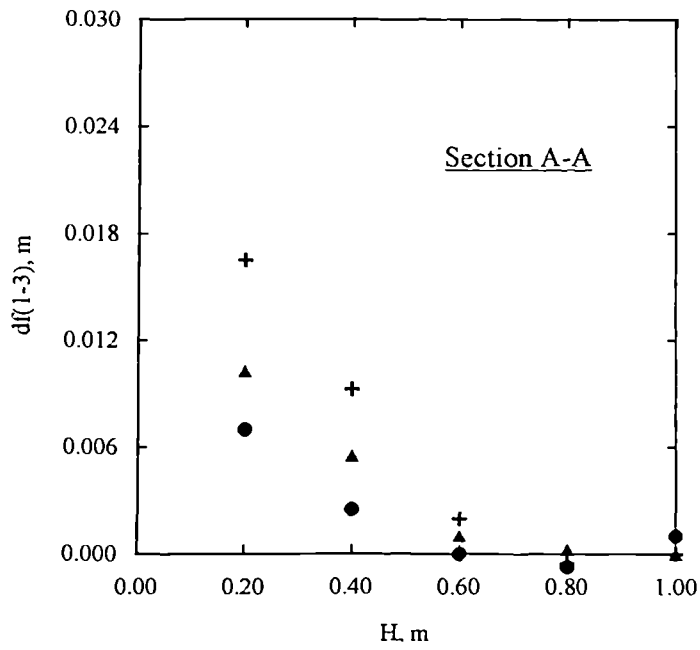
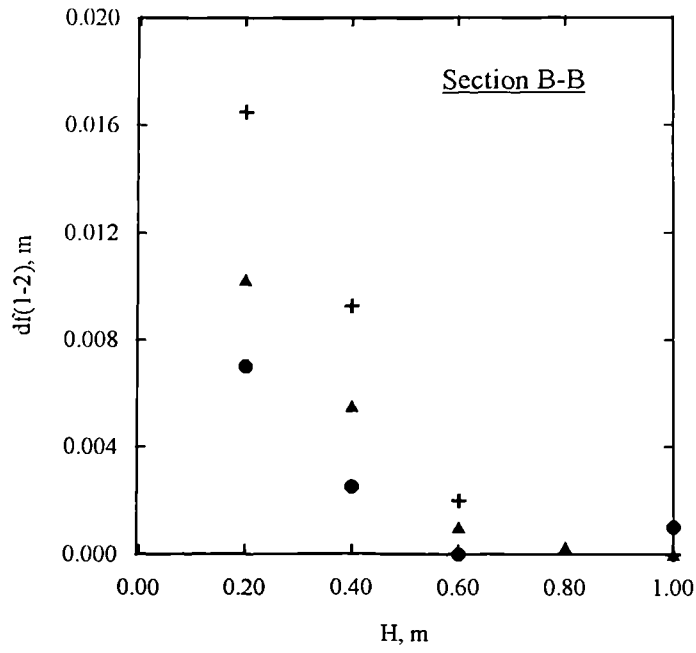
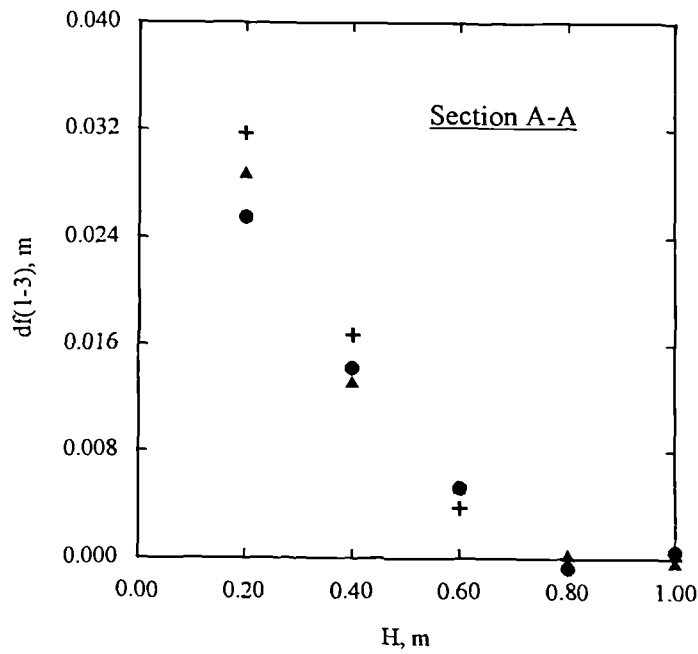
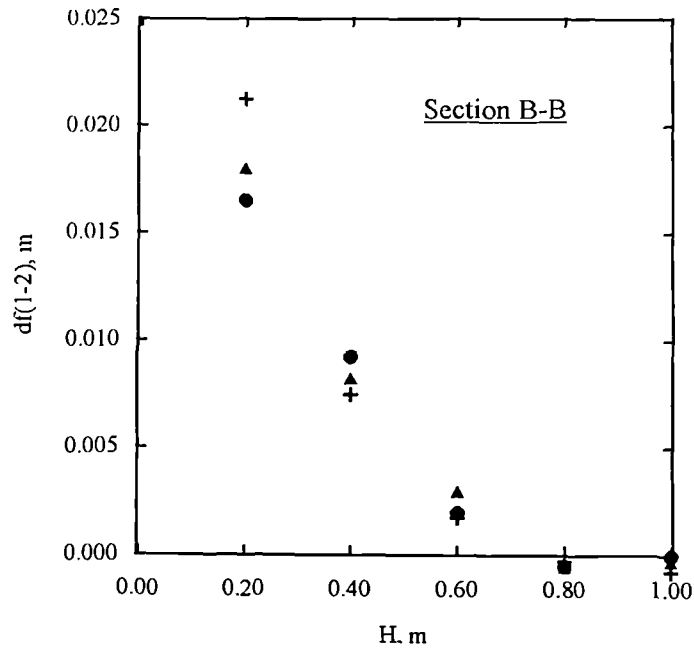
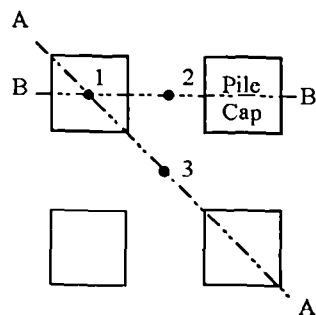


Figure 5-9. Influence of capping ratio (b:s') on surface differential settlement (Paraweb 500).



Legend:



Legend:

- + Paraweb 165
- ▲ Stratagrid
- Paraweb 500

Figure 5-10. Influence of geotextile material on surface differential settlement ($b:s'=1:2$).

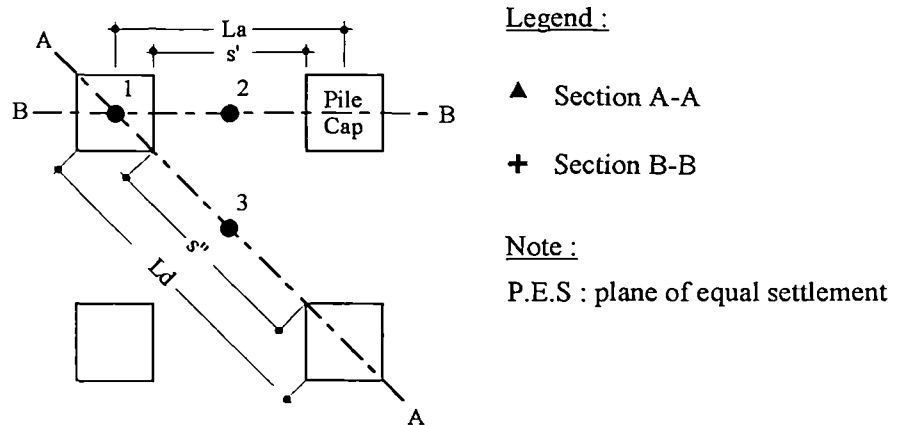
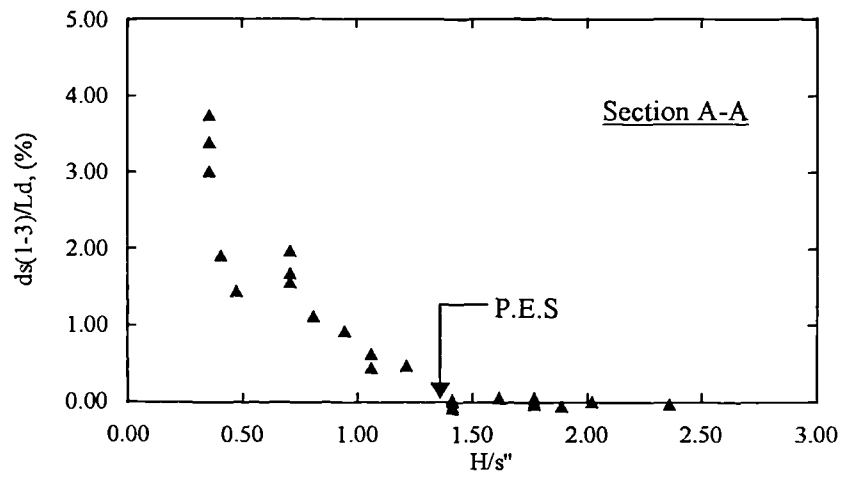
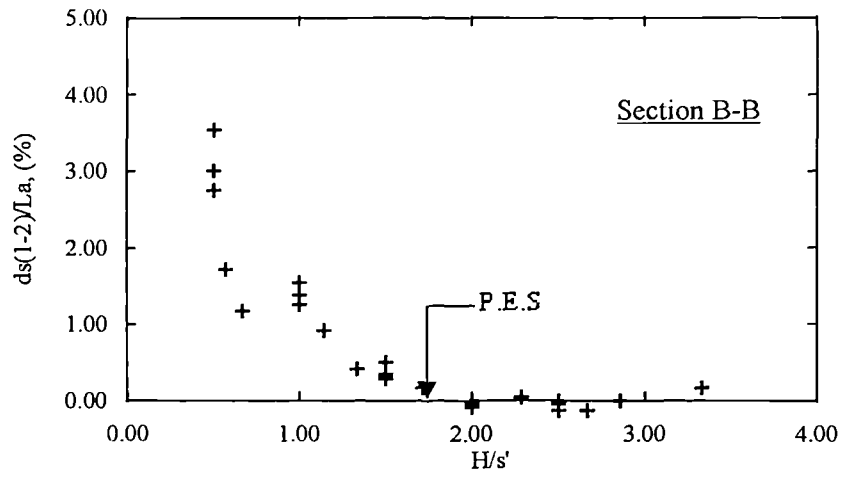


Figure 5-11. The variation of the maximum surface distortion with the depth ratio along the transverse and diagonal lines of symmetry.

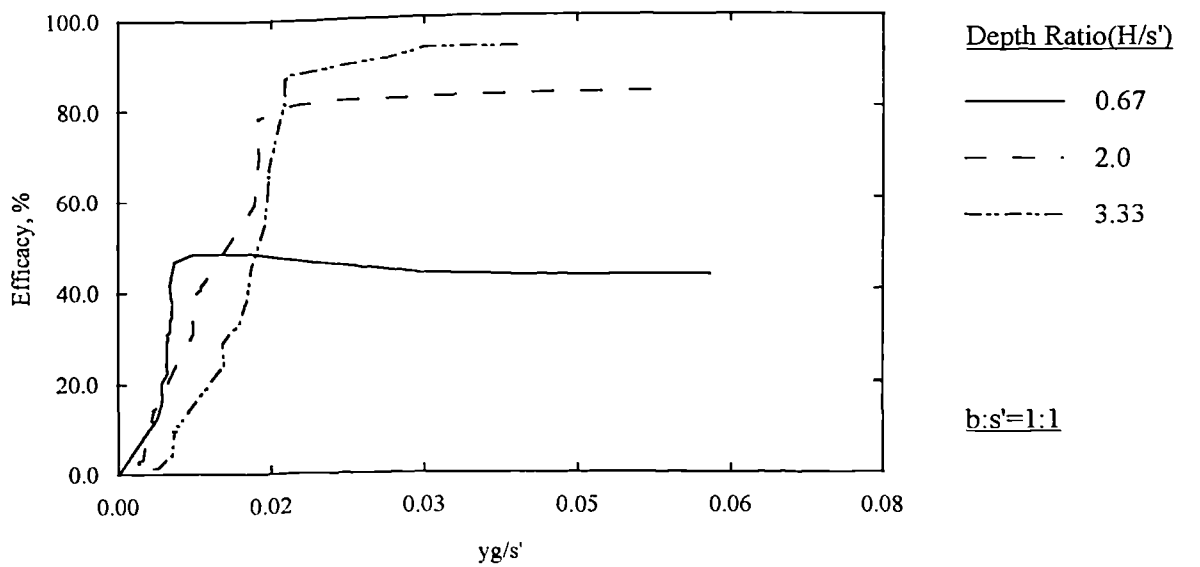
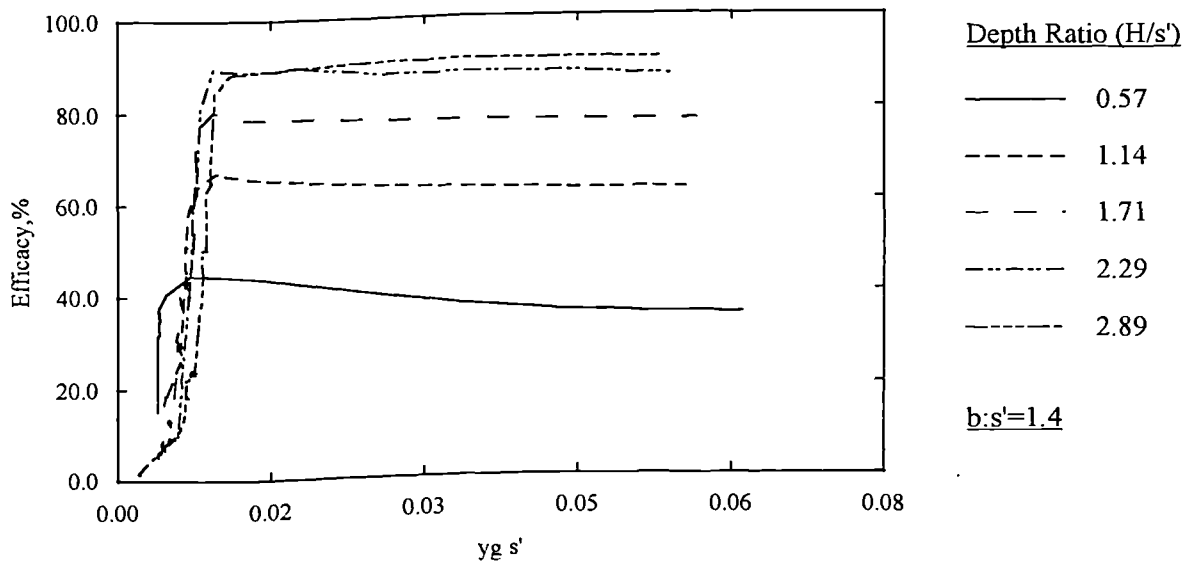
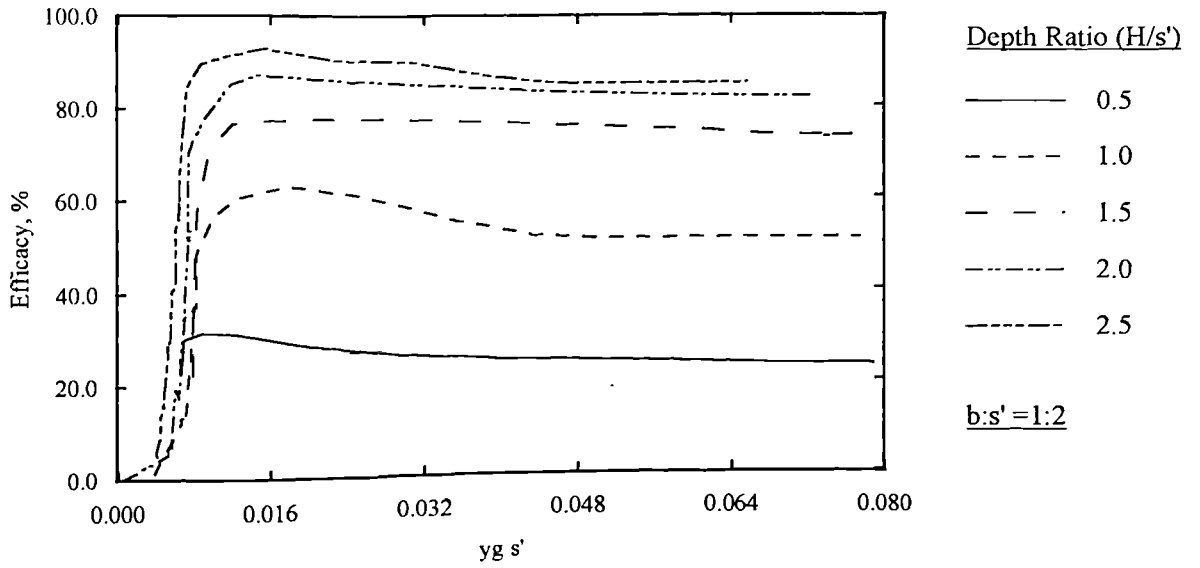
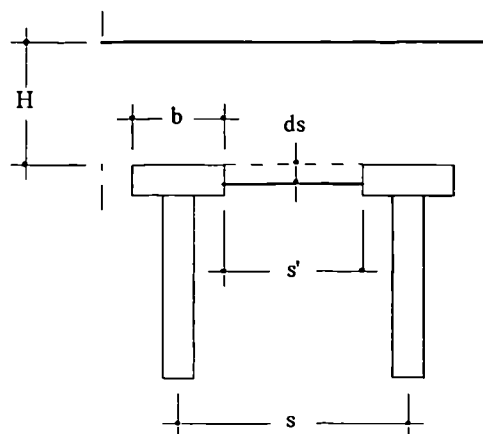
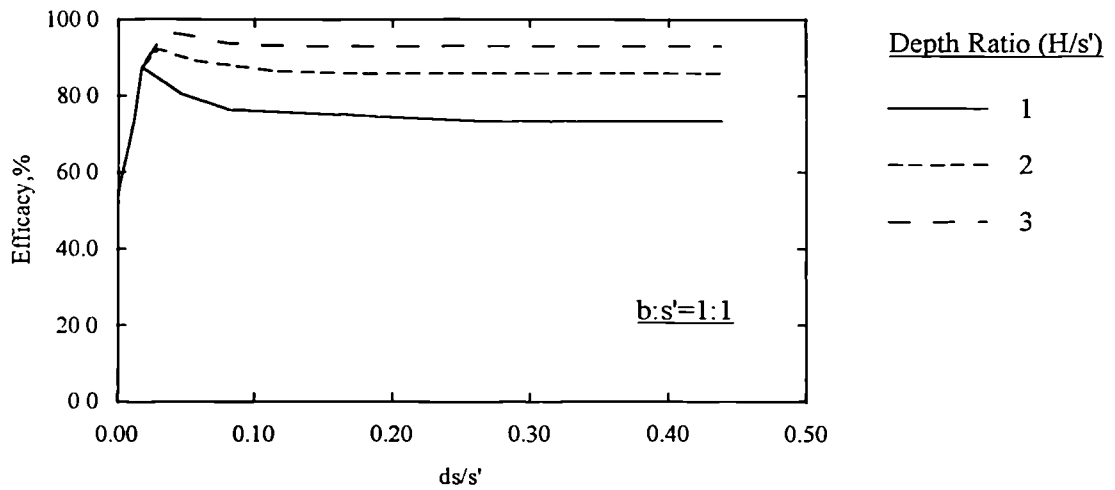
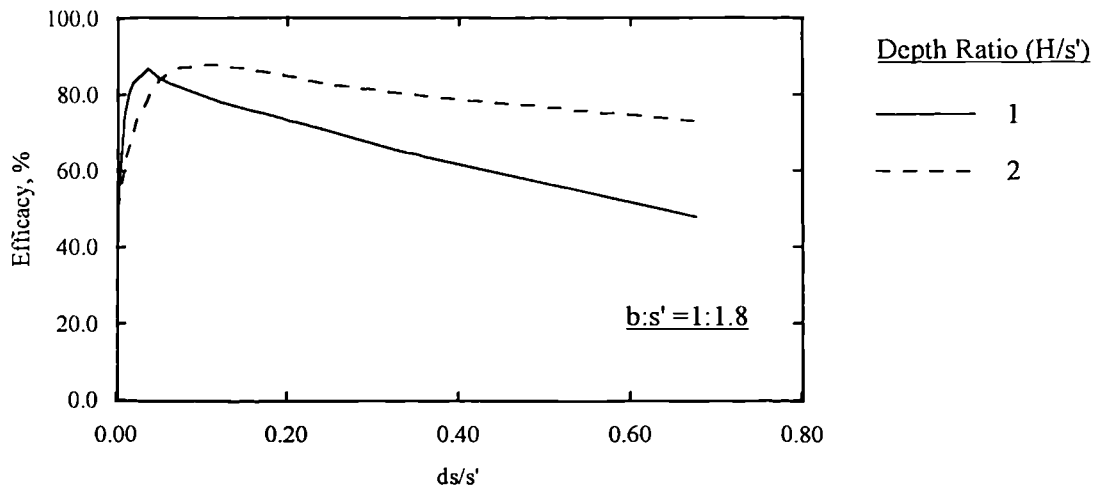


Figure 5-12. The influence of the settlement ratio on efficacy for different b/s' ratios (material : Paraweb 500).



Note:

$ds/s' =$ settlement ratio

Figure 5-13. The influence of the settlement ratio on efficacy for different b/s' ratios for an unreinforced model piled embankment, Ali (1990).

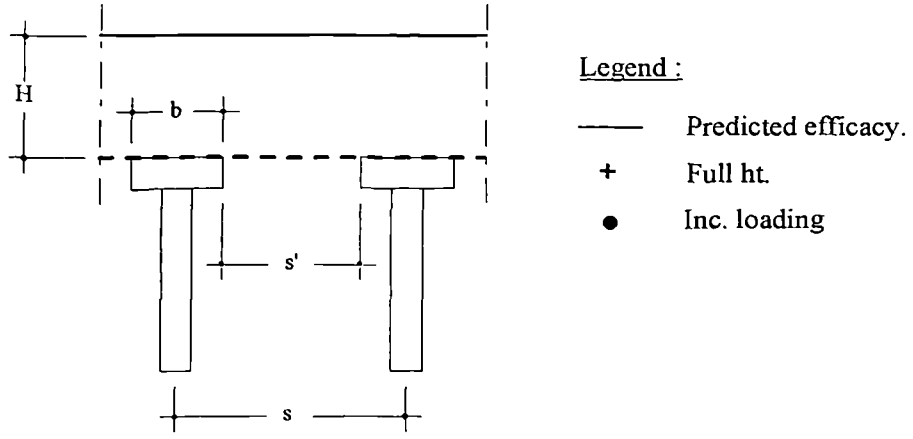
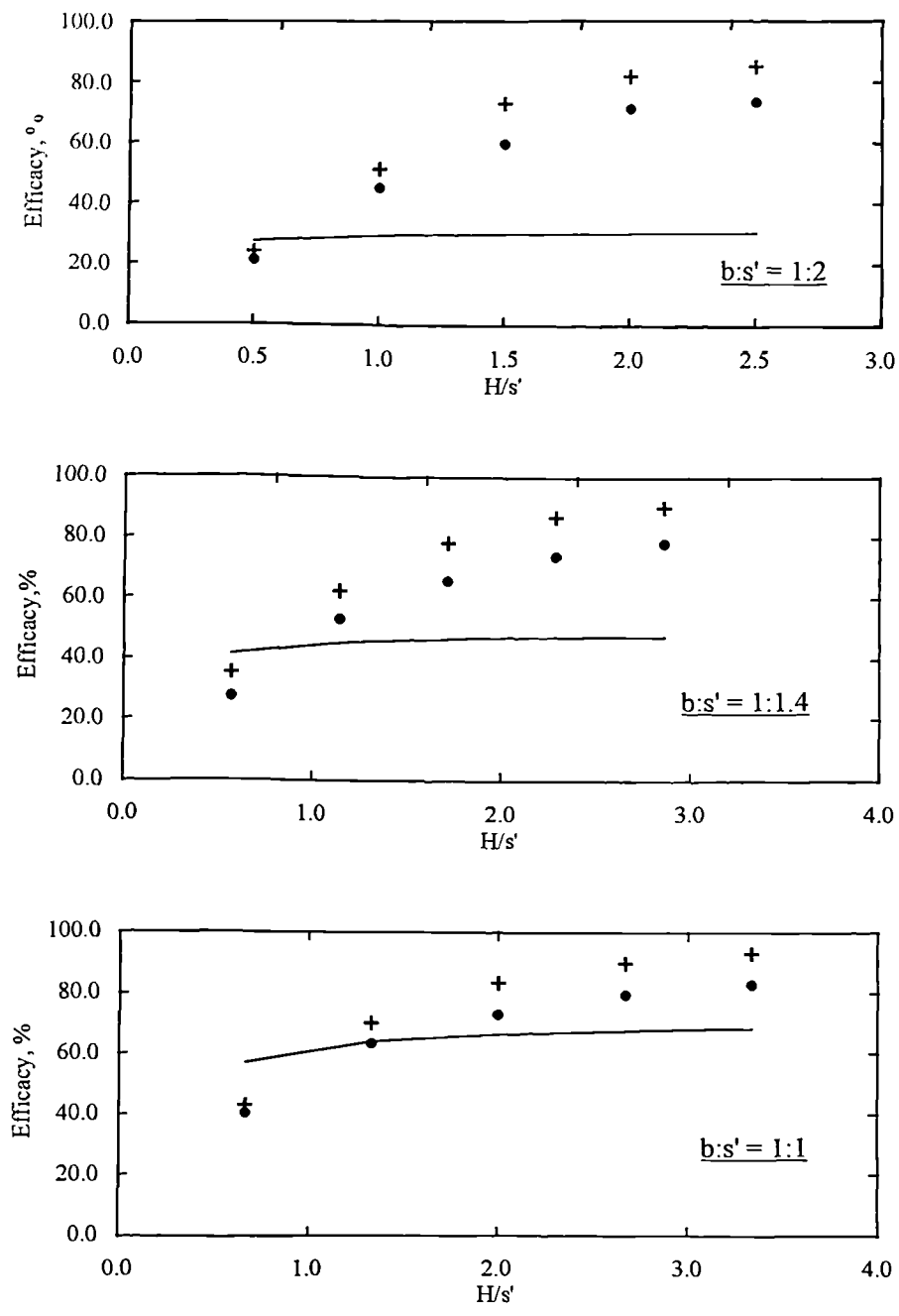


Figure 5-14. The variation of the efficacy calculated using the shear plane method proposed by John (1987).

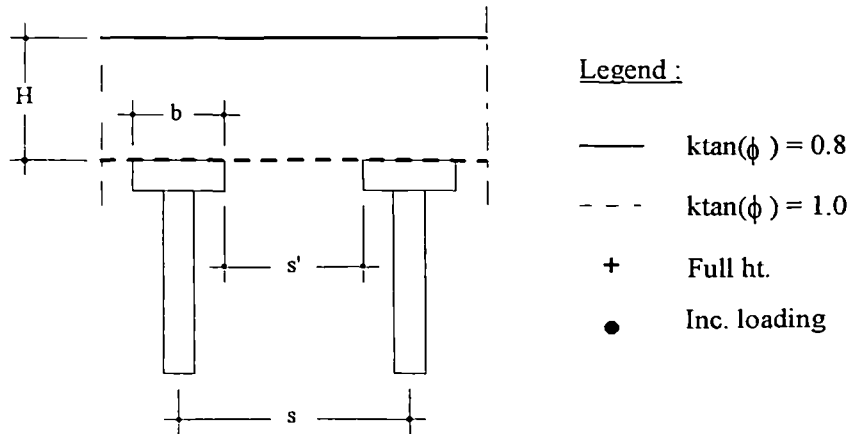
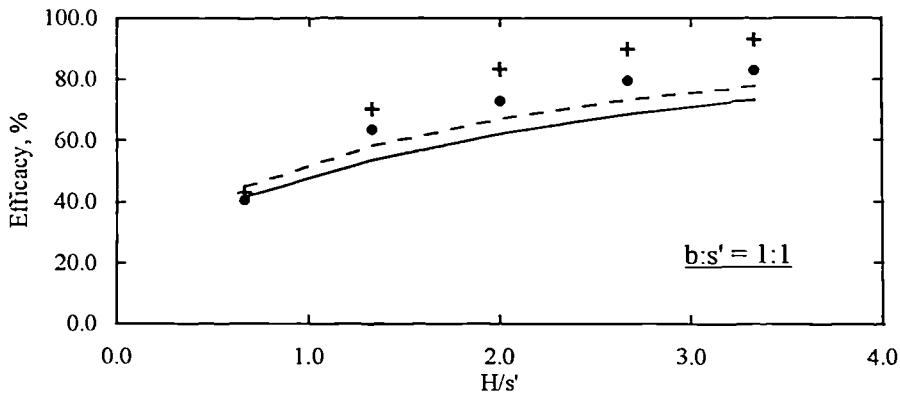
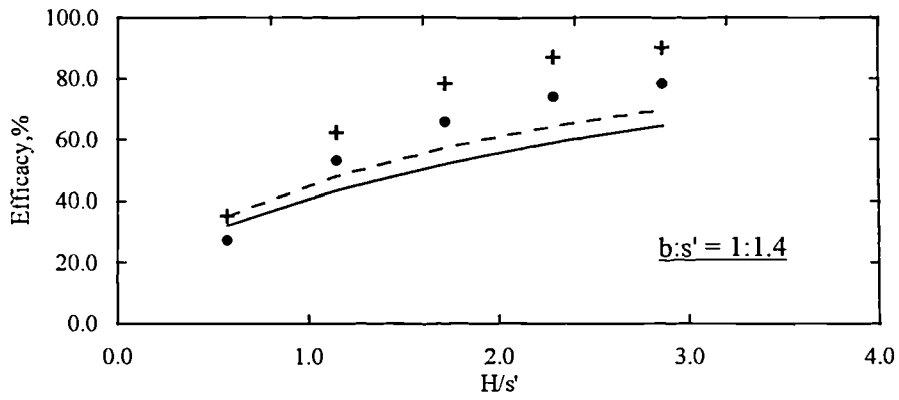
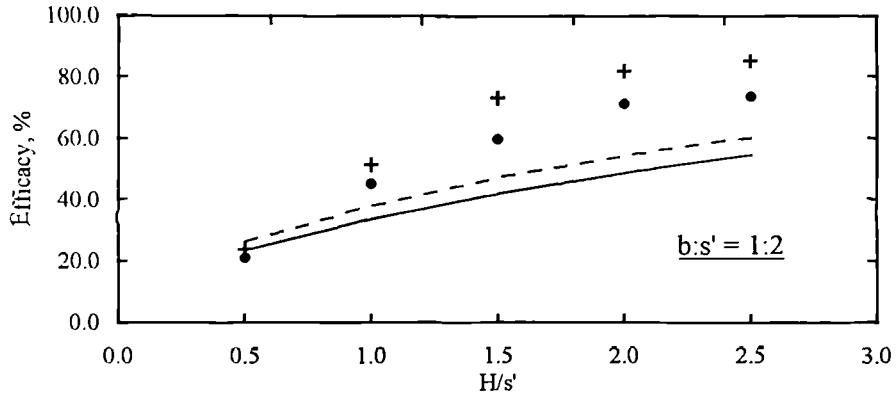
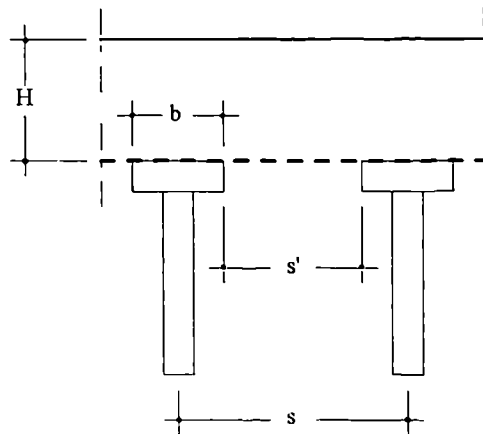
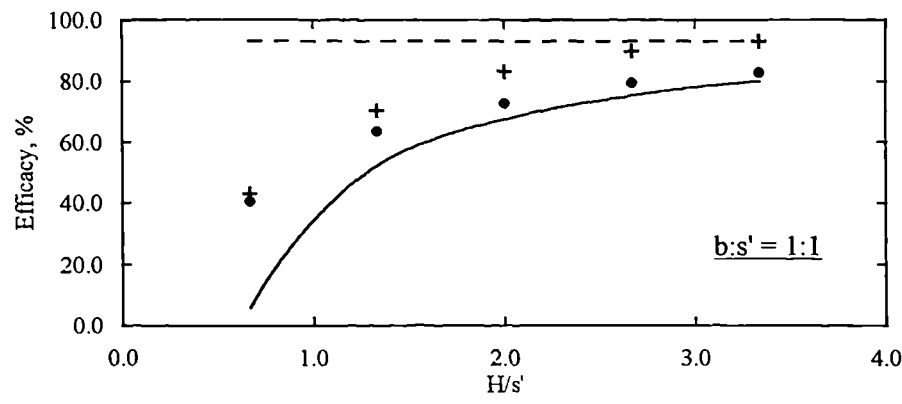
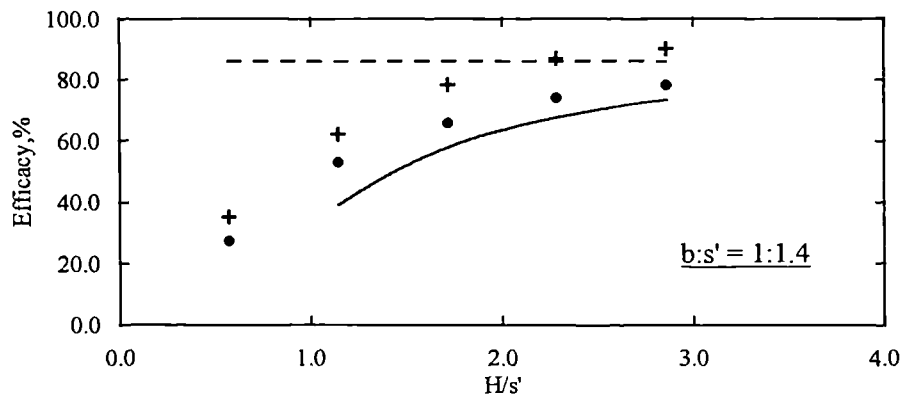
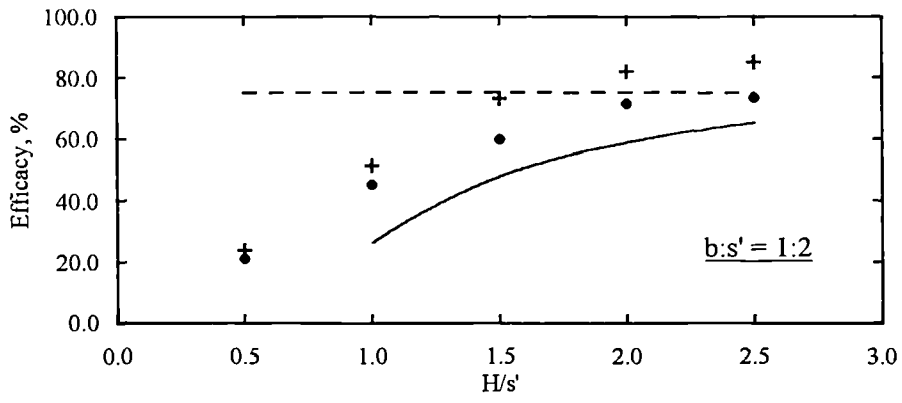


Figure 5-15. The variation of the efficacy calculated using the semi-empirical method proposed by Combarieu (1987).



Legend :

- - - Cap stability
- Crown stability
- + Full ht.
- Inc. loading

Figure 5-16. The variation of the efficacy calculated using the domed arch analysis (Hewlett et al. (1988)).

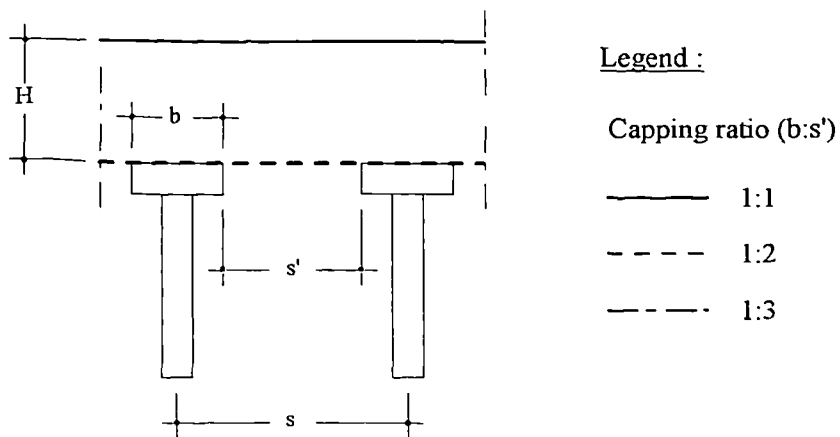
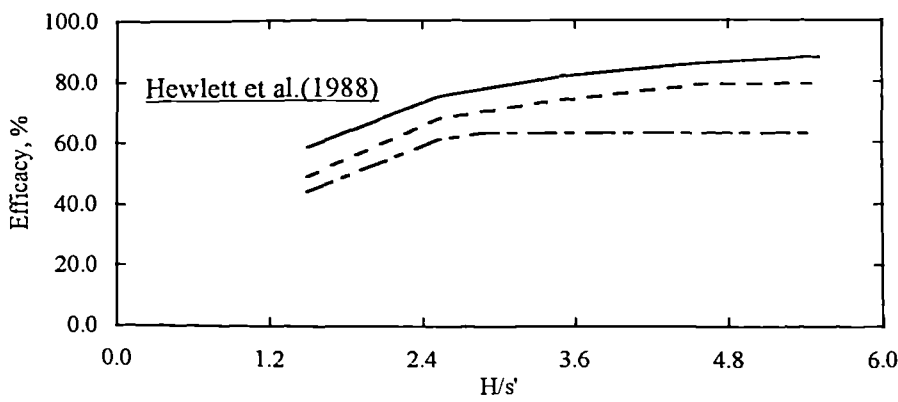
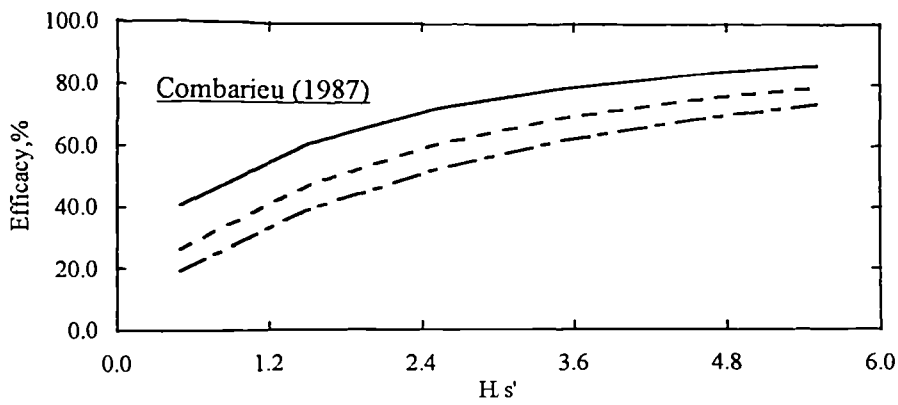
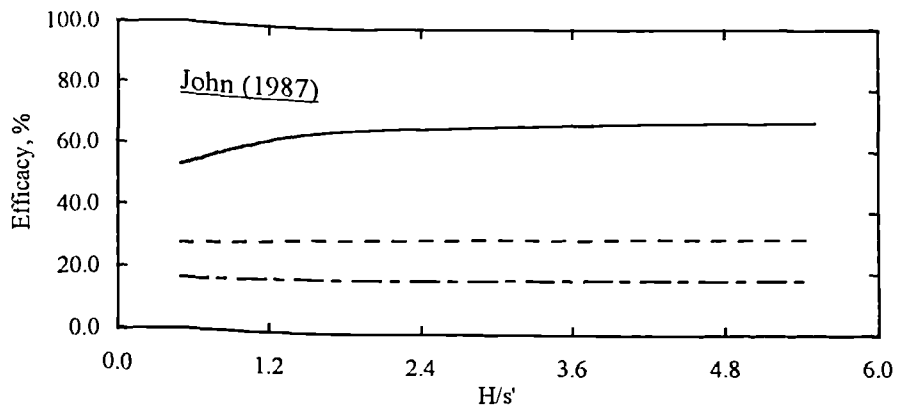
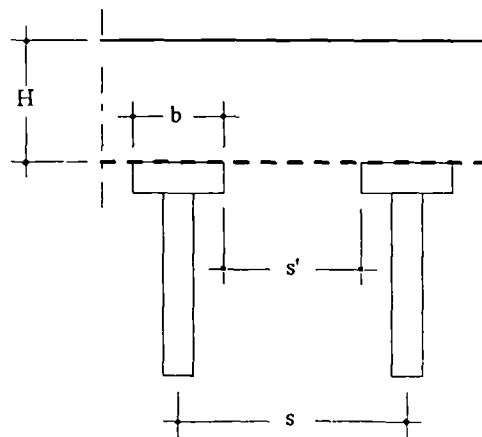
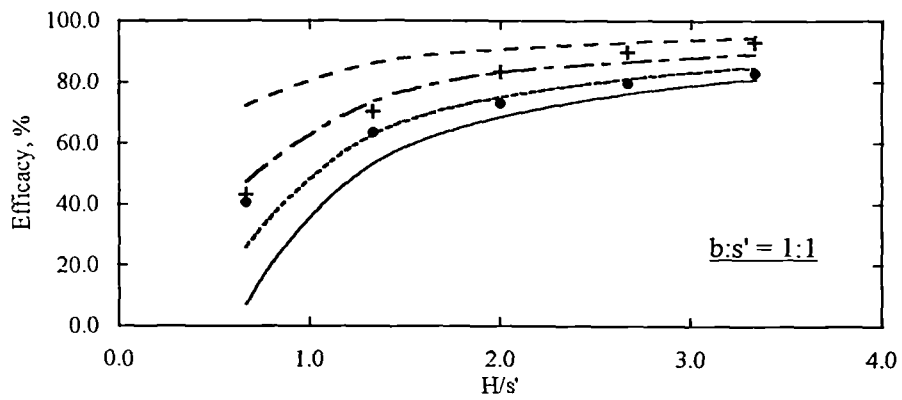
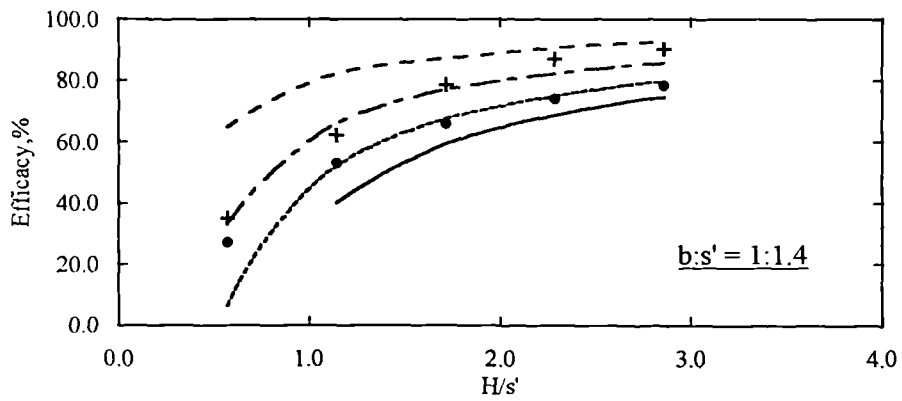
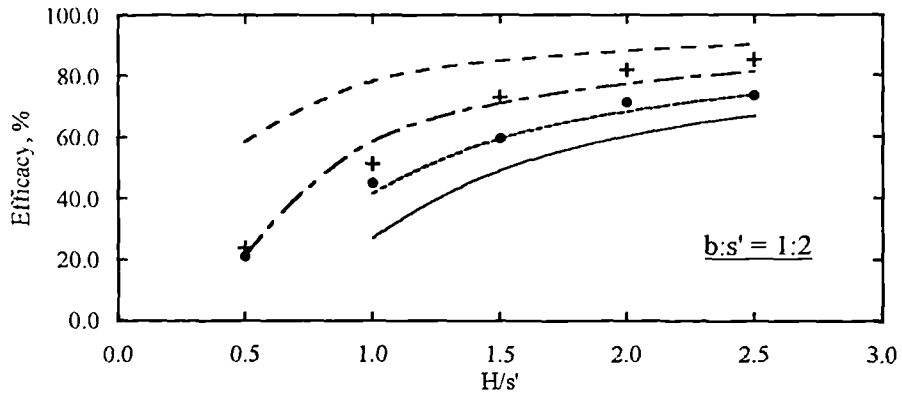


Figure 5-17. A comparison between the three methods of calculating piled embankment efficacy.



Legend :

- | | | |
|-------|-----------------|---------------------|
| — | $\alpha = 1.0$ | } Crown stability |
| - - - | $\alpha = 0.8$ | |
| - - - | $\alpha = 0.57$ | |
| - - - | $\alpha = 0.3$ | |
| + | Full ht. | } measured efficacy |
| • | Inc. loading | |

Figure 5-18. The variation of the efficacy calculated using the domed arch analysis (Hewlett et al. (1988)) for different (α) values.

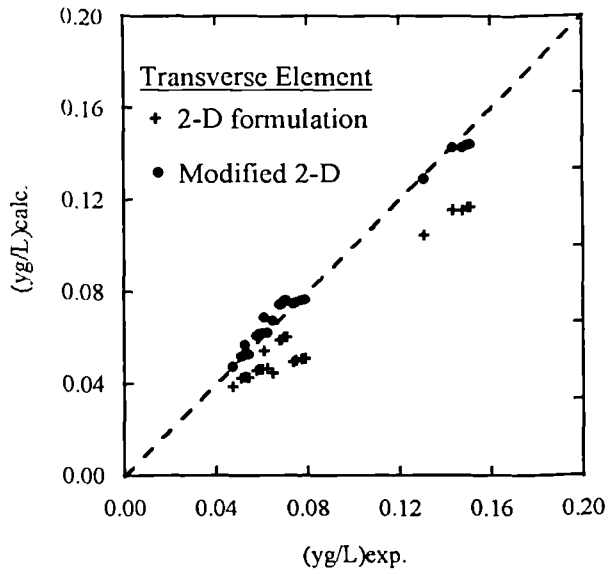


Figure 5-20a. Experimental versus calculated (yg/L) values for the 2-D and modified 2-D solutions along the transverse line of symmetry.

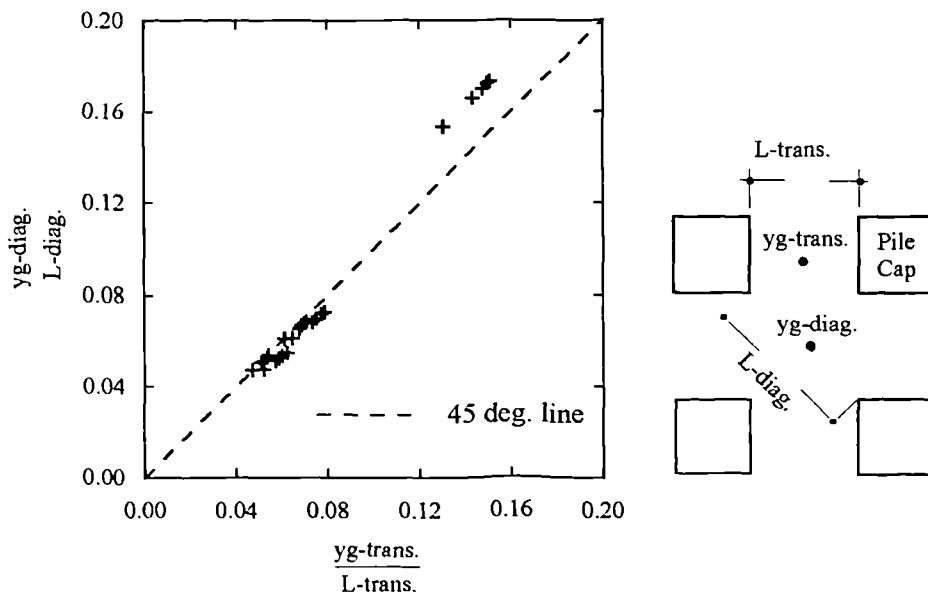
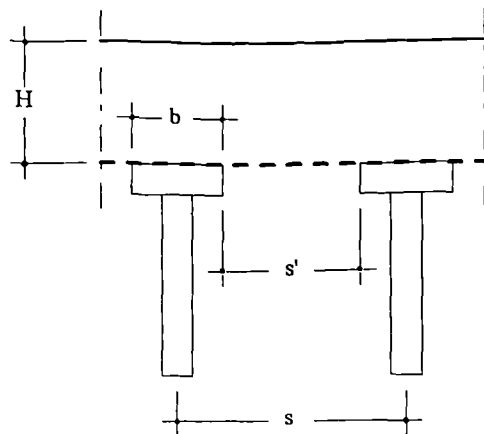
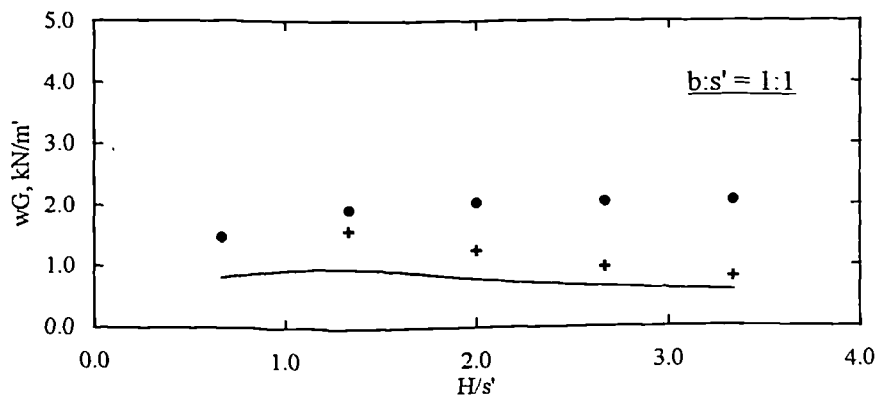
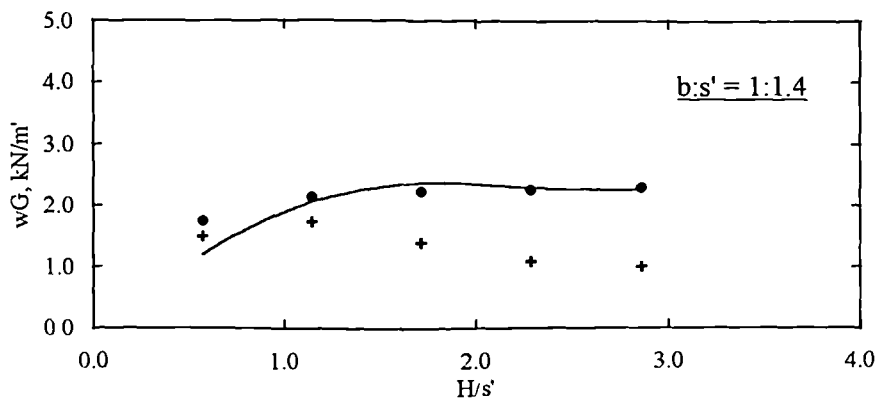
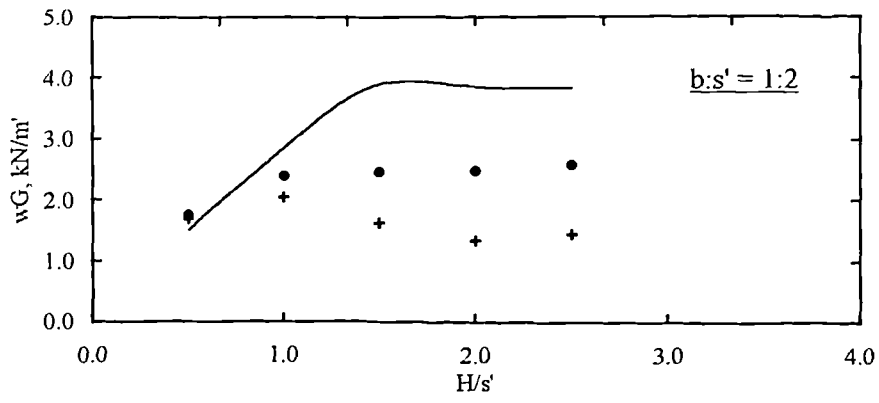


Figure 5-20b. Relationship between (yg/L) for the transverse and diagonal lines of symmetry



Legend :

• Incremental

+ Full height

— BS 8006:1995

Figure 5-21. The variation of the distributed load (wG) for different piled embankment configurations (after BS 8006:1994).

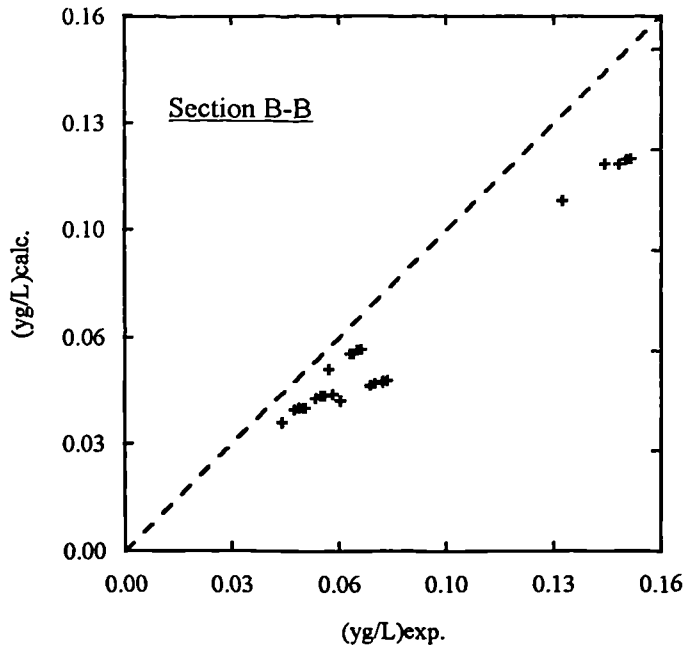


Figure 5-19a. Comparison between calculated and measured (yg/L) .

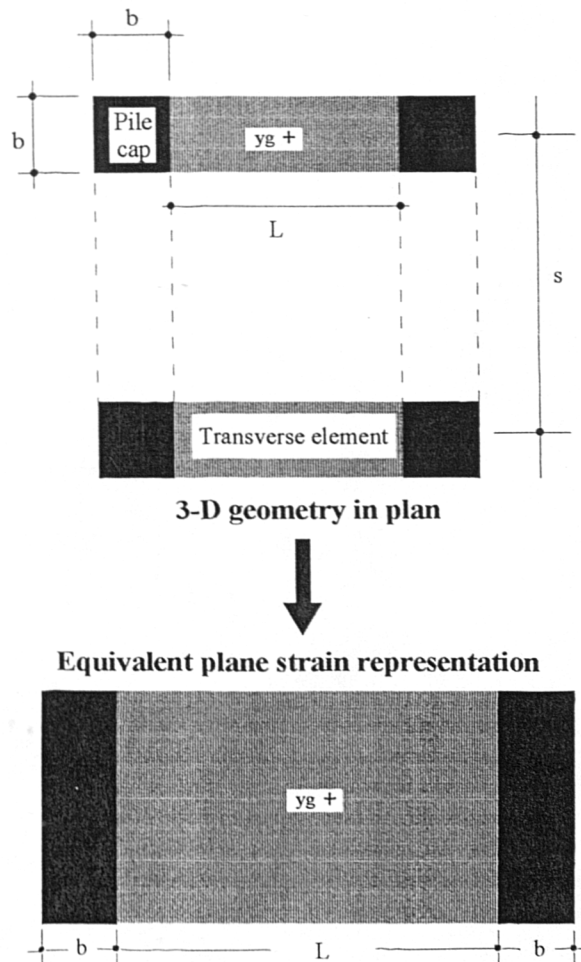
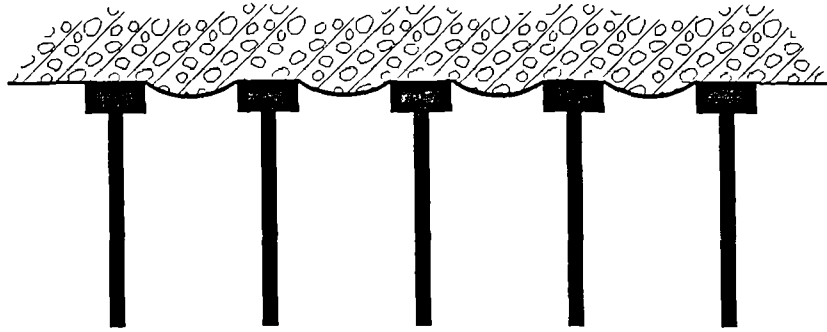
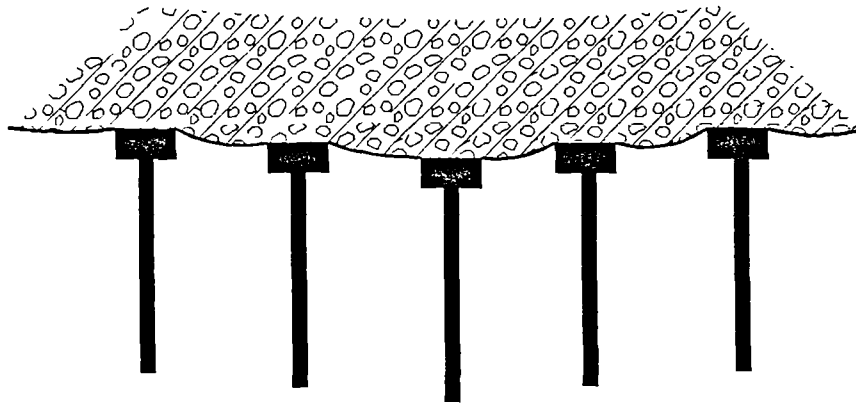


Figure 5-19b. Equivalent plane strain geometry.



a) Reinforcement Strain



b) Foundation Settlement

Figure 5-22. Serviceability limit states for basal reinforced piled embankments

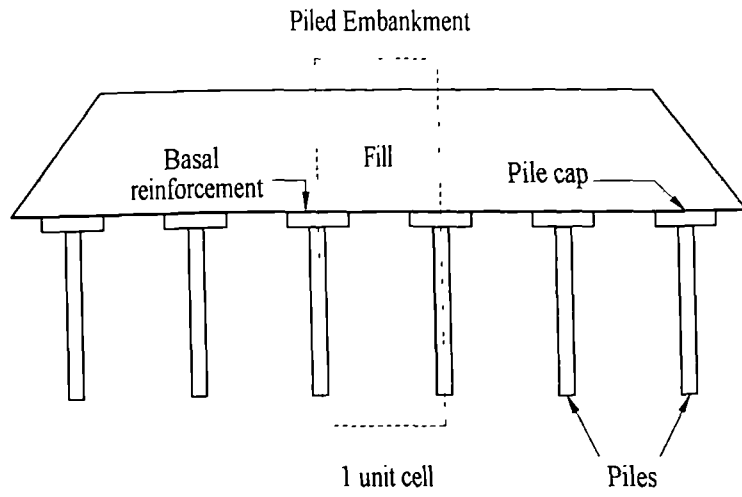


Figure 6-1. Typical piled embankment layout.

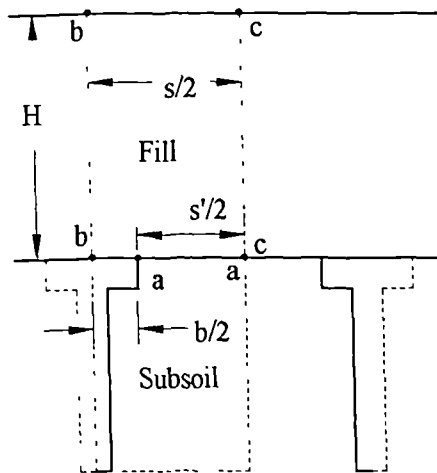


Figure 6-2. Unit cell of a piled embankment.

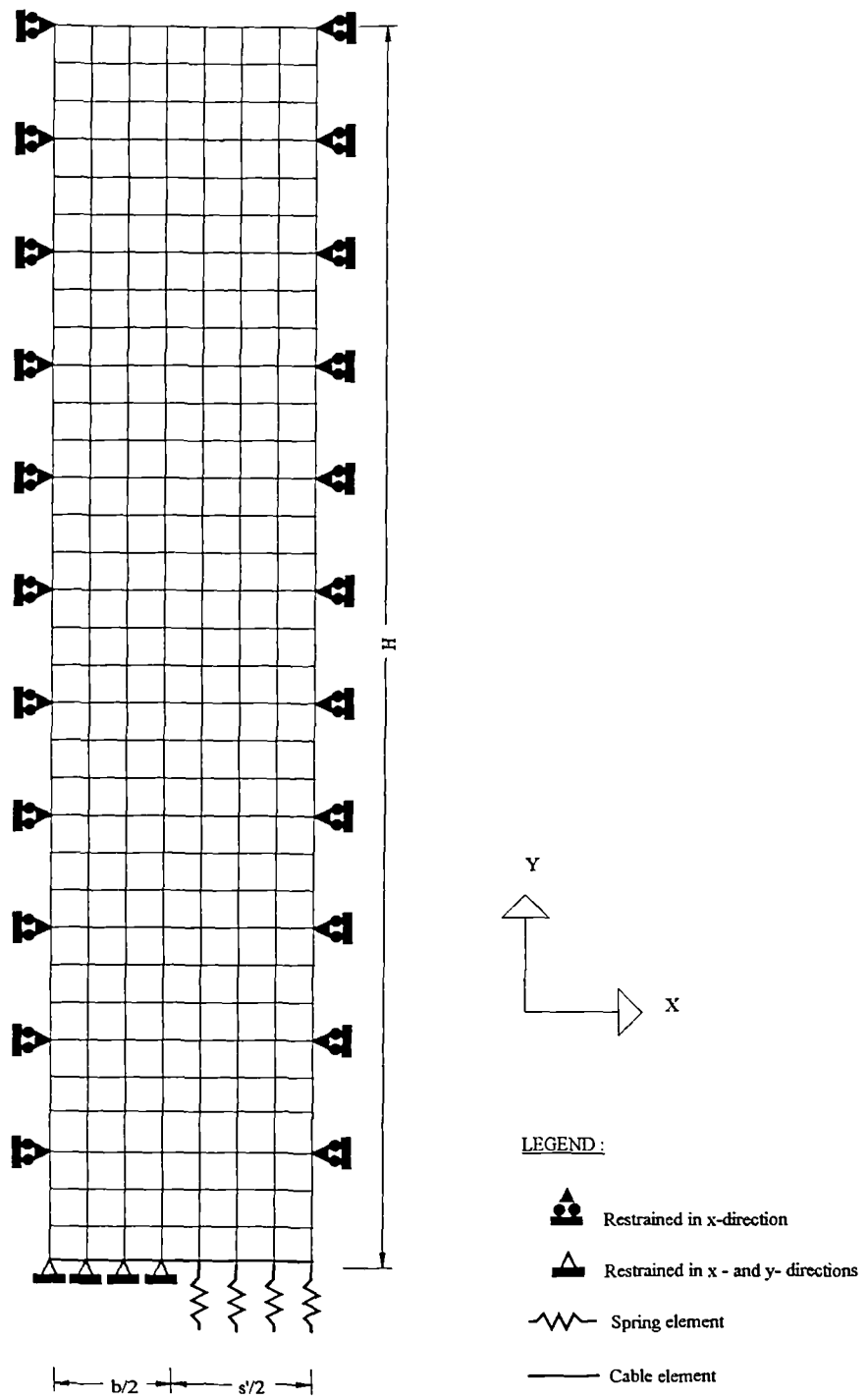
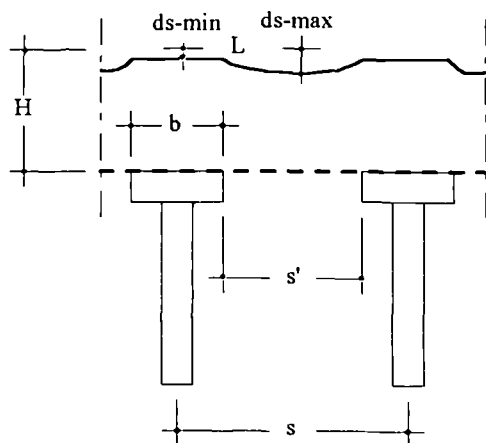
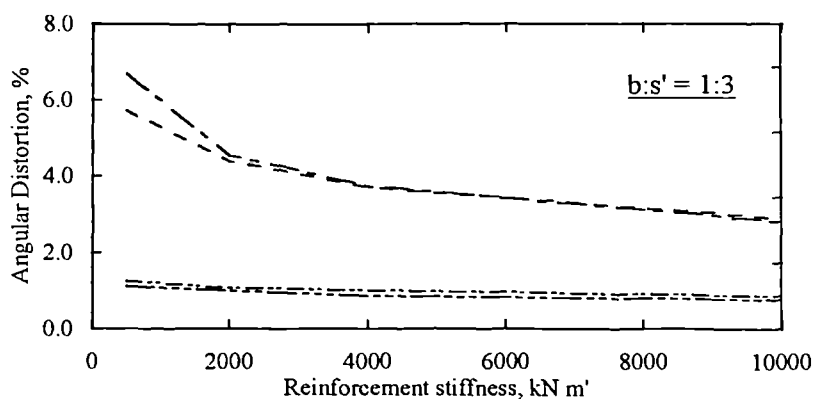
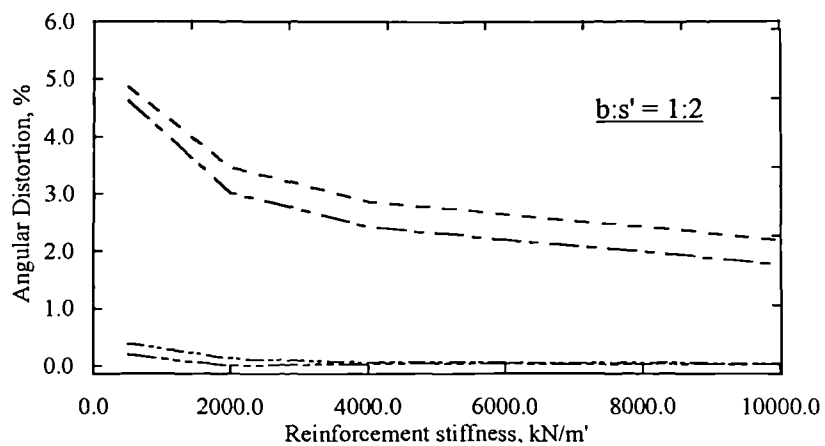
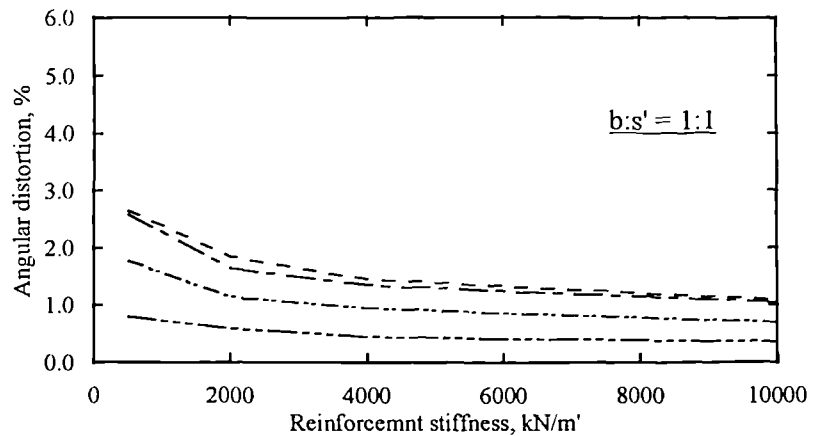


Figure 6-3. Typical finite difference mesh and boundary conditions used in the study.



Legend :

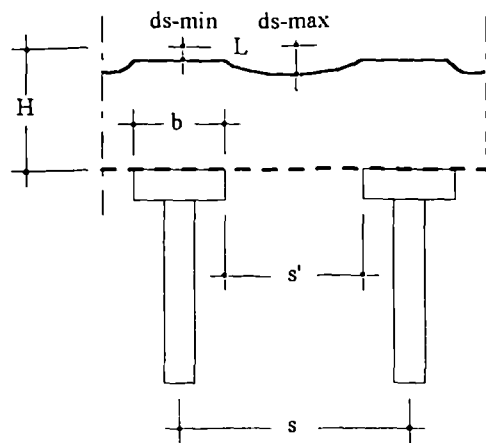
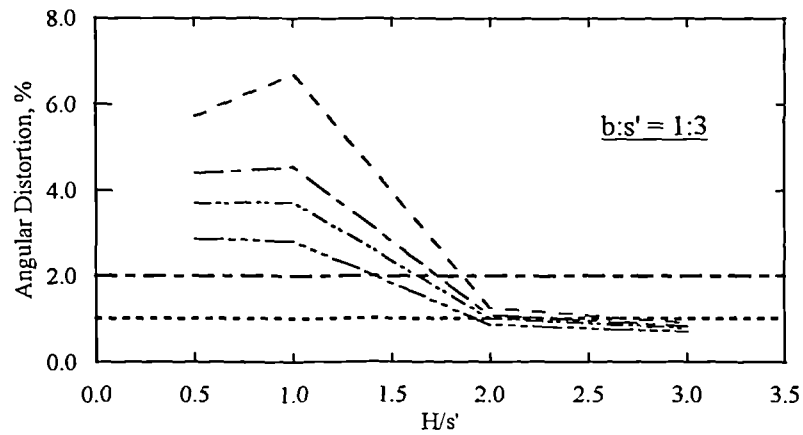
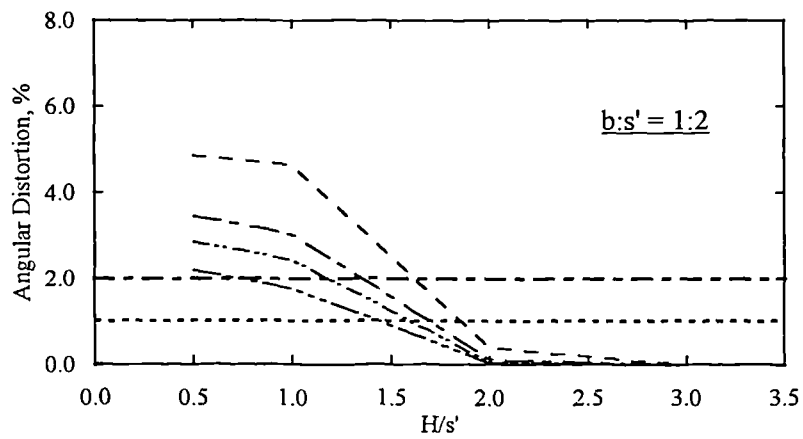
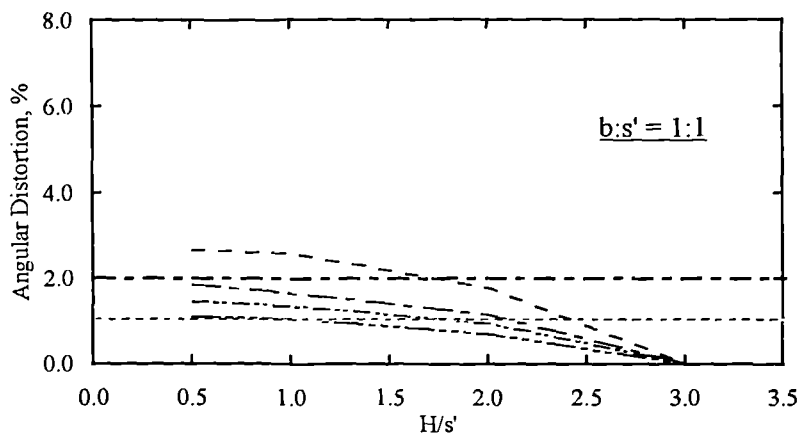
- $h/s' = 0.5$
- - - $h/s' = 1.0$
- · · $h/s' = 1.5$
- · — $h/s' = 2.5$

Note :

Angular distortion is defined as:

$$\frac{(ds-max - ds-min)}{2L} \times 100$$

Figure 6-10. The variation of the angular distortion with the depth ratio (H/s') for different geotextile stiffnesses.



Legend :

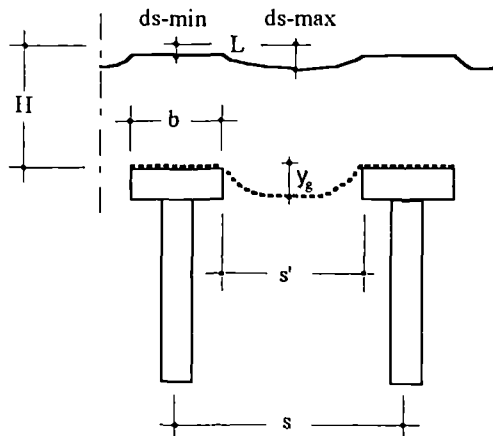
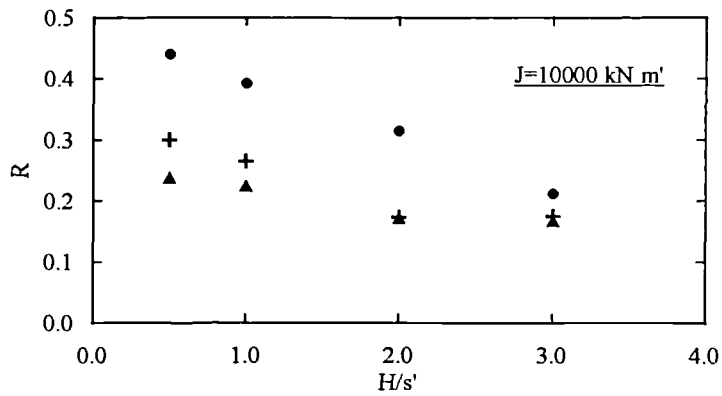
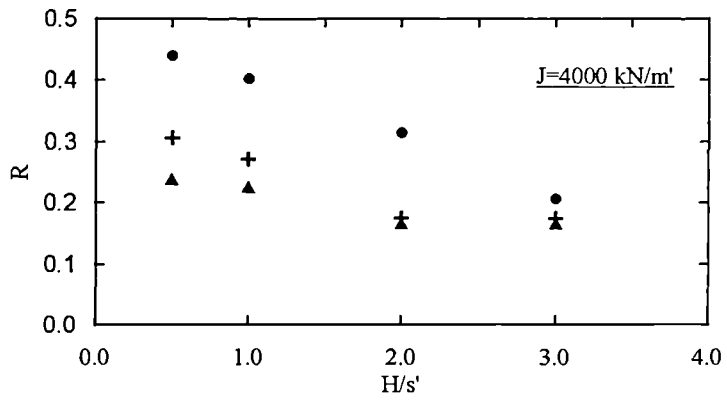
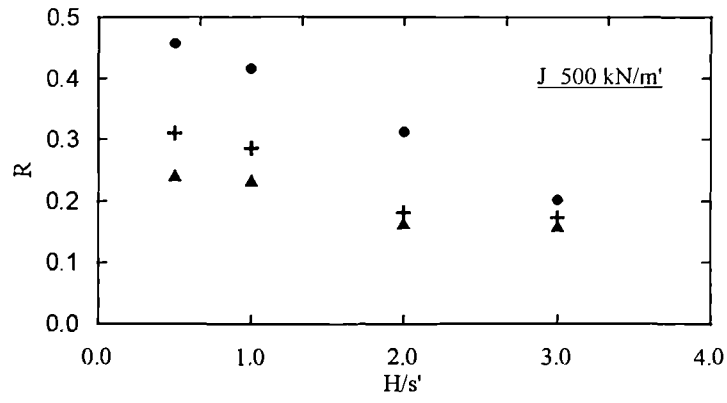
- J1 = 50 kN/m'
- J2 = 200 kN/m'
- J3 = 400 kN/m'
- J4 = 1000 kN/m'
- 1% principal roads
- 2% non-principal roads

Note :

Angular distortion is defined as:

$$\frac{(ds-max - ds-min)}{2L} \times 100$$

Figure 6-11. The variation of the angular distortion with the depth ratio (H/s') for different geotextile stiffnesses.



Legend :

- $b:s' = 1:1$
- + $b:s' = 1:2$
- ▲ $b:s' = 1:3$

Note

$$R = \frac{d\text{-max}}{yg} \cdot \frac{b}{s}$$

Figure 6-12. The variation of the dimensionless parameter (R) with depth ratio.

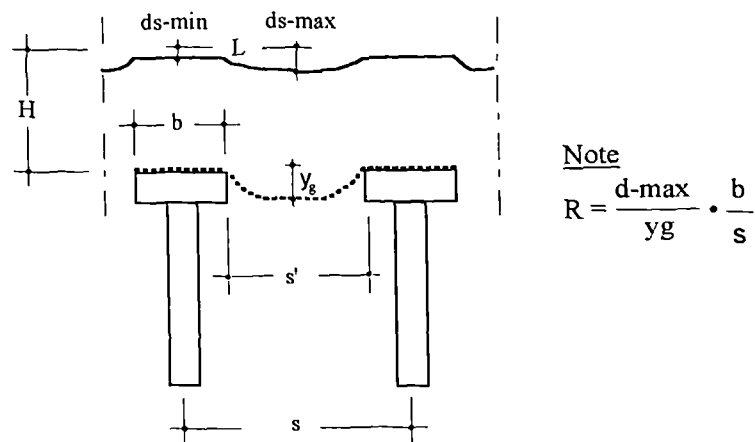
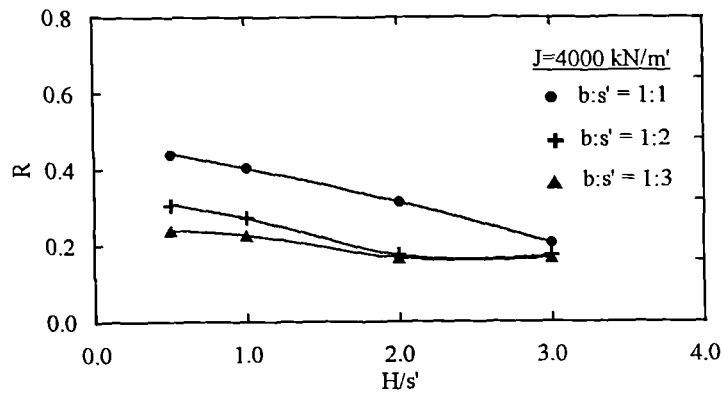
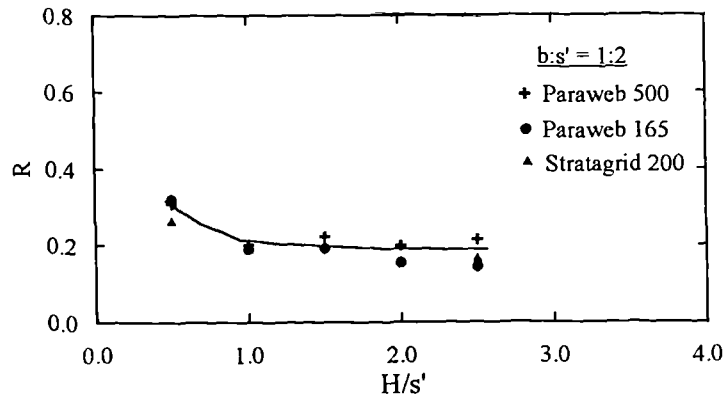
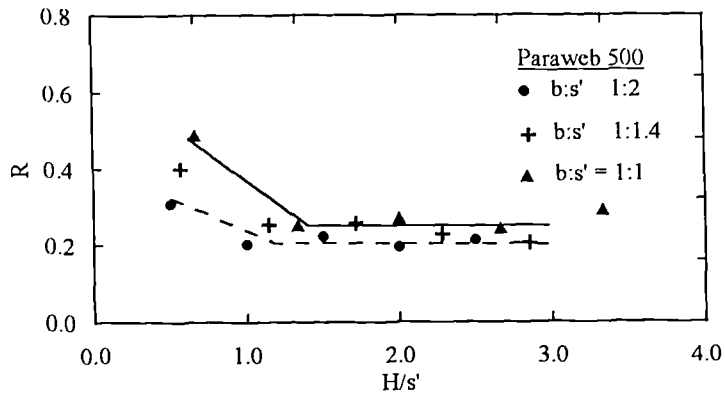


Figure 6-13. The variation of the dimensionless parameter (R) with depth ratio for the full height tests.



Plate 1. Overall view of apparatus.

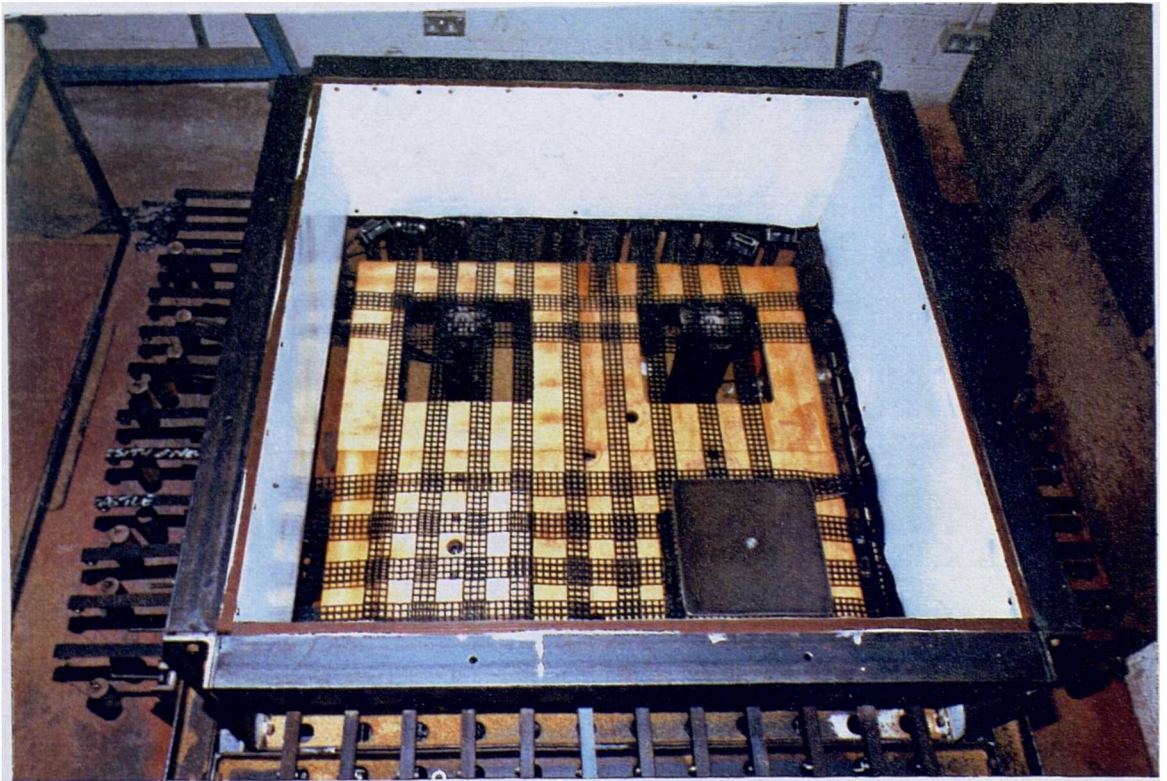


Plate 2. Plan view showing geotextile mesh, pile caps and movable base.

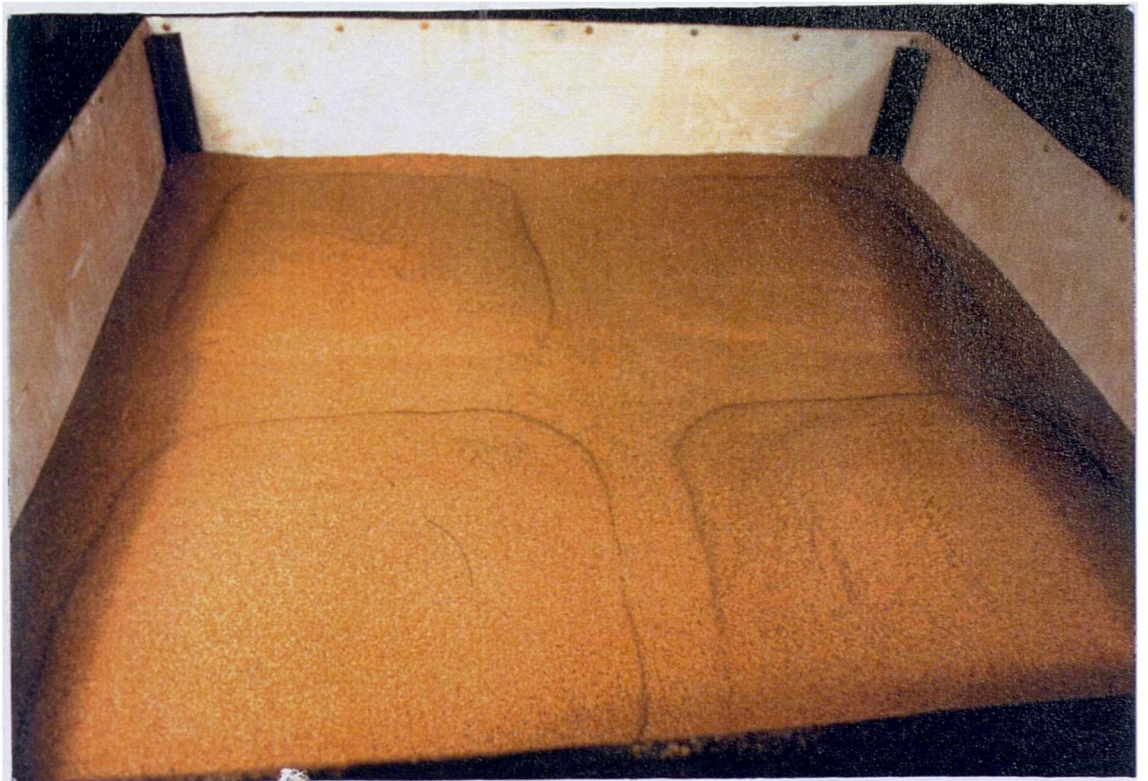


Plate 3. Typical surface settlement profile for low embankment heights.